UNIVERSITÉ DU LUXEMBOURG

PhD-FSTM-2020-079
The Faculty of Science, Technology and Medicine

DISSERTATION

Defence held on 10/12/2020 in Esch-sur-Alzette

to obtain the degree of

DOCTEUR DE L'UNIVERSITÉ DU LUXEMBOURG EN SCIENCES DE L'INGÉNIEUR

by

Vishojit Bahadur THAPA
Born on 6th October 1991 in Luxembourg City (Luxembourg)

RECYCLING OF GRAVEL WASH MUD FOR MANUFACTURING CO_2-REDUCED CEMENT

Dissertation defence committee

A-Prof. Dr.-Ing. Joachim Hansen, Chairman
Associate Professor, University of Luxembourg, Faculty of Science, Technology and Medicine

Prof. Dr. André Lecomte, Vice-Chairman
Professor, University of Lorraine, Institut Jean Lamour

Prof. Dr.-Ing. Danièle Waldmann, Dissertation supervisor
Professor, University of Luxembourg, Faculty of Science, Technology and Medicine

Prof. Dr. Jean-Frank Wagner
Professor, University of Trier, Department of Geology

Dr. Claude Simon
Expert, Head of Quality Management, Cimalux S.A.

Preface and acknowledgements

This doctoral dissertation presents the results of my investigations on the topic of "Recycling of gravel wash mud for manufacturing CO_2-reduced cement", which were realised during my PhD journey at the Institute of Civil and Environmental Engineering (INCEEN) of the University of Luxembourg. This research project was mainly carried out at the Laboratory of Solid Structures (LSS) of the University of Luxembourg. It deals with the revalorisation of an unused industrial waste product, namely gravel wash mud (GWM) and its utilisation for the conceptualisation of potential "low carbon" cements. The execution of the present project and the writing of this dissertation were carried out in the period from the 1st of September 2016 to the 10th of November 2020.

My sincere and special thanks go to Prof. Dr.-Ing. Danièle Waldmann for her trust and her confidence in my actual potential and capabilities in the scientific field by offering me this unique opportunity to carry out a doctorate under her supervision. I want to express my profound gratitude to Prof. Dr.-Ing. Danièle Waldmann for her clear and continuous guidance throughout my PhD journey, her permanent availability for any exchange (very appreciated as this is not always obvious), her trust on the quality of my independent work, her constructive feedback and criticisms, her understanding for personal concerns, and her professionalism and efforts to provide an inspiring and motivating working environment.

I want to express my sincere thanks to Prof. Dr. Jean-Frank Wagner, Professor and Head of the Department of Geology at the University of Trier, for his support during the elaboration of the actual research question of this project. Furthermore, his contributions and inputs to extend my understanding of the geological origin and the mineralogy of the gravel wash muds were precious for the progress of the project.

My sincere thanks and appreciations go to A-Prof. Dr.-Ing. Joachim Hansen, Professor in Engineering Science in the field of Hydraulic Engineering and Urban Water Engineering at the University of Luxembourg, and to Prof. Dr.-Ing.André Lecomte, Professor at the Department of Chemistry and Physics of Solids and Surfaces (Institut Jean Lemour) of the University of Lorraine, for their participation as Chairman, respectively, Vice Chairman in my dissertation defence committee. Their remarks and comments on the content of my PhD work during the different meetings of the thesis supervision committee (CET) and their detailed communication of their expectations on the final work were extremely valuable and allowed to improve my final dissertation.

I am deeply grateful to Dr. Claude Simon from Cimalux S.A. for his willingness to participate as a member of my thesis supervision committee (CET). Without his eagerness to support this research project actively, major milestones and some of the significant findings would have been difficult or more time-consuming to reach. I consider his unique contributions by giving me access to various high sensitive and cost-intensive characterisation methods at his company's expenses and linking me up with different topic-related experts as a key factor to the success of this project. His expertise and his suggestions were a precious contribution to the work and allowed me to clarify my doubts by bringing me back to the right track to succeed at fulfilling my research goals.

Furthermore, I am sincerely thankful to Carlo Spina from Contern S.A. and Paul Wertz, from Carrières Feidt S.A., for the supply of various raw materials and tools used in the realisation of this research work, and their valuable inputs and feedback on the progress of my research work during our regular meetings. Especially, I am grateful to Paul Wertz for his valuable inputs and responses to diverse questions related to the current, historical and regional availability of gravel wash muds and the regional occurrence of similar products.

Moreover, I would like to express my gratitude to Dr. Marcus Paul and Astrid Becker from the Wilhelm Dyckerhoff Institut (WDI) for their valuable contributions to various applied characterisation techniques. Additionally, I am grateful to Dr. Oscar Baeza-Urrea from the University of Trier and Zornitza Tosheva from the Department of Physics and Materials Science at the University of Luxembourg for providing support to the microstructural analysis.

I would also like to thank my colleagues and friends from the laboratories in Campus Kirchberg of the University of Luxembourg, Gilbert Klein, Marc Seil, Claude Collé, Logan Freitas, Vicente Reis Adonis, Ed Weyer, Markus Schlienz, Ralph Reiter, Ken Adam, Cédric Bruyère, Grace Ligbado and Remi Radinovic for sharing their valuable time at countless occasions for technical support or memorable discussions as short distractions from everyday work. Special thanks go to Marc Seil and Gilbert Klein for their excellent and experienced research support capabilities in a friendly, pleasant and cooperative atmosphere. I could contact them at any time, and I always found appreciative advice and help regarding the provision of materials or tools, the appropriate setup of the experiments, the introduction to the operation of new machines and tools, and much more.

Heartfelt thanks and highest appreciations go to my fellow PhD and Post-doc colleagues, Dr.-Ing. Michel Weiler, Dr.-Ing. Dolgion Erdenebat, Patrick Pereira Dias, Dr.-Ing. Gael Chewe Ngapeya,

Lorenc Bogoviku, Hooman Eslami, Dr.-Ing. Laddu Bhagya Jayasinghe, Dr.-Ing.Thanh Tung Nguyen and Tarik Camo, for the numerous and endless rounds of discussions on professional and private matters, for the share of knowledge as well as for getting me out of my monotonous work routines throughout my PhD journey.

I am also grateful to the staff members of the University of Luxembourg for their helpful administrative support, especially Simone Drees, Annabella Simon, Marielle Mabille, Mike Hansen, Shayan Weber, Inmaculada Peral Alonso, Silvia Vendetti, Berta Rato, Rita Giannini and Suzanne Biwer.

Furthermore, I would like to thank the students Sinan Kaassamani, Alejandra Mora Rincón (University of Trier), Jasmin Riem (University of Trier), Stefan Habetz (University of Trier), Nico Moes, Vincent Bamberg, Joe Gengler, Kristian Vidovic, Gilles Kayser, Jérome Pauly and Kauyne Parise for their active contributions to the global project through their successful Bachelor's theses, Master's theses and semester projects under my personal supervision.

The greatest and deepest thanks go to my parents, for their admirable and selfless love, support, trust, and patience in all stages throughout my life without ever expecting anything in return.

Luxembourg, 10th November 2020

Vishojit Bahadur THAPA

Abstract

The present research project “CO2REDCEM” is carried out at the Laboratory of Solid Structures (LSS) of the University of Luxembourg, in close collaboration with Luxembourgish industrial partners (Cimalux S.A., Carrières Feidt S.A. and Contern S.A.). This project aims at reducing the generation of CO_2 emissions during cement production by minimisation of the use of cement clinker or its complete replacement by new binder compositions and concepts, containing novel material resources derived from local unused industrial waste products. Such a potential raw material is gravel wash mud (GWM), which occurs as a waste product from gravel mining. This clayey mud is collected from a sludge reservoir, located in the North West of Luxembourg. Currently, this waste product is landfilled without any further use. However, this prime material offers very promising properties, which require a thorough characterisation and verification before its revalorisation as a viable supplementary cementitious material (SCMs).

Reusing or recycling of waste elements into goods has been among the greatest ambitions of our and earlier generations, and it will take a more important role in the future economy. One primary goal of this project is to replace the “end-of-life” concept of gravel wash mud by reusing it as new raw material. This endeavour will bring double benefit to environment as the waste is prevented from landfilling, and it is revalorised as a prime resource in another system.

This research work shares the outcomes from the assessment of the performance of the prime material GWM within the following binder concepts and binder reaction mechanisms:

- The use of gravel wash mud (GWM) powders as a precursor material for the synthesis of alkali-activated binders: A “cementless” binder is synthesised by alkaline activation of processed and calcined GWM powders. The mitigation of the CO_2 emissions is achieved by the calcination process of the clayey gravel wash mud, which requires less thermal energy and thus lower energy consumption than for cement clinker production.
- Substitution of Ordinary Portland Cement (OPC) by calcined GWM powders: Cement and concrete mixtures are prepared based on partial replacement of Portland cement by calcined GWM powders. This study presents the investigations on the involved reaction mechanisms (pozzolanic and cementitious hydration reactions), the optimal mixture configurations and the optimal material treatment processes.
- The development of lime-Metakaolin-GWM binder concepts: Mixtures without cement are developed using GWM and other constituents, classified as industrial by-products. This research includes the mineralogical and microstructural characterisation of the constituents, the understanding of the reaction mechanism, and the optimisation of the mixtures to enhance the performance of the novel cementitious products.

This thesis allowed to assess the performance of the waste product GWM as a valid pozzolanic prime material and to understand the requirements on physical, chemical and mineralogical characteristics of any potential raw material to ensure its permissibility as an alternative supplementary cementitious material (SCM).

Keywords:

Gravel wash mud (GWM), Alternative clay materials, Calcined clays, Supplementary cementitious material (SCM), Pozzolanic activity, Illite, Kaolinite, Metakaolin, Lime, Alkali-activated binder, Blended cements, blended lime-clay pastes, Concrete, Mineralogy, Mechanical properties, Microstructural analysis, Hydration kinetics, Drying shrinkage.

Kuerzfaassung

Déi virleiend Fuerschungsaarbecht „CO2REDCEM“ gouf an enker Zesummenaarbecht mat lëtzebuergeschen Industriepartnern (Cimalux S.A., Carrières Feidt S.A. a Contern S.A.) am „Laboratoires des Structures Solides (LSS)“ vun der Universitéit Lëtzebuerg duerchgefouert. Dëse Projet zielt op eng Reduzéierung vun den CO_2 Emissiounen aus der Zementindustrie aus duerch e partiellen oder kompletten Ersatz vum Zementklinker duerch nei Bindemëttelkompositioune a -konzepter, déi Romaterialien enthalen, déi vu lokalen industriellen Offallprodukter ofstame. Sou e potenzielle Material ass de Kiselwäschschlamm (KWS), den als Offallprodukt an lëtzebuergesch Steebréchanlagen entsteet. Dëse tounhaltege Schlamm gouf aus enger Steekaul am Nordweste vu Lëtzebuerg gesammelt. Aktuell gëtt dëst Offallprodukt ouni weidere Notzen deponéiert. Allerdéngs bitt dëst Primärmaterial ganz villverspriechend Eegeschaften, déi eng grëndlech Charakteriséierung a Analys erfuerdert hun éier eng Revalorisatioun als „Supplementary Cementitious Material (SCM)“ a Fro koum.

D‘Verwäertung oder de Recyclage vun Offallelementer an nei Wueren gehéiert zu de gréissten Ambitiounen vun dëser a fréierer Generatiounen, an et wäert ganz bestëmmt eng méi wichteg Roll an der zukünfteger Wirtschaft anhuelen. Ee Haaptzil vun dësem Projet ass et den „End-of-Life“ Konzept vum Kiselwäschschlamm durch eng Verwäertung als Ressource fir néi Rostoffer ze ersetzen. Dës Ustrengunge bréngen e duebelt Virdeel fir d’Ëmwelt, well eng Deponéierung vun

engem Offall verhënnert gëtt, an duerch seng Verwendung als Haaptressource an engem anere System revaloriséiert gëtt.

Dëst Fuerschungsaarbecht deelt d'Resultater iwwert d'Leeschtungscapacitéit vum Haaptmaterial KWS an folgend Bindemëttelkonzepter a -reaktiounsmechanismen mat:

- D'Verwendung vu KWS-Polver fir d'Synthees vun engem alkalesch-aktivéierten Bindemëttel: En Bindemëttel gëtt duerch alkalesch Aktivatioun vu traitéierte a kalzinéierte KWS-Polver synthetiséiert. D'Reduktioun vun den CO_2 Emissioune gëtt duerch de Kalkzinéierungsprozess vum KWS erreecht, wat manner Hëtzt erfuerdert an domat e geréngere Energieverbrauch ewéi bei der Zementklinkerproduktioun opweist.
- Ersatz vum Portlandzement (OPC) duerch kalzinéiert KWS-Polver: Zement a Bëtonmëschunge ginn produzéiert baséiernd op engem partiellen Ersatz vu Portlandzement duerch kalzinéiert KWS-Polver. Dës Etüd präsentéiert d'Analysen iwwer déi involvéiert Reaktiounsmechanismen (pozzolanesch an zementarteg Hydratatiounsreaktiounen), déi optimal Mëschungskonfiguratiounen an déi optimiséiert Materialbehandlungsprozesser.
- D'Entwécklung vu Kallek-Metakaolin-KWS Bindemëttelkonzepter: Mëschunge ouni Zement ginn ënnersicht mat KWS-Polver an aner Bestanddeeler, déi als industriell Nieweprodukter klasséiert sinn. Dës Fuerschung enthält eng mineralogesch a mikrostrukturell Charakteriséierung vun de Bestanddeeler, eng détailéiert Etüd vum Reaktiounsmechanismus, an eng Optimiséierungsetüd vun de Mëschunge fir d'Performance vun den neien zementarteg Produkter ze verbesseren.

Dës Aarbecht erlaabt et d'Performance vum Offallprodukt KWS als e pozzolanescht Material ze bewäerten an d'Ufuerderunge un physikalesch, chemesch a mineralogesch Charakteristike vu

potenziellen Rostoffer ze verstoen fir hir Admissibilitéit als alternativ „Supplementary Cementitious Material (SCM)“ ze iwwerpréiwen.

Schlësselwieder:

Kiselwäschschlamm (KWS), Alternativ tounhalteg Matière, Getëmpert Toune, Supplementary cementitious material (SCM), Puzzolanech Reaktioun, Illit, Kaolinit, Metakaolin, Kallek, Alkalesch-aktivéiert Bindemëttelen, Mëschzementer, kallek- an tounhalteg Bindemëttel, Bëton, Mineralogie, Mechanesch Eegenschaften, Mikrostrukturanalys, Hydratatiounskinetik, Dréchenschwinden.

Kurzfassung

Das vorliegende Forschungsprojekt „CO2REDCEM“ wurde im „Laboratory of Solid Structures (LSS)“ der Universität Luxemburg in enger Zusammenarbeit mit luxemburgischen Industriepartnern (Cimalux S.A., Carrières Feidt S.A. und Contern S.A.) durchgeführt. Diese Arbeit befasst sich mit der Reduzierung des CO_2-Ausstoßes bei der Zementherstellung durch eine partielle oder vollständige Substitution von Zementklinker durch neuartige Bindemittelzusammensetzungen und -konzepten, die aus unverwendeten, lokalen Industrieabfallprodukten stammenden Rohmaterialien enthalten. Ein solcher Rohstoff ist der Kieswäscheschlamm (KWS), der als Abfallprodukt beim Kiesabbau anfällt. Dieser tonhaltige Schlamm wurde aus einem Dekantierbecken einer Steinbruchanlage im Nordwesten Luxemburgs entnommen. Bisher wurde dieses Abfallprodukt ohne jegliche Weiterverwertung deponiert. Jedoch zeigt dieser Rohschlamm vielversprechende Materialeigenschaften auf, die einer gründlichen Charakterisierung und Überprüfung unterzogen wurden, bevor eine Aufwertung zum „Supplementary Cementitious Material (SCM)“ erfolgte.

Die Wiederverwendung oder das Recycling von Abfallelementen zu neuen Gütern gehört zu den ehrgeizigsten Bestrebungen heutiger und früherer Generationen, und sie wird in der künftigen Wirtschaft eine wichtigere Rolle spielen. Ein Hauptanliegen dieses Projekts besteht darin, das End-of-life-Szenario von KWS durch eine Wiederverwertung als neuen Rohstoff zu ersetzen. Dieses

Vorgehen wird der Umwelt einen doppelten Nutzen bringen, da der einstige Abfall nicht mehr deponiert und in einem anderen System zum Rohstoff aufgewertet wird.

Im Zuge dieser Forschungsarbeit werden zahlreiche Ergebnisse und Erkenntnisse zur Leistungsfähigkeit des KWS in folgenden Bindemittelkonzepten und Reaktionsmechanismen vorgestellt:

- Die Verwendung von KWS-Pulvern als Ausgangsmaterial für die Synthese eines alkalisch-aktivierten Bindemittels: Ein zementfreies Bindemittel wird durch die alkalische Aktivierung von getemperten KWS-Pulvern hergestellt. Die Reduzierung der CO_2-Emissionen erfolgt durch den Kalzinierungsprozess des tonhaltigen KWS, der weniger Wärmeenergie und damit einen geringeren Energieverbrauch als bei der Zementklinkerherstellung erfordert.
- Substitution von Portlandzementanteilen durch getemperte KWS-Pulver: Herstellung von Zement- und Betonmischungen durch partielles Ersetzen von Portlandzementanteilen durch getemperte KWS-Pulver. Diese Studie stellt die Ergebnisse der Untersuchungen zu den auftretenden Reaktionsmechanismen (puzzolanische und zementartige Hydratationsreaktionen), zur optimalen Mischungskonfiguration und zum geeigneteren Materialbehandlungsprozess vor.
- Die Entwicklung von Kalk-Metakaolin-KWS Bindemittelkonzepten: Es werden zementfreie Mischungen unter Verwendung von KWS und anderen Bestandteilen entwickelt, die als industrielle Nebenprodukte eingestuft werden. Diese Forschung umfasst die mineralogische und mikrostrukturelle Charakterisierung der Bestandteile, das Verständnis des Reaktionsverhaltens und die Optimierung von Mischungsrezepturen, um die Leistungseffizienz der neuartigen zementähnlichen Produkte zu verbessern.

Diese Arbeit ermöglichte es, KWS als ein puzzolanischer Zusatzstoff nachzuweisen und die Anforderungen an physikalischen, chemischen und mineralogischen Eigenschaften potenzieller Rohstoffe sicherzustellen, um deren Zulässigkeit als alternatives SCM zu überprüfen.

Schlüsselwörter:

Kieswäscheschlamm (KWS), Alternative tonhaltige Materialien, Getemperte Tone, Supplementary cementitious material (SCM), Puzzolanische Reaktion, Illit, Kaolinit, Metakaolin, Kalk, Alkalisch aktivierte Bindemittel, Mischzemente, kalk- und tonhaltige Bindemittel, Beton, Mineralogie, Mechanische Eigenschaften, Mikrostrukturanalyse, Hydratationskinetik, Trockenschwinden.

Résumé

Le projet de recherche « CO2REDCEM » est réalisé dans le Laboratoire des Structures Solides (LSS) de l'Université du Luxembourg, en étroite collaboration avec des partenaires industriels luxembourgeois (Cimalux S.A., Carrières Feidt S.A. et Contern S.A.). Ce projet vise à réduire les émissions de CO_2 lors de la production de ciment en minimisant l'utilisation de clinker de ciment ou en le remplaçant complètement par de nouvelles compositions et concepts de liants, contenant des matières dérivées de déchets industriels locaux non utilisés. Les boues de lavage de gravier (BLG) sont de telles matières premières, qui se présentent en tant que déchets de carrières de pierres. Ces boues argileuses sont collectées d'un bassin de décantation d'une carrière de sables et graviers, situé dans le nord-ouest du Luxembourg. Actuellement, ce déchet est mis en décharge sans autre utilisation. Toutefois, ce matériau de base offre des propriétés très prometteuses, qui nécessitent d'une étude de caractérisation approfondie avant sa revalorisation en tant qu'ajouts cimentaires.

La réutilisation ou le recyclage des éléments de déchets en produits figure parmi l'une des plus grandes ambitions de notre époque et des générations précédentes, et elle jouera un rôle plus important dans l'économie future. L'un des principaux objectifs de ce projet est de remplacer le concept de fin de vie de boues de lavage de gravier (BLG) par leur réutilisation comme nouvelle matière première. Cet effort apportera un double avantage à l'environnement, puisque les déchets

ne seront plus mis en décharge et qu'ils seront revalorisés en tant que ressource principale dans un autre système de produits.

Ce travail de recherche présente les résultats de l'évaluation des performances des boues argileuses dans les concepts et les mécanismes de réaction de liants suivants :

- L'utilisation de poudres de BLG comme matériau de base pour la synthèse d'un liant à activation alcaline: Un liant « sans ciment » est synthétisé par activation alcaline des poudres de boues argileuses traitées et calcinées. L'atténuation des émissions de CO_2 se résulte du processus de calcination des boues argileuses, qui nécessite moins d'énergie thermique et donc une consommation d'énergie plus faible que lors de la production de clinker de ciment.
- Remplacement du ciment Portland ordinaire (CPO) par des poudres de BLG calcinées: Des mélanges de ciment et de béton sont produits en se basant sur le remplacement partiel du ciment Portland par des poudres de boues argileuses. Cette étude présente les recherches sur les mécanismes de réaction impliqués (réactions pouzzolaniques ou réactions d'hydratation du ciment), les configurations optimales des mélanges et les processus de traitement des matériaux optimisés.
- Le développement de concepts de liants chaux-métakaolin-BLG: Des mélanges sans ciment sont développés à partir de poudre de BLG et d'autres constituants, classés comme sous-produits ou déchets industriels. Cette recherche comprend la caractérisation minéralogique et microstructurale des constituants, la compréhension du mécanisme de réaction et l'optimisation des mélanges pour améliorer les performances des nouveaux produits cimentaires.

Cette thèse a permis d’évaluer la performance du produit déchet BLG en tant que matériau pouzzolanique et de comprendre les exigences relatives aux caractéristiques physiques, chimiques et minéralogiques de toute matière première potentielle afin de veiller à sa validité en tant qu’ajouts cimentaires.

Mots clés:

Boues de lavage de gravier (BLG), Matériaux alternatifs argileux, Argiles calcinées, Ajouts cimentaires, Activité pouzzolanique, Illite, Kaolinite, Métakaolin, Chaux, Liant à activation alcaline, Ciments mélangés, Liants à base de chaux et d'argile, Béton, Minéralogie, Propriétés mécaniques, Analyse microstructurale, Cinétique d'hydratation, Retrait au séchage.

Table of Contents

List of abbreviations

AASHTO	American Association of State Highway and Transportation Officials
ASTM	American Society for Testing and Materials
BET	Brunauer-Emmett-Teller method
BJH	Barrett-Joyner-Halenda method
BLG	fr. Boues de lavage de gravier; Gravel wash mud
BSE	Backscattered electrons
C_2S	Dicalcium silicate, Belite
C_3A	Tricalcium aluminate
C_3S	Tricalcium silicate, Alite
C_4AF	Tetracalcium aluminoferrite
CAH	Calcium aluminate hydrates
CASH	Calcium aluminosilicate hydrates
CCS	Carbon capture and storage
CDW	Construction and demolition waste
CEN	fr. Comité Européen de Normalisation; European Committee for Standardization
CET	fr. Comité d'Encadrement de Thèse; Thesis Supervisory Committee
CFCs	Chlorofluorocarbons
CG	Prefix for lime-metakaolin binder using calcined GWM
CG10	Blended cement pastes including 10 wt.% of calcined GWM
CG20	Blended cement pastes including 20 wt.% of calcined GWM
CG30	Blended cement pastes including 30 wt.% of calcined GWM
CGS	Prefix for mortar mixtures (binder and sand)
CGWM	Calcined GWM; calcined at 850°C if not indicated differently
CH	Calcium hydroxide, Portlandite
CO2REDCEM	Recycling of gravel wash mud for manufacturing CO_2-reduced cement
CO2REDRES	Traitement de ressources secondaires pour une réduction des émissions de CO_2 dans l'industrie de la construction
CPO	fr. Ciment Portland Ordinaire; Ordinary Portland Cement
CSH	Calcium silicate hydrates
CT	Calcination temperature
DIN	ger. Deutsches Institut für Normung; German Institute for Standardization
DS	Dolomitic sand
DSC	Differential scanning calorimetry
DTA	Differential thermal analysis
DTG	Differential Thermogravimetric analysis
EDS, EDX	Energy-dispersive X-ray spectroscopy
EDTA	Ethylenediaminetetraacetic acid

FA	Fly ash
GGBS	Ground-granulated blast-furnace slag
GWM	Gravel Wash Mud
HFC	Hydrofluorocarbons
HL1	Hydrated lime from Lhoist - CL90-S
HL2	Hydrated lime from Carmeuse S.A. - CL80-S
HL3	Hydrated lime from Carmeuse S.A. - CL90-S
HPC	High-performance concrete
ICSD	Inorganic Crystal Structure Database
IR	Infrared spectroscopy
ISO	International Organization for Standardisation
KASH	Potassium aluminosilicate hydrates
KOH	Potassium hydroxide, alkaline solution
KWS	lu. Kiselwäschschlamm; ger. Kieswäscheschlamm; Gravel wash mud
LCA	Life cycle assessment
LSS	Laboratory of Solid Structures, University of Luxembourg
LOI	Loss on ignition
MIP	Mercury intrusion porosimetry
MK	Metakaolinite, Metakaolin
MSG	Mosel sand and gravel mix
NASH	Sodium aluminosilicate hydrates
NHL	Natural hydraulic lime from Chaux et enduits de Saint-Astier - NHL 3.5
OPC, PC	Ordinary Portland Cement
PGWM	Pure GWM, unprocessed GWM
PSD	Particle size distribution
REF	Reference mixture
REM	ger. Rasterelektronenmikroskop; scanning electron microscope
RHA	Rice husk ash
RP	Real potential
RSI	Relative strength index
SAI	Strength activity index
SCM	Supplementary cementitious material
SEM	Scanning electron microscope
SF	Silica fume
SJR	Scientific Journal Rankings
STA	Simultaneous thermal analysis
TAM	Thermal activity monitor
TG, TGA	Thermogravimetric analysis
UG	Prefix for lime-metakaolin binder using uncalcined GWM
UG10	Blended cement pastes including 10 wt.% of uncalcined GWM
UG20	Blended cement pastes including 20 wt.% of uncalcined GWM
UG30	Blended cement pastes including 30 wt.% of uncalcined GWM
UGWM	Uncalcined GWM, dried GWM
UHPC	Ultra-high performance concrete
WDI	Wilhelm Dyckerhoff Institut
XRD	X-ray diffraction
XRF	X-ray fluorescence

Chapter 1 General

1.1 Motivation

The relevance of this thesis is established on the following four main backgrounds and motives at global, international, regional and national level, which prompted the need for the present research project:

I. Global concern - Mitigation of climate change: Climate experts agree that the excessive generation of anthropogenic greenhouse gases such as water vapour (H_2O), carbon dioxide (CO_2), ozone (O_3), methane (CH_4), nitrous oxide (N_2O) and fluorinated gases (CFC's and HFC's), will intensify the global greenhouse effect and lead to greater global warming potential with its subsequent effects on all ecosystems on Earth. This priority issue is of global relevance, and research should contribute to creating a scientific and technological basis towards durable and eco-friendly solutions.

II. International motives - The cement industry as significant CO_2 emitter: The cement manufacturing itself generates less CO_2 per kg of product than other industrial products like steel, plastics, aluminium, insulations material, glass, and many more. However, the enormous cement production volumes required to fulfil the current demand for concrete

and cementitious products overshadow any comparative assessment of the total CO_2 emissions with other products. These facts explain the current race to reduce concrete's carbon footprint by developing eco-friendly cements and alternative binder concepts.

III. Regional factor - Scarcity of traditional raw materials: In the Greater Region, the occurrence of traditional aggregates and "mainstream" industrial pozzolans/cementitious materials has significantly declined due to excessive exploitation of the regional resources or due to environmental limitations and technological developments imposed to the primary industrial sectors by the local authorities. It is of great interest for the regional industry to investigate the potential of a diversity of unused mineral resources, which after undergoing basic treatment processes, can become a viable solution to the impending shortage of traditional raw materials.

IV. National incentives - Valorisation of local unused industrial wastes: Current national obligations and laws on the management of industrial wastes restrict the excessive landfilling of quarrying and mining wastes, and it has become a substantial challenge of local quarrying plant operators to get authorisations for new landfills or future landfilling activities. Therefore, there exists a genuine interest in promoting national and regional research projects to develop concepts and solutions for alternative applications of these industrial waste products.

1.2 Scope and Aims

The main focus of the research project CO2REDCEM relies on the revalorisation of gravel wash mud (GWM) as a novel raw material by assessing the optimal treatment processes and developing new binder compositions, adapted to the characteristics of GWM. Another important objective of this work is to ensure that the developed concepts contribute to the reduction of the overall high carbon footprint of the cement production industry by lowering the clinker factor in cement compositions or by developing “cementless” binder concepts.

This work presents the investigations on three different binder concepts, namely “the use of gravel wash mud (GWM) for the synthesis of an alkali-activated binder”, “the substitution of Ordinary Portland Cement (OPC) by calcined GWM powders” and “the development of lime-Metakaolin-GWM binder concepts”. Furthermore, in a subsequent study, the performance and the characteristics of binary blended concretes using GWM powders were successfully analysed.

During the evaluation of the different binder concepts, the main objective was to assess the performance of the waste product, GWM, as a potential pozzolanic prime material, and to understand the physical, chemical and mineralogical characteristics of the raw material as well as to ensure its validity as a supplementary cementitious material (SCM) in each examined binder technology.

Within the framework of this research work, the criteria of success of the proposed concepts are exclusively restricted to the characteristics and performances of the reaction products based on one single raw material, namely gravel wash mud (GWM). Therefore, it is not recommended to project the compositions of the developed concepts on other “similar” raw materials without actually carrying out all the relevant investigations. Depending on the nature and the reactivity of the

examined material, greater respectively lower performances of the proposed binder concepts can be expected.

1.3 Contents and structure of the thesis

The present thesis consists of a cumulative dissertation based on four peer-reviewed publications, which are published (resp. submitted) in globally renowned top-ranking journals. The different topics and the elaborated contents of this dissertation are subdivided into nine chapters. A general overview of the structure of this thesis is shown in **Figure 1.1**. The first three chapters act as an introductory part of this writing. A brief introduction to the motivations, the objectives and the publication metrics of the four research papers are provided in **Chapter 1** and **Chapter 2**. The idea is to give a short insight into the backgrounds of this thesis as well as to provide an understanding on how the four publications are interlinked. In this way, it will be possible to establish direct connections between the investigated topics in all writings and to create a fluent transition between each research paper. Furthermore, the presentation of the structure of this document supports the comprehensibility of the contents by the readers and also allows understanding the author's line of thought during the preparation of this dissertation.

The first part of **Chapter 3** presents the literature review on a diversity of topics related to Ordinary Portland cement, cement alternatives, characterisation techniques, evaluation methods and criteria related to the present research topic. The second part of **Chapter 3** focuses on the introduction of the main raw material, the gravel wash mud (GWM), around which different investigations were carried out. A set of relevant details about its origin, the involved processing and treatment stages, and the available data on the quantitative and qualitative aspects of GWM are given.

Chapter 4 reproduces the original content of the first published research paper, entitled as "Assessment of the suitability of gravel wash mud as raw material for the synthesis of an alkali-activated binder".

Chapter 5 presents the original content of the second published research paper, entitled as "Gravel wash mud, a quarry waste material as supplementary cementitious material (SCM)".

Chapter 6 repeats the original content of the third published research paper, entitled as "Performance of lime-metakaolin pastes using gravel wash mud (GWM)".

Chapter 7 recreates the original content of the fourth research paper (submitted manuscript), entitled as "Properties of binary blended concrete using gravel wash mud (GWM) powders".

A summary of the core findings of this research project is highlighted in **Chapter 8** and **Chapter 9** gives an outlook on future research works.

Important note: *No changes or corrections of the contents of the four publications were undertaken. Only some figures were exchanged with figures of higher resolutions to maintain the quality of the present document without changing or replacing any information to the published versions.*

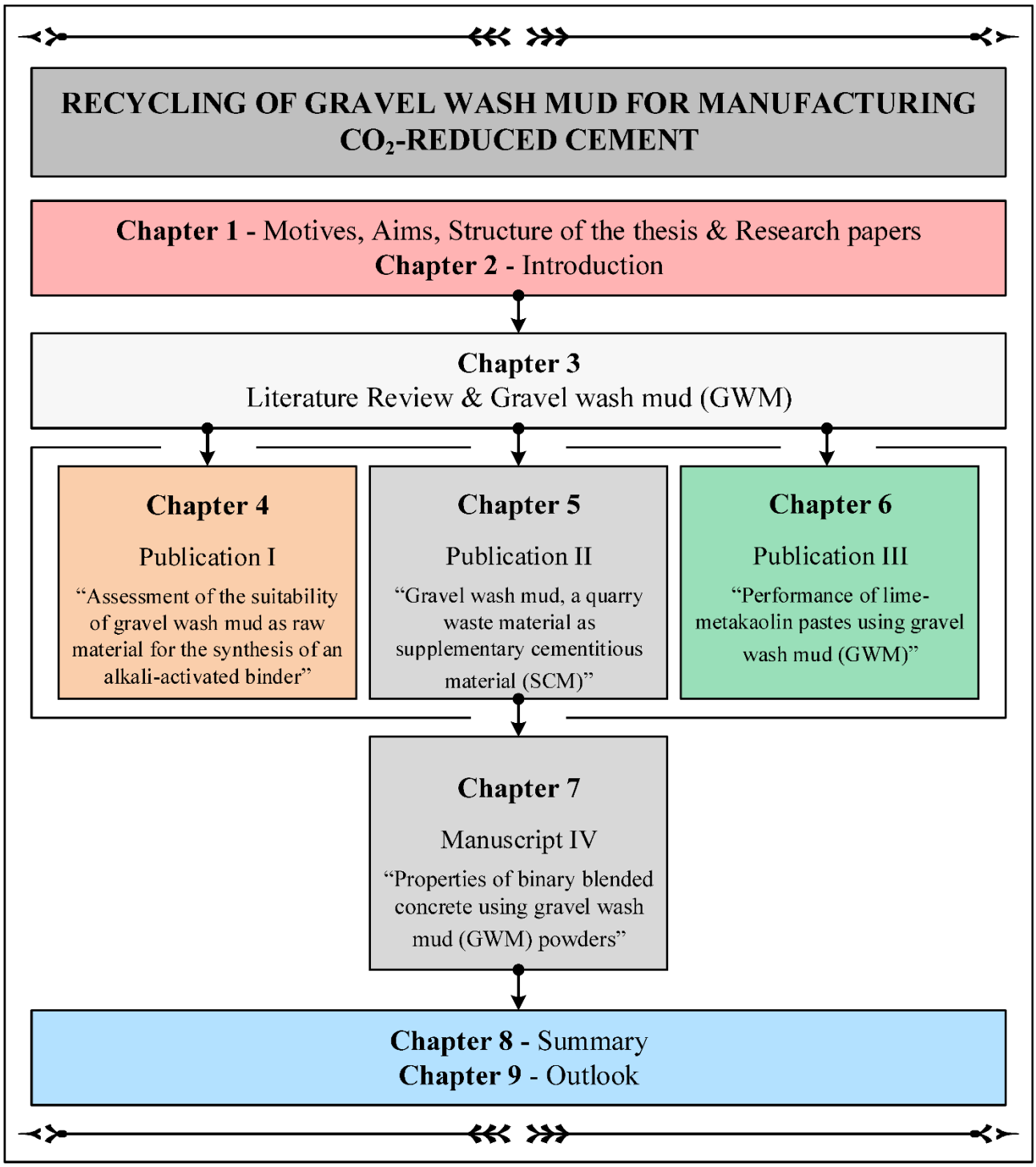

Figure 1.1 *- Structure of the thesis*

1.4 Presentation of the research papers and the links between each publication

This subchapter is dedicated to give a brief presentation of each research paper of this cumulative dissertation and to express the genuine links and the transitions between each document.

1.4.1 Published papers (peer-reviewed) and manuscripts

1.4.1.1 Publication I

Reference [1] - V.B. Thapa, D. Waldmann, J.-F. Wagner, A. Lecomte, Assessment of the suitability of gravel wash mud as raw material for the synthesis of an alkali-activated binder, Appl. Clay Sci. 161 (2018) 110–118. doi:10.1016/j.clay.2018.04.025.

Journal metrics and citations

- Status: Published in September 2018 in Applied Clay Science, Elsevier BV (Netherlands)
- Q1 rating in Geology (SJR Journal Ranking)
- Current impact factor (IF): 4.605 (2019)
- Citations (Nov. 2020): Cited 4 times (Web of Science) / 5 times (Google Scholar)

1.4.1.2 Publication II

Reference [2] - V.B. Thapa, D. Waldmann, C. Simon, Gravel wash mud, a quarry waste material as supplementary cementitious material (SCM), Cem. Concr. Res. 124 (2019) 105833. doi:10.1016/j.cemconres.2019.105833.

Journal metrics and citations

- Status: Published in October 2019 in Cement and Concrete Research, Elsevier Ltd. (United Kingdom)
- Q1 rating in Building and Construction (TOP 1; SJR Journal Ranking)
- Current impact factor (IF): 8.328 (2019)
- Citations (Nov. 2020): Cited 4 times (Web of Science) / 4 times (Google Scholar)

1.4.1.3 Publication III

Reference [3] - V.B. Thapa, D. Waldmann, Performance of lime-metakaolin pastes using gravel wash mud (GWM), Cem. Concr. Compos. 114 (2020) 103772. doi:10.1016/j.cemconcomp.2020.103772.

Journal metrics and citations:

- Status: Published in November 2020 in Cement and Concrete Composites, Elsevier Ltd. (United Kingdom)
- Q1 rating in Building and Construction (TOP 3; SJR Journal Ranking)
- Current impact factor (IF): 6.257 (2019)
- Citations (Nov. 2020): /

1.4.1.4 Manuscript IV

During the finalisation of this cumulative dissertation (November 2020), this research paper has been submitted for revision to the journal “Construction and Building Materials” after completion.

As the paper is considered as a submitted manuscript and not published yet, the document will be hereafter referred to as manuscript, respectively Manuscript IV.

Reference [4] - V.B. Thapa, D. Waldmann, Properties of binary blended concrete using gravel wash mud (GWM) powders. Unpublished Paper. Submitted on the 2nd of November 2020.

Journal metrics and citations:

- Status: Submitted for revision in Construction and Building Materials, Elsevier Ltd. (Netherlands)
- Q1 rating in Building and Construction (TOP 15; SJR Journal Ranking)
- Current impact factor (IF): 4.419 (2019)

1.4.2 Generalities and the coherence between each paper

1.4.2.1 General strategies for the reduction of the total carbon footprint of the cement industry

The implementation of the concepts of sustainability in the construction industry is essential for the reduction of environmental impacts generated by concrete, respectively, the cement industry. In general, the consumption of natural resources (depletion of unsustainable resources and growing material shortages worldwide), the generation of excessive industrial waste and the emission of harmful greenhouse gases are major factors for the growing negative image of the concrete-related industries. Nonetheless, the reliable quality, performance, and beneficial properties of concrete as the most used construction material and the related detrimental impacts to the environment are two sides of the same coin. In fact, according to current statistics, a decline in the production of concrete (resp. cement production) in the near future is not in sight due to rapidly growing populations worldwide (mainly in emerging industrial nations). Furthermore, its performance efficiency, as well as its cost-effectiveness compared to other construction materials, guarantees the continuous production and usage of concrete in the global construction industry until competitive alternatives are developed. It is important to differentiate that concrete as a standalone construction material is not as highly harmful (CO_2 emissions/tonne of concrete) as it is currently portrayed compared to other construction materials like steel, aluminium, insulations material, and more. It is the massive production volume of concrete required for shaping the modern cities and infrastructures worldwide, which outweighs any process-related assessment of the total CO_2 emissions compared to other production industries.

Over the last decades, the cement industry has significantly reduced its CO_2 emissions per tonne of produced cement by adopting various methods of energy efficiency like the usage of waste materials as fossil fuels, the optimisation of the clinkerisation process by conservation and recirculation of thermal energy for preheating the raw materials or the reduction of the clinker factor by incorporating portions of additives. However, the increasing political and societal awareness on reducing the immediate impacts of climate change have imposed massive pressure on the high CO_2-emitting industrial sectors like the cement industry. Therefore, in recent decades, the challenge and the race among the research and development (R&D) institutions to find viable and sustainable solutions has led to remarkable findings and process-related optimisations of the cement industry. In general, all the developed solutions and research progressions can be fitted within the following four main strategies, which were adopted to reduce the CO_2 emissions related to the cement industry (**Figure 1.2**).

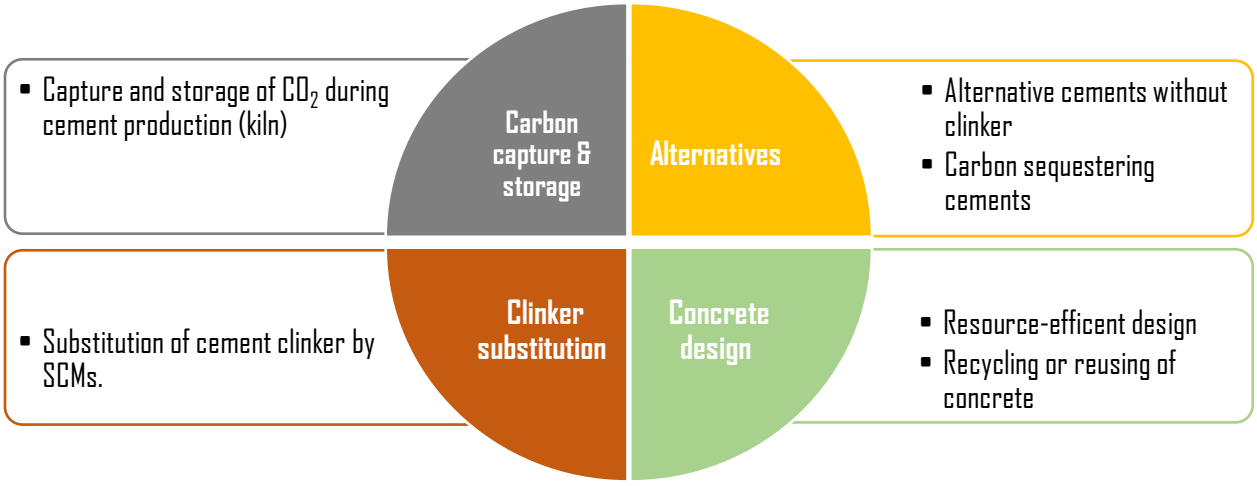

***Figure 1.2** - Strategies for the reduction of total CO_2 emissions of the cement industry*

In the following paragraphs, each global strategy for the reduction of CO_2 emissions generated from the cement industry is shortly explained:

I. **Carbon capture & storage:** This strategy aims to minimise the release of CO_2 into the atmosphere from the cement production plants. Different carbon capture and storage (CCS) technologies are applied to collect carbon dioxide from the combustion of fossil fuels in electricity generation plants and the CO_2 emissions from the clinkerisation processes. Each CCS method consists of three main stages: capture, transport and storage of carbon dioxide. There exist three main carbon capture methods, namely pre-combustion carbon capture, post-combustion carbon capture and oxy-fuel combustion carbon capture. Further details about the different carbon capture methods can be found in [5].

II. **Cement clinker substitution:** Clinker substitution figures among the most widely investigated and developed methods for the reduction of the CO_2 emissions related to cement manufacture. This strategy suggests that portions of the clinker content in cement can be substituted by a broad range of reactive materials (SCMs). The clinker replacement levels are already fully regulated in international standards for specific materials like calcareous and siliceous fly ashes, silica fumes, granulated blast furnace slags, limestone and natural pozzolans. As the cement production sites worldwide are dependent on the local availability and the regional acquirability of these materials, there exists a vital, continuous search for new potential alternative SCMs based on waste materials or unused industrial by-products to anticipate and ensure future cement demands.

III. **Alternative concepts:** This option promotes the idea of entirely dispensing the usage of Portland cement clinker as the principal binding agent by using other cementitious (cement-like) concepts like alkali-activated materials, geopolymer cements, lime-based pastes, and so on. These concepts are mainly developed using SCMs (established SCMs and alternatives from a broad range of industrial waste streams after undergoing physical

and thermal processes) and various activators or main reaction agents other than Portland cement clinker. An entirely novel and specific portion of the alternative concepts also focuses on carbon-sequestering cementitious products, where the main objective is to develop binder concepts which absorb and store CO_2 during its hardening process (carbonation hardening) and continuously proceed to absorb CO_2 over their effective usage time to become carbon neutral at long-term.

IV. **Concrete design:** The first part of this strategy consists of using quantitatively less concrete in the design of concrete structures by developing optimised structural systems. The general and self-explanatory idea behind this strategy is that if the same level of structural performance can be assured by design with less consumption of concrete, then less cement clinker needs to be produced (less CO_2 emission). It is vital to rethink the general consideration of concrete as an abundant and cheap construction material, and conceptualise structural elements like beams, columns, slabs, floors, walls and foundations as material-efficient structures by optimising their topology, shape and material composition. Additionally, there is currently a scientific debate whether the use of recycled aggregates from construction and demolition waste (CDW) in concrete mixtures is efficient, as there exist high variabilities in the quality of CDW depending on its structural and regional origin. Therefore, still no overall accepted quality characterisations, code of practice, regulations or standards could be developed regarding the reusability of CDW. Nonetheless, research on pure recycled concrete aggregates shows that to some substitution degree, the replacement of natural aggregates by high quality recycled concrete aggregates is feasible without loss in strength and durability performances [6,7].

1.4.2.2 Chronology and relationship between the research papers and the link to the global strategies

This PhD thesis project is entitled “Recycling of gravel wash mud for manufacturing CO_2-reduced cement”. As suggested by its title, the primary scope of this research work is to use the gravel wash mud (GWM), a waste product from sand/gravel quarrying, as a novel raw material to develop CO_2-reduced cement concepts. Therefore, in all the subsequent research papers, GWM in its various forms is used as the common raw material.

1.4.2.2.1 Publication I – Alkali-activated binder

The initial objective of this project was to use GWM as a raw material for the development of an alternative binder concept, namely an alkali-activated binder. The investigated concept complies with the **Strategy III** presented in **section 1.4.2.1**.

From preliminary tests, performed prior to the investigations carried out in Publication I, the requirement of thermal treatment was observed during the curing process of the specimens due to low to none reactivity of the initial GWM powders with the alkaline solution. In addition, several tests were conducted to assess the impact of varying calcination time and temperature on the mineralogy of the raw material. Further evaluations were carried out to assess the quantities of GWM and the concentrations of alkaline solutions (NaOH solutions) required to prepare a homogenous mixture with good workability. The optimal curing ages and conditions were simultaneously assessed to ensure a hardening of the mixes with achievable mechanical performances.

Within Publication I, the main idea behind the first concept of binders consisted of the alkaline activation of calcined GWM. Prior to the experimental investigation, the exact terminology of the

investigated binder concept was justified by debating on the differences between the reaction mechanisms of alkali-activated binders and geopolymers using extensive literature research.

In the experimental part, the chemical composition, the mineralogy and the particle size distribution of the calcined GWM powders (uncalcined, 550°C, 650°C, 750°C, 850°C and 950°C) were examined to assess the optimal material preparation parameters of the GWM powders, more specifically in combination with alkaline activation. Finally, extensive series of mixtures with varying parameters, including different calcination temperatures of the GWM powders and different concentrations of the alkaline solution as well as different mixture compositions were prepared. Subsequently, the resulting mechanical strengths of the investigated mixtures and the microstructure of alkali-activated GWM-based binders were analysed. These analyses and evaluations allowed verifying the potential of the synthesis of a GWM-based alkali-activated binder. It also gave essential knowledge whether the concept of alkali-activated binder is applicable or not to the specific raw material.

1.4.2.2.2 Transition from Publication I to Publication II and Publication III

The outcome of the first paper suggested the conclusion that the concept of alkali-activated binder does not apply to thermally treated GWM powders. The morphology of the different binders and the achieved compressive strengths were not satisfying to continue the research on the synthesis of alkali-activated binders based on gravel wash mud due to lack of performance of the resulting reaction products.

However, the chemical composition of the investigated powders confirmed that GWM is an aluminosilicate-rich raw material and its mineralogy includes moderate contents of clay minerals, namely illite and kaolinite, which become amorphous at higher calcination temperatures.

Therefore, further preliminary trials using different binder concepts were conducted on calcined GWM to find more appropriate and more substantial reaction products. The investigated concepts were in one hand, the direct substitution of cement proportions by calcined GWM in blended cements in compliance with **Strategy II** presented in **section 1.4.2.1** (Publication II) and the incorporation of calcined GWM in lime-metakaolin pastes (binders without OPC content) in compliance with **Strategy III** presented in **section 1.4.2.1** (Publication III).

1.4.2.2.3 Publication II – Blended cement pastes: GWM as a supplementary cementitious material

From Publication I, the results suggested the physicochemical and mineralogical adequacy of calcined GWM powders to exhibit some degree of pozzolanic activity. Therefore, prior to the investigations presented in Publication II, preliminary mixtures with blended cement paste mixes using GWM calcined at 650°C and 750°C with OPC substitution degrees at 0 wt.% (control mixture), 20 wt.%, 40 wt.% and 60 wt.% were prepared and examined using compression strength tests on prismatic samples (40x40x160 mm^3) at 28 days. From the results of these preliminary experiments, it was concluded that blended cement pastes containing 20 wt.% of GWM powders calcined at 750°C showed a positive impact on the mechanical performance of the hardened binary blended cement pastes.

From the preliminary test, strong indications about the pozzolanicity of calcined GWM powders were provided; therefore, the primary objective of Publication II was to prove the pozzolanic activity of calcined GWM and to find the optimal calcination temperatures for further confirmation of its usage as SCM in blended cement pastes. For the verification of latter hypotheses, various characterisation methods including particle size distribution (PSD), X-ray fluorescence (XRF), X-ray diffraction (XRD) were applied on the calcined GWM powders at 750°C, 850°C and 950°C

and the simultaneous thermal analysis (STA) was performed on uncalcined GWM powders to determine the optimal calcination temperature. Furthermore, large series of blended cement mixtures using GWM powders calcined at 750°C, 850°C and 950°C at OPC replacement percentages from 0 wt.% up to 30 wt.% and selected mortar mixes were prepared to determine the potential of calcined GWM powders as SCMs. The pozzolanic activity of the GWM powders was verified by applying strength-based evaluation methods, STA and SEM on hardened samples. Overall, reliable strength-enhancing capacities of calcined GWM were observed for a limited range of mixture proportions and calcination temperatures with best performances achieved by samples containing GWM powders calcined at 850 °C at an OPC replacement level of 20 wt.%.

1.4.2.2.4 Publication III – Cementless binder concept: Lime-MK-GWM pastes

One of the first objectives of this research project was to develop an alternative binder concept without OPC content using GWM powders as a raw material. Although the first study secured valuable findings regarding alkali-activated binders carried out in Publication I, the non-applicability of alkaline activation to the GWM powders due to its lower reactivity lead to the non-fulfilment of own initial targets. Therefore, the search for a more suitable binder concept compatible with the slower reaction kinetics of the GWM powders was initiated.

Most of the research works investigate the partial substitutability of Portland cement by alternative SCMs without loss in workability, performance and durability. However, the initiative for the present concept arises from the motivation to develop concrete products without any Portland cement by using other cementitious materials resp. SCMs. Therefore, prior to the investigations presented in Publication III, a series of preliminary feasibility tests were conducted on a large variety of mixtures proportions using metakaolin (MK), lime and pure GWM (the initial constituent) as main components to evaluate the degree of performance in terms of compressive

strength of the proposed ternary binder concept. This ternary binder concept is based on the same reaction fundamentals as between OPC and SCMs, namely the pozzolanic reaction. Similar strength-building pozzolanic reactions were expected to occur between the calcium hydroxide-rich limes and both pozzolans (MK and calcined GWM powder). The preliminary results showed very promising compressive strengths for the ternary GWM-lime-MK blends. However, further investigations regarding the optimal composition, the achievable performances, the study of the involved reaction mechanics and the microstructural compositions were required.

Within Publication III, the main objective was to confirm the suitability of the proposed ternary MK-lime-GWM pastes as an alternative to OPC-based products for constructive applications. Massive series of varying mixture proportions and mixture compositions were prepared using four different types and compositions of limes, GWM powders in three different treatment levels (pure, uncalcined and calcined at 850°C), MK and dolomitic sand as inert filler material. In a primary phase, the selection of the optimal composition of raw material was prioritised, followed by the assessment of the governing reaction mechanisms to confirm the achievable performances of the examined binder concept. Finally, the outcomes of the different investigations allowed reconfirming the moderate level of pozzolanicity of calcined GWM. Furthermore, the usage of hydrated lime was suggested for the ternary paste mixtures, and the incorporation of calcined GWM in the ternary lime-MK-GWM system revealed as very efficient in terms of mechanical performance compared to the binary lime-MK binder system used as the reference mixture.

1.4.2.2.5 Transition from Publication II to Manuscript IV

Considering the suggestions of the thesis supervisory committee (CET) members, the interest of the involved project partners (Cimalux S.A., Carrières Feidt S.A. and Contern S.A.), and by weighing the attractiveness of the different investigated binder concepts for the continuation of the

research work, the choice was made to proceed with further investigations on the usage of calcined GWM as SCM for OPC substitution.

1.4.2.2.6 Manuscript IV – Properties of concrete using GWM powders as SCM

Manuscript IV is considered as a continuation (complementary work) to the research work presented in Publication II, but it has its full validity as a standalone paper. In the outlook of the study carried out in Publication II, further research regarding the impact of incorporating calcined GWM as SCM on long-term behaviours and durability of the hardened pastes as well as on the properties of the fresh and hardened concrete mixtures was suggested.

These suggestions and further evaluations were taken into consideration and incorporated in the investigative program carried out within the study presented in Manuscript IV. The experimental program is subdivided into two major parts. The first part consists of a series of investigations applied on blended cement pastes incorporating uncalcined and calcined GWM at selected OPC replacement levels. The evaluation of the early reaction kinetics (evolution of early hydration heat flow), the assessment of the time-dependent hygric volume change (dry shrinkage) and the evolution of the mechanical performances at two different curing conditions (air- and water curing) for selected curing ages is carried out on the blended cement paste mixtures. The second part is dedicated to the investigations on the durability (depth of carbonation), the properties of fresh concrete, the mechanical properties (compressive strength and elastic modulus) and the microstructural composition of concrete mixtures using the blended cement paste proportions of the first part as the binder.

Important notes concerning Manuscript IV: During the submission of the final version of the cumulative dissertation, the manuscript was submitted for revision to the journal "Construction and Building Materials" after completion and should be considered as a submitted manuscript.

Chapter 2 Introduction

Concrete is known as the second most consumed substance in the world after water and ranks unquestionably as the most used construction material. Its most important constituent is Ordinary Portland Cement (OPC) with an average annual production volume of around 4.1 billion tonnes worldwide over the last years. Although Ordinary Portland Cement is cost-effective, easy to handle for concrete production and allows realising high mechanical strengths, its enormous production volumes implicate that up to 5-6 % of the global annual anthropogenic CO_2 emissions result from the cement industries. The high contributions to the carbon footprint of the cement industry are process-related to the cement clinker production, where the largest portion of CO_2 emissions is generated during the sintering of the clinker raw materials at temperatures above 1400ºC. Furthermore, the rising demand for concrete and cementitious products opposed to the growing challenges regarding the acquirability of traditional raw materials for cement clinker production has promoted the research on cement alternatives and new binder technologies.

In parallel, the current trend of recycling or revalorising of unused waste products or industrial by-products for their usage as potential raw materials has stimulated the research on their suitability in alternative binder concepts to reduce the clinker factor in cement compositions or the OPC contents in concrete products.

Within this context and based on existing valuable research works in this field, this thesis presents its investigations on the revalorisation potential and later on the performance of a local industrial waste product, namely gravel wash mud (GWM), as a competitive alternative supplementary cementitious material (SCM), compared to already established and commercially available cement additions.

This research work presents the findings from the assessment of the performance of the prime material GWM within the three different binder concepts and reaction mechanisms:

- Alkali-activated binder: The use of gravel wash mud (GWM) powders as a precursor material for the synthesis of an alkali-activated binder.
- Blended cement pastes and binary blended concrete: Cement paste mixtures and concrete formulations based on partial replacement of Portland cement by calcined GWM powders as SCMs.
- Lime-Metakaolin-GWM binder pastes: The development of “cementless” lime-based binder compositions incorporating calcined GWM powders and other constituents, classified as industrial by-products.

The following chapter introduces an extensive literature review on the current state-of-the-art and the most relevant findings of existing works related to each of the binder concepts mentioned above. In the subsequent chapters, the findings of the numerous investigations on each individual concept are presented by the corresponding published research papers of this research project, before ending this cumulative dissertation with a short recapitulation of the core findings and a personal outlook on future research works.

Chapter 3 Literature review and Gravel wash mud

This chapter presents a comprehensive overview of the state-of-the-art, the existing knowledge and the valuable contributions of previous research works on a multitude of fields and areas related to the investigated research topics. The main focus is dedicated to the presentation of the different thematic aspects and the elaboration of significant findings and recent developments discussed within the thesis.

It is a crucial prerequisite to identify the various backgrounds and contexts of a research field and to present an extensive and detailed literature review to carry out a trustworthy, fact-based and structured scientific research work. The topics discussed in this chapter build the fundamental knowledge and the frameworks, based on, which this research project has been carried out. These previous vital contributions provided the platform and set the qualitative benchmarks for the successful completion of the investigations conducted within this work.

This detailed review consists of four subchapters, which are thematically interrelated. The structure of the literature review follows a logical pyramidal sequence by starting from a broad topic like Ordinary Portland cement, its production and its characteristics to the reasons for the necessity of alternative solutions, followed by more specified topics, namely the existing solutions, the alternative concepts, the recent developments, and the current discrepancies and circumstances.

Finally, the last subchapter introduces the local primary raw material (GWM) of this research work by presenting its geographical and geological description, the different processing steps, and the process of activation of the raw materials by thermal treatment as well as the estimative indications on the available quantities and the consistency of quality of the raw materials.

This extensive literature review prior to the actual research work does not only allow starting the investigations based on in-depth knowledge on the different topics but also provides the basis for the identification of potential research gaps to elaborate more precisely the scientific research question of the present research work. It supports the formulation of the research hypotheses and also significantly contributes to their argumentations and demonstrations.

The examination of previous works and literature immensely assisted the investigations carried out in this work at three levels:

- First, the examined literary works allowed diminishing the risk of heading off-topic and the risk of putting unnecessary efforts in irrelevant directions and topics. The proof-based contributions and the references allowed gathering further in-depth readings and the determination and inclusion of most of the crucial and relevant aspects of the research field.
- Second, the benefit of working based on the results of extant research literature allowed developing theoretical and experimental confidence during the investigative procedures. Furthermore, this practice permitted to maintain the general overview and continuous verification of the findings at each stage of the investigations. This retrospective method allowed not losing the target on the main research topic.
- Finally, the analysis of previous works contributed to the deeper understanding and the knowledge of the research field and allowed to develop a more critical view on the applied techniques and methods, leading to the reported findings. This critical evaluation also

provided the basis for verification of existing methods and their confirmation or not, in case of the used raw material, GWM. For example, some disagreements related to the topics of alkali-activated binders and geopolymers were found during the literature analysis. The observed discrepancies were critically discussed in **section 3.2.1.2**.

The primary bibliographic sources for the presented literature review were majorly collected through online journal databases, like Science Direct, Springer, Taylor and Francis, Scopus, Statista, Web of Science, Wiley Online Library, etc. Overall, about 650 articles and documentations were thoroughly consulted to collect and isolate the significant contents related to the examined topics. Most references were relevant published research papers from a broad spectrum of internationally renowned journals and online databases, followed by suggested recommendations and citations from these research works. Additionally, scientific and educational books, various review studies, international standards and regulations, individual online documentation from reliable sources were broadly covered to complete the literature review.

3.1 Ordinary Portland cement (OPC)

3.1.1 Cement

3.1.1.1 From raw materials to Portland cement

The history of cement can be followed back to the Roman Empire, and its development over time has undoubtedly made out of cement today's most widely used construction raw material [8]. In contrast to reality, one would expect that the requirements for raw materials for cement production are very limited and strict. However, the origin and the chemical composition of the natural raw products can differ significantly. The choice of the mix of raw ingredients rather depends on the required proportions of compounds formed from oxides of calcium, silicon, aluminium, and iron. **Table 3.1** shows the sources of raw materials used in Portland cement production.

Calcium	Iron	Silica	Alumina	Sulphate
Alkali waste	Blast-furnace dust	Calcium silicate	Aluminium-ore refuse	Anhydrite
Aragonite	Clay	Cement rock	Bauxite	Calcium sulphate
Calcite	Iron ore	Clay	Cement rock	Gypsum
Cement kiln dust	Mill scale	Fly ash	Clay	
Cement rock	Ore washing	Fuller's earth	Copper slag	
Chalk	Pyrite cinders	Limestone	Fly ash	
Clay	Shale	Loess	Fuller's earth	
Fuller's earth		Marl	Granodiorite	
Limestone		Ore washing	Limestone	
Marble		Quartzite	Loess	
Marl		Rice-hull ash	Ore washings	
Shale		Sand	Shale	
Slag		Sandstone	Slag	
		Shale	Staurolite	
		Slag		
		Traprock		

***Table 3.1** - Raw materials used for Portland cement production (adapted Table 3-1 from [9])*

The specific processes in cement production plants might differ from one plant to another. However, the fundamental characteristics and production chains of each cement manufacturing

plant are similar. The general processes of cement production are presented/explained using **Figure 3.1**.

As listed in **Table 3.1**, most of the ingredients are materials occurring in nature or by-products from industrial productions. Depending on the origin and nature of the raw materials, the pre-treatment of the ingredients can differ. Nevertheless, most of the raw materials originate from quarries, as huge quantitative availability of the base materials is crucial for the production of cement clinker. The excavation of materials is generally realised in two phases: quarrying and processing. During extraction or quarrying, in a first phase, superfluous layers or large pieces of stone are removed to get access to the more valuable identified geologic deposits. The layers of earth, vegetation, rocks and poor-quality stones of the raw material, which are unsuitable for other production processes, are called “overburden”, and are removed with heavy equipment and transferred to onsite storage to be used as cover material for rehabilitation and renaturation purposes after the end of the quarry’s operating life. For this kind of fills, overburden materials and construction and demolition, (C&D) wastes are used to cover and replace the removed strata.

There exist diverse quarrying methods depending on the variations of the physical properties (such as density, fracture properties and stratifications), the profitability and finally the site owner’s preferences.

Nevertheless, regardless of the used quarrying technique by the quarries, the general processes for each raw material consist of the following steps:

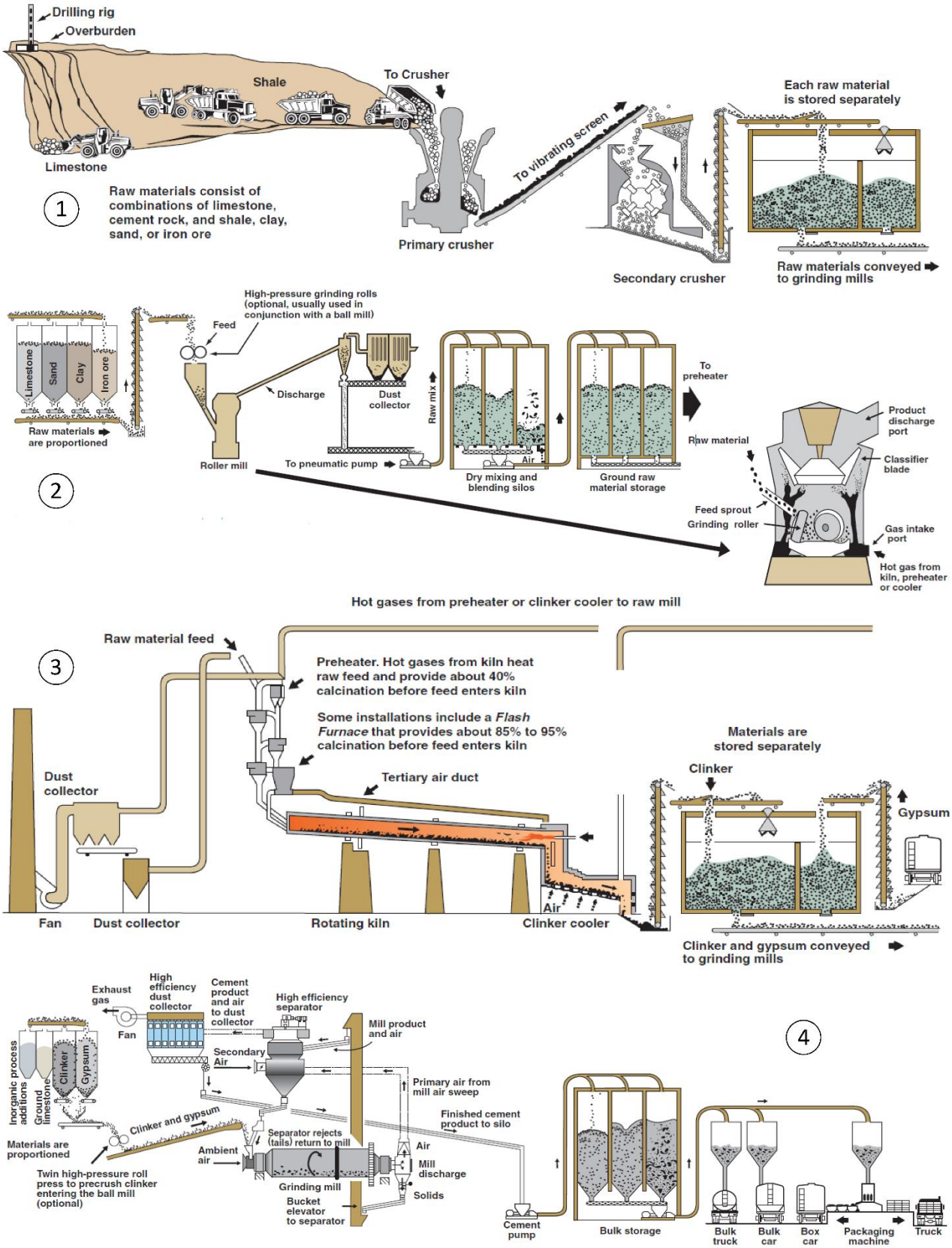

Figure 3.1 *- Cement production: From raw materials to Portland Cement (Figure 3-3 from [9])*

In first phase as shown in **Figure 3.1-1**, minimal fractures are located or drilled in the stone to simplify material extraction and using different techniques [10], and the stones are removed using heavy machinery. After, the material is loaded on a vehicle for transport to a stationary or mobile crushing unit, where the larger stone blocks are primarily coarsely crushed into a manageable size and screened into a secondary crusher for further processing. In this unit, the coarser material is crushed into a smaller particle size depending on the requirement for the next production process and stocked in a temporary storage unit.

In the next production step, as illustrated in **Figure 3.1-2**, the different primary materials are stored separately before each material is released in a predefined proportion on a conveyor belt and carried to high-pressure grinding rolls, which serves as a feeding unit for a vertical roller mill. The vertical roller mill combines the functions of crushing, grinding, drying and classifying units in one equipment [9]. The drying heat in the roller mill comes from heat recovery from the powder preheater or the clinker cooler. Before the discharged raw mix from the roller mill is pneumatically pumped to the mixing and blending silos [11], it passes through a recipient linked to a recipient linked with a dust collector. The dust collection captures the dust occurring during each production step of the cement and allows to control the air quality inside the manufacturing plant and to minimise the exhaustion of dust into the atmosphere. From the blending silos, the finely ground and mixed raw powder is pumped in a storage before entering the clinker burning process. At the same time, a storage of gypsum is set up to prevent early reaction of the cement clinker.

The subsequent step of cement production is the pyro-processing of the fine raw mix into the final powder called cement clinker. Before entering a high-temperature rotary kiln, the blended mixture of raw ingredients often undergoes a few preheating and pre-calcining processes. The raw powder is fed from the storage unit into a multi-stage preheating system (**Figure 3.1-3)**, where it meets hot

gases rising from the actual rotary kiln. Preheating of the raw mix before calcination allows saving overall energy consumption during the burning process as the heat loss from the rotary kiln is revalorised as a heat input. These preheating units function as dehydration and calcination zones. At up to ~ 450°C, in the dehydration zone, free water is evaporated, and moisture in the raw mix is removed. At the preheating unit up to ~ 900°C, the powder undergoes a calcination process. During calcination, the bound water is driven out of the clays, and the calcium carbonate is decomposed. At this stage, the raw mix is still available in powder form, as the melting point of materials is not reached [12,13]. After passing the preheating stages, the powder is fed downwards to the rotary kiln, where the temperature increases over its length from ~ 900°C up to ~ 1500°C. The kiln is built of cool-rolled steel shell tubes, and its length and diameter can vary according to the size of the cement production plant. The cylindrical vessel is slightly sloped and slowly rotates about its axis, which allows to control the passing of the raw mix and to stir the material during the burning process. The temperature range above ~ 900°C up to ~ 1300°C is defined as the solid-state reaction zone, where the first cement minerals, also known as clinker minerals, begin to form.

Calcium oxide and reactive silica react to form dicalcium silicate (C_2S) crystals. Additionally, intermediate calcium aluminates and calcium ferrites are formed. They function as a fluxing agent to accelerate the clinker formation by decreasing the melting temperature and by increasing the amount of liquid phase during the clinkerisation process. Above ~ 1300°C up to ~ 1500°C, the actual clinkerisation phase starts by melting of the intermediate crystals, which leads to the clumping of the powder mix into an agglomeration of fine particles enclosed by a thin layer of liquid formed by reacting dicalcium silicates. The clinker mineral tricalcium silicate (C_3S) is formed by the reaction of C_2S crystals and calcium oxide (CaO). During this reaction, the C_3S crystals increase in amount and size, whereas the C_2S crystals increase in size. This reaction

prevails until the quantity of reactive silica in the reacting calcium silicates (C_2S and C_3S) and the quantity of free lime (CaO) are reduced to a minimum. [12,13]

Due to the temperature drop at the end of the rotary kiln (the cooling zone), the tricalcium aluminate (C_3A) and tetracalcium aluminoferrite (C_4AF) crystallise in the liquid phase, and the C_2S crystals acquire a lamellar structure. The clinker nodules remain unchanged during cooling and harden, and the resulting product is called cement clinker nodules. Nonetheless, the rate of cooling is essential for the production of more reactive cement as C_3S crystals can disintegrate to their initial components.

The output of the rotary kiln is pulverised into a fine material using a grinding mill, and small quantities of gypsum are added (**Figure 3.1-4)**. The addition of gypsum allows regulating the setting time of the cement, improving shrinkage and strength development properties [14]. The final cement powder is pumped in bulk storage until it is collected by bulk trucks or sent to the bagging machine unit for final packaging before the sale.

3.1.1.2 Cement hydration

3.1.1.2.1 Clinker minerals

When the cement clinker exits the rotary kiln, it consists mostly of four main mineral crystalline compounds, the so-called clinker minerals, presented in **Table 3.2**.

Clinker phases	Oxide spelling	**Abbreviated form**	Colour of the pure phase	Proportion in clinker in %
Alite (Tricalcium silicate)	$3\ CaO \cdot SiO_2$	**C_3S**	White	45...80
Belite (Dicalcium silicate)	$2\ CaO \cdot SiO_2$	**C_2S**	White	0.2…32
Aluminate phase (Tricalcium aluminate)	$3\ CaO \cdot Al_2O_3$	**C_3A**	White	7…15
Ferrite phase (Tetracalcium aluminoferrite)	$4\ CaO(Al_2O_3,Fe_2O_3)$	**C_4AF**	Dark brown or greyish-green (MgO content)	4…14

***Table 3.2** - Portland cement clinker (modified and adapted Table 9.4 from [15])*

Other constituents are residuals in small quantities from the clinkerisation process like calcium sulphate, alkali sulphates, unreacted calcium oxide, magnesium oxide, salt phases and other intermediate chemical species.

Therefore, individual clinker constituents are not only recognised for their different chemical composition, but they also differ in terms of hardening time rate, resistance to sulphate and regarding the released hydration heat during hardening.

ALITE - C_3S

Alite represents one of the main minerals in cement clinker. It primarily consists of tricalcium silicate, which can be considered as the most important carrier during the hydraulic hardening. Furthermore, pure C_3S is highly reactive (unstable) and therefore, agglomerates other oxides like MgO, Al_2O_3 and Fe_2O_3 in its grid and can be considered as tricalcium silicate doped with other ions. Pure C_3S stabilises at temperatures above 1250°C. During slow cooling below 1250°C, a disintegration leads to the formation of C_2S and CaO; therefore, rapid cooling of the clinker down to 150°C must be provided.

BELITE – C_2S

Belite is an essential component of cement clinker. Dicalcium silicate can be divided into three polymorphs: an α-C_2S structure at high temperature, a β-C_2S structure at an intermediate temperature and a γ-C_2S structure at low temperature. Although the γ-C_2S crystal is stable, it does not show any hydraulic activity in the presence of water, and therefore the occurrence of this form is avoided in Portland cement. However, by rapid cooling, the metastable, reactive β-polymorphic form of dicalcium silicate β-C_2S can be quickly stabilised by binding other oxides like Al_2O_3, Fe_2O_3, K_2O and Na_2O in its composition matrix. The other metallic oxides are prone to build together with C_2S solid solutions of different concentrations. Therefore, the crystalline structure of C_2S contains higher levels of impurities than C_3S. Nevertheless, compared to C_3S crystals, β-C_2S crystals have a less irregular structure leading to a lower reactivity than that of C_3S. [12,13]

TRICALCIUM ALUMINATE – C_3A

The main constituents of the aluminate phases in clinker are the tricalcium aluminates. Pure C_3A melts at 1542°C and consists mainly of cubic or orthorhombic crystal structures [12]. The

relatively close Ca-O distance creates a certain tension in the crystal. This tension and the large cavities in the composition matrix explain the rapid reaction of the C_3A with water. The aluminate phase also binds other ions in the C_3A-matrix like Fe_2O_3, MgO, SiO_2, Na_2O and K_2O. The C_3A content directly influences the essential properties of the clinker like the strength of the cement and the water demand in the clinker. With increasing C_3A content, the early strength and water demand are increased, but the final strength is reduced. [15]

TETRACALCIUM ALUMINOFERRITE – C_4AF

The ferrite phase mainly consists of a stable compound with any composition between dicalcium aluminate and dicalcium ferrite resulting in a tetracalcium aluminoferrite. The aluminium content in the cement clinker minerals is higher than the iron content, and C_4AF considerably binds other ions like SiO_2 and MgO. Like most of the ferrous (Fe^{3+}) compounds, pure C_4AF has a brown colour. Due to the binding of MgO in the C_4AF matrix, the Portland cement receives its characteristic grey to greyish green colour. The ferrite phase is less reactive than the aluminate phase in the clinker, and it becomes more inert, the higher the Fe_2O_3 content.

3.1.1.2.2 Cement Hydration Process – Hydration of the clinker phases

In general, the addition of water to the cement leads to the formation of the so-called liquid cement paste. It has a plastic, thixotropic consistency, binds the aggregates and fills the cavities between the grains. After, different processes and reactions lead to the stiffening, solidification and hardening of the cement paste into the so-called cement stone. During these processes, the previously introduced clinker phases react into hydrated compounds, the so-called hydrate phases. The entire process of cement hardening is referred to as cement hydration. The term “hydration”

becomes self-explanatory as, during the mixture of cement with water, all the processes occur in an environment in excess of H_2O.

The metastable clinker phases are only involved in a chemical reaction when they are brought into contact with water. The hydration process can be considered as a two-stage system: dissolution and precipitation. This two-stage system in cement hydration was first mentioned in the early 20th century by the French chemist Herny Louis Le Chatelier [16].

Due to the dissolution of clinker in water, the particles attain better mobility leading to improved rearrangements, which result in more stable hydrate phases. The related gain of stability is a thermodynamic prerequisite for the rearrangements and the hydrate formation. During the dissolution of cement minerals, ions are released into the water, also known as pore solution. Due to their high intrinsic solubility, the cement minerals C_3S and C_3A dissolve quickly and increase the concentrations of ions in the pore solution. Once the pore solution is (over)saturated, the ions tend to interconnect into a new solid phase, which is more favourable in energetic terms instead of remaining dissolved [12,13].

This step initiates the precipitation process of cement hydration. As the newly formed solid phases differ from the initial cement minerals, they are called hydration products. This precipitation allows reducing the ionic concentration (oversaturation) of the pore solution leading to further dissolution of the cement minerals. This replacement process of cement minerals by hydrate products is a continuous reaction where the pore solution functions as the transitional medium between the two solid phases. Beside the dissolution of the cement minerals, the water also functions as a provider of ions, mainly hydroxyl groups.

Moreover, it is well known that all chemical or thermal processes tend to shift towards thermodynamic equilibrium. Thus, the solid phases precipitating in the pore solution are the most

stable phases at the given conditions. As the cement minerals are stabilised at high temperatures, at low temperatures, they remain unstable and highly soluble. Therefore, after dissolution in water, the minerals tend to form new solid phases. During the formation of the more stable solid phases with lower free energy, there is the release of the exothermic heat defined as the heat of hydration.

The formation of gel, as well as the formation of crystals, are the most decisive processes during cement hardening. The complexity of the different thermochemical processes derives from the interdependency of the clinker phases during the reaction process. The hydration of the four clinker phases occurs with different intensities defining the various characteristics of the cement. **Figure 3.2** illustrates the compressive strength of each clinker mineral over time and **Table 3.3** summarises the characteristics of the clinker minerals regarding the reaction speed during hardening, their contribution to the strength and the scale of the heat of hydration. [17]

As illustrated in **Figure 3.2** and indicated in **Table 3.3**, the hydration of alite (C_3S) is characterised by its early and fast reaction with high release of hydration heat contributing to high early and high ultimate strength to the cement matrix. In contrast, belite (C_2S) solidifies slowly and continuously with low hydration heat leading to low early strength but provides a more considerable contribution to the high ultimate compressive strength. The aluminate phase (C_3A) is the most reactive mineral of all clinker phases. It stands out by its rapid solidification with the high release of hydration heat. However, its contribution to strength development is relatively low. The ferrite phase (C_4AF) is of low importance for the actual hydraulic solidification as it reacts slowly with moderate hydration heat and contributes very little to the early respectively ultimate strength of the cement matrix. However, it contributes positively to the corrosion and sulphate resistance of the hardened cement. [13,17]

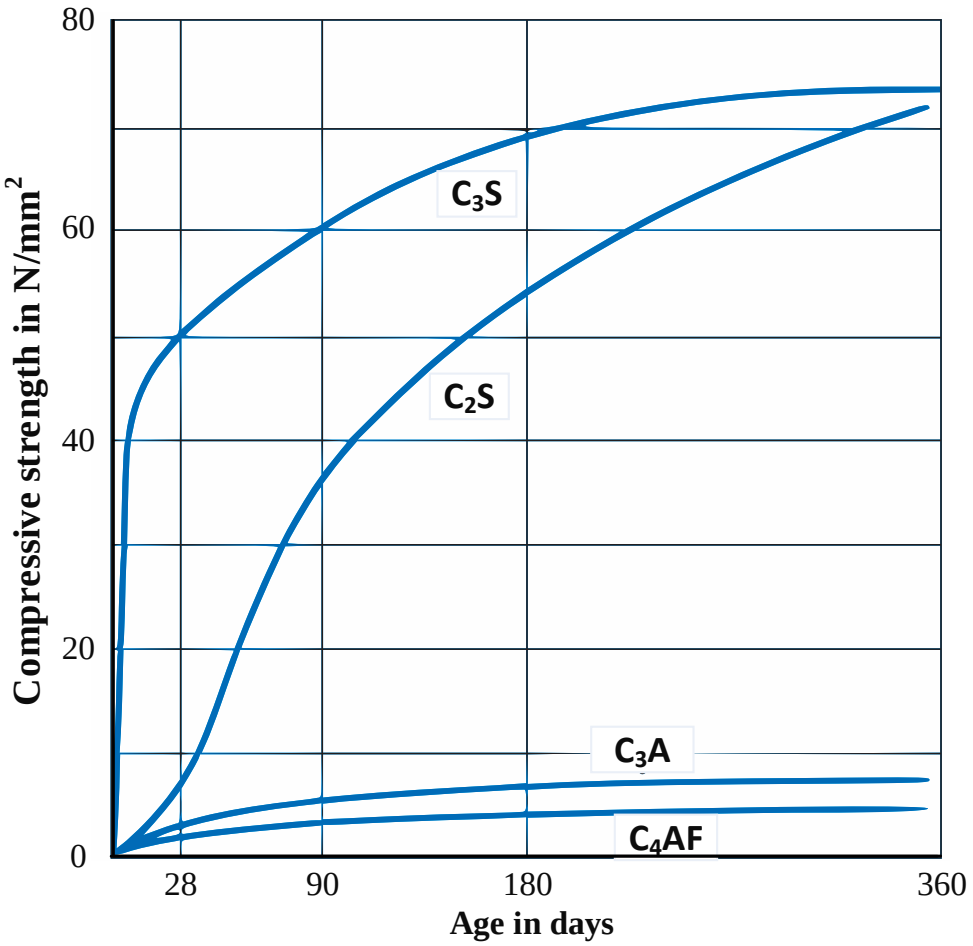

Figure 3.2 *- Cement production: From raw materials to Portland cement (Figure I.4.1-1 from [17])*

Clinker phases	Reaction speed	Heat of hydration	Contribution to strength
Alite, C_3S (Tricalcium silicate)	fast	high	High early and high ultimate strength
Belite, C_2S (Dicalcium silicate)	slow and continuous	low	Low early and high ultimate strength
Aluminate phase, C_3A (Tricalcium aluminate)	early and fast	very high	Low early and low ultimate strength
Ferrite phase, C_4AF (Tetracalcium aluminoferrite)	slow and continuous	moderate	Low early and low ultimate strength

Table 3.3 *- Cement clinker: Composition and hydration characteristics (Table 9.4 from [15])*

3.1.1.2.3 Hydration of the silicates with the formation of the calcium silicate hydrates

The cement hydration process can be considered as the result of numerous exothermic processes and can be divided into several phases: the initial phase, the dormant phase, the acceleration phase, the retardation phase and the final phase. Different reactions describe each of these phases; therefore, the released hydration heat, the speed of reactions and the exact composition of the hydrates considerably vary from one cement clinker mineral to another. **(Figure 3.3a)**

Calcium silicate hydrates are built quickly and are responsible for the solidification of cement. These hydrates are formed by reaction with water of the siliceous clinker phases, mainly alite (C_3S) and belite (C_2S). The hydration of these minerals is of high importance as strength-building phases and play an essential role in the strength development of the cement stone. These hydrates of different stoichiometry primarily contain burnt lime (CaO), quartz (SiO_2) and water (H_2O) and their composition depend in particular on the water-cement ratio (w/c ratio). Therefore, the hydration products can vary within a wide range, but in general, calcium silicate hydrates can be described by the following formula:

$$m\mathbf{CaO \bullet SiO_2 \bullet}\ n\mathbf{H_2O} \qquad \text{(Eq. 1, [17])}$$

where: m represents the molar ratio between CaO/SiO_2

n represents the number of H_2O molecules bound by the calcium silicate

Alite (C_3S) is the most available and most important Portland cement clinker mineral as it contributes to most of the early strength development. Its hydration reaction can be simplified, as shown in **Eq. 2**.

$$2\ (\mathbf{3\ CaO\ \bullet SiO_2}) + 6\ \mathbf{H_2O} \rightarrow \underbrace{\mathbf{3\ CaO\ \bullet 2\ SiO_2 \bullet 3\ H_2O}}_{\boldsymbol{C-S-H\ phase}} + 3\ \underbrace{\mathbf{Ca(OH)_2}}_{Portlandite} \qquad \text{(Eq. 2, [17])}$$

After addition of water (H2O), the hydrolysis of C3S begins with a quick release of calcium (Ca2+) and hydroxide (OH-) ions with a large amount of hydration heat release. After saturation of the

system, the calcium hydroxide starts to crystallise, and calcium silicate hydrates begin to form continuously, which intensifies the hydration reaction again. Once the hydration products become thicker (crystallisation), the water is obstructed from reaching the unreacted C3S leading to a decrease of the formation of the calcium silicate hydrates which reduces the speed of the reaction and the release of heat (**Figure 3.3b**).

Belite (C_2S) hydrates slower than alite. After the release of the reacting ions due to its lower solubility in water, the amount of portlandite formed is less. However, the actual hydration reaction runs similarly as for alite (**Eq.3)**.

$$2\ (\mathbf{2\ CaO\ \bullet SiO_2}) + 5\ \mathbf{H_2O} \rightarrow \underbrace{\mathbf{3\ CaO\ \bullet 2\ SiO_2 \bullet 4\ H_2O}}_{\boldsymbol{C-S-H\ phase}} + 3\ \underbrace{\mathbf{Ca(OH)_2}}_{Portlandite} \qquad \text{(Eq. 3, [17])}$$

After the hydration of both clinker minerals, there is the formation of portlandite, which mainly consists of calcium hydroxide crystals. Due to the smaller size of the portlandite crystal compared to other hydrates and its very high solubility in water, it contributes very low to the strength and the impermeability of the cement paste. Calcium hydroxide is mostly unaffected during the reduction of water in the pore system and can be beneficial in limiting the amount of shrinkage. It can function as a restraining element when the calcium silicate hydrates start to shrink [17].

3.1.1.2.4 Hydration of the aluminate and aluminate ferrite

The formation of aluminate and aluminate ferrite hydrates is a more complicated process than the formation of calcium silicate hydrates. C_3A does not contain sulphate ions and is highly soluble in water leading to a faster formation of the aluminate hydrates [12]. Gypsum is added to the clinker during the grinding process to delay the reaction of C_3A with water by the formation of calcium sulfoaluminate hydrates ($3CaO•Al_2O_3•3CaSO_4•32H_2O$), also known as ettringite around C_3A particles. This formation provides additional time to the hydration of C_3S by refraining the faster reaction of C_3A and thereby permits the occurring of natural setting.

The nature of the formed aluminate hydrates is dependent on the available amount of sulphate agents. In the absence of sulphate (**Eq. 4a** and **Eq. 4b**), thin hexagonal tetracalcium aluminate hydrates are formed. In the presence of sulphate, calcium sulfoaluminate hydrates are preferably formed. At high sulphate concentration, the hydration reaction results in the formation of ettringite (**Eq. 4c**), whereas at low-sulphate and calcium-rich conditions, the monosulfoaluminate hydrates are built (**Eq. 4d**). [12,13,17]

$$2\ (\mathbf{3\ CaO\ \bullet Al_2O_3}) + 21\ \mathbf{H_2O} \rightarrow \underbrace{\mathbf{4\ CaO \bullet Al_2O_3 \bullet 19\ H_2O}}_{C_4AH_{19}} + \mathbf{2\ CaO \bullet Al_2O_3 \bullet 8\ H_2O} \quad \text{(Eq. 4a)}$$

$$\mathbf{4\ CaO \bullet Al_2O_3 \bullet 19\ H_2O} + \mathbf{2\ CaO \bullet Al_2O_3 \bullet 8\ H_2O} \rightarrow 2\ \underbrace{(\mathbf{3\ CaO \bullet Al_2O_3 \bullet 6\ H_2O})}_{C_3AH_6} + 9\ \mathbf{H_20} \quad \text{(Eq. 4b)}$$

$$\mathbf{3\ CaO\ \bullet Al_2O_3} + \mathbf{3}\ \underbrace{(\mathbf{CaSO_4 \bullet 2\ H_2O})}_{gypsum} + 26\ \mathbf{H_2O} \rightarrow \underbrace{\mathbf{3\ CaO \bullet Al_2O_3 \bullet 3\ CaSO_4 \bullet 32\ H_2O}}_{ettringite} \quad \text{(Eq. 4c)}$$

$$2\ (\mathbf{3\ CaO\ \bullet Al_2O_3}) + \mathbf{3\ CaO \bullet Al_2O_3 \bullet 3\ CaSO_4 \bullet 32\ H_2O} + \mathbf{4\ H_2O} \rightarrow$$

$$3\ \underbrace{(\mathbf{3\ CaO \bullet Al_2O_3 \bullet CaSO_4 \bullet 12\ H_2O})}_{monosulfoaluminate} \quad \text{(Eq. 4d)}$$

The hydration reaction of the ferrite minerals takes place in a similar way. Compared to the hydration products of C_3A, some portion of the aluminates is substituted by the ferrite minerals. Therefore, the reaction products of the hydration process depend on the composition of the aluminoferrite minerals and reaction conditions of the cement paste (Eq. 5a and Eq. 5b).

$$\mathbf{4\ CaO \bullet (Al_2O_3, Fe_2O_3)} + 3\ \underbrace{(\mathbf{CaSO_4 \bullet 2\ H_2O})}_{gypsum} + 21\ \mathbf{H_2O} \rightarrow$$

$$\underbrace{\mathbf{3\ CaO \bullet (Al_2O_3, Fe_2O_3) \bullet 3\ CaSO_4 \bullet 32\ H_2O}}_{aluminoferrite\ trisulphate\ hydrate\ (AFt)} + \mathbf{(Al_2O_3, Fe_2O_3) \bullet 3\ H_2O} \quad \text{(Eq. 5a)}$$

$$\mathbf{4\ CaO\ (Al_2O_3, Fe_2O_3)} + \mathbf{3\ CaO \bullet (Al_2O_3, Fe_2O_3) \bullet 3\ CaSO_4 \bullet 32\ H_2O} + 7\ \mathbf{H_2O} \rightarrow$$

$$3\ \underbrace{(\mathbf{3\ CaO \bullet (Al_2O_3, Fe_2O_3) \bullet CaSO_4 \bullet 12\ H_2O})}_{aluminoferrite\ monosulphate\ hydrate\ (AFm)} + \mathbf{(Al_2O_3, Fe_2O_3) \bullet 3\ H_2O} \quad \text{(Eq. 5a)}$$

The different hydration reactions of the clinker minerals take place at several levels and different degrees of intensity (heat of hydration) with a wide variety of final hydration products.

Consequently, the cement hydration is a complex system with numerous, partly interdependent reactions. Over time due to the different hydration products forming during the different stages of the hydration process of the cement paste, the cement particles are more rigidly interconnected. This process leads to the solidification of the cement paste into cement stone. [12,13,17]

Overall, Concrete can be considered as a solid artificial stone, which is formed by a hydraulic hardening process of a mixture of cement, aggregates and water. As long as the concrete is still workable, it is called fresh concrete. After the solidification of the cement matrix, it is called “hardened” concrete. Responsible for the strength of the cement stone are the shape and size, spatial arrangement as well as the packing density of the formed hydrate phases.

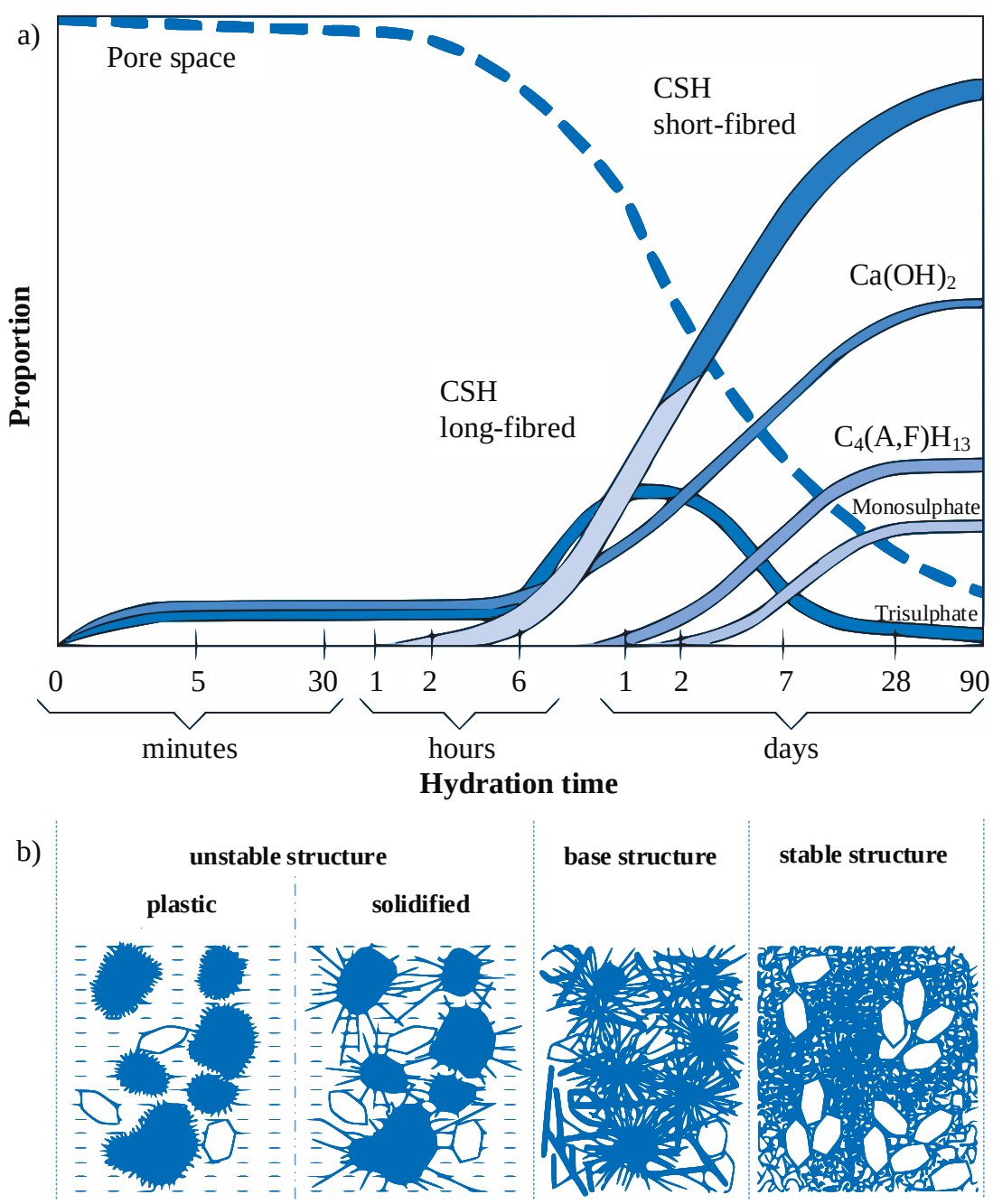

Figure 3.3 *- Schematic representation of the formation of hydrate phases and the development of the cement matrix during the hydration of cement (Figure I.4.1-5 from [17])*

3.1.2 Deterioration of OPC binders

Structures, which were built using OPC-based concrete a few decades ago, currently show deterioration problems, as these structures tend to disintegrate due to various reasons and highlight the limitations of OPC structures. The main reasons for concrete deterioration are exposure to chlorides, carbonation, freeze-thaw deterioration, chemical attacks from acids, salts, alkalis or sulphates, aggregate reactivity, abrasion of the surfaces, thermal influence and overload damage [18].

Jacobsen et al. [19] studied the influence of chloride migration due to freeze-thaw exposure on the compressive strength of OPC concrete. The results showed a deterioration of the binders in the form of compressive strength reduction of 45 to 68 %. Furthermore, the speed of chloride migration was increased from 2.5 to 8 times in contrast to unexposed conditions and the penetration time was reduced from more than 2.5 days down to few minutes leading to severe cracking of the specimens.

The corrosion of the steel reinforcement is associated to the carbonation of concrete, which occurs due to the dissolution of CO_2 in the pore solution and its reaction with the calcium from the cement hydrates leads to the formation of calcium carbonate. Over time, this process penetrates through the concrete and drops the pH level of concrete from around 12.5 towards 7 at the affected areas. Carbonation slightly increases the strength of the concrete due to the reduction of porosity and permeability. Nevertheless, in the case of reinforced concrete, the lower pH level leads to corrosion of the steel reinforcement due to reduction of the passivating environment provided by the alkaline conditions of concrete. Cabrera [20] carried out experimental tests on the deterioration of

reinforced concrete due to the corrosion of the steel reinforcement. His results indicated that a 9% corrosion damage leads to 1.5 times higher deflection compared to a non-corroded beam.

The sulphate attack on concrete is associated with the formation of ettringite due to the reaction of calcium hydroxide and the hydrated aluminate phases with the sulphate ions. This mode of deterioration occurs due to the reduced granular cohesion by the formation of gypsum and ettringite, leading to the expansion and cracking of the concrete. Piasta [21] carried out an experimental study on the performance of concrete exposed to carbonisation and sulphate attack on two concrete elements, a 23-year-old concrete slab from a 3-storey car park and a 50-year-old concrete column from a roofless gypsum storage hall. The analysis confirmed the presence of calcium carbonate in the hardened cement paste originating from carbonation for both concrete specimens. However, due to the contact with gypsum in the wet air, the concrete column underwent a simultaneous sulphate and carbonate attack. The exposure to carbon dioxide and humidity conducted ettringite to instability and carbonation, leading to ultimate failure.

In general, these apparent deteriorating issues are related to the intrinsic properties of concrete. Its permeability, porosity and the presence of unreacted calcium hydroxide form an exposed target for aggressive components to penetrate the concrete, leading to its disintegration. The unfavourable environmental impact of cement production and the intrinsic properties of concrete confirm the necessity to promote the development of novel, eco-friendly, more resistant and durable alternatives to conventional concrete formulations and traditional cementitious products.

3.2 Cement alternatives

Cement provides excellent binding properties and allows preparing high performing construction elements. However, cement production is related to high-energy consumption and high emissions of CO_2 and other greenhouse gases. Moreover, concrete has its unfavourable intrinsic properties, mostly related to the characteristics of cement. Furthermore, in recent years, the demand for infrastructures has strongly risen and is still growing, and therefore, the quantity of cement requirements is also increasing. Therefore, if no sustainable solution is found, the emissions of greenhouse gases related to cement industries cannot be reduced to prevent an intensification of the global warming effects.

Over the last decades, research was carried out to develop binder concepts and technologies, which do not contain cement clinker. Concepts with auspicious characteristics to be investigated are alkali-activated binders and geopolymer cements. The main idea was to use industrial by-products or industrial waste as prime material in combination with an alkaline solution to form a binder, which performs similar to OPC.

Simultaneously, since the middle of the last century, research on alternative cementitious materials has been extensively carried out, and many very promising alternatives have been developed. There are alternative materials or technologies, which allow supplementing or substituting cement clinker without loss of performance as a construction material. Regarding supplementary materials, there are some potential raw materials, which show cementitious qualities and their use allows enhancing physical and chemical properties of the final concrete. Moreover, these materials reduce the production costs by decreasing the amount of clinker produced with consequently associated savings in raw materials, energy consumption and greenhouse gas emissions. These

materials are called cementitious admixtures or supplementary cementitious materials (SCMs) and mainly include fly ash, silica fume, ground granulated blast furnace slag, natural or artificial pozzolans and many others. These raw materials are either incorporated to the cement clinker during the grinding stage, by blending with cement after grinding or during the concrete mixture. Their use at adequate proportions make concrete mixtures more economical, increase durability, reduce permeability, increase strength and influence other properties of the fresh or hardened concrete.

The fundamental principles and the reaction mechanisms of these concepts as well as the different categories of the broad selection of potential raw materials are explained in detail in the following subchapters.

3.2.1 Alkali-activated materials

As cement alternatives are attracting increasing interest, alkali-activated binders and geopolymer technology have shown great potential to be developed as OPC replacement and have been extensively investigated over the last decades. The following sections regarding the topic of alkali-activated binders and geopolymers are partly reproduced, adapted and complemented based on an article, entitled “A short review on alkali-activated binders and geopolymer” published in a book [22], written by the author of this dissertation.

Before discussing details about the potential and the reaction mechanisms of these binder concepts, it is necessary to point out that there is a terminology issue concerning certain technologies. Even if the geopolymer technology and the concepts of alkali-activated materials are researched since the last mid-century, there is no overall accepted consensus about the terminology of these materials. The most common descriptions, which are found in literature, are “alkali-activated materials”, “inorganic polymers” and “geopolymer”. There are also many other terminologies which are formed by combinations of these terms and do not give any logical meaning from the chemical reaction point of view. It is complicated to give a complete overview as some experts use the notions and denominations based on the OPC hydration chemistry.

In contrast, others demand an adapted terminology due to the differences in the chemical processes, structures and properties of the final products. Furthermore, this demand for proper terminology is justified by some authors, who claim that the expressions “alkaline cement” or “alkali-activated cement” are irritating and are not accurate because OPC hardens in alkaline conditions and, thus, it can be considered as an alkali-activated calcium silicate [23]. The generally accepted classification of alkali-activated materials is illustrated in **Figure 3.4**. However, still today, there

is a disagreement in the research community, whether “geopolymer” can be considered as a subset of “alkali-activated binders”. For greater insight into these issues, it is essential to understand the historical background and the mechanisms of the different systems to have a more transparent overview [24,25].

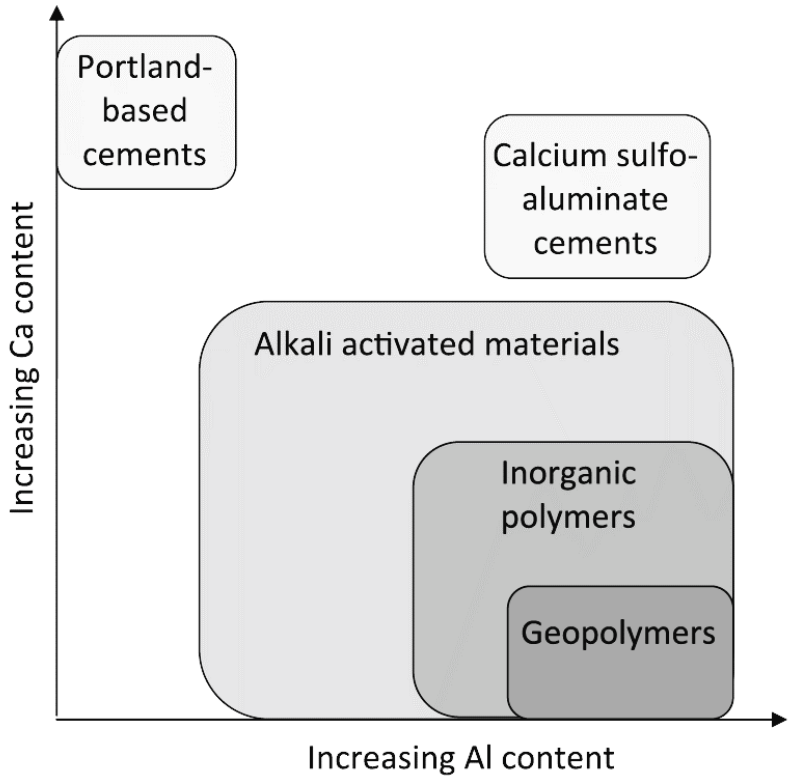

Figure 3.4 *- Classification of different subsets of alkali-activated binders with comparisons to OPC and calcium sulfoaluminate cements [26]*

Already before the 1940s, references to alkali-activated materials [27,28] existed, however, Glukhovsky [29] was the first researcher who extensively studied the presence of analcime phases in the binders applied in ancient constructions and later developed himself binders made from aluminosilicates in reaction with alkaline industrial wastes, which he named “soil silicate concrete” and “soil cements”. The early investigations on alkali-activated binders mainly focused on the activation of blast furnace slag, a by-product of the metallurgical industry. After, the next wave of interest raised after the results of Davidovits [23,30], who developed and patented a novel binder

[31,32] which he named “geopolymer cement”. The first geopolymer binder was a slag-based geopolymer cement, which consisted of metakaolin, blast furnace slag and alkali silicate. The benefit of this technology compared to OPC technology is that it hardened faster while reaching the maximal strength at early hours and provided a durable and compact microstructure. Subsequent studies have been carried out based on these original structures, and different authors have done substantial research on the understanding of the chemical mechanism and the development of alkaline binders [33–50].

Today, after several decades of development and the occasional application of alkali-activated materials, the interest has once again increased due to the high potential of reducing the carbon dioxide footprint of constructions by replacing OPC by alkali-activated binders or geopolymer cements. In addition, the known contribution of high carbon emissions to climate change and its severe consequences for the environment and humans have initiated the research for alternative solutions in almost every industrial sector. In the case of “low-carbon binders”, these high levels of CO_2 emissions savings are not yet wholly approved and indeed are not necessarily provided by the material’s intrinsic properties. These benefits are more gained due to appropriate design and the choice of the right chemical mechanism for each application. Moreover, in the past decades, there has been some progress in the conflict of the definition of alkali-activated materials and geopolymer. A clear division has been made between alkali-activated materials based on calcium-rich raw materials and alkali-activated materials based on low-calcium raw materials. Popular high-calcium precursors are blast furnace slags and other calcium-rich industrial by-products. Low-calcium or calcium-free (“geopolymer”) precursors are mainly fly ash or clay-based raw materials which allow developing durable and robust binder systems. However, the reaction mechanism of alkali-activated compounds is still not completely understood because the

solidification and the setting mechanisms are very dependent on the raw materials and the used alkaline solution. In the following sections, the mechanism of alkali-activated binders and geopolymers are discussed using different research works, followed by recent works dealing with the application of these concepts to other industrial by-products and waste products.

3.2.1.1 Reaction mechanism of alkali-activated binders

Most of the works on alkali-activated binders have been carried out for the activation of granulated blast furnace slags by an alkaline solution. Blast furnace slag is a calcium-rich by-product of the metallurgical industry and can achieve high compression strengths after activation with an alkali solution. Shi et al. [51] succeeded in reaching compression strengths of about 160 MPa after 90 days of curing at ambient temperature by alkali-activation of blast furnace slag with sodium silicate. Before, Glukhovsky et al. [33] already did valuable work on "alkali-activated slag cement" and defined the following reaction mechanism of alkaline activation. The reaction mechanism of alkali-activated binders is a synthesis process occurring in a solution and is very much dependent on the raw material and the alkaline solution. It involves the dissolution of the aluminosilicate material in the alkaline medium, transportation of the dissolved species, followed by a condensation process into a polymeric network of aluminosilicates species and finally re-solidification. During the exothermic process of dissolution phase, due to the increased alkalinity (pH rises) in the system, the aluminosilicate solids are disintegrated into unstable, reactive units consisting of covalently bond Si-O-Si and Al-O-Si species. After, new phases are formed by penetration of the Al atoms into the Si-O-Si compounds leading to the formation of a coagulated structure, the aluminosilicate gels (colloid phase) [24]. Then, there is the generation of a condensed structure and crystallization.

In general, two types of reaction mechanisms of alkali-activated binders can be established [34]. The first system involves the activation of calcium-rich raw materials like blast furnace slags, with a high content of Si, Al and Ca atoms. The activation is realised using moderate alkaline solutions leading to calcium silicate hydrates (CSH)-like phases as reaction products. The second mechanism involves the alkali activation of low-calcium, respectively, calcium-free prime materials using medium- to high alkaline solutions, leading to a polymeric network with the formation of amorphous zeolite-like phases and high mechanical strength.

Provis [52] presented an approximated schematic representation (**Figure 3.5**) of the phases formed within alkali-activated binders depending on the Si/Al ratio to the content of calcium and magnesium. It is difficult to determine the exact phases formed because of the high chemical complexity of the system related to the content of the reaction components, the alkaline activation, the liquid/solid ratio and the curing conditions. High content of calcium-rich aluminosilicates leads to the formation of calcium aluminosilicate hydrate (C-A-S-H) gels. The use of precursors with a high content of magnesium will lead to the assemblage of hydrotalcite phases, instead of zeolites, which would be the case for low calcium and magnesium contents. The alkali-activation of low calcium aluminosilicates leads to the formation of so-called sodium aluminosilicate hydrate (N-A-S-H) gels. Furthermore, in high pH conditions, the presence of aqueous aluminate and aqueous calcium modifies N-A-S-H gels leading to the partial substitution of sodium with calcium to form “C-(N)-A-S-H gels”.

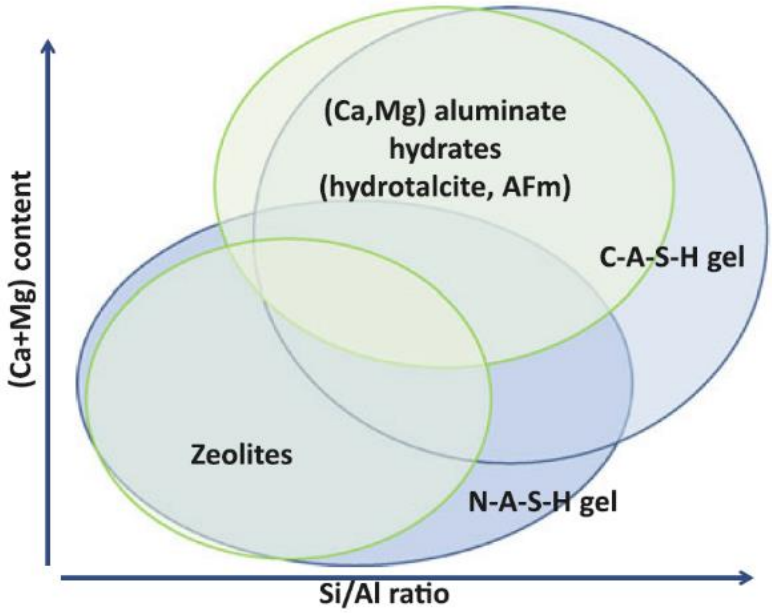

Figure 3.5 *- Schematic representation of phase formation within alkali-activated binders; green: ordered products; blue: disordered products [52]*

In the case of calcium-rich raw materials, blast furnace slag is the more reactive raw material used for alkali-activation. It, therefore, can be processed using a broader range of activators like hydroxides, silicates, alkali carbonates or sulphate solutions. However, usually higher concentrations of alkaline solutions are used as these promote faster setting and better strength development at ambient curing temperatures. The binder formed by alkaline activation form aluminium-rich secondary phases like hydrotalcites and zeolites, and C-A-S-H phases depending on the aluminium and magnesium content of the raw material [43–50]. Song et al. [35] reported similar reaction products after alkali activation of blast furnace slag. He observed the formation of C-S-H gels with traces of hydrotalcite phases by X-ray diffraction. Puertas et al. [36] investigated the reaction of blast furnace slag with activation by sodium hydroxide solutions and observed the presence of C-S-H gel phases, hydrotalcite and calcite by XRD analysis.

The low-calcium alkali-activated material technology can be divided in low-calcium alkali-activated binders based on fly ash as a precursor and calcium-free alkali-activated binders formed

by alkali activation of clay-based raw materials, mainly metakaolin. These precursors are most commonly activated with hydroxide or silicate solutions. Even if there are confusions on the terminology and the notions of alkali-activated binders, there is no doubt that the first development of low-calcium alkali-activated binders was conducted by Joseph Davidovits [23]. The initial purpose was to develop fire-resistant inorganic polymeric binders using clay-based raw materials.

In the case of "low-calcium" raw materials, fly ash or metakaolin are the more reactive raw materials used for alkali-activation and commonly is processed using strong alkaline activators like hydroxides and silicates. The final reaction products are strongly dependent on the prime materials. Xie and Xi [37] studied the reaction products of fly ashes alkali-activated with mixed solutions of sodium hydroxides and sodium silicates, and noticed the presence of crystals, mainly unreacted sodium silicate phases. Furthermore, the XRD analysis led to the detection of only small reaction products. Other authors [38,39] reported the formation of hydroxysodalite and herschelite as final hydration products.

Phair and Deventer [40] reported that at pH of 12, the dissolution of metakaolin in the form of Si and Al species is very high. The aluminium of metakaolin disintegrates ten times higher, and the silica dissolves two times higher than its uncalcined raw material (kaolin). Yunsheng et al. [41] investigated on three key parameters (SiO_2/Al_2O_3, M_2O/Al_2O_3 and H_2O/M_2O) composition design method based on chemical characteristics analysis of calcined kaolin-based geopolymer cement. The results showed that the ratios Na_2O/Al_2O_3 and H_2O/Na_2O had a significant effect on compressive strength. The highest compressive strength achieved was 34.9 MPa, and the analysis of the IR spectra indicated that cement with the highest strength was the most fully reacted one and possessed the most considerable amount of geopolymers. According to Rowles et al. [42], in the production of the inorganic polymer, the amounts of OH^- and Na^+ are coupled, as the ions of

the NaOH are their only source in the activating solution. In samples with low sodium content, there would be both insufficient OH^- to dissolve Si^{4+} and Al^{3+} from the metakaolinite completely, and insufficient Na^+ to allow complete polymerisation of the network. This content leads to unreacted metakaolinite, which results in a lower strength material. In samples with high sodium content, an excess of OH^- allows a complete dissolution of Si^{4+} and Al^{3+} from the metakaolinite. However, excess sodium would weaken the structure.

3.2.1.2 Geopolymer vs Alkali-activated material

The term "geopolymer" was mentioned for the first time by the chemist Joseph Davidovits in 1975 to classify all forms of inorganic polymeric material synthesized by chemical reaction of alumina silicates and an alkaline activating solution. Initially, the term defines silicon-based polymers, which use raw materials from mainly rock-forming minerals of geological origin. However, in the last decades, the term "geopolymer" has been "misused" to describe all sorts of alkali-activated materials based on low-calcium precursors, which does not suit to the initial definition of geopolymer. Therefore, Davidovits [23,53] reminds the scientific community and points out in his speeches and writings that it is a scientific mistake to use alkaline activated materials and geopolymer as synonyms because, according to him, not all alkali-activated materials are not polymers considering their chemistry and therefore cannot be considered as geopolymers. Furthermore, his main issue is that the scientific community applies the concept of geopolymer cement as being a derivative of the calcium silicate hydrates from OPC hydration leading to the wrong formulation like NASH and KASH depending on the alkaline solution. According to Davidovits, during geopolymerisation, there is never the formation of a hydrate nor a gel, but the formation of a polymer by polycondensation of reactive ortho-sialate units.

According to [53], “geopolymer cements” are binder systems which solidify at ambient temperature and if heat treatment is required for hardening, then the geopolymer compound is called “geopolymer binder”. Geopolymer cements can be considered as a valid alternative to Ordinary Portland cement for different applications from fast hardening to durable compounds for infrastructure and construction. Furthermore, geopolymer cement requires mild alkaline soluble silicates or hydroxides. Therefore, the alkaline reagents can be classified as “user-friendly”, as opposed to strong alkaline solutions required for alkali-activated binders.

The characteristics of clay-based alkali-activated geopolymer binders have been extensively investigated over the last decades. Regarding kaolinite-based raw materials, the production of geopolymer cement comprises two main procedures: calcination and geopolymerisation. The calcination process consists of the thermal treatment of the raw material, which leads to dehydroxylation of clay mineral into a high-energy and nearly amorphous meta-state. One of the main reason to use clay-based geopolymer binders as cement alternative is the fact that the dehydroxylation process occurs at lower temperatures than the burning of cement clinkers. After the addition of the alkaline solution to the meta-clay, the geopolymerisation is initiated and is based on three complementary processes, namely, the depolymerisation of the minerals into monomers by condensation of the alkaline component, the formation of oligomers and the polycondensation into a geopolymer ribbon by the combination of the oligomers into a covalently bonded network. The synthesized geopolymers show interesting characteristics like good mechanical properties, high strength and good durability [54].

3.2.1.3 Concept of geopolymerisation

The concept of a geopolymer structure is explained in the example of an alkaline reaction of metakaolin. Generally, the complete mechanism of geopolymerisation can be divided into 3 stages, which consist of seven phases/steps (**Figure 3.6**).

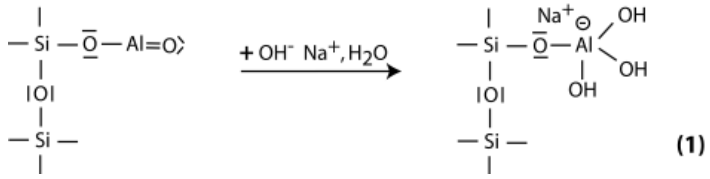

Alkalinisation

Formation of a tetravalent aluminium group

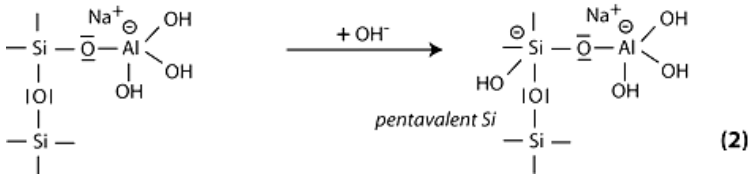

Reaction of the hydroxide with the silicon and formation of pentavalent silicon with a negatively charged Si atom

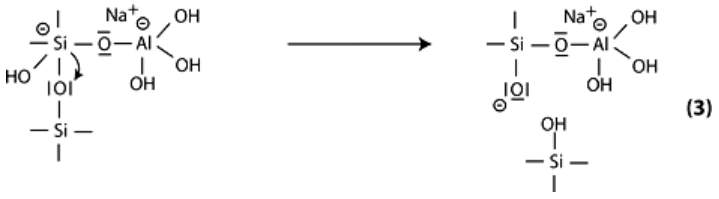

Cleavage of a silanol group

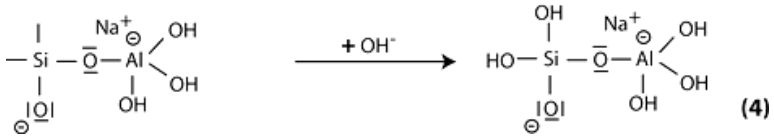

Formation of an ortho-sialate molecule

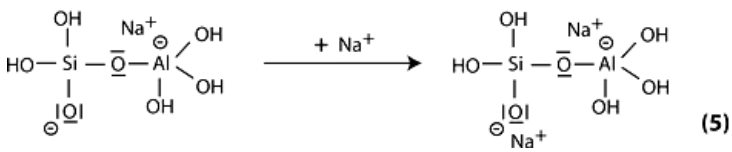

Bond of the cation with the basic ortho-sialate

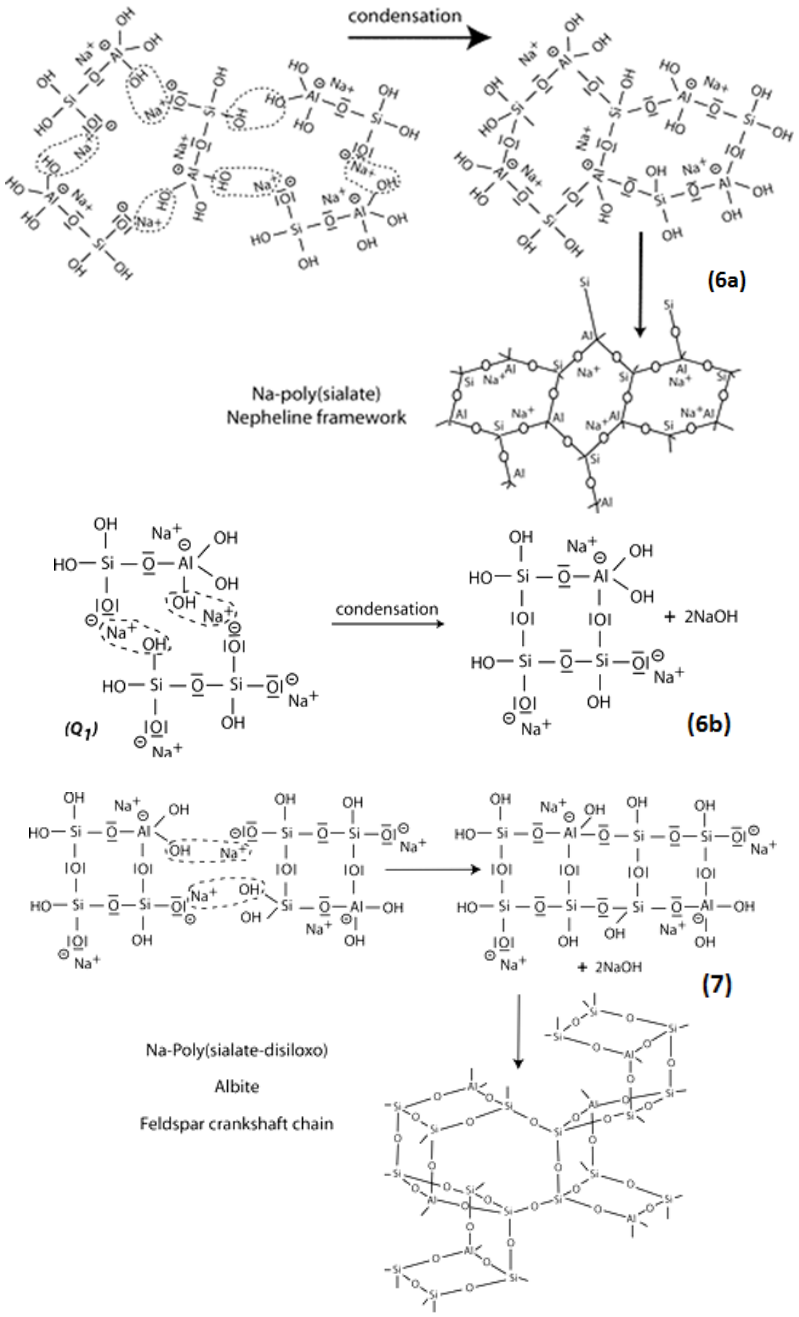

Condensation and polycondensation

Polymerization of the subunits into the larger ribbons

Final geopolymer

Figure 3.6 *- Explanation of the mechanism of geopolymerisation [54]*

At the first stage of geopolymerisation, depolymerisation is initiated, which starts with alkalisation of the clay layers. The alkaline solution (OH^-, Na^+ and H_2O) reacts with the aluminosilicates, leading to the formation of a tetravalent aluminium Al in the sialate group (1). Then, the hydroxide anion OH^- attaches to the silicon atom Si. This attachment promotes the central silicon atom Si to

the penta-covalent state with a negative charging (2). In the next step, as the pentavalent silicon atom Si is in an unstable state, the silicon of the siloxane group transfers an electron to the oxygen atom. This transfer leads to the cleavage of the siloxane group Si-O-Si, leading to the formation of silanol group Si-OH on the one hand and a basic siloxo Si-O- on the other hand (3). In the presence of hydroxide anions OH^-, further silanol groups Si-OH are formed, and an ortho-sialate molecule is isolated, which represents the primary unit in the geopolymerisation mechanism (4). In the final step of the first stage, the sodium cation Na^+ reacts with the basic siloxo Si-O- group to form a -Si-O-Na terminal bond. This molecule represents the reactive unit of the geopolymerisation process (5).

In the second stage, the polymerisation of the reactive subunits is launched by the condensation between the ortho-sialate molecules, reactive groups Si-O-Na and aluminium hydroxyl. These reactions lead to the formation of a cyclo-tri-sialate structure and the production of alkaline sodium hydroxide NaOH, which reacts again to ensure the final stage, the polycondensation into a complex Na-polysialate framework (6a). However, in the presence of waterglass, the condensation between the di-siloxonate, ortho-sialate molecules, reactive groups Si-O-Na, Si-OH and aluminium hydroxyl OH-Al- leads to the formation of an ortho-disiloxo cyclic structure and the production of sodium hydroxide, which react again to ensure polycondensation into a framework (6b). Finally, further polycondensation promotes the formation of a Na-polysialate-disiloxo albite framework (7).

The geopolymerisation of aluminosilicates leads into the formation of larger amorphous units that build the final structure of the Na-poly sialate (or –disiloxo) framework. This mechanism is the same for both the sodium Na and potassium K based geopolymer structures. [54]

3.2.1.4 Alkali-activated binders from waste products

Most of the previous investigations used pure metakaolin or slag-based premium materials with a high content of reactive SiO_2 and Al_2O_3 as raw materials for cement substitution. However, the application of inorganic polymers as construction materials is unfavourable due to the high price of commercially available raw materials. For example, the price of metakaolin has risen during the last years due to its high demand. Therefore, in the recent year, there is a trend to investigate alternative prime materials to be revalorised for development of alkali-activated binders. In recent literature, other raw materials than metakaolin, mainly waste products from different industrial origins, are increasingly studied to being processed to synthesise an alkali-activated binder or geopolymer binder, and promising results have been found, but also indicate that further research is needed [55–57].

Table 3.4 lists a selection of compressive strengths of different binders from literature. It can be considered that in terms of mechanical performance, alkali-activated binders based on industrial by-products or waste material already fulfil or even outperform the standard strength requirements for conventional OPC-based products. Therefore, it is essential to continue the research work on alkali-activated binders to understand their behaviour entirely in structural systems and harmful environments to confirm it as a valid alternative to OPC.

Type of binder	Specifications / based on	Strength [MPa]
OPC according to EN 197-1 [58]	CEMI 32.5	$32.5 \leq x \leq 52.5$
	CEMI 42.5	$42.5 \leq x \leq 62.5$
	CEMI 52.5	≥ 52.5
Alkali-activated binder based on traditional SCMs	Ground granulated blast-furnace slag [59]	40.0
	Fly ash [60]	59.0
	Metakaolin [60]	38.5
Alkali-activated binder based on industrial waste products	Waste ceramics [61]	71.1
	Calcined reservoir sludge [55]	56.2
	Tungsten mine waste mud [56]	60-75
	Waste treatment sludge & Rice husk ash [57]	16.0

***Table 3.4** - Comparison of compressive strength of different binders*

The revalorisation of waste products has become a subject of intense study for the development of novel alkali-activated binders or geopolymer cements. Some of the results seem to be very promising; however, the exact reaction processes and reaction products are not yet entirely understood. Furthermore, these results are mostly valid for specific raw materials, available at regional level under given specific conditions and therefore the interest for research on these materials is mainly of local or regional interest. [22]

Therefore, in this research project, investigations on the suitability of a waste product (gravel wash mud) as raw material for the synthesis of a novel geopolymer binder were carried out and presented as early indications, and examples from the literature suggest its potential of performance without addition of further strengthening components.

3.2.2 Cementitious admixtures, pozzolans and pozzolanic activity

The current necessity and demand for sustainable concepts in cement and concrete industries have driven the interest for innovative measures and sustainable concrete products, mainly by driving the trend of mixing cementitious minerals or reactive pozzolanic material with cement for economic and environmental benefits.

3.2.2.1 Nomenclature

Before explaining the details about the different types of materials and reaction processes, some essential terminologies are explained and discussed using the terminological clarification of ASTM C125 [62] as reference:

- **Admixture** - a material other than water, aggregates, cementitious material, and fiber reinforcement that is used as an ingredient of a cementitious mixture to modify its freshly mixed, setting, or hardened properties and that is added to the batch before or during its mixing. [62]
- **Mineral admixture** - deprecated term (old). [62]

  DISCUSSION - this term has been used to refer to different types of water insoluble, finely divided materials such as pozzolanic materials, cementitious materials, and aggregate. These materials are not similar, and it is not useful to group them under a single term. The name of the specific material should be used, for example, use "pozzolan," "slag cement," or "finely divided aggregate," as is appropriate.

- **Supplementary cementitious material (SCM)** – an inorganic material that contributes to the properties of a cementitious mixture through hydraulic or pozzolanic activity, or both. [62]
- **Cementitious material** - an inorganic material or a mixture of inorganic materials that sets and develops strength by chemical reaction with water by formation of hydrates and is capable of doing so under water. [62]
- **Pozzolan** - "a siliceous or siliceous and aluminous material that in itself possesses little or no cementitious value but will, in finely divided form and, in the presence of water, chemically react with calcium hydroxide at ordinary temperatures to form compounds possessing cementitious properties. [62]

In the past, pozzolans, cementitious materials and aggregates were classified under the terminology of "mineral admixtures". However, as these materials do not share the same properties, neither similar compositions, the term, "mineral admixture", is classified as outdated. A more recent and widespread terminology for pozzolans and cementitious materials is "Supplementary cementitious materials (SCM)", which due to its broader definition encloses these materials as any inorganic material that contributes to the properties of a cementitious mixture through hydraulic or pozzolanic activity or both.

Since the middle of the last century, research on alternative materials has been extensively carried out to diminish or entirely cease the use of Ordinary Portland cement. Several raw materials and different technologies were studied to supplement or substitute cement clinker without loss of performance as a construction material or even improving specific physical and/or chemical properties of the resulting concrete products.

In the following sections, cementitious admixtures will be shortly presented, followed by an extensive discussion about the pozzolans and the pozzolanic reaction.

3.2.2.2 Cementitious admixture

According to [62], cementitious materials describe any material, which fulfils following definition: "*An inorganic material or a mixture of inorganic materials that sets and develops strength by chemical reaction with water by formation of hydrates and is capable of doing so under water*."

In general, these materials comprise Ordinary Portland cement and other cementitious materials, which, in the presence of water, form, hydrate products, whether by hydration or chemical reaction with other concrete components. The cementitious potential of OPC and other similar hydraulic binders, which by definition figure among cementitious materials, is widely known/discussed. Furthermore, these constituents are the main binding agents of the whole concept of concrete products and therefore, will not be discussed in the following sections. In the case of cementitious materials/admixtures, a classification into two categories can be made:

- **Pozzolanic materials**: This category of material essentially consists of siliceous or aluminosilicate materials that undergo a chemical reaction with calcium hydroxide in the presence of water to form additional calcium silicate/aluminosilicate hydrate phases. Pozzolanic materials can have a wide range of origin (natural product, secondary industrial product or waste product) and their mineralogical and chemical composition also spans a broad spectrum from mainly siliceous nature to different ratios of alumina and silica-based phases. Further detailed explanations and discussions on pozzolans and their reaction mechanism are presented in **section 3.2.2.3**.

- **Cementitious admixtures**: This category of materials mainly consists of calcium aluminosilicates, which own latent hydraulic properties. Latent hydraulic materials exhibit hydraulic behaviour after the addition or presence of an alkaline activator. In concrete mixture, the role of the alkaline activator is often lead by calcium hydroxide ($Ca(OH)_2$) or similar compounds. The contents of reactive calcium oxide (CaO), silica (SiO_2) and alumina (Al_2O_3) in the cementitious material are decisive for the hydraulic effectiveness to form compact CSH, CAH and CASH phases in the presence of water.

In the following paragraphs, the most used and known cementitious admixtures, namely blast furnace slags and calcareous fly ashes are shortly presented.

BLAST FURNACE SLAG

Slag, also referred to as Blast Furnace Slag (BFS) or Granulated Blast Furnace Slag (GGBFS or GGBS) is a secondary product of the iron and steel manufacturing industry. It is an example of a latent hydraulic binder and is classified as a cementitious material due to its high CaO content. In the blast furnace, slag at a liquid, molten state from iron production is rapidly cooled leading to instantaneous granular solidification. After, the granules are dried out and ground into a fine powder known as GGBS. Slag consists essentially of silicates and aluminosilicates of calcium developed in a molten state simultaneously with iron in a blast furnace. The mineralogical composition of slag depends on the cooling rate. A faster cooling leads to the formation of amorphous calcium aluminosilicate phases, which possess a latent hydraulic potential. Whereas, a slow cooling, leads to a crystalline microstructure with no hydraulic properties, but can be used as fine aggregate. The presence of water can improve latent hydraulic properties of GGBS and alkaline activation using sodium hydroxide (NaOH), potassium hydroxide (KOH), calcium

hydroxide ($Ca(OH)_2$), clinker minerals, sodium carbonate (Na_2CO_3), and sodium silicate (Na_2SiO_3) [63,64]. The alkaline activation leads to the dissolution of the amorphous phases into reactive ionic groups. Finally, due to its hydraulic activity, different C-A-S-H phases are formed depending on the reacting precursors. [64–67]

CALCAREOUS FLY ASH

Fly ashes occur as secondary products during the combustion of coal in electric power plants. During the coal combustion process, mineral impurities in the coal are fused and leave the combustion unit with the exhaust gases and solidify into fly ash by accumulating in the filters of the industrial dedusting plant. The chemical and mineralogical composition of fly ashes has an extensive range of variety and strongly depends on the mineralogical nature of the coal used for combustion. However, fly ash's composition consists of various contents of calcium oxide, silica and alumina. The European Standard for "composition, specifications and conformity criteria for common cements" [66] divides fly ashes into two categories depending on their calcium oxide (CaO) content: siliceous and calcareous fly ash. Fly ashes with a calcium oxide content below 10% are classified as siliceous fly ashes also known as low-calcium fly ashes and can be considered as pozzolans, whereas calcareous fly ashes (CaO content above 10%) are referred to as high calcium fly ashes, which can possess hydraulic properties.

The impact of cement products using fly ashes highly depends on their chemical and mineralogical composition as well as physical properties of the particles. In general, the incorporation of fly ashes results in similar long-term concrete strengths to that using only cement, and it increases resistance against alkali-silica reactions. It decreases the release of hydration heat of the concrete

(c.f. Table 1.14 in [64]). However, the use of calcareous fly ashes also decreases the early strengths of concrete and worsens the workability of fresh concrete pastes. [13,64,66,68,69]

3.2.2.3 Pozzolans & pozzolanic reaction

There is evidence that in the ancient empires of Egypt, Greece and Rome, pozzolans were used as an essential component of cement pastes to build ancient structures. Already at that period, the potential of fine pozzolanic powders was examined to make cements as previously these natural raw materials were mainly used to make pottery. The term pozzolan or pozzolana is derived from an Italian toponym, "Pozzuoli", a village in the proximity of Naples. Initially, the Roman used the term "pulvis puteolanus" to describe red or purple volcanic tuff/ash, a reactive siliceous material of volcanic origin, which was mined in that region. Further readings about the history of the development of pozzolans can be found in [70,71].

As previously mentioned in the terminologies, pozzolans are siliceous or alumino-siliceous fine materials, which do not own or only slightly possess any hydraulic activity. Nonetheless, pozzolanic material can chemically react with calcium hydroxide $Ca(OH)_2$, also known as Portlandite (CH), in lime or cement mixtures in the presence of water to form calcium silicate hydrates (CSH) and/or calcium aluminosilicate hydrates (CASH).

Portlandite is the main constituents of hydrated lime. During the production of hydrated lime, Portlandite is formed after the addition of water to quicklime (CaO) which is obtained after calcination of limestone ($CaCO_3$). If a controlled amount of water is added to quicklime to make a more stable powder, it is called hydrated lime. If excess water is added, then the calcium hydroxide compound is referred to as lime putty.

Calcination of limestone at around 1000°C:

$$\underbrace{CaCO_3}_{\substack{calcium\ carbonate\\ limestone}} \xrightarrow{Heat} \underbrace{CaO}_{\substack{calcium\ oxide\\ quicklime}} + \underbrace{CO_2}_{carbon\ dioxide} \quad (1)$$

Addition of a controlled amount of water to quicklime to form hydrated lime:

$$\underbrace{CaO}_{\substack{calcium\ oxide\\ quicklime}} + \underbrace{H_2O}_{water} \rightarrow \underbrace{Ca(OH)_2}_{\substack{calcium\ hydroxide\\ portlandite}} \quad (2)$$

In case of the reaction of pozzolans with Ordinary Portland cement, the main portion of Portlandite occurs during the hydration reaction of the cement clinker phases. After addition of water, the clinker phases (calcium silicate phases) start to hydrate and form the calcium silicate hydrates (CSH). The hydrolysis of C_3S begins with a quick release of calcium (Ca^{2+}) and hydroxide (OH^-) ions with a large release of hydration heat. After saturation of the system, the calcium hydroxide starts to crystallize, and calcium silicate hydrates begin to form continuously, which intensifies again the hydration reaction (cf. **section 3.1.1.2.3**). At this stage, excess Portlandite can be bound by pozzolans to form additional calcium silicate hydrates (CSH), calcium aluminosilicate hydrates (CASH) and other cementitious hydration products depending on the nature of the pozzolan. This chemical reaction is called the pozzolanic reaction.

This reaction is essential to improve the performance of concrete and to reduce concrete from carbonation, as free calcium hydroxide in concrete tends to react with carbon dioxide (CO_2) from the air. Primarily, the outer surface of the concrete is affected, and the carbonation slowly and continuously progresses inwards. Even though carbonation slightly increases the mechanical performance of concrete due to the reduction of porosity and permeability, its disadvantage derives from the reduction of the pH level of concrete, which leads to the corrosion of steel rebars due to the dissolution of the passivating environment provided by the alkaline conditions of concrete.

$$\underbrace{Ca(OH)_2}_{\substack{calcium\ hydroxide \\ portlandite}} + CO_2 \rightarrow \underbrace{CaCO_3}_{calcium\ carbonate} + \underbrace{H_2O}_{water} \quad (3)$$

In general, excess $Ca(OH)_2$, a by-product of concrete hydration, has to be reduced/eliminated by the pozzolanic reaction to enhance the durability and the strength of the final concrete product. During hydration of cement or lime pastes, a pozzolanic reaction occurs due to liberation of Ca^{2+} and OH^- ions from excess hydrated CaO ($Ca(OH)_2$):

$$\underbrace{Ca(OH)_2}_{\substack{calcium\ hydroxide \\ portlandite}} \rightarrow Ca^{2+} + 2OH^- \quad (4, [72])$$

When significant quantities of reactive Al_2O_3 and SiO_2 are present in the mixture, then CSH, CAH or even CASH phases can be formed:

$$Ca^{2+} + 2OH^- + SiO_2 \rightarrow \underbrace{CSH}_{calcium\ silicate\ hydrates} \quad (5a, [72])$$

$$Ca^{2+} + 2OH^- + Al_2O_3 \rightarrow \underbrace{CAH}_{calcium\ aluminate\ hydrates} \quad (5b, [72])$$

These compounds are essential for the enhancement of the mechanical characteristics of the mixtures as a result of the progression of pozzolanic reactions over time.

The capacity of pozzolans to bind calcium hydroxide (CH) in the hydration process of cement/lime pastes to produce hydration products is referred to as the pozzolanic activity.

The definition of pozzolan is extensive, and therefore it encloses a broad panoply of materials of a variety of origins, chemical compositions and physicochemical characteristics. In general, one can primarily divide pozzolanic materials into two categories: artificial and natural pozzolans. However, this source-related classification has no relevant purpose, as it is irrelevant for the performance of the pozzolans whether the pozzolan is of “artificial” or “natural” origin.

3.2.2.4 Artificial pozzolans

Artificial pozzolans also incorporate “industrial pozzolans” and comprise pozzolanic materials, which undergo an industrial process like thermal activation or occur as waste or by-products from usually high-temperature processes from higher-level industrial productions. Artificial pozzolans include materials such as fly ash, silica fume, blast furnace slag, rice husk ash, calcined clays, burnt brick powder, calcined siliceous and opaline shales, spent oil shale, burnt banana leaves, burnt sugar cane stalks and bauxite waste, bagasse ash, laterite soils and red tropical soils and more. [8]

In the following, selected varieties of artificial pozzolans are shortly presented, as there exist numerous subtypes depending on their mineralogical nature, and geological origins. The detailed reaction properties and -mechanisms of these materials after addition to cement will not be elaborated in this dissertation.

SILICA FUME

Silica fume also referred to as microsilica or condensed silica fume, is formed as an industrial by-product during silicon smelting for the production of silicon metals and ferrosilicon alloys. These amorphous, fine and spherical-shaped particles occur during the melting of high-purity quartz into silicon at high temperatures. In general, its chemical composition comprises a very high percentage of SiO_2 (90 wt.%), and it has a high specific surface area of about 20000 m^2/kg. This high content of very reactive silica and high specific surface makes the silica fume a very reactive pozzolanic material. Furthermore, its inter-granular potential as a filler between cement particles allows densification and homogenisation of the cement matrix. These advantages make silica fume the ideal ingredient to make high performance concretes (HPCs). Moreover, intrinsic, deleterious

reactions and behaviours of concrete are reduced as well as the resistance against external chemical impacts is improved due to denser microstructure and compact interfacial transition between cement paste and aggregates. [64,73]

SILICEOUS FLY ASH

The origin of fly ashes has been presented in **section 3.2.2.2**. As already mentioned, the European Standard for "composition, specifications and conformity criteria for common cements" [66] divides fly ashes into two categories depending on their calcium oxide (CaO) content: siliceous and calcareous fly ash.

In contrast to calcareous fly ash, siliceous fly ash exhibits pozzolanic behaviour as it consists essentially of reactive silica and alumina. For siliceous fly ash, the calcium content is negligible to non-present and its chemical and mineralogical composition, as well as physical properties of the particles, highly depend on its origin. Furthermore, as this type of fly ash mainly contributes to the pozzolanic reactions in the presence of clinker in the cement, the concrete mixtures, for similar particle sizes (fineness), usually show lower early strength compared to traditional OPC. However, its addition to concrete mixtures improves the workability and the water demand of the paste, while also positively contributing to higher long-term strength compared to traditional concrete products. [13,64,66,68,69]

METAKAOLIN

Unlike the previously presented material, Metakaolin (MK) or metakaolinite is not a waste product or industrial by-products depending on a primary production process. Metakaolin is an industrially processed material based on naturally available clay minerals. It is classified as an artificial pozzolan because the achievable high pozzolanic reactivity of Metakaolin usually is not an intrinsic characteristic; it is achieved after industrial treatment of the raw material, kaolinite. Metakaolin is aluminosilicate material obtained after low-temperature calcination of the clay mineral kaolinite up to temperatures ranging from 500°C to 800°C depending on the nature of the kaolinite mineral. During the thermal treatment, at temperatures above 100°C, the absorbed water is removed (dehydration) from the kaolinite minerals and with increasing temperatures above around 500°C; the chemically bonded hydroxyl ions are removed. This process is called dehydroxylation of kaolinite into a largely amorphous, highly pozzolanic meta-state, namely Metakaolin. Metakaolin meets the requirement of ASTM C618 [74] for calcined natural pozzolan for its use as an admixture in concrete. Furthermore, cementitious mixtures based on Metakaolin by direct substitution of Portland cement or by alkali-activation to form polymeric cements are highly popular topics in current research investigations as “traditional” industrial pozzolans depending on primary industrial processes are limited or already exhausted. In general, the benefits of using Metakaolin are a denser microstructure of the final product, increased compressive strengths (early and long term), increased durability, reduced permeability, increased resistance to chemical attack and alkali-silica reaction, improved shrinkage behaviour, etc. [74–76].

RICE HUSK ASH

Rice husk ash combines all the origins of the previously presented pozzolanic materials. It is generated from the waste material, rice husk, occurring as a by-product from agro-industrial production of rice, and it has to undergo an industrial treatment to acquire pozzolanic reactivity. Rice husk is the covering element of rice grains and is separated from the corn during the milling process. As rice husk is a plant-based organic matter, it mainly consists of cellulose and lignin, but also a moderate amount of silica. After the burning of rice husk at temperatures between 500°C and 700°C, the predominately silicon-based matter, the so-called rice husk ash (RHA) remains. RHA is collected from the combustion plant and ground into a fine powder. Its physical properties and mineralogy are highly sensitive to the applied burning conditions and procedure [8,77]. Rice husk ash's pozzolanic reactivity depends on the content of amorphous silica, its surface area and its fineness. Furthermore, the availability of rice husk in large quantities in many parts of the world makes it an attractive raw material for use as SCM in concrete after industrial processing. The advantages of incorporation of RHA in blended cements or high-performance concrete are the high reduction potential of greenhouse gases, its contribution to the reduction of permeability, the increased resistance to chemical penetration and alkali-silica reaction, the enhancement of resistance to chloride penetration, the significant improvements in workability and durability, etc. [57,75,78,79].

3.2.2.5 Natural pozzolans

In contrast to pozzolanic industrial by-products or industrially processed waste materials, natural pozzolans are highly reactive pozzolanic materials by nature and usually do not require any important industrial processing. According to ASTM C618 [74], the requirements to the chemical composition of natural pozzolan are approximately 70% in contents of silica (SiO_2), alumina (Al_2O_3) and iron oxide (Fe_2O_3) combined and the required loss on ignition should be maximum 10%. Furthermore, calcined clay, metakaolin and calcined shale are also often classified as natural pozzolans, but the classification depends on the definition of natural pozzolans adopted by some authors. In this writing, these pozzolans are considered as artificial pozzolans as they undergo heavy industrial processing (high-temperature treatment) to exhibit pozzolanic behaviour. In contrast, natural pozzolanic materials already show pozzolanic behaviour without or with minimal industrial operations.

The quality and reactivity of natural pozzolans depend on their physical and compositional nature, which is strongly related to their origin. In general, natural pozzolans are abundantly available only at a local level at specific spots in the world, as they originate from natural minerals and volcanic deposits, which are related to the paleogeology of a region. However, the stock of high-quality, naturally occurring pozzolans is limited and already face a high degree of exploitation, leading to a scarcity of these materials.

According to [70], natural pozzolans can be classified into two categories:

- Pozzolans originated from volcanic origin, basically consisting of non-crystalline (amorphous) glass from fusion during volcanic eruptions or similar natural events. This category encompasses volcanic ashes, vitreous pumices, amorphous volcanic glasses like

obsidians, different volcanic rocks, volcanic and zeolitised tuffs, etc. In this category, rocks from meteorite impacts are included.

- Pozzolans derived from sedimentary origins, which contain a high percentage of opal (hydrated amorphous silica) or argillaceous substances. This category encompasses diatomaceous earths, bauxite, cinder, shales and naturally burned clays, but also specific types of argillaceous sands such as schist, basalt, feldspar and mica, which can have low pozzolanic properties.

These materials are generally only available at local scales, and their source is limited. Furthermore, as there exist numerous subtypes depending on their mineralogical nature, and geological origins, the short presentation of some selected natural pozzolans in detail has been omitted in this writing.

3.2.2.6 Assessment methods of pozzolanic activity

A pozzolan is defined as "*a siliceous or siliceous and aluminous material that in itself possesses little or no cementitious value but will, in finely divided form and in the presence of water, chemically react with calcium hydroxide at ordinary temperatures to form compounds possessing cementitious properties.*" [62]

Furthermore, besides the known environmental impacts of the use of Portland cement, the current exploitation of "traditional" pozzolanic materials is also a driver for the necessity of alternative sources of pozzolanic materials. Therefore in recent years, different methods have been developed, respectively, optimised to assess the pozzolanic activity of potential new raw materials. In literature, there is a vast range of studies and reports on various test methods to determine the reactive behaviour of a material. [80–90]

Most of the authors are in agreement that all the assessment methods of pozzolanic activity can be classified into two categories: direct or indirect methods.

3.2.2.6.1 Direct methods for assessing pozzolanic activity

Pozzolans are defined by their ability to react with calcium hydroxide to form compounds with additional calcium aluminosilicate phases, which improve the cementitious properties. Therefore, the fundamentals behind direct methods of assessing pozzolanic activity are chemical and comprise measurement techniques, which track the amount of $Ca(OH)_2$ present in the mix over time. The direct methods allow assessing the reduction of calcium oxide over time as the pozzolanic reaction progresses using classical chemical procedures or modern mineralogical and thermogravimetric analysis methods.

The direct method comprises the Frattini test, the saturated lime test, the Chapelle test, the isothermal calorimetry, the thermogravimetric analysis and the XRD analysis. In the following sections, the basic ideas of these methods are shortly described, and their approach to evaluating pozzolanic reactivity is explained.

FRATTINI TEST

The Frattini test is a widely used standard test procedure specified in EN 196-5 [91] for the assessment of the pozzolanicity of potential raw materials for pozzolanic cement. The Frattini test method evaluates the pozzolanic activity by measuring the amount of $Ca(OH)_2$ in an aqueous solution of a hydrated pozzolan-cement mix after a specific time. An active pozzolanic reaction is measured if a reduction of additional calcium hydroxide is evidenced, respectively, the concentration of $Ca(OH)_2$ in the tested solution is lower than the saturation concentration.

According to the procedure specified in the standard, 20g of the investigated blended cement consisting of 80% of Portland cement and 20% of the tested pozzolanic materials is mixed with 100 ml of boiled distilled water. This mix is stored in sealed recipients in a laboratory oven at a constant temperature of 40°C. After specific periods, the samples are vacuum filtered through filter paper. After cooling down to room temperature, the filtered material is chemically analysed for the concentration of OH^- and Ca^{2+} ions by titration methods using a dilute hydrochloric acid solution, an ethylenediaminetetraacetic (EDTA) acid solution and a Patton-Reeder indicator triturate [92].

This chemical analysis provides data that can be plotted in an XY graph with the Ca^{2+} concentration in [mmol l^{-1}] on the y-axis and the OH^- concentration in [mmol l^{-1}] on the x-axis. The Frattini test results are compared with the solubility curve of $Ca(OH)_2$ (**Figure 3.7**) and the

results from some control samples. A positive indicator for pozzolanic activity is given if the plotted points remain below the standard curve. [82–84,90,91,93]

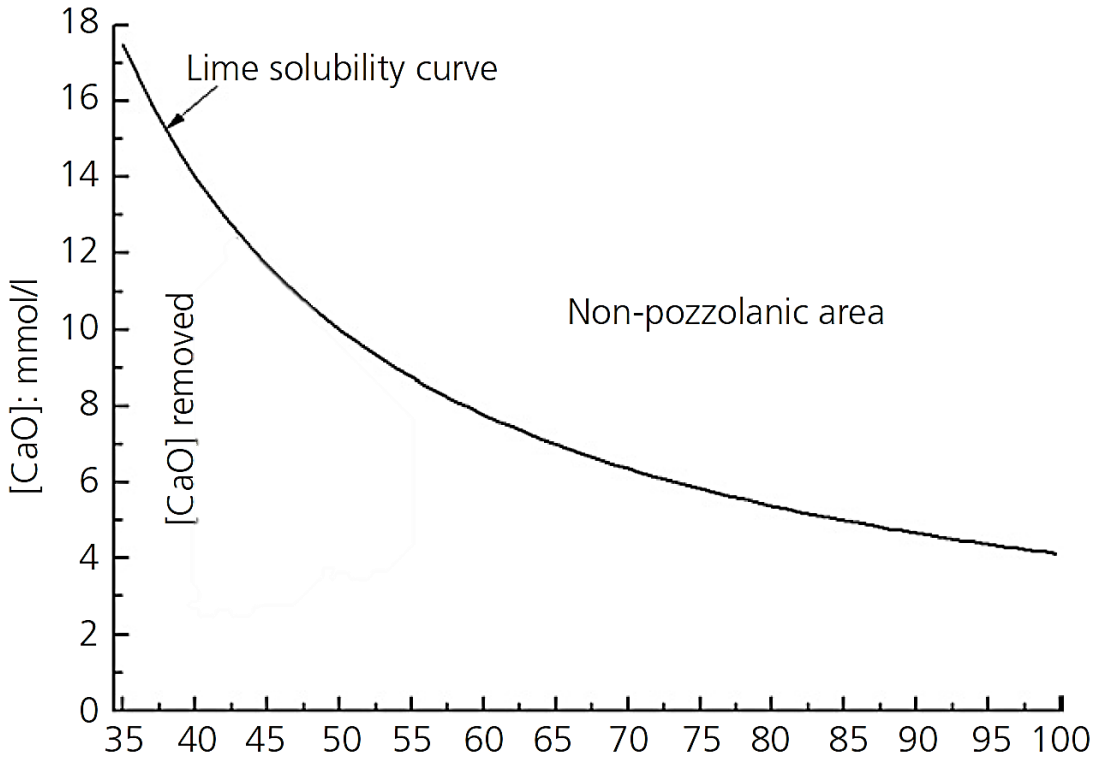

Figure 3.7 *- Schematic diagram of quantified Frattini test (modified Figure 2 from [94])*

SATURATED LIME TEST

The saturated lime test is also known as the modified Frattini method. It investigates the pozzolanic activity of an investigated material by fixing the quantity of $Ca(OH)_2$ available in an aqueous solution [95,96]. 1g of the test pozzolan is added to a plastic recipient filled with 75 ml of a saturated lime solution. Then, the recipient is sealed and stored in a laboratory oven at 40°C for a specific time. At the end of each period, the sample solution is filtered and the CaO contents are chemically determined like for the Frattini test. The advantage of this method is that the quantity of Ca^{2+} is known and it is evident that Ca^{2+} can only react with the test pozzolan or water, which allows quantifying the absolute consumed/fixed lime contents. [83,86,93]

CHAPELLE TEST

The Chapelle activity test, especially the modified Chapelle test, is a commonly performed method to determine the pozzolanic reactivity of different materials. This method is carried out by dissolving and 1g of the test pozzolan in an aqueous solution consisting of 1g of calcium oxide (CaO) and 250ml of distilled water. After a short stirring process, the solution is heated up to about 90°C for 16h. Afterwards, as the exact quantity of CaO is known, the lime consumed is calculated by the difference between the initial and the final lime concentrations. This quantification is performed by filtration of the solution and the determination of the concentration of unreacted CaO by titration with a dilute hydrochloric acid solution using a phenolphthalein indicator. [89,96]

THERMOGRAVIMETRIC ANALYSIS

In recent years, thermal analysis methods have become quite popular for the determination of pozzolanic materials and DTA-TG analysis are usually used for quick testing and early indicator for pozzolanicity of a material. These measurements figure among complementary tests to verify the consumption of calcium hydroxide by the pozzolanic reaction between the test pozzolan and the cementitious component. The blended cement pastes and a control mixture are prepared and cured over a specific time (usually 2 and 28 days). After each period, the samples are immersed in acetone for 24h to stop the hydration reaction and dried in a laboratory oven at 40°C for 24h. Afterwards, the samples are finely ground and analysed by the DTA-TG analysis method. The mass of the consumed $Ca(OH)_2$ is determined by the loss of mass at temperatures between around 400 and 550°C due to the dehydroxylation of the $Ca(OH)_2$ minerals. The calcium hydroxide content available in the paste consists of the calcium hydroxide produced during the hydration reaction of cement clinker subtracting the quantities consumed due to pozzolanic reaction. The

pozzolanic activity is determined by the difference between the amount of fixed $Ca(OH)_2$ of the investigated sample and the amount of consumed calcium hydroxide of the control sample. [81,82,84,88–90,93,96]

MINERALOGICAL ANALYSIS

The crystal minerals and amorphous phases are determined by the X-ray diffraction method, and the assembled data about the crystallography of a substance provides information about the spatial arrangement of atoms at specific physicochemical conditions. Furthermore, the quantitative evaluation of the mineralogy allows determining the presence of pozzolanic amorphous meta-clay phases and amorphous glassy phases. The hardened blended cement is prepared like for the previously described thermogravimetric analysis method and then analysed by XRD. The pozzolanic activity is determined by recording the newly formed hydration products and changes in the amounts of Portlandite and calcite phases using qualitative XRD analysis or quantitative XRD analysis. [82,84,86,88,89]

3.2.2.6.2 Indirect methods of assessing pozzolanic activity

Indirect test methods of assessing pozzolanic activity measure changes of physical properties of hydrated concrete products, including the investigated pozzolanic material. These methods are classified as indirect techniques as they do not directly quantify the amount of calcium hydroxide fixed by the pozzolan or monitor the $Ca(OH)_2$ consumption due to pozzolanic reaction over different periods. Indirect methods comprise techniques like electrical conductivity test, heat evolution by conduction calorimetry or the widely known strength-based Strength activity index (SAI).

ELECTRICAL CONDUCTIVITY TEST

The electrical conductivity method is an alternative and indirect technique for monitoring the pozzolanic reactivity of potential substitution materials during the early concrete hydration phases. In literature, the sample preparation slightly varies from one author to another. Nonetheless, mostly, mixtures with specific quantities of the test pozzolan and saturated calcium hydroxide solution are used for the analysis. However, the basic idea of this method consists of recording at regular intervals of time the electrical conductivity of the sample. Several studies have concluded that the rate of change of conductivity is a valid parameter to quantify pozzolanicity during the hydration of concrete as low electrical resistance corresponds to high $Ca(OH)_2$ consumption. In contrast, high electrical resistance corresponds to low $Ca(OH)_2$. In other words, the monitored electrical conductivity decreases with time when the investigated material exhibits pozzolanic behaviour and therefore fixes a certain amount of Ca^{2+} and OH^- ions due to the pozzolanic reaction. [82,93,96,97]

ISOTHERMAL CONDUCTION CALORIMETRY

The isothermal conduction calorimetry method, also known as hydration heat test is an adiabatic technique. Isothermal conduction calorimetry monitors the heat generation during cement hydration of a pozzolan-lime based mixture in a thermally isolated bottle in a climatic chamber at constant room temperature to avoid external thermal influences. The sample preparation, according to [98], consists of injecting 3g of water into the same quantity of test pozzolan in a sample cup. Then, the sample is sealed with plastic film and placed in the calorimeter. Afterwards, the rates of heat evolution in [mW/g] are recorded using an appropriate monitoring system. The fundamental idea of this method relies on the increase of heat liberation due to the additional pozzolanic reactions, co-occurring to the heat generation from cement clinker hydration. [98–100]

STRENGTH ACTIVITY INDEX (SAI)

The strength activity index (SAI) counts among the most used evaluation techniques to assess the pozzolanicity of a reactive material incorporated in concrete mixtures. The advantage of this "indirect" method is that it measures the actual physical performance in the form of compressive strength of the mixtures incorporating the investigated pozzolanic material compared to a reference mixture. This method evaluates the strength contribution of a mineral admixture in a cement-based mixture. It, therefore, permits to determine the potential of the pozzolanic material directly as a cement substitution considering the performance of the final product. Basically, within this method, the compressive strength and the flow of the mixtures is assessed according to EN-196-1 [101] or similar international standards.

The control mixtures may vary from one standard to another or even from one author to another. Control mixtures are prepared by adding water to a mixture of standard sand (1:3 sand/cement

ratio) and Ordinary Portland cement at a w/b ratio of 0.50. Samples using the same quantities mixtures are prepared, while a Portland cement is substituted at 25 wt.% by the investigated pozzolanic material. The mixtures are stored and cured for specific curing ages (usually 2, 7, 28, etc.) according to the used standards or the followed test procedure. Afterwards, the specimens are tested using a standardised compressive strength test unit. Finally, the strength activity index (SAI) is calculated as the ratio of the compressive strength of the test specimen to the compressive strength of the control unit. The evaluation of the SAI criteria for pozzolanic activity depends on the used standards. [62,74,81–85,88,102,103]

3.2.2.6.3 Remarks on the methods of assessing pozzolanic activity

In the previous sections, different methods of assessing pozzolanic activity were presented, and it is a complex task to evaluate which method can be considered superior to the others. Each method has its advantages and disadvantages, which are mostly related to the wide variety of materials (cf. **sections 3.2.2.4** and **3.2.2.5**) that are being examined. Nonetheless, specific methods are used preferably in some scientific fields due to faster investigation speed, better compatibility and the availability of existing data and verified reference studies. Furthermore, other factors like the rheology of the mixtures, specific surface or particle size distribution of the investigated pozzolanic material play also a significant role in the outcome of the tests. In literature, we find comparative studies [83] that conclude that the outcomes regarding the pozzolanic activity of certain materials do not always correlate to each other and strongly depend on the test procedures and conditions of each method. Finally, the general practice is to support/confirm the findings from the indirect pozzolanic activity tests using direct tests.

3.2.2.7 The three governing effects

The reaction mechanisms leading to the hardening of concrete mixtures and their final properties are based on very complex mechanisms, as it simultaneously comprises several physical and chemical processes. Since a long time, numerous research studies from different material-related engineering fields have done extensive and valuable work to understand the complex mechanisms of concrete hardening process from concrete paste to the final hardened concrete product with a broad range of different characteristics and performances. Furthermore, the substitution of Portland cement by pozzolanic or cementitious materials puts additional factors into the existing complexity of the concrete hardening process.

Nonetheless, it is intuitive that each constituent of the cementitious paste, with or without additional admixtures, engages in a different way inside the cement matrix. However, this involvement occurs in a coordinated and interdependent form as otherwise the well-known characteristics and performances of concrete products would not be achievable.

The interaction of the constituents of the cementitious paste occurs at different levels and depends mainly on factors like particle size, chemical and physical activity of each component. In the following paragraphs, the different processes leading to the “generally” increased compressive strength of cement pastes containing pozzolanic materials are shortly discussed.

According to [104–106], the addition of pozzolans or cementitious materials in cement-based mixtures, which generally consist of fine particles, can lead to compressive strength improvements due to three possible effects, which can co-occur as coexisting processes or at distinctive stages over time:

- **Chemical effect – Hydration reaction**

Depending on the mineralogical and chemical nature of the substitutive material, in presence of water, the particles can hydrate and form hydration products coexisting with the clinker hydrate phases from the hydration of Portland cement. Contrary to hydration, these fine particles can react with a cement component (usually $Ca(OH)_2$) to form CAH, CSH or CASH phases as a consequence of a pozzolanic reaction (cf. **section 3.2.2.3**).

- **Physiochemical effect – Chemical effect related to the particle surface**

Fine materials may not directly interact chemically with the cement due to its inert nature. Still, they can indirectly contribute positively by influencing the early chemical reactions of the cement paste. The finer particle size distribution of the added filler material is often correlated to a larger contact surface area of the small particles, which provide a better interfacial area for the hydration reactions by surrogating as nucleation sites. Nucleation sites are essential for the growth of the hydration reactions, as individual ions or molecules involved in hydration reactions might not have enough impact overcome the physical obstruction of the surrounding viscous medium. Therefore, additional agglomeration surfaces allow more molecules to bond to a more compact form by physical proximity to overcome the obstructive and viscous resistance in early cement hydration phases.

- **Physical effect – Packing/filler effect**

The physical effect leading to strength enhancement of concrete products, known as packing effect, filler effect or even micro-filler effect, is related to the size and shape of the particles of the filler or cement substitute. The addition of filler material to a cement paste considerably improves the compactness of the concrete as the added fine particle build a more effective cement-aggregate-

paste matrix bond by filling the gaps between the cement particles themselves and between the cement particles and the aggregates.

The functionality of the filler effect is based on the fact that the density of concrete is significantly related to the particle size distribution of the concrete constituents. The denser the packing of the constituents, the higher the density of the composite concrete product. A better packing of the multi-component mixture is achievable by filling the voids with different fractions of fine particles. In his study, Isaia et al. [105] have discussed two packing phenomena, which shows the significant importance of filler material in concrete mixtures and the choice of the right relative particle size distribution of the concrete constituents for optimal packing leading to higher cement matrix-aggregate bond: [75,81,86,104–109]

- The "**wall effect**" (**Figure 3.8**) describes the difficulty of particles in the fresh concrete paste to pack the spaces efficiently in the proximity of larger aggregate particles. Furthermore, this phenomenon is intensified by the tendency of fresh concrete mixture to segregate of water, and cement particles by the shearing stresses exerted by the aggregate particles during mixing. The packing issue arising with the wall effect is the reduced concentration of hydratable clinker particles near larger aggregate leading to a more porous paste filling at the contact areas, which directly affect the strength of the final concrete.

- The "**two-wall effect**" describes a similar phenomenon to the "wall effect", but in this case, the less dense packing is provoked by the obstruction of clinker grains in the space between coarser aggregate particles. When two coarser particles occupy close positions, then the fluid medium of cement paste can enter the narrow gaps between coarser particles, but the clinker grains cannot pass through the small space. Even if the particle size of the clinker grains is smaller than the opening, the passage through the voids between coarser

aggregates remains complicated due to the interlocking effect of the fine particles leading to an agglomeration of the particles near the openings as shown in **Figure 3.9**.

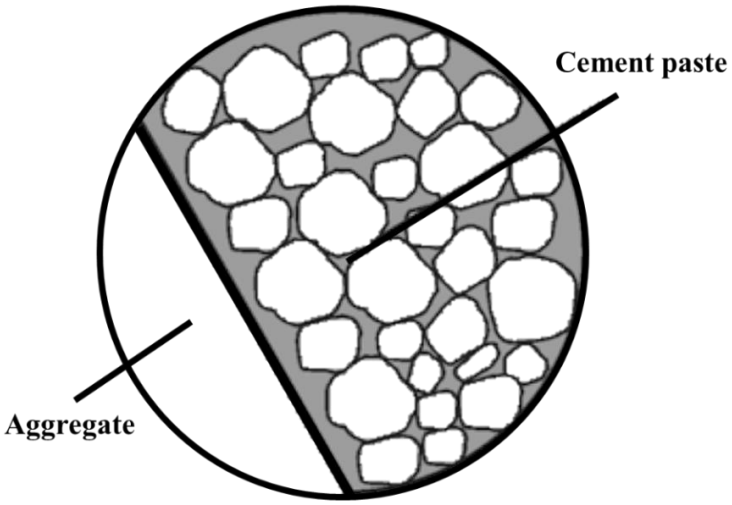

Figure 3.8 *- The wall effect (modified and adapted Fig.1 from [105])*

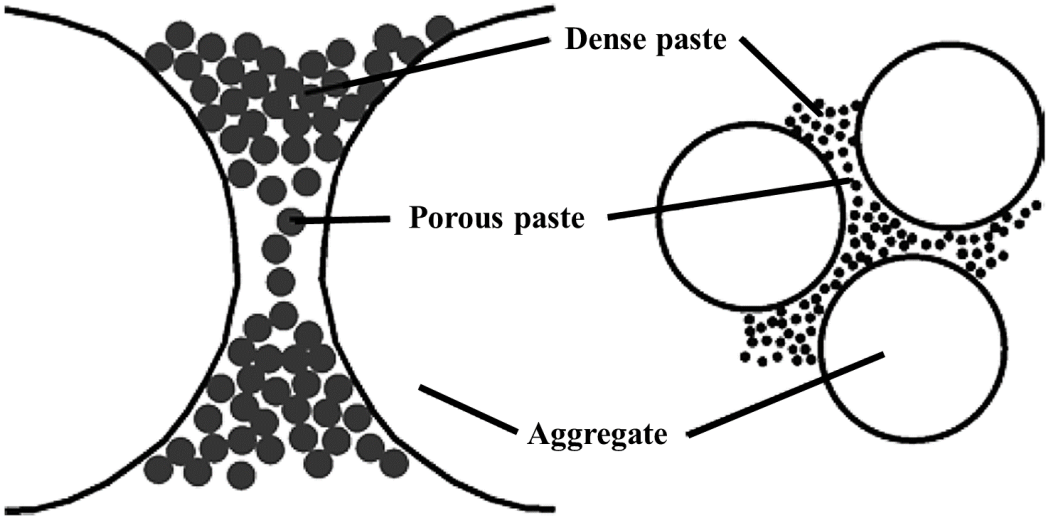

Figure 3.9 *- The two-wall effect (modified and adapted Fig.2 from [105])*

3.2.3 Supplementary cementitious material (SCM)

A more recent and widespread terminology, a recent umbrella term for pozzolans and cementitious materials is "Supplementary cementitious materials (SCMs)", which due to its broader definition encloses these concepts as any inorganic material that contributes to the properties of a cementitious mixture through hydraulic or pozzolanic activity or both.

All the types of materials, reaction mechanisms and assessment methods presented and discussed in **section 3.2.2** are comprised within the overall concept of Supplementing cementitious materials (SCM). However, even if some SCMs have similar origins, there can be considerable variability in the physicochemical properties. Each SCM can be decomposed in a ternary CaO-SiO_2-Al_2O_3 system. **Figure 3.10** depicts an estimative categorisation of novel SCMs using their chemical composition and predicts possible behaviour, reaction mechanisms and reaction products.

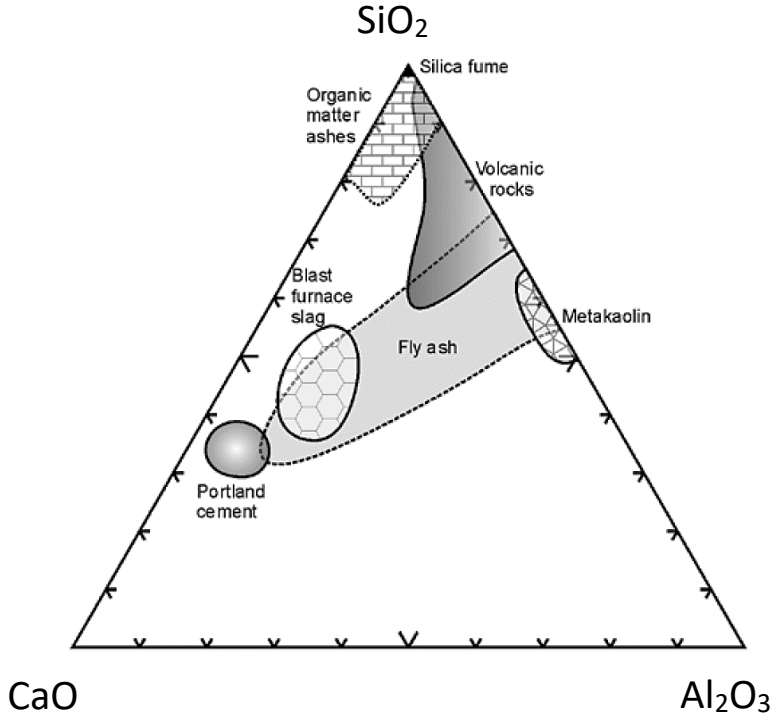

***Figure 3.10** - Ternary CaO-SiO_2-Al_2O_3 variation diagram of different SCM groups (adapted and modified Figure 3 from [110,111])*

Since the middle of the last century, research on alternative materials has been extensively carried out to diminish or entirely cease the use of Ordinary Portland cement. Several raw materials and different technologies were studied to supplement or substitute cement clinker without loss of performance of the resulting construction materials or even improving specific physical and/or chemical properties of the concrete products.

In the previous chapters, a large number of works and studies related to the understanding of the behaviour of supplementary cementitious materials and their characterisation have already been presented and explained. Therefore, a short selection of studies on the performance of supplementary cementitious materials (SCM) using industrial, substitutive materials is presented to complement the literature on SCMs. Furthermore, as one of the key objectives of this project is dedicated to highlighting the performances of clay-based OPC substitutions, a major portion of the presented reviews consists of studies related to clay-based SCMs.

Juenger and Siddique [112] evaluated the role of SCMs in concrete by reviewing the impact of the interaction of SCMs with OPC on early hydration, fresh concrete paste properties, mechanical performances and long-term durability.

Regarding the early hydration, the “filler effect” due to the addition of fine SCMs in blended cements brings a double-benefit to the hydration kinetics. In one hand, by acting as nucleation sites for the clinker hydrates and in the other hand, by delaying the stabilization period of the hydration products by dilution of the cement content, leading to better growth of the CSH phases [112,113]. In a study with calcined clays, Tironi et al. [114] examined the influence of Portland cement substitution by metakaolinite-based clays. The physiochemical properties, as well as the mineralogy of two different Metakaolins, was determined using TG-DTA, XRD, BET method, Blaine test and using mercury intrusion porosimetry (MIP). The results from DTA and XRD

confirmed the considerable fixation of calcium hydroxide by the SCM clays compared to control mixtures due to pozzolanic reaction and also the formation of additional crystalline hydration products like C_4AH_{13} which formed by the reaction of metakaolinite with calcium hydroxide. The meta-stable structure of clays containing high amounts of metakaolinite showed auspicious pozzolanic activity, performance and durable properties for its applicability as SCMs.

The impact of SCMs on the workability of concrete mixtures is detrimental, as in most cases, the water demand increases due to the fineness or higher water absorption of the supplementary cementitious material [86,112].

Quercia et al. [115] conducted investigations on the physiochemical and morphological characteristics of six different amorphous silica-based materials using various electron microscopy techniques, XRD-EDS, laser granulometry, Brunauer-Emmett-Teller (BET) test and Barrett-Joyner-Halenda (BJH) method. Furthermore, the slump flow test and the performance-based tests on hardened specimens were carried out. The examined materials consisted of different micro-silica and nano-silica materials, which covered a wide range of particle size distributions between 1nm up to a few micrometres. Quercia et al. concluded that despite the versatility of the siliceous materials in terms of pore diameters, pore size distributions and particles shapes, the principal parameters influencing the workability and the performance of the final product are related to the specific surface area, pore volumes and the agglomeration behaviour of the fine particles. They suggest the optimal dispersion of the silica in the cement matrix allows achieving the desired improvement of the final concrete’s characteristics.

The effect of these cement substitutes on the mechanical performance of concrete is mostly led by an increase of the long-term strength due to the additional hydrate products from pozzolanic reaction and a better packing of the cement matrix. Zhang et al. [116] examined series of high

strength concrete mixtures based on Portland cement and calcium sulfoaluminate cement with different mix proportions of two silica sands, silica fume, GGBS and fly ash. They reported that the addition of SCMs and the optimization of the water to binder ratio led to a significant increase of the compressive and bending strength of the tested mortars. Overall improvements in the strength range with 20%-70% increase for the compressive strengths and the bending strengths were achieved at different curing ages compared to the reference mixtures. Fernández et al. [117] analysed the interdependent effects of different SCMs (blast furnace slag, siliceous fly ash and limestone filler) depending on the composition of OPC (CEM I 42.5 R-SR and CEM I 42.5 R) by evaluating the mechanical performances, the changes in the pore solution and the resulting microstructure of the mixture pastes and mortars. They confirmed the formation of a higher amount of hydrates at early hydration phases than for the reference. For mixtures containing silica fume as SCM a significant strength gain at advanced hydration ages was measured for both cement types. However, the low alkali and low C_3A cement (CEM I 42.5 R-SR) achieved 15% less strength than the CEMI 42.5 R cement. This study concludes that the reactivity of SCMs leading to enhanced performances of concrete is influenced by the composition of the cement as the C_3A content has a significant influence on the reactivity of the pozzolanic material.

Regarding clay-based blended cements, Taylor-Lange et al. [118] investigated the pozzolanic behaviour and the mechanical performance of mortars containing kaolinite-calcium bentonite and a laboratory blended kaolinite-sodium bentonite and compared them to the performance of a known pozzolanic material, Georgia kaolinite, and an inert filler quartz. A combination of XRD and TG analyses was applied to determine the optimal calcination temperature for each clay sample, and the performance was evaluated by examining the pozzolanic behaviour and the resulting compressive strengths. Taylor-Lange et al. affirmed previous studies by confirming the

relationship between the degree of Portlandite fixation of the SCM paste and the related compressive strength achieved (**Figure 3.11**).

Abdelli et al. [119] studied the chemical-, the mineralogical composition and the pozzolanic activity of three different metakaolins using XRD, TGA, SEM and the strength activity index. One of the metakaolins showed a high content of calcium oxide, while the other two mainly consisted of aluminosilicates. The XRD and TGA results verified the formation of additional hydration products due to the consumption of Portlandite due to pozzolanic reactions. All the samples exhibited strength activity indices above 1 for all curing ages. However, the samples with the CaO-rich metakaolin showed less performance than the other two metakaolins. This difference can be explained by the additional CaO content, which explains the lower capacity of the SCM (metakaolin) to consume additional Portlandite (pozzolanic reaction). These findings confirm the high pozzolanic activity of the different used metakaolins. In another study, El-Diadamony [76] examined the effect on the hydration products of mixtures with up to 20 wt.% OPC substitution by a calcined Egyptian kaolinite clay using XRD, DTA and DTG techniques. The evaluation of the optimal thermal treatment of the applied clay is suggested at a calcination temperature of 850°C for two hours.

Furthermore, the consumption of free lime was observed over time due to the pozzolanic reaction of metakaolinite (MK) using XRD and DTA. Finally, the compressive strength development also confirms the positive impact of MK as SCM. At 5 wt.% of MK addition, the highest performance (above OPC reference mixture) was achieved mainly due to the optimised packing (filler effect) of the constituents. Furthermore, for blended cement pastes containing 10-20 wt.% MK no significant difference in the mechanical performance was observed, which supports the applicability of the used MK as SCM. Similar results were also found by Beuntner [120], who

investigated the pozzolanic activity of low kaolinite clays in cementitious mixtures (20 wt.% OPC substitution) using XRD, BET method, Chapelle test and compressive strength test.

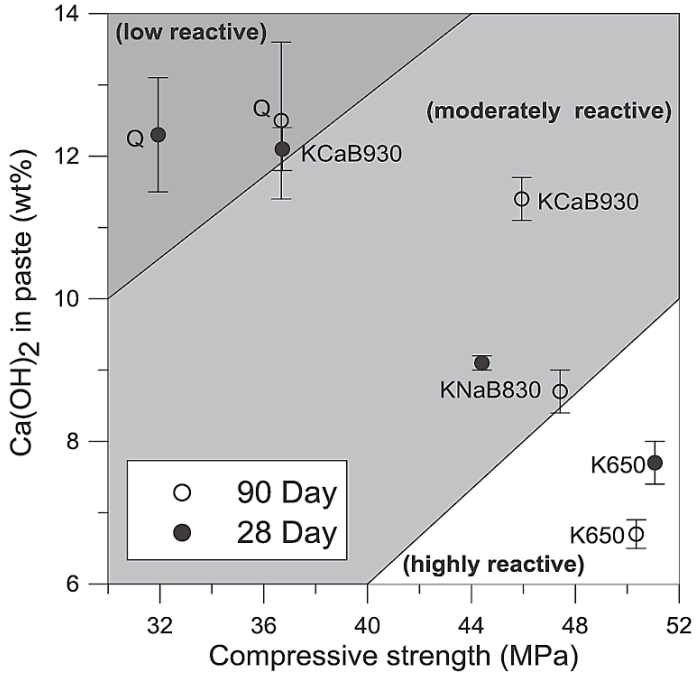

Figure 3.11 *- Remaining Portlandite content as function of compressive strength of the investigated samples; mortars containing Q:quartz, KCaB:Texas kaolinite–calcium bentonite, KNaB: laboratory blended kaolinite–sodium bentonite and K: Georgia kaolinite (K) (Fig.6 from [118])*

Badogiannis et al. [121] focused their work on the improvement of the thermal activation of four Greek kaolin clays, and the performance and the reactivity of the corresponding metakaolins. The dehydroxylation conditions of the clays were examined by DTA-TG, and the resulting mineralogical shifts were analysed by XRD. Pozzolanicity was evaluated using the Chapelle test and the mechanical performance compared to a reference sample. Badogiannis et al. suggested that an efficient thermal treatment for most of the tested kaolinites at 650°C for 3h as optimum and led to the highest pozzolanicity, also supported by the corresponding Portlandite fixation by the results of the Chapelle test. The optimal thermal treatment conditions were verified using the mechanical performances of mortars using 20% OPC substitution by each metakaolin. The high pozzolanic reactivity was confirmed for the metakaolins with a chemical composition of

SiO_2/Al_2O_3 ratios of 3.5:1 or 3:1, whereas the metakaolin at 1:1 ratio did not perform as good as the other samples.

Considering the long-term durability of concrete with the addition of SCMs, generally, it is reported that the detrimental deterioration effects of traditional concrete are reduced. A denser microstructure is developed due to the fixation of free $Ca(OH)_2$ leading to additional CSH phases, which occupy more void spaces of the microstructure. Additionally, this refinement of the pore microstructure also significantly reduces the permeability of the concrete, leading to a significant reduction of carbonation and the improvement of its resistance against chemical attacks from acids, salts, alkalis, sulphates or gas intrusions. Even the alkali-silica reaction in concretes is reduced due to the absorption of the reactive, amorphous silica by the high aluminate content in the SCM, preventing the reaction of silica with alkali reagents in concrete to form a gel that swells and damages the concrete by expansion. Farnam et al. [122] investigated on the enhancing contribution of silica fume, fly ash and slag in binder mixtures based on Ordinary Portland cement and OPC V cement (cement mix classified as high sulphate resistant due to very low C_3A content) to resist to chloride attacks (de-icing salts) by preventing the formation of calcium oxychloride. In other words, SCMs restrict the reaction between chloride-based de-icing salts and calcium hydroxide in concrete by fixing $Ca(OH)_2$ due to pozzolanic reaction. The specimens were exposed to $CaCl_2$ solutions, and the specific latent heat associated with the formation of calcium oxychloride was quantified using low-temperature differential scanning calorimetry (LT-DSC). Furthermore, the TGA methods were applied to quantify the calcium hydroxide content in the examined specimens and compared to the $Ca(OH)_2$ content of control mixtures. The results from LT-DSC and TGA analysis confirmed the positive effect of SCM to reduce the formation of calcium oxychloride due to the dilution effect and the pozzolanic reaction, compared to samples without SCM addition.

SCMs are also used in high-performance concrete (HPC) or ultra-high performance concrete (UHPC), and several studies confirm the optimisation regarding the denser packing, the filler effects as well the pozzolanic reaction leading to a significant increase of the performances of UHPC. Vejmelková et al. [123] investigated on HPC mixtures including finely ground ceramics as SCM alternative and examined various concrete-related characteristics like material compositions, mechanical properties, fracture behaviour, long-term durability as well as hydric and thermal properties compared to a reference OPC concrete. The HPC containing fine-ground ceramics outperformed the reference OPC mixtures in terms of frost resistance up to a substitution degree of 40%. However, resistance to de-icing salts, in other words, preventing the formation of calcium oxychloride was improved only for mixtures containing up to 10% of fine-ground ceramics. Overall, Vejmelková et al. concluded that HPC mixtures with fine-ground ceramics at lower OPC substitution degrees could be considered as a promising alternative to metakaolin as SCM in concrete.

There exist a lot of valuable and reliable studies on industrially used SCM, but also on alternative SCMs like rice husk [78,79,124], industrially processed clays [125], calcined clay-brick wastes [126–129], volcanic tuffs [130,131], pumices [132], modified reservoir sludge [133,134], waste expanded perlite [135] and many more. All these materials show cementitious behaviour and lead to enhancements of the concrete properties in terms of durability, mechanical performances, hydration characteristics, resistance to internal and external detrimental effects, etc. These materials behave similarly to the materials already extensively discussed in this writing and mainly follow the same reaction mechanisms. The properties and the resulting performances only differ due to their mineralogical nature, particle size and the physiochemical properties.

3.2.4 Clay-lime-based binders and mortars

The use of lime-based mortars revived since the 1970-80s because the application of OPC-based products for the refurbishment of historic masonry was detrimental due to its high stiffness, shrinkage, cracking behaviour and poor adhesion to the traditional (historic) building materials leading to poor compatibility for its usage in historic masonry. Sepulcre-Aguilar and Hernández-Olivares [136] studied the performance of masonry conservation mortars based on three different lime compounds containing metakaolin and sepiolite using simultaneous thermal analysis, SEM, XRD, Surface EDX and compressive strength tests. They confirmed the formation of hydration products and additional stratlingite and C_4AH_{13} phases. In addition, the water/binder ratio plays a major role in the formation of hydrogarnet phases, and the addition of sepiolite has significantly reduced the formation of C_4AH_{13} phases, resulting to a loss in mechanical performance by 66% compared to mixtures without the addition of sepiolite. Finally, Sepulcre-Aguilar and Hernández-Olivares concluded that mortars containing lime and white Portland cement portions could be more suitable as alternative mortars for refurbishment applications. Another investigation related to masonry conservation mortars was conducted by Aggelakopoulou et al. [137], who evaluated metakaolin-hydrated lime mortars to be used for restoration purposes Mortars consisting of commercial Metakaolin and hydrated limes were prepared at different MK-lime ratios for various curing periods and evaluated using TG-DTA, mercury intrusion porosimetry (MIP) and strength-based evaluations. Overall, all mortars achieved acceptable performances required for restoration mortars compared to traditional structural materials. Furthermore, higher consumption of hydrated lime was observed for mortars with higher Metakaolin content leading to better performances. However, a decrease of strength was observed for all mortars after 3 months of curing time due to the failure in the microstructure due to shrinkage with increasing MK content.

Wild et al. [138], as well as Arizzi and Cultrone [139], agreed in their studies on the lime-based pastes, respectively, cement-based pastes containing MK as SCM that the substitution of 20 wt.% of the cementitious materials offered the optimal improvement of the mechanical performance compared to lower substitution degrees. Similar conclusions were made by Vejmelková et al. [140] and Nežerka et al. [141].

Gameiro et al. [142–144] focused on a series of investigations on the analysis of the microstructure, the determination of hydration products, the influence of binder:aggregate ratio of lime-metakaolin mortars. In [142], the physiochemical characteristics and microstructure of lime-metakaolin paste systems were examined using XRD, TG-DTA and SEM-EDS. The formation of additional and higher quantities of hydration products (calcium aluminate- and calcium silicate hydrates) was detected by all applied techniques for higher quantities of Metakaolin. Furthermore, the variation of hydration products observed simultaneously with variations in Portlandite content changed with the MK content for increasing curing ages. Similar results were found in [143], where the phase development and the stability of the formed hydrates were evaluated over time for lime-MK mortar pastes cured at ambient conditions. The examination over time confirmed the previously mentioned fluctuations of hydrates formed with time, directly related to the release of Portlandite due to later formation of CSH phases.

Furthermore, crystalline phases like tetra calcium hydrate phases (C_4AH_{13}) resulting from the pozzolanic reaction of Portlandite with Metakaolin is found in a very unstable state over time for all pastes. In [144], the influence of the binder:aggregate ratio of lime-metakaolin-based pastes for restoration application was evaluated based on the mineralogical analysis and the mechanical performance analyses using TG-DTA, XRD and strength tests. According to the authors, the binder:aggregate ratio allows controlling the desired level of desired mechanical performance

depending on the application conditions. However, the primary influence in performance due to binder:aggregate ratio is related to the proportions of lime and MK present in the systems as these factors specify the extent of carbonation and pozzolanic reaction. In terms of performance, a binder:aggregate ratio of 1:1 promotes the pozzolanic reaction during a more extended period with increasing MK content, but these systems are more affected by long-term hygric effects like shrinkage and might not be compatible for restoration purposes. Similar results were found in [145]. Additionally, the authors stated that the presence of katoite (occurrence in some samples) has detrimental effects on MK-lime blended systems at long-term as this compound reduces the mechanical performance.

Cabrera and Rojas [146,147] analysed the reaction kinetics of lime-MK mixtures using TG-DTA and XRD using a rapid method. The determination of the lime content was accelerated by drying the samples at 60°C using a microwave oven. The formed hydration products were C_2ASH_8 and C_4AH_{13} in metastable states at early hydration phases that after long curing periods might convert to hydrogarnet. Furthermore, for the same curing period (9 days), samples cured at 60°C in the microwave oven showed a portion of 82% of reacted lime, while for the sample cured at 20°C, only 18% of lime was fixed. In [147], the authors stated that the hydrogarnet is not formed by the transformation reaction of the metastable hydrate phases, but as a result of the pozzolanic reaction between MK and lime.

Bakolas et al. [148] prepared several pastes by mixing commercially available products, metakaolin and hydrated lime in different proportions and examined them using TG-DTA analysis, XRD, MIP and compressive strength tests. Mineralogical results revealed the formation of hydrate phases due to hydration of cementitious material and phases formed due to the pozzolanic reaction between MK and hydrated lime. Furthermore, excellent results for lime consumption have been

achieved for paste with lime/MK ratio of 1. Finally, a clear shift in pore size distribution is observed with increasing MK contents, leading to a reduction in porosity and cumulative volume.

Additional studies have been carried out on systems based on air lime-based compounds [149,150].

In terms of finding the optimal compositional configuration of lime-MK-based systems, Vimmrová et al. [151] suggested the sequential simplex optimization methods as a promising technique for the design of composite building materials. Especially, for components exhibiting synergies, this method seems to be prospective as traditional optimization methods are very laborious, time-consuming and material-intensive.

Further studies on lime mortars containing treated clays and calcined ceramic wastes are extensively reviewed and presented by Matias et al. [152]. This review covers very well different topics like historical background, reaction mechanisms, pozzolanicity related lime-based mortars with clay-based admixtures, use of ceramic waste materials etc. and complements the literature, which are not discussed in this writing.

3.3 Gravel wash mud (GWM)

As the title of this research project "Recycling of gravel wash mud for manufacturing CO_2-reduced cement" suggests, one of the primary ambitions of this work is to reuse gravel wash mud (GWM), a waste product from sand/gravel quarrying, as a novel raw material to develop and manufacture CO_2-reduced cements. Therefore, the presentation and description of the prime raw material of this project, GWM, serves as a substantial part of this dissertation. The raw material was extracted from a settling basin of a sand/gravel quarry in Folschette, located in the Northwestern of Luxembourg. The mud-like residue is generated during the gravel extraction process, more precisely during the washing of sand and gravel aggregates.

The rock strata around the quarry primarily consist of red sandstone (ger. Bundsandstein); therefore, which explains the excavated rocks' reddish-brown outer layer: However, this clayey layer is removed as impurity by washing during the sieving and crushing processes of the rocks due to the quality requirements on the commercially sold aggregates. Theoretically, the washing of the aggregates is not required, however product guidelines and the clients' preference to buy the traditional, yellow-brownish aggregates, require the aggregates to undergo additional post-processing to fulfil the requested quality standards.

After the cleaning of the granules, the wastewater containing large quantities of clayey residues is pumped into a series of decanting basins, where the solid particles of wastewater start to settle, leading to the separation of decanted water and the sludge. The reddish-brown sludge is relatively homogeneous and has a very plastic consistency. After, the sludge is transported to a sludge lagoon, where it is temporarily stored until it is mostly transferred to landfilling. Usually, the

separation process is accelerated by applying a flocculating agent. For this work, the GWM was extracted a sludge lagoon and stored into plastic buckets or a storage vessel.

In the following sections, the regional origin and the general aspects of the raw material are portrayed and explained, followed by further details about the processing of the raw material, its regional acquirability and its consistency in quality.

3.3.1 Geography and Geology

The Grand Duchy of Luxembourg has a surface area of 2586 km^2, which is relatively small compared to its neighbouring states. Nonetheless, it offers a wide range of impressive geological diversity as depicted in **Figure 3.12**. Around 400 million years ago, during the Devonian geological period, a sea covered the entire territory of current Luxembourg and left behind sediments, which form the oldest layers of sedimentary rocks of the country. In a later period, these rock strata, which mainly consist of shale, were folded and stacked up to form a mountain range. Later, the layers of shale in the southern part of Luxembourg were covered by other sediments, so that the layers of shale are only visible on the surface of the northern part. These geological formations lead to the division of Luxembourg into two geological and geographical regions, namely the northern region called the Oesling (Éislek) and the southern region called the Gutland. This geological distinction is the result of an uplift motion of strata during the Late Tertiary. This movement leads to erosions of layers of sedimentary rock or soil that drew the current zonal irregularities between the Devonian and the Triassic rocks of Luxembourg. As the uplift movement of the regions was more pronounced in the northern part than in the southern part of Luxembourg, the erosion of the Mesozoic strata led to the current two geomorphological units [153].

The southern part, which covers two-thirds of the Luxembourgish territory, is composed of younger sedimentary rocks of the Trias and the Jurassic. These layers of sedimentary rocks or soils consist of soft units that are vulnerable to erosion like marls and erosion-resistant units like limestones, sandstones, dolomites and iron ores. The northern region, covering one-third of Luxembourg is part of the Ardennes plateau and is composed of old sedimentary rocks or soils from the Devonian period, which consist mainly of slates, schists and quartzites.

The location of the gravel quarry, where the gravel wash mud occurs as a waste during the washing process of the gravels and sands is situated in Folschette (Foulscht), a small town belonging to the commune of Rambrouch in western Luxembourg. The exceptional characteristic of this quarry is that it is situated precisely on the geological border between the Oesling and Gutland territory.

Figure 3.13 illustrates the local geological situation of Folschette. The gravel quarry is located in a zone, mainly consisting of red sandstone (pink; ger. Buntsandstein), which borders the first shale (green, schist; ger. Schiefer) unit of the northern region. Furthermore, the red sandstone sediments are surrounded by sediments of shell sandstone (blue, ger. Muschelsandstein) and “Schilfsandstein” (yellow).

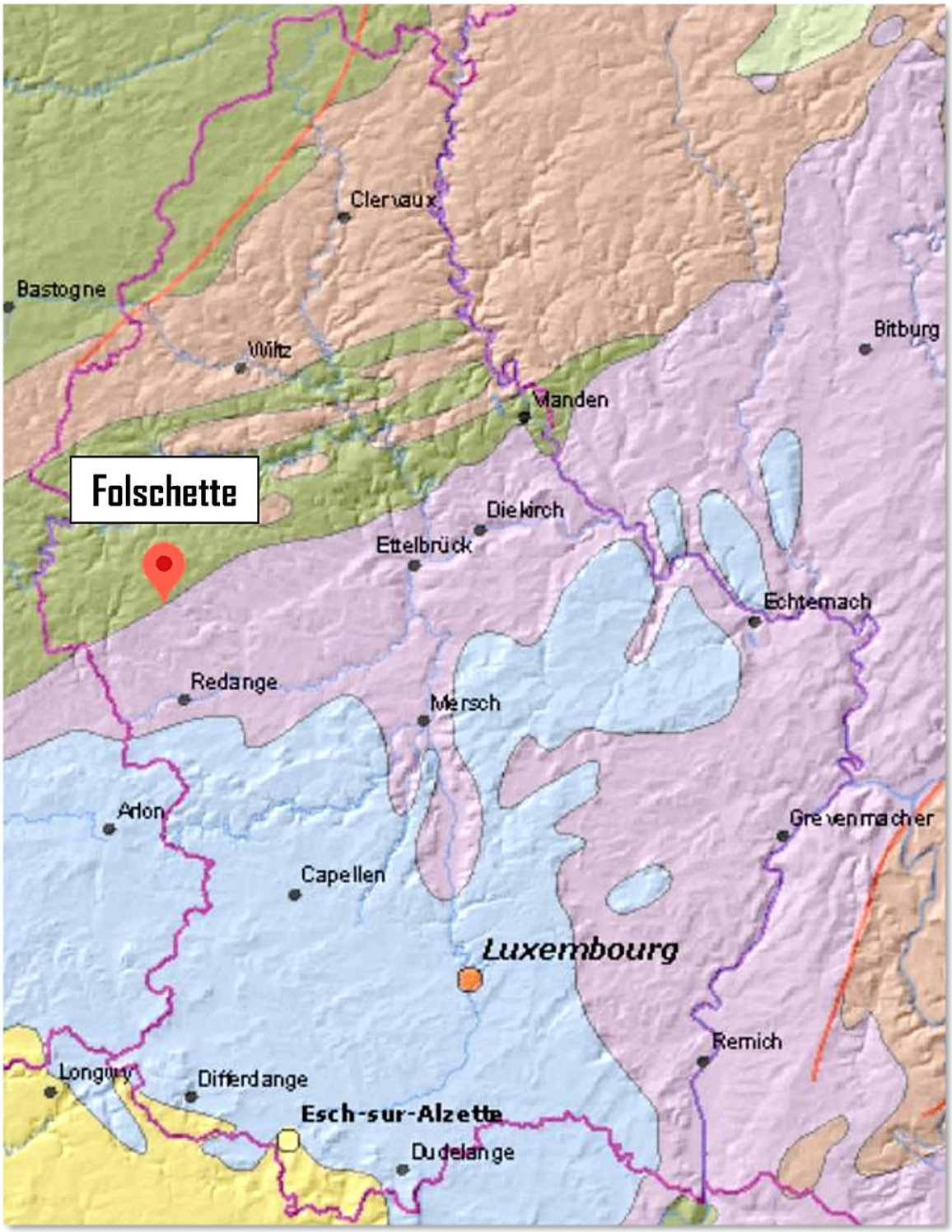

Figure 3.12 *- Geological map of Grand Duchy of Luxembourg (generated and modified from [154])*

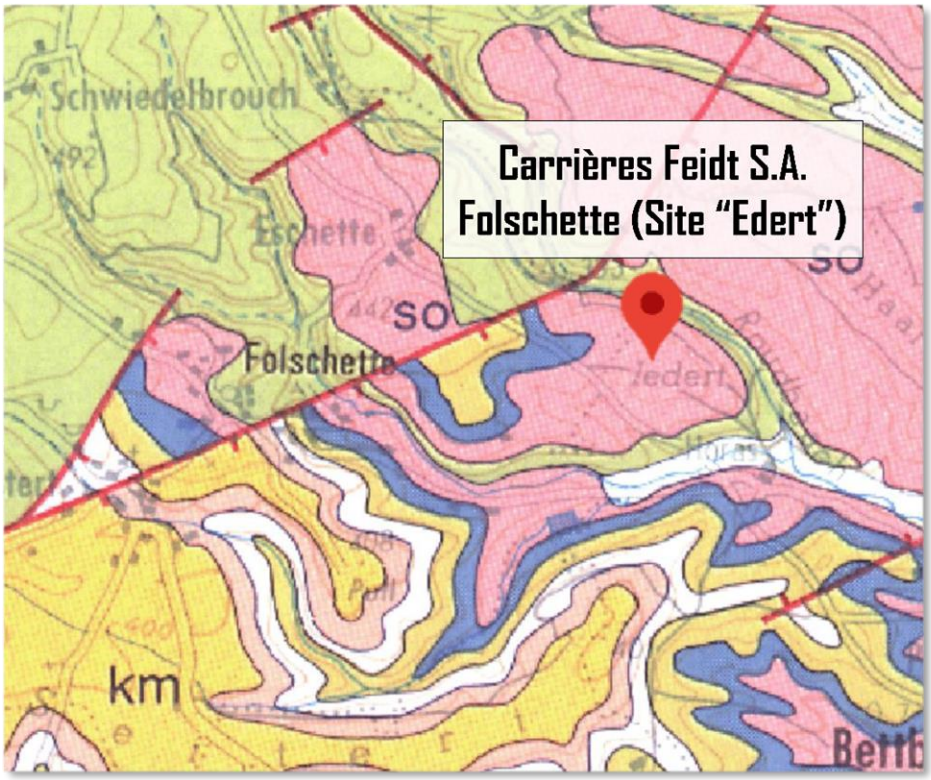

Figure 3.13 *- Geological map of the quarry site "Edert" in Folschette (modified from [155])*

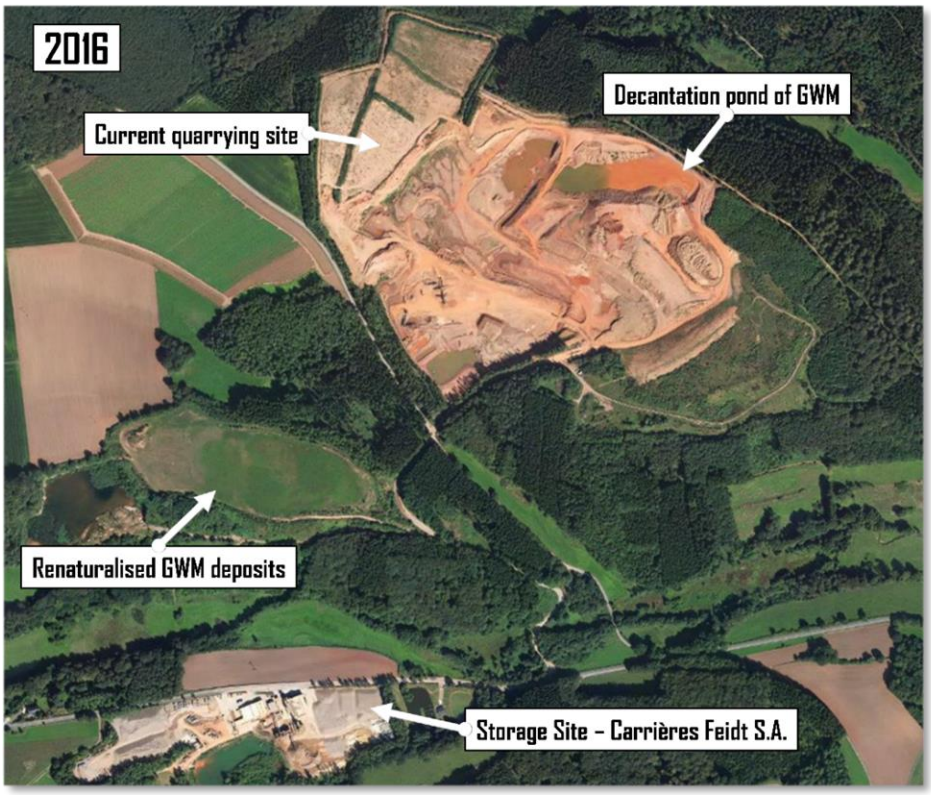

Figure 3.14 *- Overview of the sandstone quarry site (Carrières Feidt Folschette); GWM used in work is collected from the presented basin (generated and modified from [155])*

The sandstone quarry in Folschette is operated by a local private company called Carrières Feidt S.A., which is specialised in extraction and processing of natural stone, production of sand, gravel and crushed stone, sales of gabions and filler materials, and operation of landfills for inert waste. As illustrated in **Figure 3.14**, the site is divided into two parts. The first part is the material post-processing and storage site, where depending on the current site workload, the removed materials like stones, gravels and sands are directly delivered by trucks (**Figure 3.15**) from the excavation pit to the processing plant (**Figure 3.16**). The processing consists of several degrees of crushing, washing and screening processes depending on the excavated material. After processing, the materials are stored on-site until delivery to the clients.

Figure 3.15 *- Loading of the truck using a shovel excavator (Carrières Feidt Bruch)*

Figure 3.16 *- Fix processing plant next to the material storage site (Carrières Feidt Folschette)*

The second part encompasses the actual excavation site, where different layers of rock strata are removed by heavy machinery. There exist different quarrying techniques depending on the variations in the physical properties of the deposit such as density, fracturing and bedding planes, and of course, the site owner's preference. Nevertheless, the primary process consists in the identification of an appropriate geologic deposit, followed by localisation or creation of minimal breaks in the stone. Then, the material is excavated using heavy machinery and secured on-site for transport to the processing unit.

The excavated material is fed to the mobile processing plant consisting of a primary crushing unit, a jaw crusher, which breaks the stones by moving a heavy metal plate backwards and forwards against a fixed plate. The broken material is dropped on a conveyor belt, which leads to the first vibrating sieve where the fine material is collected. Depending on the required granulometry and the type of material, the crushing process is repeated in several stages with different crushing machinery. After each crushing process, the material is screened, and the oversized material is conveyed to the next crushing unit. In case of the processing unit depicted in **Figure 3.17,** already pre-processed material is fed to a cone crusher, and the crushed material is conveyed to a washing unit before it is screened and heaped at a temporary storage area.

After the washing of the aggregates, the water has become reddish slurry, and it contains a high portion of silt and clay. The thin slurry is pumped into a temporary storage basin before it is finally stored in a storage bond. Due to the setting of the slurry in the basin, there is the sedimentation of particles leading to the formation of the gravel wash mud. The material used as a raw material for this project was extracted from the GWM storage basin, which can be seen in the top right corner of **Figure 3.14**.

Figure 3.17 *- Mobile processing plant: washing and screening unit (Carrières Feidt Folschette)*

3.3.2 Processing of the raw material into the GWM powders

After extraction from the storage pond, the GWM was sealed into plastic buckets or a storage vessel and stored at ambient temperature. For the first batch of GWM, the mud contained a high portion of water, as, over time, the sedimentation of the particles separates a certain quantity of water from the sediment. Before beginning with preparation, the excess water was removed (**Figure 3.18-1**). For later batches of GWM, less excess water was present as the usage of flocculating agents at the storage basin, already reduced the water content of the collected pure GWM.

The sticky material is decanted from the bucket into a steel bowl (**Figure 3.18-2**). Then, the recipient is put in a laboratory oven at 105°C for 2 days for dehydration. The required time for dehydration depends on the quantity of material put in the bowl and the type of recipient used. However, once the GWM is dried out (**Figure 3.18-3**), it was fragmented into coarse pieces (**Figure 3.18-4**) using a hammer, so that it could fit the feed of the laboratory jaw crusher (**Figure 3.18-5**). The size of the crushed material, which passes through the jaw crusher, is dependent on the opening at the bottom of the crusher (**Figure 3.18-7**). The dried GWM is crushed twice to work more efficiently. First, the dried GWM was crushed coarsely to have a simple, workable material (**Figure 3.18-6**) and then it was finely crushed by setting the opening gap of the crusher to about 2 mm to have a fine GWM powder. (**Figure 3.18-8**). After milling, the fine powder material, uncalcined GWM (UGWM), was poured into a bucket and sealed until it was used for the thermal treatment process (calcination).

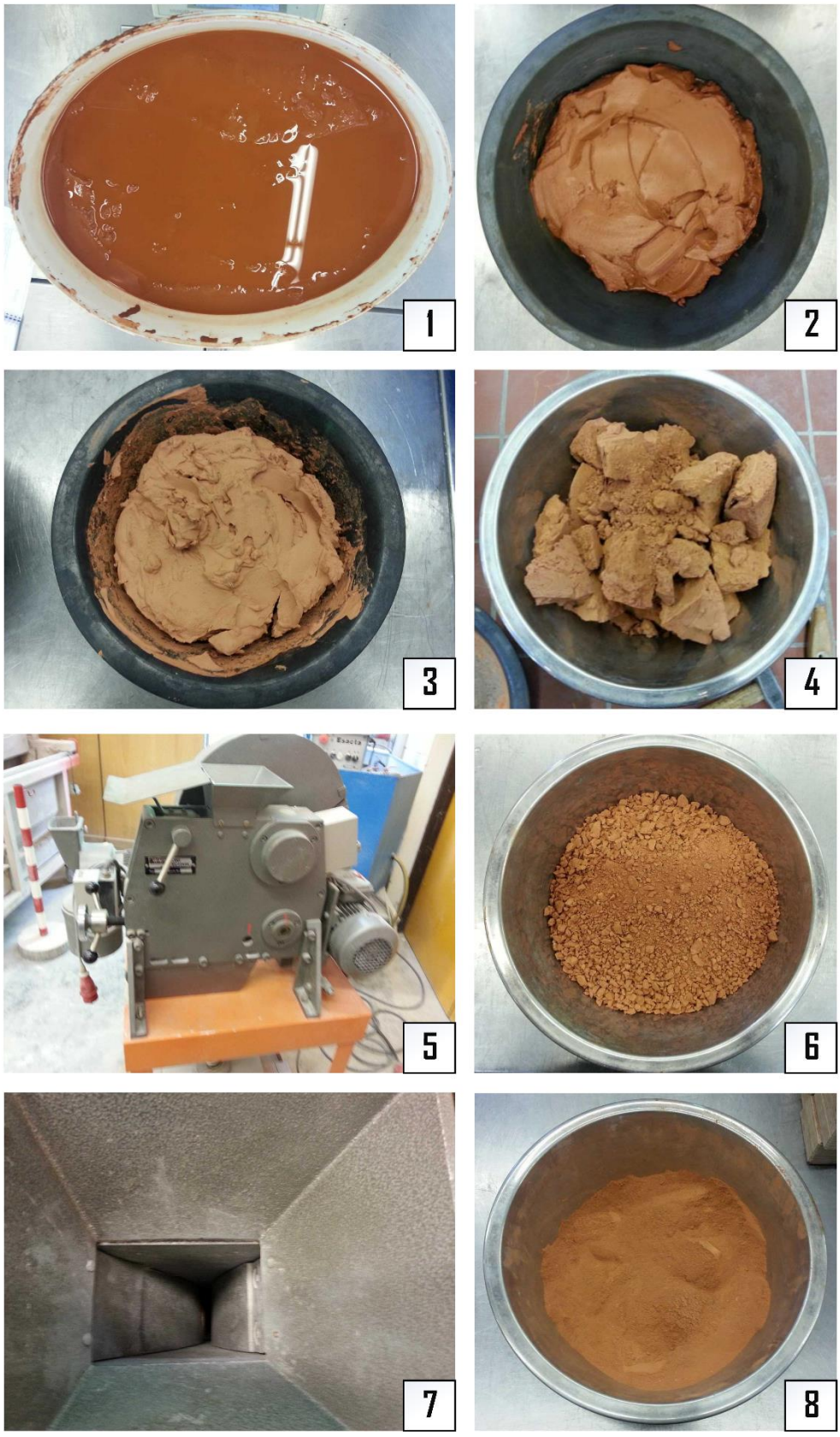

Figure 3.18 *- Material preparation: From GWM to raw material*

3.3.3 Thermal treatment process of the GWM powders

The thermal treatment of the GWM powders consists of the calcination of the raw material in a laboratory chamber furnace to impose a thermal decomposition of its minerals without reaching its fusion point. In general, calcination is used to modify the chemical or physical composition of a material by driving off crystalline water and volatile substances from the constituents or oxidizing a portion of the substance. In case of the GWM powders, the calcination is required for the dehydroxylation of clay minerals into a high-energy and nearly amorphous meta-state. One of the main reason to use the concept of calcined clays to develop alternative cementitious binders is the fact that the dehydroxylation process occurs at lower temperatures than the burning of cement clinkers.

The calcination of the dried GWM powder is carried out using a laboratory chamber muffle furnace with radiation, branded as m “Nabertherm, Model N41/H” with adjustable duration and temperature control unit (**Figure 3.19-1**). The maximum reachable temperature is about 1200°C. The GWM powders are poured in porcelain crucibles (**Figure 3.19-2**) and placed in the furnace heated from two sides by ceramic heating plates.

The heating of the furnaces starts after the crucibles are put in the oven, and the temperature is increased until reaching the target temperature. The temperature is held for one hour, and the calcined material is let to cool down to room temperature naturally inside the oven before the crucibles are taken out. Finally, the calcined material is stored in sealed buckets until their use in the preparation of mixtures.

Technical note: At the beginning of the project, small porcelain crucibles were used for calcining the GWM powders. Therefore, only small quantities of material could be processed, and the

preparation of the material was inefficient and laborious. Hence, those crucibles were replaced by larger ones to be able to calcine larger quantities of GWM powder and to have better stability during the handling of the heated material.

Figure 3.19 *- Calcination of the fine GWM powder*

3.3.4 Fractions of GWM powders

In a subproject related to this research project, the physical and chemical characteristics of different fractions of the GWM were studied, and their potential for alkali-activation was examined. These investigations were conducted by Alejandra Mora Rincón as the main topic of her master thesis, entitled as "The effect of alkali-activated binder on clay-silt (PS<20µm) from gravel wash mud" [156]. This study was carried out partly in the Laboratory of Solid Structures at the University of Luxembourg and in the laboratories at the Department of Geology of the University of Trier under the supervision of Ass. Prof. Dr.-Ing. Danièle Waldmann-Diederich, Prof. Dr. rer. nat. Jean Frank Wagner and M.Sc.Eng. Vishojit Bahadur Thapa.

The main emphasis of the following sections relies on showing the different fractions in the particle size distribution of GWM, which were examined by Mora Rincón [156]. Therefore, the applied methods are shortly introduced, and the different fractions are presented.

One of the objectives of this subproject was to analyse the different particle sizes independently and to evaluate various fractioning procedure to ensure the separation of different particle size ranges. The applied fractioning methods were the wet sieving method for the coarser fraction and the suspension methods for the finer fractions. The GWM was separated into four different size ranges:

< 2 µm	**→**	**clay**
2 – 20 µm	**→**	**fine-silt**
20 – 63 µm	**→**	**coarse-silt**
> 63 µm	**→**	**sand**

The wet sieving method on the GWM was performed by adaptation of the procedures according to AASHTO T11 [157]. In **Table 3.5**, the procedure of the sieving method is shortly presented and explained.

A quantity of GWM of max. 600 g is washed through a 63 µm sieve (#230) until the wash water becomes clear.
The retained fraction on the sieve is stored at room temperature for drying:

PS > 63µm – sand

The fractions passed through the 63 µm sieve is then sieved through a 20 µm sieve (#635), and the retained fraction is stored at room temperature for drying:

20 < PS < 63µm – coarse silt

***Table 3.5** - Wet sieving method (modified and adapted Figure 12 from [156])*

The wet sieving method does not apply to, respectively, is not suitable for the fractions of the GWM smaller than 20 µm; therefore, the gravimetric sedimentation method is used. In **Table 3.6**, the procedure of the sieving method is shortly explained and visualised using pictures.

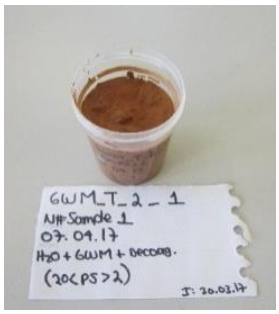

A quantity of GWM of approx. 500g is put in a cylindrical glass. Then, 500ml of distilled water and 25ml of dispersing solution are added. Subsequently, the cylindrical glass is thoroughly mixed for 60min and left for equilibration for 24 hours. After, the recipient is filled up with distilled water up to the 1L mark and left to rest for approx. 14 hours. Finally, the suspended material is put into another plastic cylinder, whereby the settled material remains in the initial recipient.

Note: This procedure is repeated until the water becomes as clear as possible.

The settled material is weighted and stored at room temperature for drying:

2 < PS < 20µm – fine silt

The suspended matter (Non-settled material) is transferred into a plastic cylinder, centrifuged for 60min and the excess water is removed. Subsequently, the settled fraction is weighted and stored at room temperature for drying:

PS < 2µm – clay

Table 3.6 *- Suspension method (modified and adapted Figure 13 from [156])*

Figure 3.20 shows the colour differences from one fraction to another of GWM powders. The coarser fraction has a more yellowish colour tone as it mainly consists of sand and coarse silt material. The finer the GWM, the more the colour tone shifts towards a reddish-brown colour, which is typical for fine silt to clayey materials.

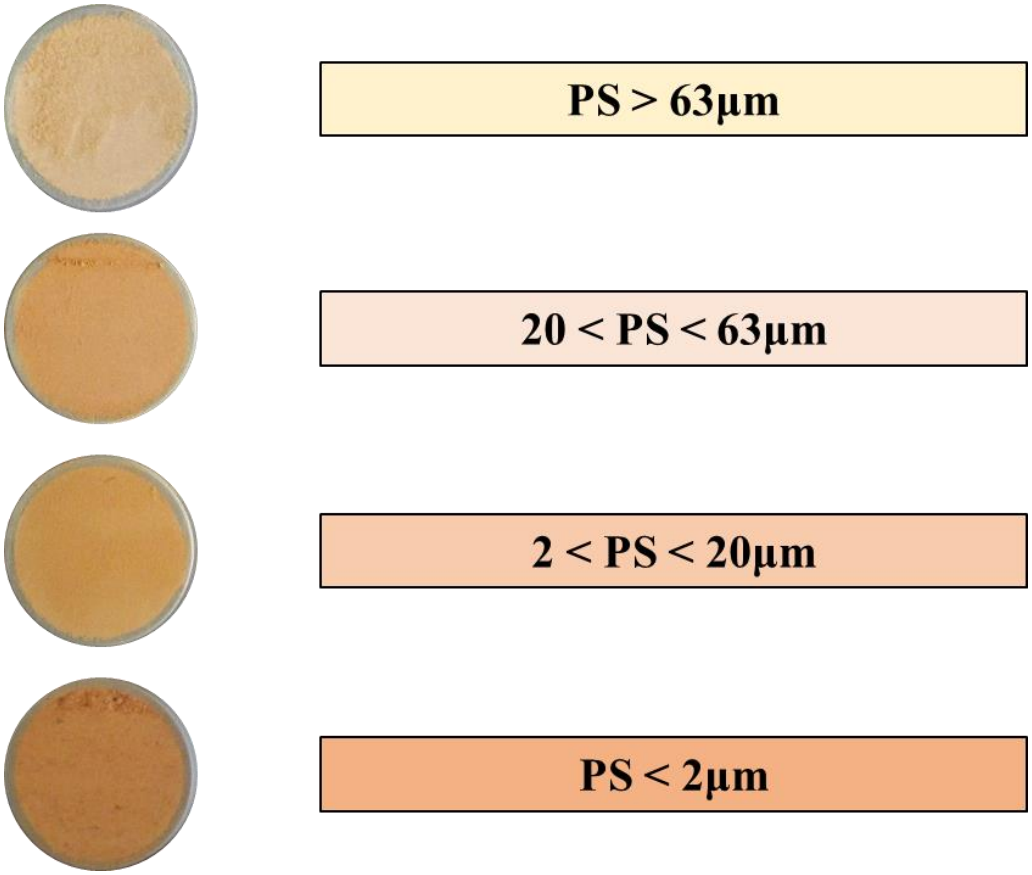

***Figure 3.20** - Colour tone of each GWM fraction (modified and adapted Figure 18 from [156])*

3.3.5 Quantity and Quality of GWM

This section provides data, knowledge and responses to three major questions concerning gravel wash mud (GWM), which are not directly related to its performance as a SCM in the different binder concepts. These enquiries interrogate the long-term acquirability, the qualitative and quantitative stability of GWM as a local resource (an industrial waste product), and the existence of unexploited deposits with similar potentials.

3.3.5.1 Quality and homogeneity of GWM

Industrial manufacture is significantly dependent on the ability of suppliers to provide quality raw materials. Therefore, an essential prerequisite for the usability of GWM as a long-term resource arises around the consistency of its quality and its homogeneity, as a large heterogeneity of its chemical and mineralogical composition as well as a wide range of its particle size spectrum would not be economically and technically justifiable from an industrial standpoint.

According to the head geological expert of Carrières Feidt S.A., Paul Wertz, considering the current activities and the organisation of the quarry in Folschette, two sources of GWM can be foreseen for revalorisation: the old backfills and heaps of GWM and the GWM from the decantation basins that are currently being filled. Other GWM deposits are buried under the landfill deposits of the extraction site and therefore currently inaccessible and unusable. Nonetheless, the GWM from the potential sources was prepared following the same process, namely decantation (gravitational precipitation). Overall, a certain degree of variety of the granulometry and compositions of the deposits can be expected. This vertical and horizontal heterogeneity is linked

to the configuration of the discharge circuits of the muds and to the involved hydrodynamic motions inside the full width and depth of multi-layered decantation basins.

However, over the last decade and even earlier, various samples of the GWM in Folschette were collected at different times for various studies on their potential. Based on the data of the present research work and the findings reported in the theses of Andreas Thomé [158] and Danae Cardenas [159], a study on the evolution of the granulometry, the chemical composition and the mineralogy of dried, uncalcined GWM powders (UGWM) is presented. The different abbreviations used in the following paragraphs are explained, and some relevant details are provided in **Table 3.7**.

Sample	UGWM_2008_Thomé	UGWM_2015_Cardenas	UGWM_2017	UGWM_2018	UGWM_2019
Year of GWM collection	2007	2015	2016	*2018*	
Explanation of the used abbreviation and important details	Dried GWM reported in the diploma work of A. Thomé.	Dried GWM powders reported in the master thesis of D. Cardenas. The suffixes “unground” designate the coarsely crushed powders, and “ground” present the finely milled powders.	Dried GWM powders from the first collection of pure GWM within this work. The indication “Cimalux”, designates the powders which were milled in the laboratories of Cimalux S.A.	Dried GWM powders from the second collection of GWM within this work. The on-site separation process of these GWMs was accelerated by the usage of flocculating agents.	

Table 3.7 *- Explanation of the used abbreviations and important details*

The evolution of the particle size distribution of the different UGWM powders prepared over the period from 2008 to 2019 are presented in **Figure 3.21**. . The PSD analysis of the different GWM reveals that, independently of the date of collection and the applied powder production process, all UGWM presented almost identical a similar PSD curves, which confirms the consistency of the granulometry of the GWM powder produced within this project. Moreover, the older UGWM powder samples show close and slightly finer grain size distributions with average particle size ranges (d50) between 4-7 μm.

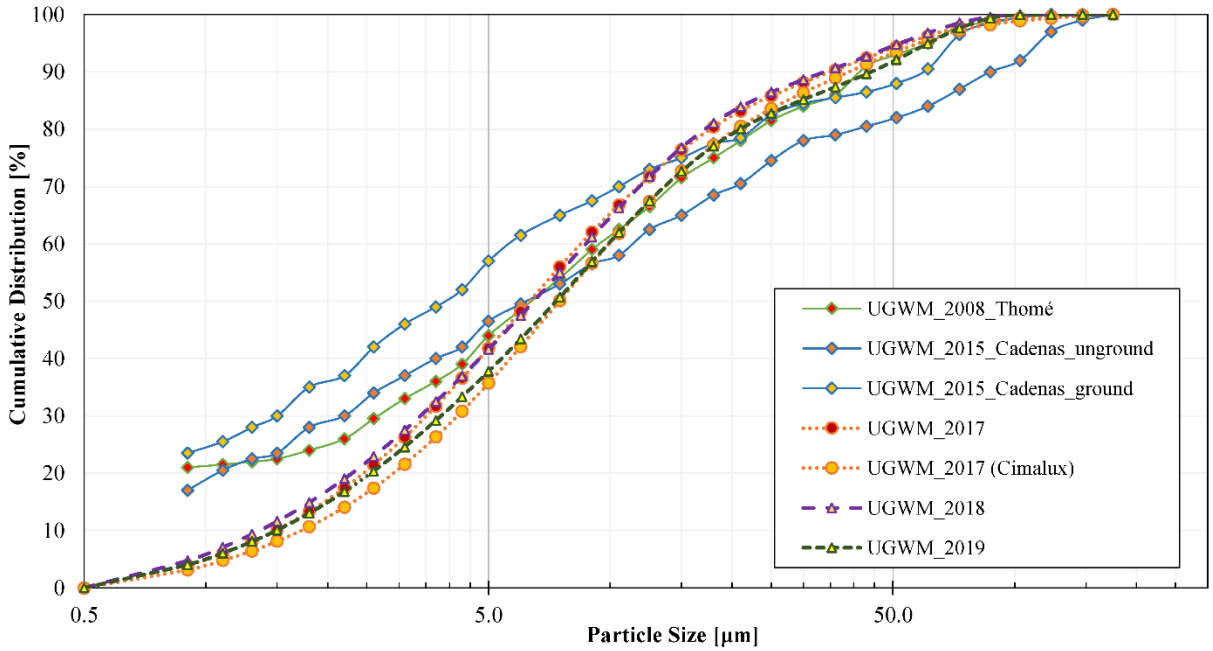

Figure 3.21 *- Evolution of the particle size distribution (PSD) of uncalcined GWM powders from 2008 to 2019*

Furthermore, **Table 3.8** presents the differences in the chemical composition of the different GWM samples. As expected, no significant differences between the UGWM powders used within this project can be reported, and only slight variations in the minor contents can be observed compared to UGWM_2015_Cardenas. Unfortunately, no data on the elemental composition of UGWM_Thomé were available.

Sample	**Chemical composition**										
	SiO_2	Al_2O_3	Fe_2O_3	FeO	CaO	MgO	SO_3	Na_2O	K_2O	TiO_2	MnO
[-]	[%]	[%]	[%]		[%]	[%]	[%]	[%]	[%]	[%]	[%]
UGWM_2015_Cardenas	56-71	12-18	5.00	1.00	1.00	1.50	-	0.50	2.00	-	-
UGWM_2017	64.95	19.98	9.02	-	0.26	1.30	-	-	3.27	0.70	0.08
UGWM_2018	65.06	19.53	9.37	-	0.41	1.66	0.09	0.24	2.72	0.85	0.06
UGWM_2019	64.97	19.50	9.35	-	0.41	1.66	0.09	0.24	2.72	0.85	0.06

Remark: Chemical composition of UGWM_2008_Thomé was not provided in [X]

Table 3.8 *- Evolution of the chemical composition of uncalcined GWM powders from 2008 to 2019*

Table 3.9 presents the crystalline phases identified during the XRD analysis of the different UGWM powders. For all investigated UGWM powders, the presence of quartz, muscovite/mica, illite, kaolinite, hematite phases were reported, and the main phases were the quartz minerals, followed by the clay minerals. In addition, from the qualitative analysis of the UGWM powder used in this work, the presence of chlorite in all samples was detected. The authors, who analysed the GWM powders from older sample collections, reported the identification of traces of smectite, calcite, plagioclase, feldspar and goethite phases, which were not identified in the GWM powders of this project. However, the "undetected" phases are subcategories of the main mineral group of Phyllosilicates. The slight variations in the mineralogical findings of the minor phases are natural and to some extent can also be explained by the differences of the applied XRD methods (quantitative and qualitative), the applied instrument configurations, user preferences and other influencing factures such as preferred orientations, impurities, sample preparation and type of x-ray sources.

Mineralogical composition (Identified phases)					
Sample	UGWM_2008_Thomé	UGWM_2015_Cardenas	UGWM_2017	UGWM_2018	UGWM_2019
XRD method	Qualitative	Qualitative	Quantitative		
Detected XRD phases	Quartz Illite Kaolinite Mica (Muscovite) Chlorite Smectite Calcite Plagioclase Hematite	Quartz Illite Kaolinite Illite - Smectite Fe-Chlorite Feldspar Goethite Hematite	Quartz Illite Kaolinite Muscovite Hematite Potassium mica ($KAl_3Si_3O_{11}$) Chlorite (qualitative) Medium content of amorphous phases		

***Table 3.9** – Overview of the identified XRD phases of uncalcined GWM powders from 2008 to 2019*

Finally, the consistency of quality of the GWM powders used in the different projects over the last years ranged within a controllable range of variability. Based on the evaluation of existing data,

no larger heterogeneity of the used GWM can be reported. A detailed assessment program on a larger set of selective GWM samples from different depths of various decantation ponds might allow giving conclusive evidence on the quality of the total exploitable GWM deposits in Folschette.

3.3.5.2 Quantitative availability of the GWM

An estimation of the available quantities of GWM in Folschette is given using a map (**Figure 3.22**) of the quarry site "Edert" by showing historical and current deposits of GWM.

Position A – Historical backfills

This location highlights the area of the historical backfills and heaps of GWM in Folschette. This area is currently in the process of renaturation and probably will never be subject to future extraction (remobilisation). The available volume of GWM can be estimated very roughly at around one million tonnes. Unfortunately, the exact surface topography of the core of the heap, the accurate composition of each stratum as well as the actual depth and the extent of these deposits are not available to provide a better quantitative assessment. However, even if these historical deposits have very heterogeneous compositions, they are included in the estimation of the total exploitable material reserves in Folschette.

Position B & C – Western and Eastern Basins of the quarry site "Edert"

This area locates the first decantation basin, the "Western" basin, which was put into place during the start of the operations of the previous processing plant at the location of the current extraction pit. This older decantation pond was entirely filled over a period of about 28 months with an estimated volume of about 80000 m^3 of GWM. At the moment, a second basin, the "Eastern" basin

is used for sludge settling, its capacity is estimated at about 105000 m^3, and the GWM disposal started in September 2019. A rough estimative calculation reveals that, in these basins, there is enough availability to extract around 0.42 Mt of pure GWM, which can be used to produce around 0.24 Mt of dry GWM powders.

Position D – Central Basin of the extraction site Edert

Another new decantation pond is currently in preparation to cover the remaining extraction pits in the central zone of the quarry site "Edert".

Overall, the sandstone quarry in Folschette, operated by Carrières Feidt S.A., has an overall hourly production volume of about 400 tonnes and around 20 wt.% to 25 wt.% of the processed raw materials is disposed and end up in the decantation basins as GWM. Considering the existing quantities of landfilled GWM, the constant daily GWM production volumes and the future excavation activities of the quarry in Folschette, it can be concluded that there is a massive availability of the GWM to be used as a local resource in other industrial activities like cement production.

***Figure 3.22** - Location of historical and current deposits of GWM on the quarry site "Edert" in Folschette (Carrières Feidt Folschette) (generated and modified from [155])*

3.3.5.3 Regional and national occurrences of similar deposits

As long as the activities on the quarry site “Edert” are in progress, further successive settling basins will be set up, and the generation of GWM as industrial production waste is unavoidable. Current estimations indicate that there are still material reserves to be exploited for the next eight years. Further reserves of exploitable red sandstones (Buntsandstein) exist in the surroundings of the quarry in Folschette; however, their exploitability depends on the expenses for the acquisition of the required lands and the approval of authorisation by of the administrations to extend the quarrying activities in that region.

Apart from the availabilities of local reserves around the quarry site “Edert” and its possible extensions, there still exist potential reserves of red sandstone in the Gutland region of Luxembourg. However, the accessibility to these lands is economically and administratively almost unviable as such an ambitious and difficult endeavour would imply the acquisition and the investment in equipment of a new quarry site and most likely the deforestation of protected zones.

There exist further rock strata of red sandstone in the marginal areas between the Northern and the Southern regions of Luxembourg in the form of conglomeratic deposits of sand and silt layers. Unfortunately, the preliminary tests on samples of potential rock strata by Carrières Feidt S.A. revealed low profitability of the reserves due to higher fineness and greater heterogeneity of the raw material.

Finally, besides of the clay-based gravel wash muds, Carrières Feidt S.A. also generates massive amounts of dolomitic gravel wash muds from the extractions of dolomite gravel for concrete production. This quarry waste product presents similar characteristics and potentials for revalorisation as the clayey GWM, which probably need to be investigated in future projects.

Chapter 4 Publication I - Assessment of the suitability of gravel wash mud as raw material for the synthesis of an alkali-activated binder

Abstract

Gravel wash mud (GWM), a waste product from gravel mining was dried and processed into a fine powder to be activated by different concentrations of sodium hydroxide (NaOH) solutions for the synthesis of an alkali-activated binder. The GWM powders were thermally treated at five different calcination temperatures 550, 650, 750, 850 and 950°C. The characterisation of the raw material comprises the particle size distribution (PSD) by laser granulometry, the chemical and mineralogical composition by X-ray fluorescence and X-ray diffraction analysis respectively, and simultaneous thermal analysis. The performance of the alkali-activated binders were examined using compression strength tests and the microstructure was observed using scanning electron microscopy (SEM). The GWM was classified as an aluminosilicate raw material with kaolinite and illite as main clay minerals. Furthermore, a mean particle size around 6.50 μm was determined for the uncalcined and calcined GWM powders. The SEM images of the developed binders showed the formation of a compact microstructure, however, relatively low strengths were achieved. This preliminary study highlights an example of an aluminosilicate prime material, which shows very promising chemical and mineralogical characteristics, but its suitability for alkaline activation without further additives was not confirmed as far as performance-based criteria are considered.

Keywords - Gravel wash mud, thermally activated clays, alkali-activated binder, illite, kaolinite.

4.1 Introduction

Today's trend of revalorising waste products or industrial by-products to reduce the use of Ordinary Portland Cement (OPC) in building or road constructions has become an ambitious goal and a key objective of current political strategies, industries and research institutions [160–162]. Concrete, mainly based on OPC, is stated as the second most used material in the world after water and its production generates up to 5% of the overall annual CO_2 emissions worldwide. One of the main factors responsible for the unfavourable ecological performance of OPC is the high CO_2 emissions linked to the cement production processes like clinker burning including the chemical conversion of limestone ($CaCO_3$) into lime (CaO) and the emissions related to the fossil fuel combustion during cement production [163]. Nevertheless, the current demand for cementitious binder is reaching record values each year and this trend is likely to increase. However, the incentive of developing sustainable and robust building concepts using alternative construction materials has become increasingly relevant. Therefore, there is a growing challenge in the research communities to develop new, durable and environmental friendly binders as an alternative to OPC binders [164].

The concepts of alkali-activated binders or geopolymer cements are intensively investigated and discussed as a very promising alternative to OPC. However, even if the concepts of alkali-activated materials and the geopolymer technology are researched since last mid-century, there are discrepancies and no overall accepted consensus considering the terminology of these materials. **Figure 4.1** shows a short illustration of the general differences between alkali-activated binders and geopolymers in terms of characteristics of the raw materials, activating solutions and reaction mechanisms.

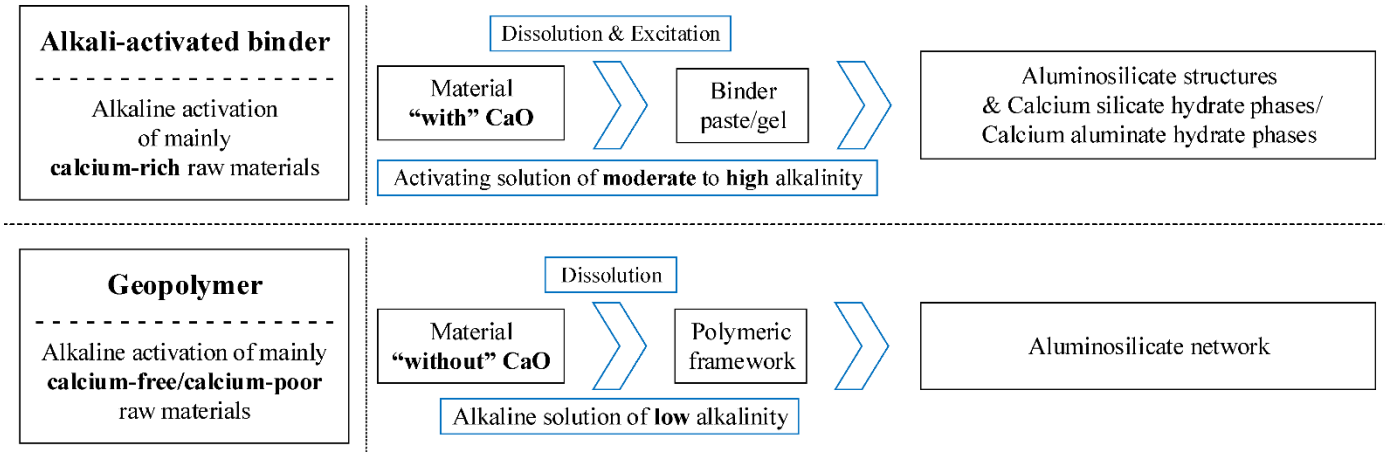

Figure 4.1 *- Overview of the general reaction mechanisms of alkali-activated binder and geopolymer*

Glukhovsky [29] was the pioneer in this field of research as he extensively studied the presence of analcime phases, which are classified as zeolites, in the cements of ancient constructions and later developed binders made from aluminosilicates in reaction with alkaline industrial wastes, which he named "soil silicate concrete" and "soil cements". The early investigations on alkali-activated binders mainly focused on the activation of blast furnace slag, a by-product of the metallurgical industry. After, the next wave of interest raised after the results of Davidovits [23,30], who developed and patented a novel binder [31,32] which he named "geopolymer cement". The first geopolymer binder was a slag-based geopolymer cement, which consisted of metakaolin, blast furnace slag and alkali silicate. The main driver for the development of this technology is the lower environmental impact compared to OPC technology. Several authors have evaluated the CO_2 emissions related to the production of these binders and have stated significant reductions of up to 80% lower CO_2 emissions compared to cement production [165,166]. Further benefits over conventional concrete is the rapid strength gain while reaching the maximal strength at early hours and the development of a durable and compact microstructure [23]. Moreover, higher thermal resistance, higher resistance to chemical attack, low permeability and better passivation of the steel reinforcement have been identified [167,168]. Finally, the production of alkali-activated binders

or geopolymer cements provides a sustainable and viable alternative use for “waste” materials, which are very uneconomically disposed in landfills.

Subsequent studies have been carried out based on these original material concepts and various authors have contributed by their research to the understanding of the chemical mechanism and the development of alkaline binders [15-29].

However, the application of these binders in construction elements has already become challenging as the price of these commercially available raw materials has risen over the last decades due to the high demand and the limited availability of adequate resources, which is highly dependent on the primary industrial processes. Therefore, there is a trend to investigate on alternative prime materials to be revalorised for development of alkali-activated binders.

Sun et al. [61] investigated on the synthesis of geopolymers out of waste ceramics, which were activated by alkali hydroxides and/or sodium/potassium silicate solutions. The maximum compressive strength for the synthesized geopolymer pastes measured after 28 days was 71.1 MPa and favourable thermodynamically stable properties in terms of compressive strength evolution after thermal exposures were observed. Pacheco-Torgal et al. [56] investigated on an alternative to OPC using tungsten mine waste mud as prime material. The mineralogical analysis indicated the presence of muscovite and quartz minerals. After activation with a mix of sodium hydroxide and sodium silicate, different fine aggregates were added and the new binders showed very high strength at early ages. The compressive strengths for the different mixtures measured after 28 days ranged from about 60 up to 75 MPa. Poowancum et al. [57] developed a geopolymer binder using water-treatment-sludge and rice husk ash as raw material. The alkaline activator used was a mixture of sodium hydroxide and sodium silicate and the resulting maximal strengths were around 16 MPa for a rice husk content of 30%. Chen et al. [55] studied the practicability of calcined sludge

from a drainage basin of a water reservoir as a precursor for alkaline activation into an inorganic polymer. The raw material consisted of a sludge containing fractions of silts and smectite clays with high content of aluminosilicates (around 85%) and some impurities. The maximum compressive strength measured after 28 days was 56.2 MPa using the raw material calcined at 850°C.

Ferone et al. [175] examined the potential of two clay sediments from different reservoirs, Occhito and Sabetta, as potential raw materials for the production of geopolymer binder. These sediments were subjected to different calcination treatments and the binder was synthesized by mixing the calcined aluminosilicates with 5 M NaOH solutions. After undergoing different curing conditions, the mechanical performance of the samples was examined. In general, a rapid strength development was reported and the maximal achieved compressive strength was around 10 MPa for the samples made of Sabetta sediments. Finally, the authors stated that the calcination temperature applied to the sediments plays a major role in the effectiveness of the geopolymerisation.

Molino et al. [176] performed a similar series of experiments on calcined sediments from Occhito reservoir to synthesise binders using various concentrations of three different alkaline solutions, namely sodium hydroxide solution, sodium aluminate solution and potassium aluminate solution. The authors recommended for impure precursors with low content of alumina to use alumina-containing activating solutions as the samples activated with the sodium aluminate solution showed the best mechanical performance and achieved compression strengths up to 7 MPa.

Recently, Messina et al. [177] conducted investigations on the production of precast building elements by the synthesis of geopolymer binders based on water potabilization sludge and clayey sediments, both considered as waste products from reservoir management. After calcination,

different proportions of the raw materials were activated using a mixture of sodium silicate solution and a 14 M sodium hydroxide solution. The highest mechanical performance of the binders is stated around 23 MPa in compression strength and around 2 MPa in tensile splitting strength.

In general, further research on potential alternative raw materials could approve their adequacy for OPC replacement as a high compressive strength and low cost alkali-activated binder [41,178–182].

In this work, the suitability of a waste material, gravel wash mud (GWM), as raw material for the development of novel binders is examined by conducting different material characterisation techniques and experimental tests. The main focus relies on finding the best parameters for the calcination of the GWM powders. An optimal calcination time and temperature range will be suggested after exposure to selected high temperatures ranging from 550°C to 950°C. The raw materials were characterised by simultaneous thermal analysis (thermogravimetric analysis and differential scanning calorimetry, TG-DSC), XRF and XRD. An optimal alkali-activated binder is selected based on mechanical testing and the evaluations based on SEM images. The findings of this study will enrich the investigations on alkali-activation of alternative raw materials to revalorise waste products economically and environmentally.

4.2 Experimental procedure

4.2.1 Materials

The prime material for this study, gravel wash mud (GWM), originates from Folschette (Rambrouch, Luxembourg) and consists of wet deposits, which occur during gravel extraction, more precisely during the washing of sand and gravel aggregates. The reddish brown mud is quite homogeneous and has a very plastic consistency. The raw material was extracted from a storage basin and provided by Carrières Feidt S.A., the operating company of the quarry. The geological analysis of the extraction site reveals that the rock strata mainly consists of red sandstone (ger. Buntsandstein) in form of conglomeratic deposits of sand and silt layers [183–185].

The GWM was dried at 105°C in a laboratory oven until reaching a constancy of mass (± 2 days) and the dried prime material was ground into a fine powder. In the following process, the powder was calcined for 1h at different temperatures 550°C, 650°C, 750°C, 850°C and 950°C (heating rate of about 5°C/min) in a laboratory chamber furnace with radiation heating (Nabertherm, Model N41/H).

The sand aggregates used were CEN-standard sands according to EN 196-1. The standard sand has a characteristic grain size distribution with particle sizes ranging between 80 µm and 2 mm.

The hydroxide (NaOH) solutions were prepared by dissolving commercially available NaOH pellets (≥ 99% purity) in different portions of distilled water to obtain NaOH solutions of different molar concentrations (8M, 10M and 14M). As the dissolution process of NaOH is an exothermic reaction, the solutions were let to cool down in sealed bottles to avoid evaporation and the capture of carbon dioxide (CO_2) from air to form sodium carbonate. The bottles were stored for 24 h at room temperature before usage.

4.2.2 Synthesis of the alkali-activated binder and mixing proportions

Two large series of alkali-activated binders were prepared (**Figure 4.2**). The first series consists of binders, which were prepared by mixing different calcined GWM powders with three concentrations of NaOH solutions, 8 M, 10 M and 14 M. The second series of mixtures comprises the same mixing materials with further addition of standard CEN sand at mass proportions of 3:1 to the calcined GWM powders. The incorporation of aggregates allows to analyse the coverage of the grains by the binder and to verify the formation of a more compact microstructure with higher mechanical performance. The liquid/solid (L/S) ratio represents the relation between the contents by mass of the alkaline solution and the solid constituents (GWM powders and sand). This ratio was kept constant for both series of mixtures at 0.7, respectively 0.8 (except 0.9 for 14M with addition of sand). Finally, nine specimens from each mixture were prepared to have specimens for different curing times, 14 days, 28 days and 56 days (3 specimens for each curing time). In total, 270 specimens were prepared using the compositions and mixing proportions as listed in **Table 4.1**.

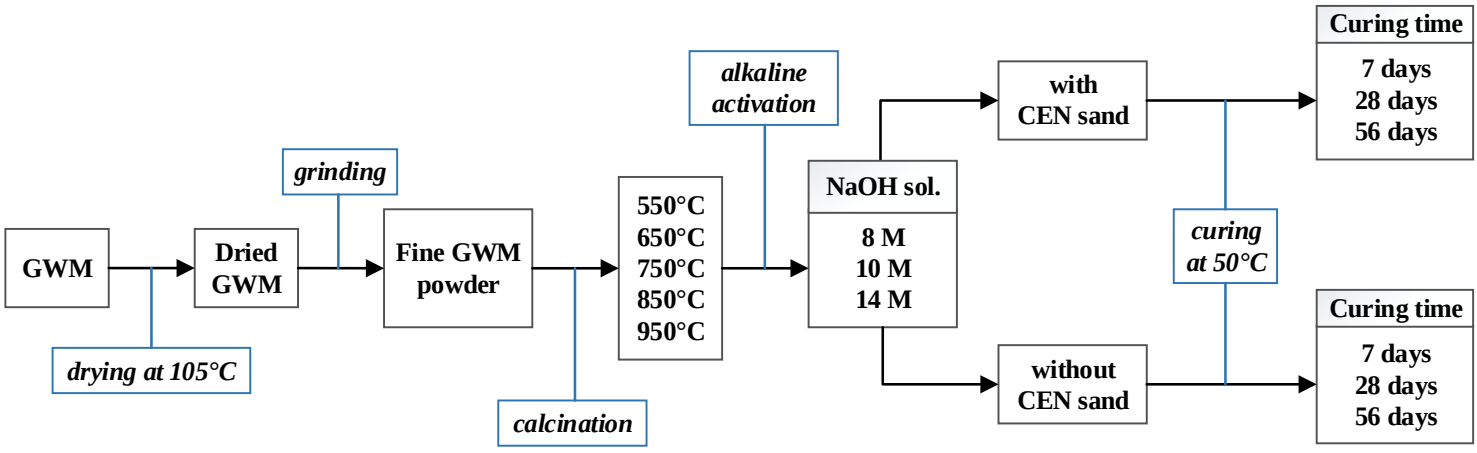

***Figure 4.2** - Overview of the mixture composition of the alkali-activated binders*

Sample ID	CT[a]	M[b]	L/S ratio[c]	S:G[d]	Sample ID	CT	M	L/S ratio	S:G
G_550_8		8 M			GS_550_8		8 M	0.8	
G_550_10	550°C	10 M			GS_550_10	550°C	10 M	0.8	
G_550_14		14 M			GS_550_14		14 M	0.9	
G_650_8		8 M			GS_650_8		8 M	0.8	
G_650_10	650°C	10 M			GS_650_10	650°C	10 M	0.8	
G_650_14		14 M			GS_650_14		14 M	0.9	
G_750_8		8 M			GS_750_8		8 M	0.8	
G_750_10	750°C	10 M	0.7	-	GS_750_10	750°C	10 M	0.8	3:1
G_750_14		14 M			GS_750_14		14 M	0.9	
G_850_8		8 M			GS_850_8		8 M	0.8	
G_850_10	850°C	10 M			GS_850_10	850°C	10 M	0.8	
G_850_14		14 M			GS_850_14		14 M	0.9	
G_950_8		8 M			GS_950_8	950°C	8 M	0.8	
G_950_10	950°C	10 M			GS_950_10		10 M	0.8	
G_950_14		14 M			GS_950_14		14 M	0.9	

Further information: Designation principle: G(S)_CT_M with "G" for GWM & "GS" for GWM with sand;
3 specimens per curing time (14 days, 28 days and 56 days) were prepared for each mixture.

[a] CT - Calcination temperature
[b] M - Molarity of activating solution
[c] L/S - Liquid to solid (mass) ratio
[d] S:G - Sand to GWM (mass) ratio

***Table 4.1** - Mixing proportions of all investigated alkali-activated binders*

The mixtures without additional aggregates were prepared by adding the calcined GWM powder in a mixing bowl and by mechanically mixing the powders at a speed of 125 rpm for 90s with gradual addition of the alkaline solution. Subsequently, the mixture was mixed at a speed of 250 rpm for 90s until a good processible compound has formed. The mixing procedure of the binders with additional aggregates consists of primarily preparing the binder (GWM and alkaline solution; at 125 rpm for 90s). Afterwards, the CEN-standard sand was gradually added and mechanically intermixed at a mixing speed of 125 rpm for 60s and later at 250 rpm for 90s until stoppage.

The prepared binder compounds were poured in prismatic moulds (40x40x160 mm^3) and vibrated for 7 seconds. Then, the moulds were covered using plastic plates of 5 mm thickness and additionally wrapped in cellophane foil to prevent desiccation of the samples and rapid loss of

moisture. The mixtures were let to cure inside the moulds in a ventilated oven at 50°C. After demoulding, the specimens were sealed in cellophane foil and stored at 50°C until 24 hours before the compression strength test.

4.3 Applied characterisation methods and results

4.3.1 Physical and chemical characterisation of the GWM powders

The PSD of the powders were evaluated by laser granulometry using a modular analysis system (HELOS and RODOS from Sympatec GmbH). Laser granulometry follows the methods of laser diffraction based on Fraunhofer diffraction physics [186]. This measurement unit is applicable on all kind of dry powders. The particle size distribution of the GWM powders is shown in **Figure 4.3**. The particle size mainly comprises within a range of 1 to 35 μm with a mean particle size (d50) around 6.50 μm, whereas, comparatively mean particle size of cement powder ranges around 10-12 μm. The PSD analysis of the GWM powders calcined at different temperatures resulted in a similar grain size distribution beside for the powders calcined at 850°C and 950°C, where a slight shift of the curves to coarser particle sizes was observed due to the clumping of the powders related to the effect of sintering of fine clay particles [187].

The specific surface area of the powder samples, determined following the BET method [188], was at 14.5 m^2/g. Furthermore, the chemical composition of the GWM powder was determined using a wavelength dispersive X-ray fluorescence spectrometer (S4 Explorer from Bruker Corporation) with a flexible integrated auto sampler. The samples were prepared by pelletisation of a mix of loose GWM powder with wax in a ring using the pressed powder technique. The calcination parameters of the GWM powders were verified by the study of mineralogical phase

transition and thermal analysis. The chemical composition of the GWM powder is listed in **Table 4.2**. The analysis of the chemical constitution verifies that the raw material mainly consists of aluminosilicate particles with primary chemical elements of SiO_2, Al_2O_3 and Fe_2O_3.

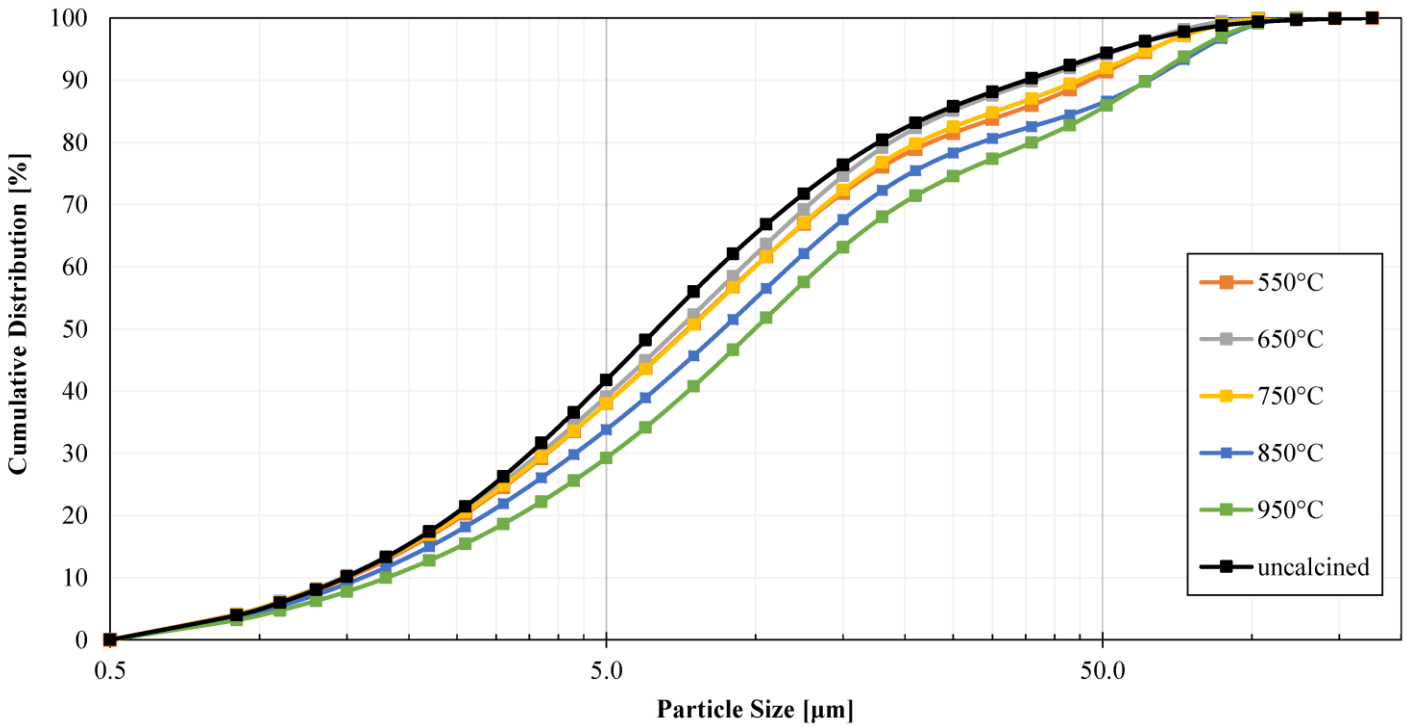

***Figure 4.3** - Particle size distribution of the uncalcined and calcined GWM powders measured by laser granulometry*

Element [-]	**Content** [%]
SiO_2	64.95
Al_2O_3	19.98
Fe_2O_3	9.02
K_2O	3.27
MgO	1.30
TiO_2	0.70
CaO	0.26

***Table 4.2** - Chemical composition of the uncalcined GWM particles determined by XRF spectrometry*

4.3.2 Mineralogical composition and thermal analysis

The GWM powders require thermal treatment at high temperatures (calcination) to increase the reactivity of the aluminosilicate materials by dehydration, dehydroxylation and change of the phase composition. This thermal decomposition provides a high-energy, distorted and amorphous raw material, which is favourable for the alkaline dissolution process.

The mineralogy of the uncalcined and the different calcined GWM powders were studied by XRD analysis. The X-ray diffractograms were collected with a D4 ENDEAVOR (Bruker Corporation) powder X-ray diffractometer using Cu Kα radiation at standard scanning parameters. A quantitative analysis was performed following the Rietveld refinement principles (TOPAS, Bruker Corporation) [189]. A quantitative phase analysis was applied instead of a qualitative crystalline phase analysis to quantify the formed amorphous phases due to different calcination temperatures. Beside the analysis of the mineralogical compositions, this evaluation in combination with the simultaneous thermal analysis (STA) enables to determine an optimum range for duration and temperature level for the thermal treatment of the GWM powder. The sample preparation for XRD analysis was the same as for the previously mentioned XRF analysis.

A quantitative XRD analysis has been carried out for the uncalcined and calcined GWM powders at temperatures of 550°C, 650°C, 750°C, 850°C and 950°C for 1 hour. The calcination time was set to 1 hour based on findings of preliminary tests and suggestions from previous research works [80,190]. **Figure 4.4** illustrates the reduction of crystalline aluminosilicate minerals with the development of new mineral phases and the rise of amorphous phases regarding the calcination temperatures. First of all, the mineralogy verifies that the aluminosilicate raw material consists of kaolinite and illite as main clay mineral. The dominant phases in all samples are the quartz

minerals, followed by clay minerals, muscovite, hematite and the amorphous portions. In addition, from the qualitative analysis of the GWM powder, the presence of low amounts of chlorite was detected, but could not be considered in the quantitative analysis. Higher calcination temperatures lead to transformation of the clay minerals into XRD amorphous phases. In fact, two stages of dehydroxylation can be observed. First, kaolinite is entirely transformed to metakaolinite at temperatures around 600°C, whereas illite becomes amorphous at higher temperatures around 900°C. Furthermore, the content of muscovite is reduced leading to an increase in the content of $KAl_3Si_3O_{11}$, which is a dehydroxilised, crystalline meta-phase of muscovite. Independent on the calcination temperature, the hematite content remains almost constant over all calcination temperatures.

The STA consists of a measurement concept that allows to perform thermogravimetric analysis (TGA) and differential scanning calorimetry (DSC) simultaneously on a single measurement unit. The analysis was carried out from room temperature until 1000°C at a heating rate of 10°C/min in a controlled nitrogen gas atmosphere.

The results of the STA analysis (TG-DSC) are presented in **Figure 4.5**. The TG curve shows two mass reduction stages (Total: - 2.62 %) of the investigated sample before 900°C. From about 30°C to 430°C, a first gradual mass loss (- 0.54 %) is observed due to the evaporation of adhesion water of the aluminosilicate minerals and the burnout of organic matters inside the samples. Furthermore, a greater decrease in mass (- 2.09 %) is observed due to the further dehydration of structural water and the dehydroxylation of the crystalline aluminosilicate minerals from 500°C to 975°C until a constant mass state is reached. The DSC curve confirms the process of dehydroxylation of the aluminosilicate matrix, followed by phase transition of the quartz minerals as an endothermic peak is observed at around 575.8°C (quartz inversion). Moreover, the crystallization of the oxides is

marked by an exothermic peak at 980°C. The findings of both analysis, mineralogical and thermal, suggest thermal treatment of the GWM powder within the range of 650°C-950°C.

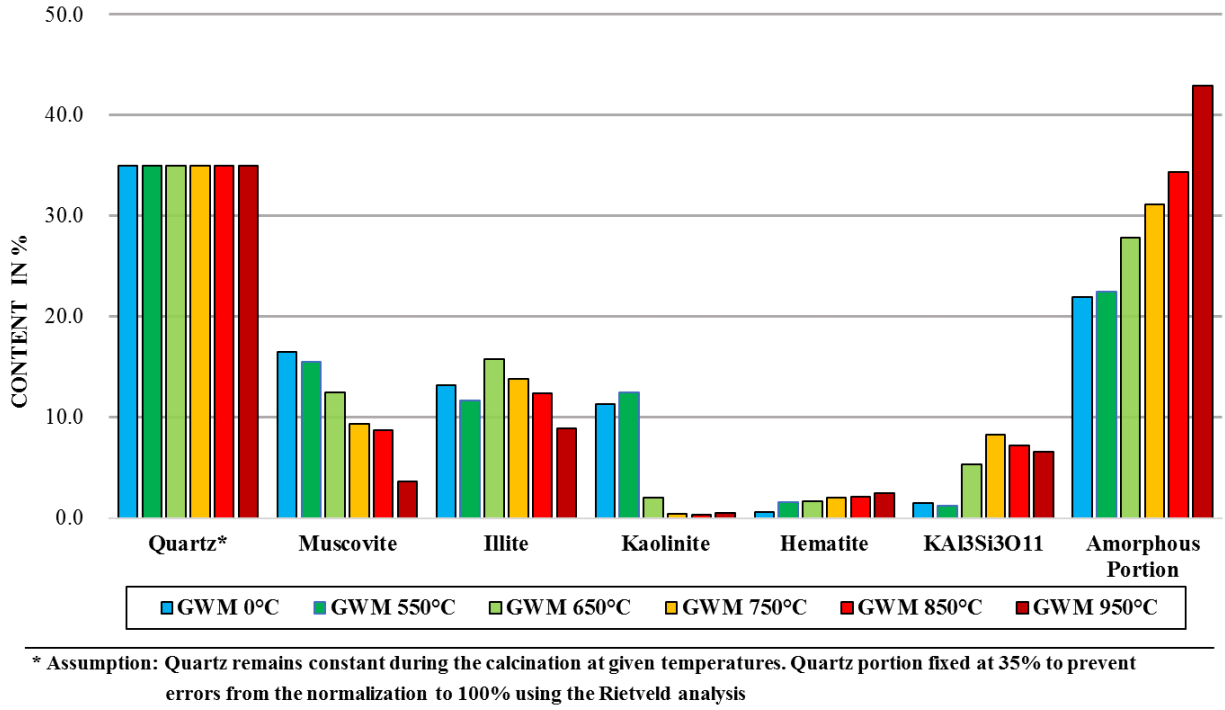

Figure 4.4 *- Results of quantitative X-ray diffraction analysis of the uncalcined and calcined GWM particles at various high temperatures*

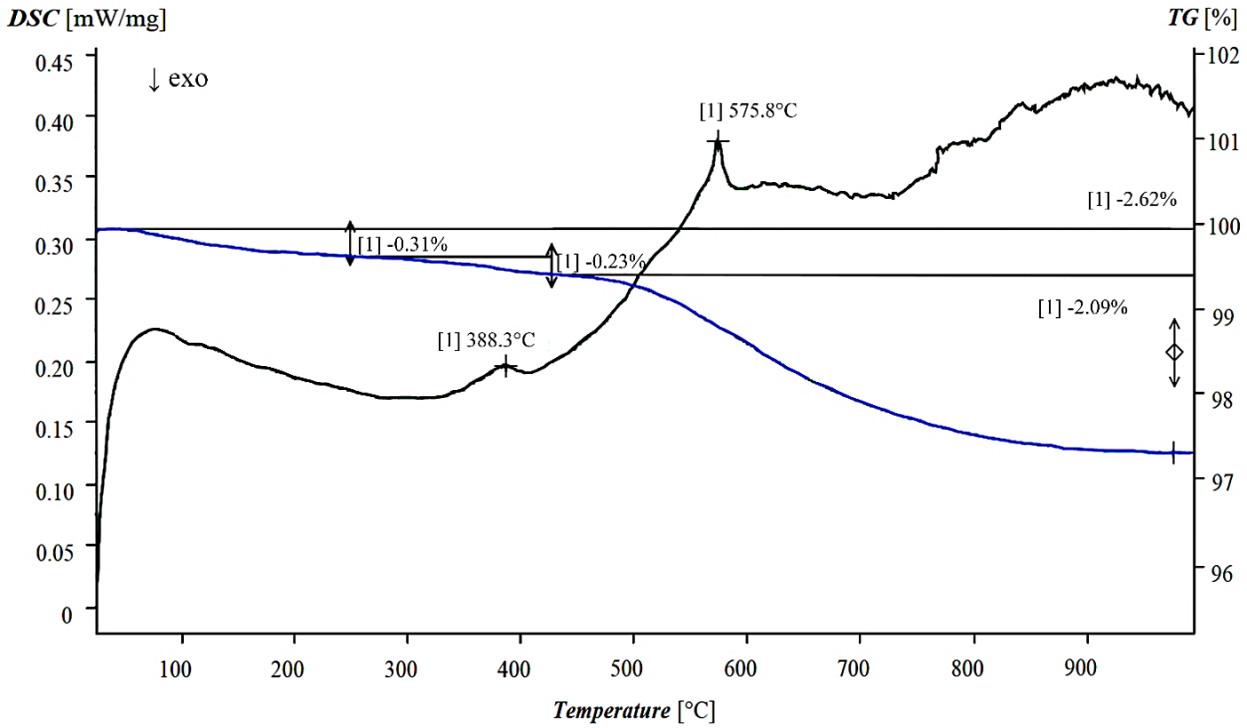

Figure 4.5 *- Results of the STA analysis (TG-DSC) on the GWM powder*

4.3.3 Compressive strength

The compressive strength was measured on three specimens of each mixture after 14 days, 28 days and 56 days using a compression test plant (Toni Technik GmbH) with additional displacement transducers. This measurement unit is optimised for compressive strength tests on prisms (40x40x160 mm^3) according to EN 196 standard. Unhardened specimens after 14 days, mainly specimens including GWM powder calcined at 550°C, were not compressed, as no sign of solidification was observable. **Figure 4.6** and **Figure 4.7** illustrates the strength development of the binders based on GWM powder calcined at different temperatures without/with sand aggregates. The specimens made with GWM powder calcined at 550°C showed very low compressive strengths and consequently low reactivity. It can be observed that for this GWM powder a higher concentration of the NaOH solution dissolved higher portions of the unreactive

aluminosilicate particles and no dense structure could be built. This observation also verifies the predictions from the mineralogical analysis discussed in **section 4.3.2**. In general, a higher thermal treatment of the GWM powders resulted in a more reactive material, which, in combination with a higher alkaline dissolution degree due to higher molarities of the alkaline solution, exhibited better compressive strengths. The highest compressive strength of 1.86 MPa was achieved by specimens calcined at 950°C and activated using 14M NaOH solution with sand aggregates. Finally, the results of the compression strength test confirm the dependency of the performance of the GWM-based alkali-activated binder on the calcination temperature of the aluminosilicate prime material, and respectively, its degree of dissolubility in the alkaline medium.

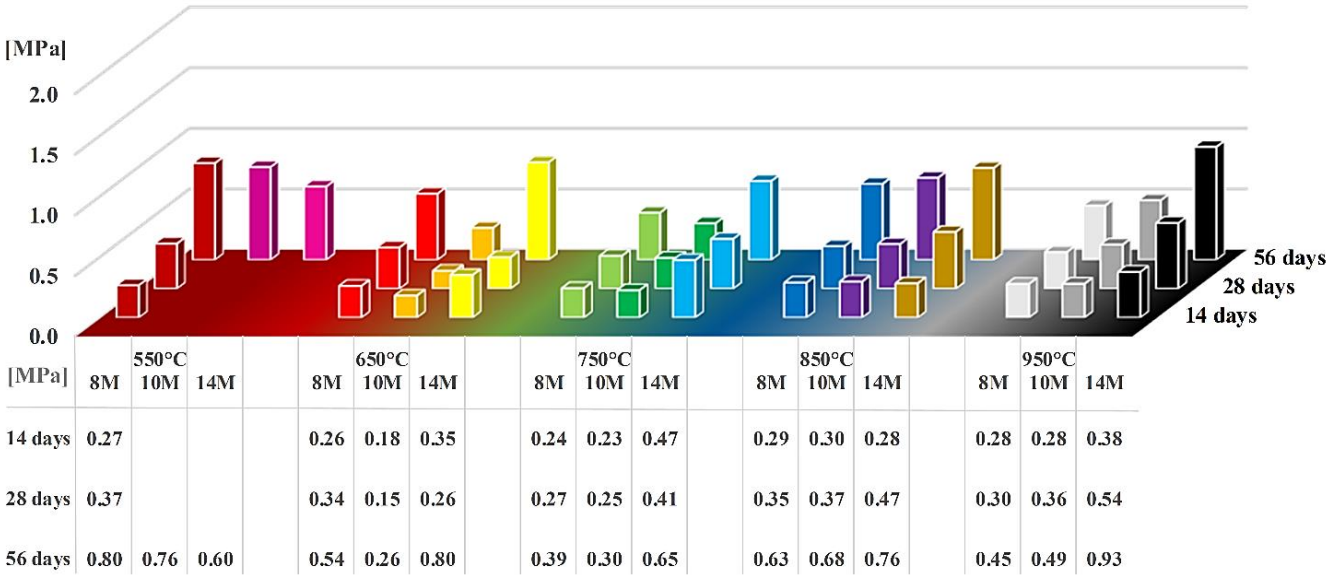

[MPa]	550°C 8M	550°C 10M	550°C 14M	650°C 8M	650°C 10M	650°C 14M	750°C 8M	750°C 10M	750°C 14M	850°C 8M	850°C 10M	850°C 14M	950°C 8M	950°C 10M	950°C 14M
14 days	0.27			0.26	0.18	0.35	0.24	0.23	0.47	0.29	0.30	0.28	0.28	0.28	0.38
28 days	0.37			0.34	0.15	0.26	0.27	0.25	0.41	0.35	0.37	0.47	0.30	0.36	0.54
56 days	0.80	0.76	0.60	0.54	0.26	0.80	0.39	0.30	0.65	0.63	0.68	0.76	0.45	0.49	0.93

Figure 4.6 *- Strength development of GWM-based binders without sand aggregates for varying calcination temperatures, varying concentrations of NaOH solutions and concrete ages*

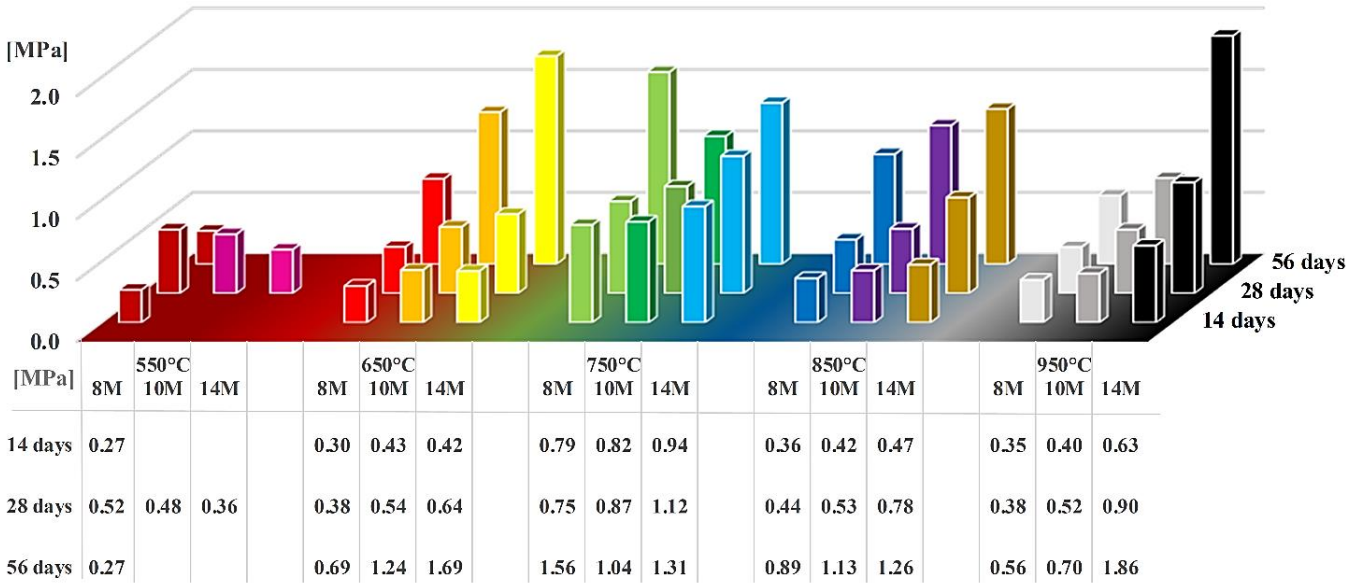

[MPa]	550°C 8M	550°C 10M	550°C 14M	650°C 8M	650°C 10M	650°C 14M	750°C 8M	750°C 10M	750°C 14M	850°C 8M	850°C 10M	850°C 14M	950°C 8M	950°C 10M	950°C 14M
14 days	0.27			0.30	0.43	0.42	0.79	0.82	0.94	0.36	0.42	0.47	0.35	0.40	0.63
28 days	0.52	0.48	0.36	0.38	0.54	0.64	0.75	0.87	1.12	0.44	0.53	0.78	0.38	0.52	0.90
56 days	0.27			0.69	1.24	1.69	1.56	1.04	1.31	0.89	1.13	1.26	0.56	0.70	1.86

***Figure 4.7** - Strength development of GWM-based binders with sand aggregates for varying calcination temperatures, varying concentrations of NaOH solutions and concrete ages*

4.3.4 Analysis of the microstructure

The microstructure of all binders was analysed by SEM using LEO 440 REM, which is a compact and high performing SEM unit that enables high quality observations of structure surfaces down to 5 nm realised by detection of secondary backscattered electrons from a high-energy beam of primary electrons in a raster scan pattern.

The images of the microstructure of selected alkali-activated binders (**Figure 4.8**) were obtained by performing SEM on small fractions of the compressed specimens. **Figure 4.8.a-b** show the microstructure of the binders realised based on GWM powders calcined at 550°C. The binder in **Figure 4.8.a** shows a compact composition, which envelops the quartz particle, whereas comparatively, the binder in **Figure 4.8.b** shows a more porous composition and the coverage of the quartz particle is loose and weak. As already supposed in the mineralogical analysis

(**section 4.3.2**) and supported by the compressive strength test (**section 4.3.3**), these binders (using calcined GWM at 550°C) possess highly disintegrated, low reactive aluminosilicate constituents formed by the dissolution in higher alkaline solutions, which lead to a weaker binder framework. In comparison with these binders (**Figure 4.8.c-f**), binders realised on the basis of GWM powders with higher thermal treatment show larger flaky, plate-like meta-clay minerals and needle-like mineral formations which provide larger reactive surfaces for the development of a compact microstructure. Finally, **Figure 4.8.g-h** presents the morphology of binders subjected to higher alkalinity and based on GWM powders calcined at higher temperatures. These microstructures present a well-formed morphology of the constituents resulting in a dense and compact matrix comprising flaky meta-clays, needle-like crystal formations and amorphous material.

The GWM's fineness with its chemical and mineralogical composition provided an auspicious base to assess its suitability for the synthesis of an alkali-activated binder. Even though the developed microstructures showed a well-developed binder framework, the achieved compressive strengths were small. These results suggest that GWM without any further additives or processing is not recommended as a precursor for alkaline activation. This outcome can be explained by the low silica content in the binder compared to the alumina content, respectively, the lower portion of reactive clay minerals compared to the dominant quartz content from a mineralogical point of view. Thereby, the calcined materials comprise lower contents of reactive meta-clays to take part in the reactions. In comparison, hardened mixtures based on raw materials with higher contents of kaolinite can achieve compressive strengths above 38.5 MPa [60] or 48.8 MPa [191] depending on the characteristics of the raw materials and the applied alkaline solution.

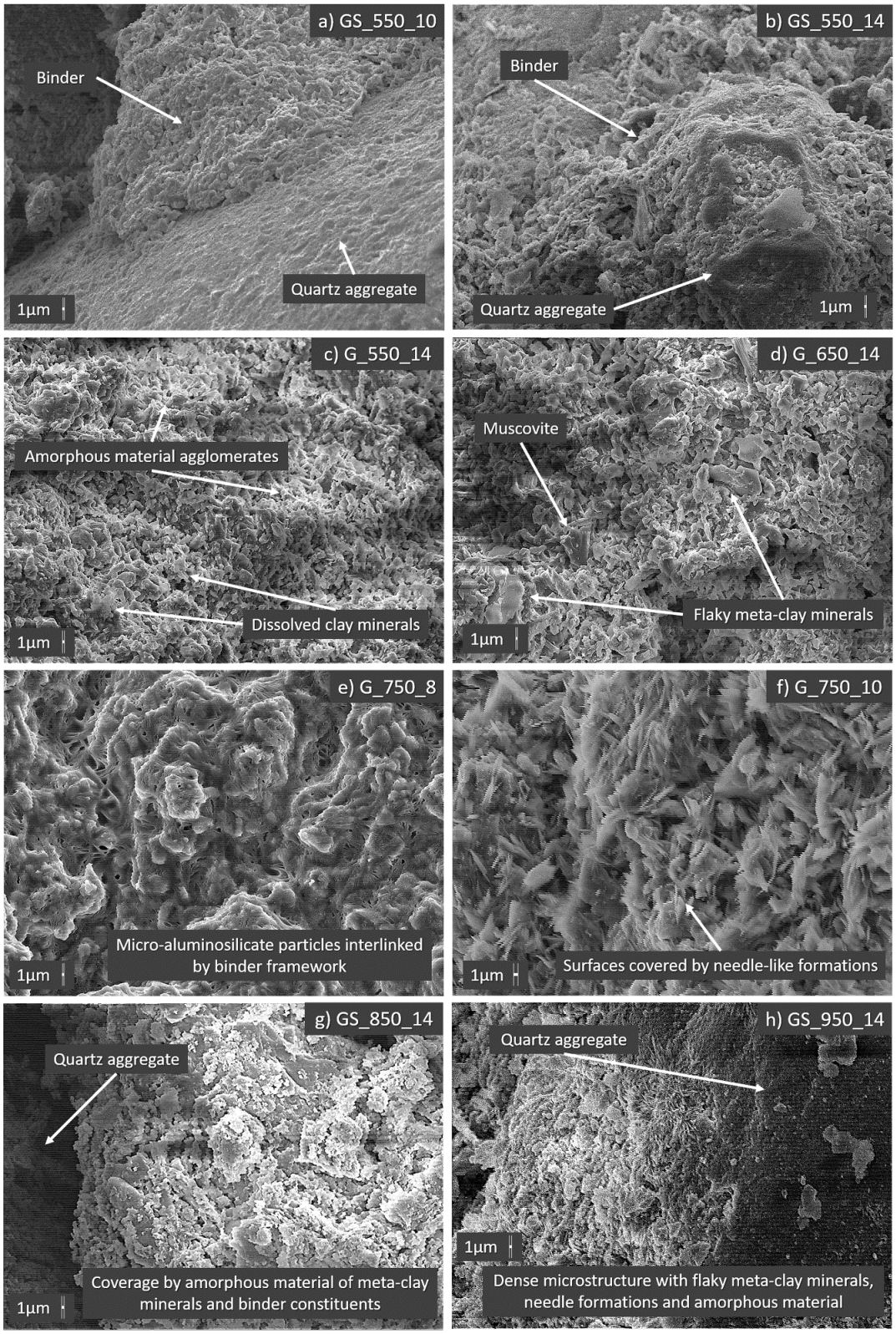

Figure 4.8 *- Scanning electron micrographs of selected specimens showing the morphology of the constituents of the alkali-activated binders in the micron range (image scale of 1µm; magnification up to 3600 x)*

4.4 Conclusion

This study presents the results of investigations carried out on alkali-activated binder using calcined GWM as prime material. The key findings from different material characterisation methods and experimental tests on specimens are summarized below:

(1) The GWM powder consists of quartz with a moderate content of clay minerals (illite and kaolinite), muscovite, and a small portion of hematite and chlorite.

(2) The XRD analysis reveals the reduction of crystalline aluminosilicate minerals with the development of new mineral phases and the rise of amorphous phases with increasing calcination temperatures from 550°C to 950°C. During calcination, two stages of dehydroxylation were observed: The complete conversion of kaolinite to metakaolinite at around 600°C and illite becomes amorphous at higher temperatures above 900°C.

(3) The results of the STA analysis confirm the process of dehydroxylation of the aluminosilicate matrix, followed by quartz inversion (endothermic peak at 575.8°C). Moreover, the crystallization of the oxides is marked by an exothermic peak at 980°C.

(4) The highest 56-day compressive strength of the binders was 1.86 MPa and occurred for the mixture using GWM powder calcined at 950°C with a 14M NaOH solution and mixed with sand aggregates.

(5) The microstructure presents a well-formed morphology of the constituents resulting in a dense and compact matrix comprising flaky meta-clays, needle-like mineral formations and amorphous material.

Further studies are required to foster greater understanding of the reactivity and reaction mechanisms of binders based on this raw material. In addition, it is necessary to investigate on the

activation effectiveness of different types of alkalis like potassium hydroxide, water glass and others. Finally, the understanding of complex solid phases is essential to analyse their effects on the long-term behaviour of alkali-activated binders.

Chapter 5 Publication II - Gravel wash mud, a quarry waste material as supplementary cementitious material

Abstract

The suitability of gravel wash mud (GWM), a sludge waste from gravel quarrying, is examined for its use as a partial Ordinary Portland cement (OPC) clinker substitute. The gravel wash mud was dried, milled into a fine powder and calcined at 750°C, 850°C and 950°C. In this study, various characterisation methods including particle size distribution (PSD), X-ray fluorescence (XRF), X-ray diffraction (XRD) and the simultaneous thermal analysis (STA) were applied on the calcined GWM powders to determine the optimal calcination temperature. Over 200 specimens were prepared based on different cement paste and mortar mixes to investigate the potential of calcined GWM powders as SCMs. The pozzolanic activity of the GWM powders was verified by applying strength-based evaluation methods, simultaneous thermal analysis and SEM on hardened samples. Very promising strength-enhancing capacities were observed for samples containing GWM powders calcined at 850°C with a OPC replacement level of 20 wt.%.

Keywords - Gravel wash mud (GWM), Supplementary cementitious materials, Alternative clay materials, Calcined clays, Pozzolanic activity.

5.1 Introduction

The inevitable CO_2 emissions related to cement manufacturing processes and its subsequent environmental impacts have received considerable critical attention worldwide and have become one of the key incentives for the development of environmental friendly and sustainable construction materials [192–194]. Furthermore, the growing demand for binders, mortars and concrete products opposed to the increasing scarcity of raw materials for cement clinker production has imperatively stimulated the research on new binder technologies to assure the current and future demands for products based on cementitious materials [195–198]. Current trends in cement research have led to a large multitude of studies that suggest the partial substitution of OPC by admixtures, known as supplementary cementitious materials (SCM). Recent investigations and existing projects validate an important reduction of OPC usage by incorporation of SCMs in cement mixes [199] and the improvements of the final products' properties in contrast to the detrimental deteriorations of conventional concrete of aesthetical, functional or structural nature [18,122]. The beneficial effects of partial substitution of OPC by various SCMs on the packing of concrete mixtures, early hydration, mechanical performances and long-term durability have been extensively examined and confirmed. These improvements of mixture properties and performances due to addition of SCMs in cement-based mixtures can be attributed to three effects, which can occur simultaneously as coexisting processes or at distinctive stages over time [104–106]:

A) The chemical reaction: hydration of cementitious materials and pozzolanic reaction by formation of additional hydration products supplementary to the hydrated clinker phases [71,89,93,112,200,201].

B) The physiochemical impact: the finer particle size distribution of the added SCMs is

correlated to larger contact surface area of the small particles, which provides larger interfacial area for the hydration reactions by performing as nucleation sites [132,202].

C) The physical effect: packing effect, respectively filler effect, leads to formation of a more effective and denser aggregate-cement paste matrix by filling the gaps between the cement particles themselves and between the cement particles and the aggregates [105–107,203–205].

Despite their high potentials and efficacy as partial OPC substitutes, the most commonly used SCMs like fly ash (FA) [206], silica fume (SF), ground granulated blast furnace slag (GGBS) and metakaolin (MK) are nowadays commercially available products and their prices have risen over the last decades due to growing demand. Thus, valuable and reliable research studies have been carried out on potential alternative SCMs and their performance as cement substitutes has been evaluated and studied mainly for local markets. The use of locally available resources as SCMs shows a considerable economical potential as short transport routes as well as very low to no competitive price variations can be expected. Alternative SCMs comprise rice husk [78,79,124], industrially processed clays [125,207], calcined clay-brick wastes [126–129], volcanic tuffs [130,131], pumices [132], modified reservoir sludge [1,133,134], waste expanded perlite [135] and more [208–212].

Investigations on alternative SCMs using processed naturally occurring raw clay mixes and waste clay products have increased worldwide. This paper focuses on the potential of a quarry waste material, namely gravel wash mud (GWM), as SCM for partial substitution of OPC in cement-based mixes by presenting a variety of selected investigations including different material characterisation analyses and performance-based experimental tests. The main objective is to suggest an optimal OPC replacement level and to evaluate the mechanical performance of the

novel cement-based products. Large series of mixtures were prepared, which consist of different cement paste and mortar mixes containing GWM powders calcined at 750°C, 850°C and 950°C. The physical and chemical properties as well as the mineralogy of the GWM powders were evaluated using laser diffraction granulometry, the BET method, the X-ray fluorescence analysis, the quantitative X-ray diffraction analysis and the simultaneous thermal analysis (STA), which combines thermogravimetric analysis (TGA) and differential scanning calorimetry (DSC). Furthermore, the hardened specimens were analysed using compressive strength tests combined with performance-based evaluation methods, thermal analysis and scanning electron microscopy. The outcome of this study will enrich the investigations on waste materials as efficient alternative SCMs for OPC supplementation. Finally, the double benefit for society and industries consists of revalorizing an industrial waste product as SCM in cement mixes in an economically attractive and environmentally friendly way.

5.2 Materials and experimental program

5.2.1 Materials

The used Ordinary Portland cement (OPC) is a commercial CEM I 42.5 R cement (clinker content ≥ 95 wt.% according to EN 197-1 [58]) from Cimalux S.A, Luxembourg and a commercially available CEN-standard sands was used for the OPC mortars, certified in accordance to EN 196-1 [101] with a characteristic grain size distribution with particle sizes ranging between 80 μm and 2 mm.

The gravel wash mud (GWM) was collected from a sandstone quarry in Folschette, Luxembourg operated by Carrières Feidt S.A. The raw mud was extracted from a settling pond and stored in

sealed recipients. The water content of the sludge was 44 wt.% and 32 wt.%, in case a flocculation reagent was applied. The reddish brown mud-like deposit has a very plastic consistency. From geological point of view, the rock strata of the quarry consists of deposits of red sandstone. The GWM was desiccated at 105°C in a laboratory oven for two days. The dried GWM chunks were fragmented and ground into a powder, henceforth referred to as uncalcined GWM (UGWM) powder. The UGWM powder undergoes a thermal treatment procedure (calcination) to improve the reactivity of the aluminosilicates by dehydration and thermal decomposition (dehydroxylation) into a high-energy, amorphous raw material (CGWM). The calcination proceeded as follows: the powders were heated from room temperature up to the target temperature of 750°C, 850°C and 950°C at a heating rate of about 5°C/min in a laboratory chamber furnace with radiation heating (Model N41/H, Nabertherm GmbH, Germany). The peak calcination temperature was maintained for one hour and left for cooling down naturally to room temperature inside the chamber furnace.

5.2.2 Mixture preparation and mix proportion design

A large series of cement paste and mortar mixes corresponding to over 200 specimens were prepared to investigate the potential of CGWM powders as SCMs using the compressive strength of the hardened sample as indicator for the pozzolanic activity of the tested SCM, the optimal calcination temperature of the UGWM powders and the range of optimal OPC replacement level. Mix proportions of all studied mixes are summarized in **Table 5.1**. Nineteen different cement paste mixes (CG) including a control mixture and four different mortar mixes (CGS) including a reference mixture were prepared for curing times of 7, 28 and 56 days. The calcination time is fixed at 1h and the calcination temperature of the GWM powders was set at 750°C, 850°C and 950°C. The water/binder ratio was fixed to 0.4. For the binder mixes, the OPC substitution degree

was varied from 5 wt.% up to 30 wt.% in steps of 5 wt.% and the mortars were prepared at an arbitrarily fixed replacement level of 15 wt.% and a binder/aggregate (b/ag) ratio of 0.75.

The mixing procedure was kept constant for all the series of binder and mortar mixes, respectively. The quantities of Portland cement and calcined GWM powder were shortly dry-mixed at a mixing speed of 125 rpm. While keeping the same mixing speed, the water is gradually added and the compound is mixed for 180 seconds, followed by a final mixing at 250 rpm for 90 seconds. For the mortar mixes, the sand aggregates were added after the binder compound was mixed for 180 seconds, followed by mixing at 125 rpm and 250 rpm for another 90 seconds each. The specimens were cast in prismatic moulds (40 x 40 x 160 mm^3 according to EN 196-1 [101]) and compacted for 7 seconds on a vibrating table. After casting, the moulds were covered with plastic plates (5 mm thick) to prevent rapid loss of moisture and after 24 hours, the specimens were demoulded, wrapped in cellophane foil and cured at ambient temperature until 24 hours before the uniaxial compression tests according to [101].

Mixture[a]	**Calcination temperature CT**[b] **= 750°C / 850°C / 950°C; curing time of 7, 28 and 56 days**					
	Substitution degree	CGWM	OPC	CEN Sand	w/b[c]	b/ag[d]
[-]	[wt.%]	[g]	[g]	[g]	[-]	[-]
CG_R	0	0	425	-	0.40	-
CG_CT_5	5	21	404	-	0.40	-
CG_CT_10	10	43	383	-	0.40	-
CG_CT_15	15	64	361	-	0.40	-
CG_CT_20	20	85	340	-	0.40	-
CG_CT_25	25	106	319	-	0.40	-
CG_CT_30	30	128	298	-	0.40	-
CGS_R	0	0	225	180	0.40	0.75
CGS_CT_15	15	64	180	180	0.40	0.75

[a] Three specimens of each mixture were prepared for each curing time (7, 28, 56 and/or 90 days)

[b] E.g. CG_CT_5 series consists of mixtures CG_750_5, CG_850_5 and CG_950_5

[c] w/b: water/binder ratio, binder equal to cement only or cement and CGWM

[d] b/ag: binder/aggregate ratio

Table 5.1 *- Mix proportions of studied series of mixes*

5.2.3 Experimental methods

5.2.3.1 Characterisation techniques applied on the primary powders and the hardened products

The laser diffraction method was used to determine the particle size distribution of the UGWM, CGWM (750°C, 850°C and 950°C) and OPC powders. A modular particle size analyser (HELOS-RODOS-VIBRI, Sympatec GmbH, Germany) was utilised to measure the powder samples by dry powder dispersion using Fraunhofer diffraction theory [41] to compute the PSD from the diffraction patterns.

The characterisation of the specific surface area was performed on UGWM and OPC powders (two samples each) using the BET nitrogen gas adsorption method [42] according to ISO 9277:2010 [43], an extended method of the Langmuir monolayer molecular adsorption [44] to multiple molecular layers. The chemical composition of the powder samples was determined by X-ray fluorescence method using a wavelength dispersive X-ray fluorescence (WDXRF) spectrometer (S8 TIGER, Bruker AXS GmbH, Germany). The test specimens were prepared by pelletisation of the samples in a ring using the pressed powder technique.

The crystalline structure was investigated by quantitative X-ray diffraction analysis using a powder X-ray diffractometer using Cu-Kα radiation (D4 ENDEAVOR, Bruker AXS GmbH, Germany). The crystalline phases present in the GWM powders were identified by their characteristic d-spacings and intensities using the XRD software DIFFRAC.EVA (Bruker AXS GmbH, Germany). The X-ray diffraction patterns were processed using the program TOPAS (Bruker Corporation) using the fundamental parameter approach for line profile fitting [213] and the powder diffractograms were refined by the Rietveld method [214] after the crystalline phases

were described using appropriate structural data from ICSD database.

Furthermore, the accurate and direct detection of non-crystalline matter in a powder sample is not possible with X-ray powder diffraction analysis, as those phases do not generate characteristic reflections peaks (X-ray amorphous). However, due to the likeliness of the presence of non-crystalline content (amorphous phases) in the GWM powders, its amorphous quantity is computed using quartz at 35% as an internal reference [215]. This procedure of quantitative phase analysis of amorphous content assumes that the internal reference quartz homogenously distributed within all powder samples, a narrow particle size distribution of all phases is ensured and a random orientation of the crystallites is assured to reduce preferred orientation effects [215,216]. With the known amount of the internal reference W_{ref} and its amount from the quantitative analysis W_q, the percentage of the amorphous content, $W_{amorphous}$, can be calculated as followed, adjusted from [215,216]:

$$W_{amorphous} = 1 - \frac{W_{ref}}{W_q} \times 10^2 \ [\%]$$

Once the amorphous content is determined and with consideration of the known quantity of the internal reference, the sum of all phases is normalized to 100%.

Simultaneous thermal analyses (STA), a combination of thermogravimetric analysis (TGA) and differential scanning calorimetry (DSC), were performed on the GWM powder and the hardened cement-based binder. The applied thermo-analytical technique consists of the monitoring of the heat flow change and mass change of a sample as a function of temperature resp. time. The temperature was increased gradually from ambient temperature to 1000°C. The analysis of the STA curves permits the assessment of the nature of changes in the samples due to the increase of temperature and whether, the endothermic and exothermic effects occur with associated mass change corresponding to e.g. a melting effect or phase transition; or without mass change

corresponding to e.g. degradation. The mineralogical analysis in combination with the STA data consists a great tool to determine the optimal calcination temperature and the phase shifts of the GWM powders and the hardened specimens.

5.2.3.2 Compressive strength test, relative strength test and pozzolanicity of the hardened binders

For each mixture, the compressive strength was measured on three specimens with same curing ages using a compression test plant (TONICOMP III, Toni Technik GmbH, Germany), conform to the standard DIN EN 196-1 [101], with additional displacement transducers. An indirect evaluation method of the pozzolanic activity, namely the strength activity index (SAI), is applied to measure physical properties of hardened test samples and to evaluate the magnitude of the pozzolanic activity [81–83,93,148,217–222]. In addition, a modified method is suggested for the determination of the level of pozzolanic reactivity of the calcined GWM powders. The proposed relative strength index (RSI) is based on the same principal as the strength activity index (SAI) using the ratio of the compressive strength of samples containing the test pozzolan to the performance of a reference/control mixture as indicator for pozzolanic reactivity. However, the RSI method follows the hypothesis that if a tested material would not show any pozzolanic activity, neither any positive packing contribution nor reactivity to the cement matrix, then the expected loss in strength would be expected to be directly proportional to the substitution degree or higher. The RSP evaluation method directly provides information about the relative strength loss or gain of the pozzolanic material to a certain OPC substitution degree. The first step of the proposed evaluation (**Figure 5.1**) is to calculate the real potential (RP) which represents the ratio between the compressive strength of the specimens containing the test pozzolan and the control mixture. In

case, the ratio is equal or above 100%, a net gain in strength was achieved from the substitution of OPC by calcined GWM powders. However, if RP value is below 100%, the consideration of the relative strength index (RSI), which is calculated by Eq. (1), provides an indication whether a relative strength gain, respectively loss occurred:

$$\mathrm{RSI} = \mathrm{RP} - (100\% - \mathrm{S}) \qquad (1)$$

where RSI is the relative strength index, RP is the real potential (%), representing the ratio between the compressive strength of the specimens containing the test pozzolan and the control mixture, and *S* is the substitution degree of OPC by the SCM (%).

5.2.3.3 Microstructural characterisation of the cured binders

The microstructure of the hardened specimens was analysed using a high-resolution scanning electron microscope (LEO 440 REM, Carl Zeiss SMT AG, Germany). This SEM unit enabled high quality observations of structure surfaces down to 5 nm realised by detection of secondary backscattered electrons (BSEs) from a high-energy beam of primary electrons in a raster scan pattern. The preparation of small fractions of hardened material was performed after compression strength tests by gold coating. The images of the microstructure of selected samples were obtained by performing SEM on small fractions of the compressed specimens.

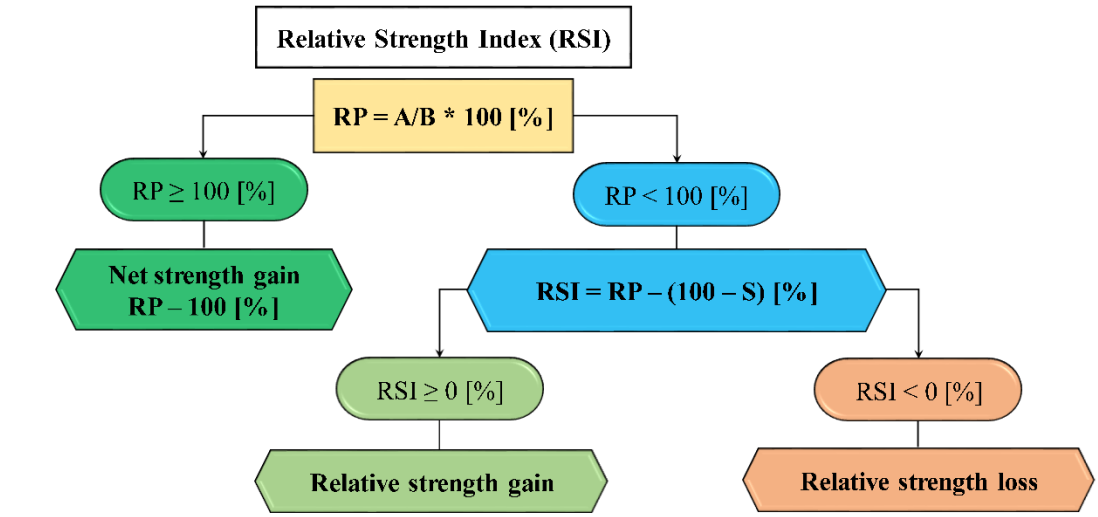

Abbreviations

A	Compressive strength of the specimen containing the test material [MPa]
B	Compressive strength of the control mortar [MPa]
RP	Real potential in strength [%]
RSI	Relative strength index [%]
S	Substitution degree of OPC by the test material [%]

Figure 5.1 *- Relative strength index (RSI)*

5.3 Results and discussions

5.3.1 Characteristics of the raw materials

5.3.1.1 Chemical analysis and PSD analysis

Figure 5.2 displays the PSD curves of UGWM, CGWM and OPC. The PSD analysis shows that the GWM powders present a very fine granulometry within a grain size range (d10-d90) from 1 to 35 µm with a mean particle size (d50) around 7-9 µm depending on the applied calcination temperature. CGWM powders at 850°C and 950°C have a slightly coarser distribution than UGWM and CGWM at 750°C due to the compaction of the minerals at high temperatures as a result of the sintering effect of clay particles [83,221]. The OPC powder showed a specific surface

area and a mean particle size of 436.50 m^2/kg and 11.58 µm, respectively. The aluminosilicate precursor UGWM showed a specific surface area of 522.49 m^2/kg with a mean particle size of 7.36 µm, whereas those for the CGWM powders, calcined at 750°C, 850°C and 950°C were 524.99 m^2/kg, 476.03 m^2/kg, 426.50 m^2/kg and 7.36 µm, 8.61 µm, 9.98 µm, respectively. The investigated CGWM powders show a finer grain size distribution than the investigated cement powder, which forecasts an enhanced packing density of the mixes, already at small OPC substitution levels [223,224].

The chemical analysis (**Table 5.2**) confirms that the GWM is an aluminosilicate-rich material, which presents an elemental composition with high silica (SiO_2), medium alumina (Al_2O_3) and low iron oxide (Fe_2O_3) contents.

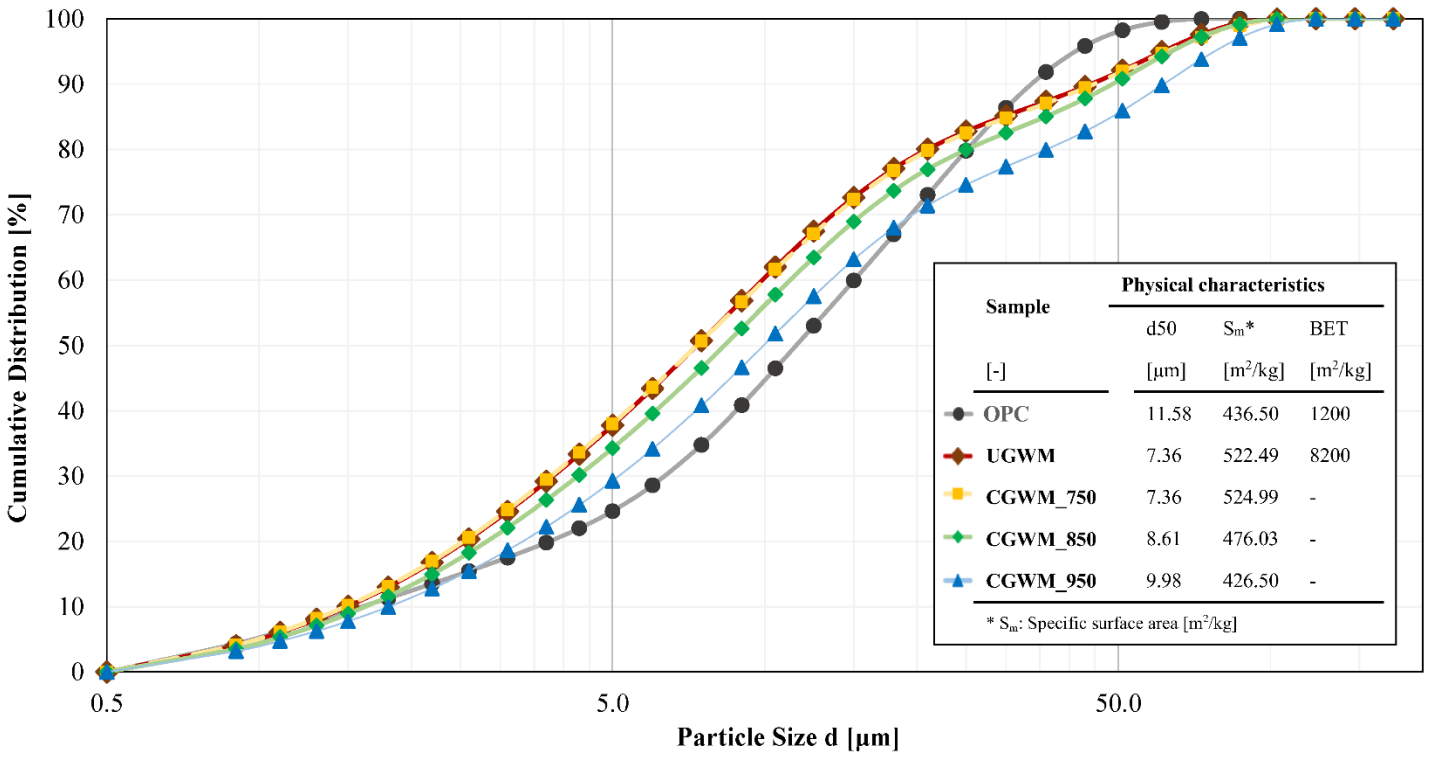

***Figure 5.2** - Particle size distribution and physiochemical characteristics of UGWM, CGWM (calcined at 750°C, 850°C and 950°C) and OPC powders*

Sample	Chemical composition											
	SiO_2	Al_2O_3	Fe_2O_3	CaO	MgO	SO_3	Na_2O	K_2O	TiO_2	MnO	CeO_2	LOI
[-]	[%]	[%]	[%]	[%]	[%]	[%]	[%]	[%]	[%]	[%]	[%]	[%]
OPC	17.10	4.23	3.84	59.20	1.10	2.91	0.19	0.47	0.30	0.31	0.15	2.4
UGWM	52.30	15.70	7.53	0.33	1.34	0.07	0.19	2.19	0.69	0.05	-	-
CGWM_750	52.71	17. 26	8.51	0.22	1.14	0.07	0.23	3.08	0.75	0.08	-	-
CGWM_850	53.70	17.00	7.47	0.34	1.52	-	0.20	2.73	0.75	0.07	-	-
CGWM_950	53.93	17.45	7.87	0.22	1.34	0.04	0.25	3.11	0.63	0.08	-	-

***Table 5.2** - Chemical composition of UGWM, CGWM and OPC powders*

5.3.1.2 X-ray diffraction (XRD) analysis a simultaneous thermal analysis (STA or TG-DSC)

Figure 5.3 illustrates the X-ray diffraction pattern of UGWM and the analysis reveals the presence of amorphous material, quartz, muscovite, illite, kaolinite, hematite and $KAl_3Si_3O_{11}$ in the GWM-based powders [1]. The quantitative analysis (**Table 5.3**), which was carried out based on the method described in [215], shows that the main crystalline phases identified were quartz, muscovite, followed by illite and kaolinite as clay minerals, hematite and the amorphous portions. The increase of the calcination temperature led to the transformation of the clay minerals into XRD amorphous phases. Two dehydroxylation phases can be pointed out with kaolinite entirely transformed to metakaolinite at temperatures below 750°C, whereas illite shifts towards amorphous phases above 850°C [1]. In addition, the quantity of muscovite is reduced above 750°C into a crystalline meta-phase, namely $KAl_3Si_3O_{11}$.

Figure 5.4 shows the curves of the STA analysis of the GWM powder, the mass loss (TGA) and the heat flow variation (DSC) of the GWM powder in function of the increase of temperature. The TGA curve shows two main phases of mass reduction (total: - 4.38%) of the investigated powder sample due to gradual increase of the applied temperature from ambient temperature up to 1000°C.

The first gradual mass loss (- 0.96%) can be perceived from 30°C to around 350°C due to the evaporation of interlayer water of the aluminosilicate phases and the burning of organic matters or volatile components from the samples. The greater mass reduction (- 3.70%) occurs from about 350°C up to about 900°C mainly driven by the dehydroxylation of the clay minerals and further dehydration of structural water until a constant mass state is reached. The DSC curve confirms the burnout of the organic matter at about 300°C and the progressive dehydroxylation of the clay mineral phases from about 400°C to 550°C, followed by the phenomenon of quartz inversion (phase transition of quartz minerals) resulting in an endothermic peak at 575.3°C [225,226]. The findings of mineralogical analysis in combination with the STA suggest a primary indication of the optimum range of calcination temperature for the GWM powder at above 750°C as the loss in mass has more or less completed and the major phase shifts have occurred.

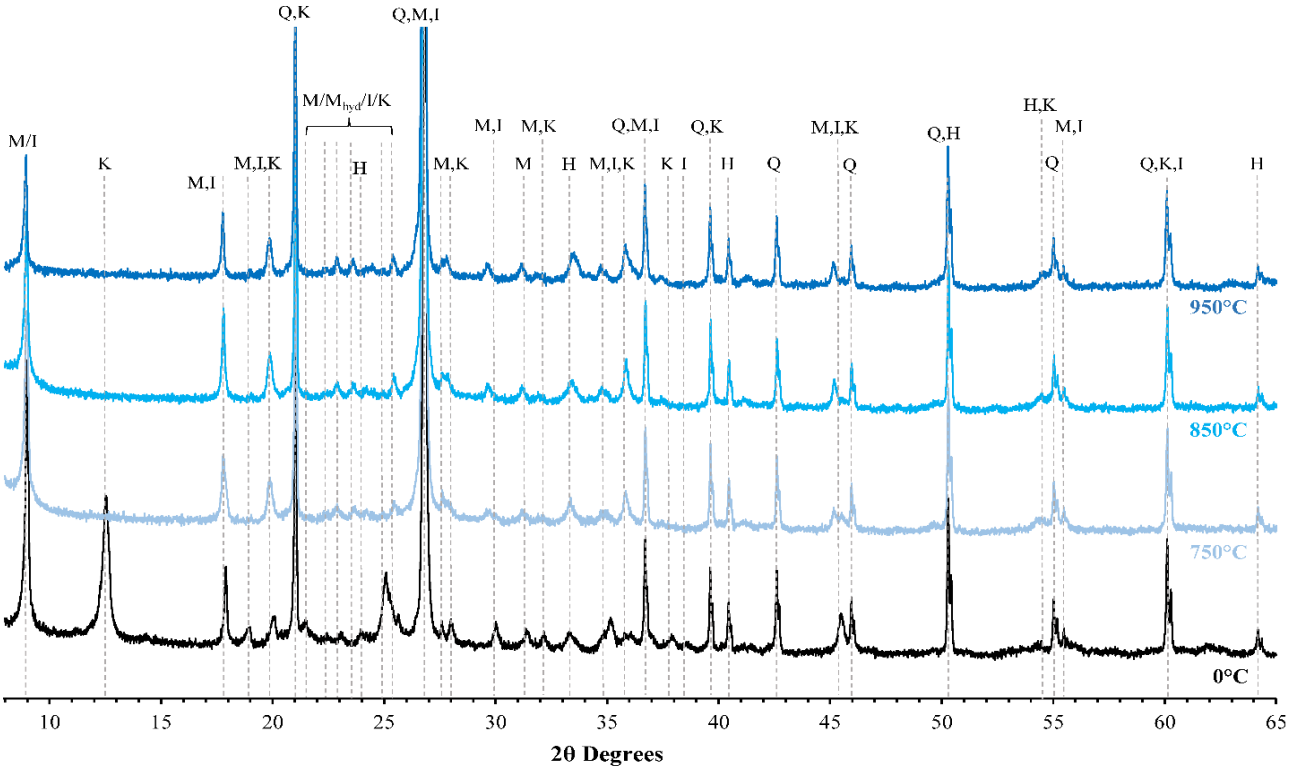

Figure 5.3 *- X-ray diffractogram of UGWM: Q - Quartz, M - Muscovite, I - Illite, K - Kaolinite, H - Hematite, M_{hyd} - $KAl_3Si_3O_{11}$*

Sample	Mineralogical composition [%]							
	C_3S	C_2S	C_4AF	C_3A	Anhydrite	Calcite	Portlandite	Quartz
OPC	51.7	24.8	12.2	1.6	2.7	4.4	1.8	0.7

Sample	Mineralogical composition [%]						
	Quartz[a]	Muscovite	Illite	Kaolinite	Hematite	$KAl_3Si_3O_{11}$	Amorph
UGWM	35.0	16.5	13.2	11.3	0.6	1.5	21.9
CGWM_750	35.0	9.3	13.8	0.4	2.0	8.3	31.1
CGWM_850	35.0	8.7	12.4	0.3	2.1	7.2	34.4
CGWM_950	35.0	3.6	8.9	0.5	2.5	6.6	42.9

[a] Quartz content fixed for normalisation of data

Table 5.3 *- Mineralogical composition of UGWM, CGWM and OPC powders*

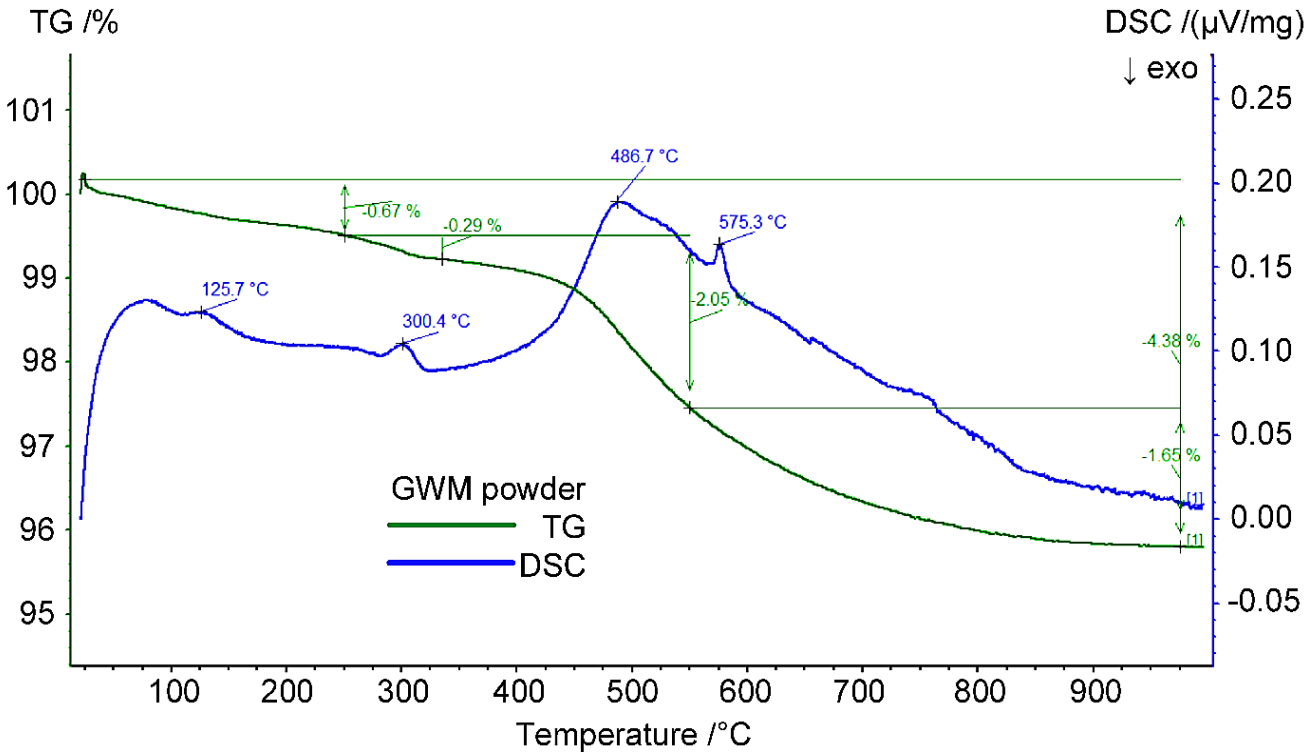

Figure 5.4 *- STA (TG-DSC) analysis of GWM powder*

5.3.2 Characteristics of the hydrated specimens

5.3.2.1 Compressive strength tests of hardened specimens and pozzolanic activity

Figure 5.5 - Figure 5.7 show the evolution of the compressive strength of hardened cement pastes containing different portions of GWM powders calcined at 750°C, 850°C and 950°C for up to 56 days of curing. Each compressive strength value represents the mean compressive strengths out of three valid specimen tests. All tested specimens showed a similar evolution of strength with a gain in compressive strength with increasing curing days. The progress of hydration of the cement clinker phases led to the formation of compact calcium silicate hydrates over the first days and months. With increasing curing ages, an additional increase in strength is considered for specimens containing CGWM powders due to the development of further reaction products from pozzolanic reaction. For example, an increase of 7.2 MPa from 28 days to 56 days of curing was observed for CG_850_15 compared to an increase of 3.5 MPa for the reference specimen over the same curing period. Moreover, an increase of the OPC replacement level by the CGWM powders, regardless the calcination temperature, did not result in a proportional loss in strength of the hardened specimens after 28 resp. 56 days. Except at 7 days of curing, where a continuous loss of performance is observable with increasing quantity of CGWM powder. This phenomenon at early curing age can be related to the low reactivity of the CGWM powder and the fixed w/b ratio, which rather builds a physical obstruction for the clinker hydration reactions in the cement matrix than an enhancement due to pozzolanic reaction or better packing of the constituents. The development of the compressive strength at higher curing ages at 28 days and 56 days does not indicate a clear decline in compressive strength with increasing OPC substitution degrees. This suggests the

formation of additional hydration products due to reactions between the CGWM powders and OPC, which is a strong indication for pozzolanic reaction. Furthermore, only the specimens containing GWM calcined at 750°C and 850°C showed an increase in strength from OPC replacement level of 15 wt.% up to 25 wt.% after 56 days of curing, whereas the development of compressive strength slightly declined for the specimens containing GWM powders calcined at 950°C. The highest compressive strengths at 56 days of curing were achieved for specimens CG_850_5, CG_950_5 and CG_850_10 with 53.97MPa, 53.07 MPa and 51.66 MPa respectively. Hardened mortar mixes (**Figure 5.8**) containing GWM powders calcined at 750°C, 850°C and 950°C at an OPC replacement level of 15 wt.% showed similar compressive strength development over the investigated time period. The compressive strength of the hardened mortars CGS_850_15 exceeded the strength of the reference mortar at 28 days and 56 days and CGS_950_15 surpassed the reference compressive strength at 56 days. At early curing ages, the achieved compressive strength of the investigated mortars were inferior to the performances of the reference mortar. However, higher compressive strength values were realised at longer curing ages. The strength enhancement might be related to the pozzolanic reaction in combination with the formation of a denser microstructure due to a better cement paste distribution leading to an improved inter-aggregate bond compared to cement matrices without aggregates.

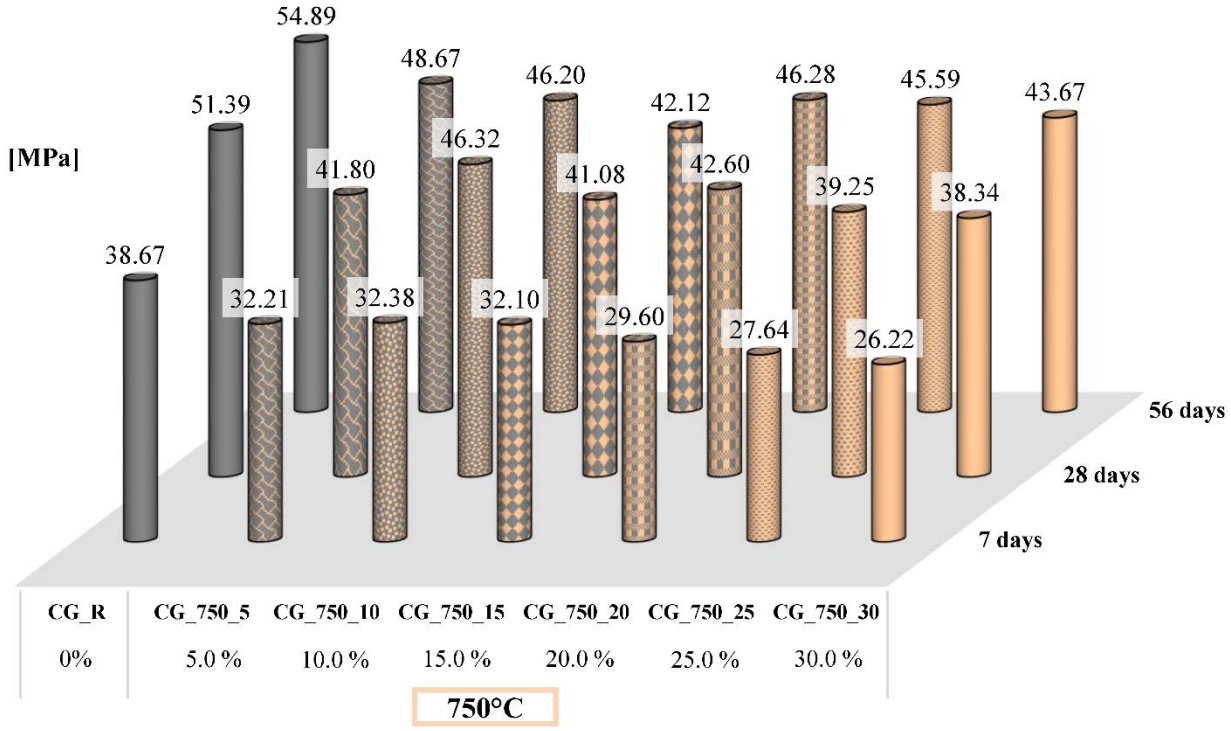

Figure 5.5 *- Development of the mechanical properties of hardened cement pastes containing CGWM (750°C) at different OPC substitution degrees*

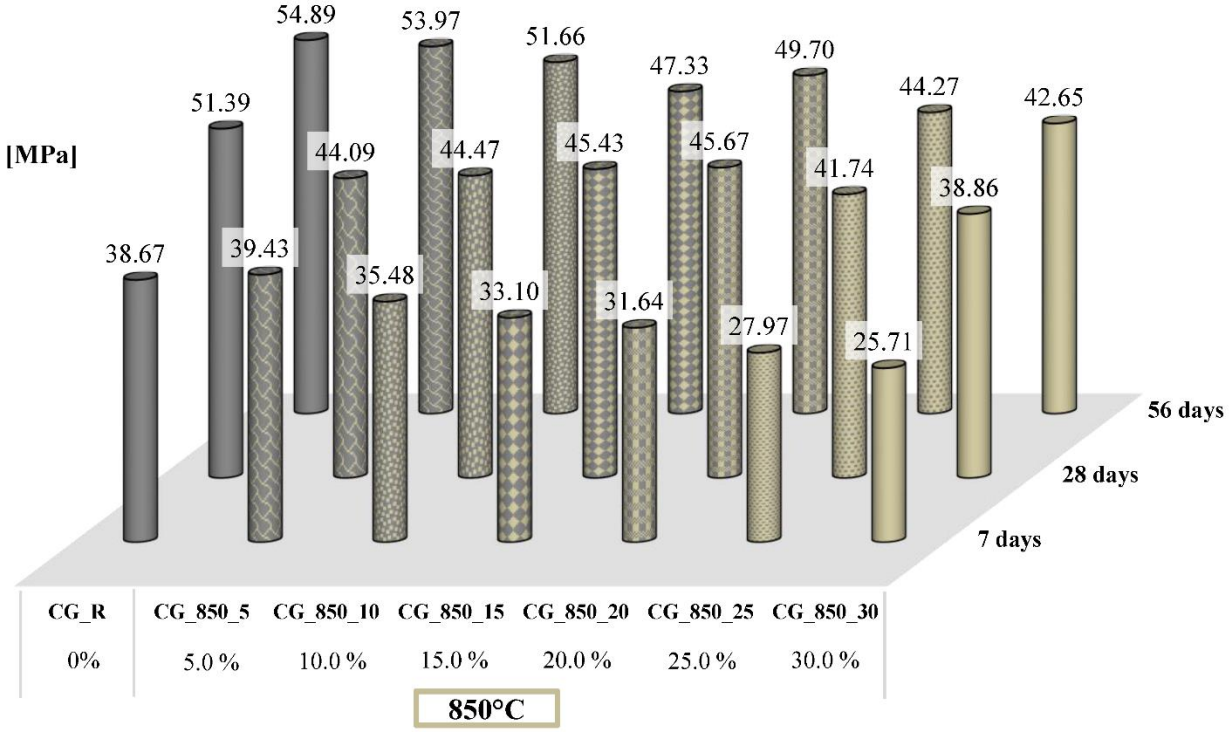

Figure 5.6 *- Development of the mechanical properties of hardened cement pastes containing CGWM (850°C) at different OPC substitution degrees*

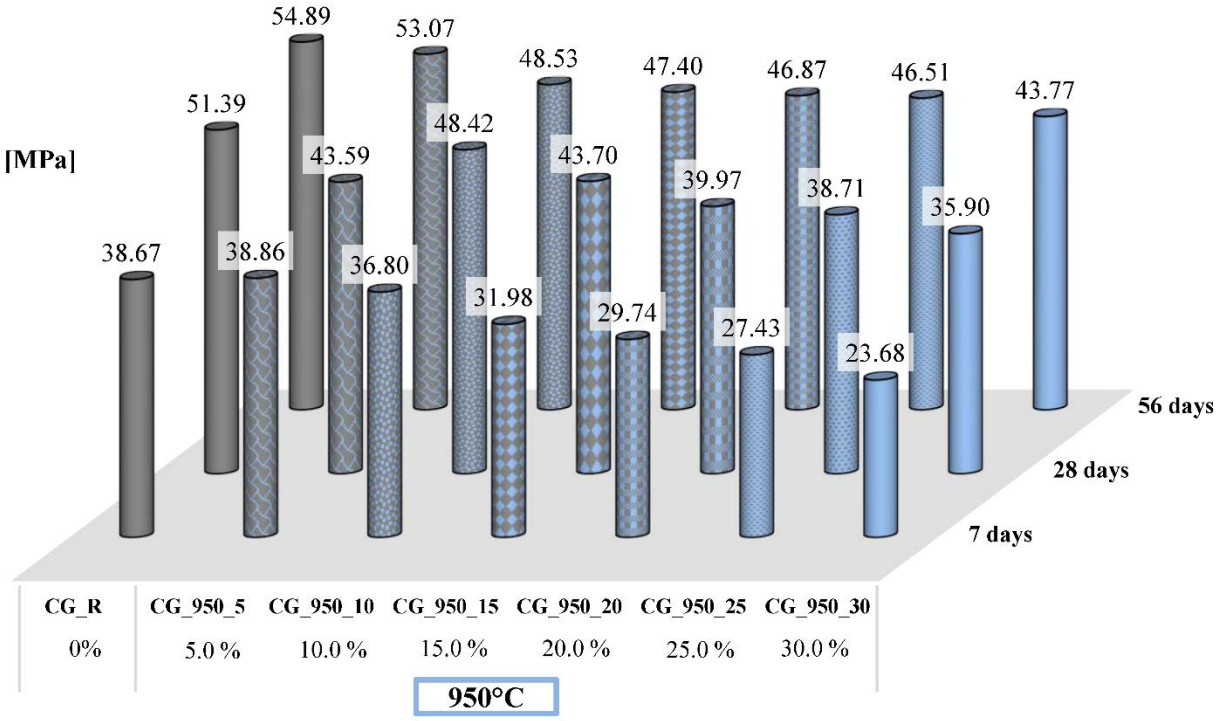

***Figure 5.7** - Development of the mechanical properties of hardened cement pastes containing CGWM (950°C) at different OPC substitution degrees*

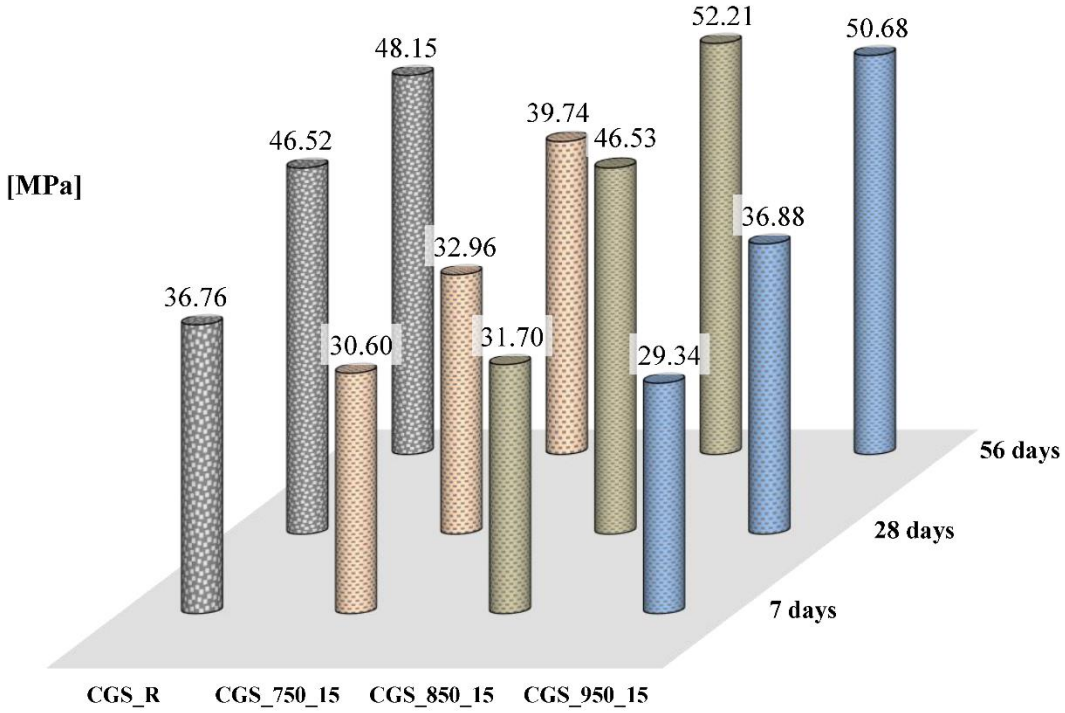

***Figure 5.8** - Development of the mechanical properties of hardened mortars containing different CGWM (750°C, 850°C and 950°C) at fixed OPC substitution degree of 15 wt.%*

The direct comparison of absolute compressive strength is not sufficient to assess the pozzolanicity of CGWM at different calcination temperatures as well as the potential of the OPC substitution. Therefore, the strength activity index (SAI) method and the relative strength index (RSI) method are applied to determine the optimal calcination temperature and the efficient OPC substitution degrees.

The chemical composition of the CGWM powders fulfils the physiochemical requirements on calcined natural pozzolan according to specification in ASTM 618 [74] for usage as Portland cement admixtures. The SAI were computed according to the test methods described in ASTM 311 [102] for hardened cement paste specimens containing CGWM powders (750°C, 850°C and 950°C) at the specified OPC replacement level of 20 wt.% (**Figure 5.9**). The dashed line at 75% represents the minimal SAI according to [102] on physical requirement on calcined natural pozzolans after 7 or 28 days of curing age. This assessment enables to evaluate if the test pozzolan reaches an acceptable level of strength development in a cement-based mixture, irrespective of whether the enhancement is from cementitious and/or pozzolanic nature.

The strength activity indices of the evaluated cement pastes were above the requirement limit of 75 % at all curing ages. The specimens containing GWM powders calcined at 850°C achieved the highest SAI of 81.8 %, 88.9 % and 90.5 % at 7, 28 and 56 days, respectively. The evaluation of the SAI confirms the potential of the CGWM powders for strength developing properties as pozzolanic materials and indicates that the optimal calcination temperature of the GWM powders is 850°C. However, the OPC replacement level of 20 wt.% should be considered as a fixed evaluation parameter according to ASTM 311 [102] rather than the recommended substitution amount of the test pozzolan. Therefore, the SAI method is extended to all tested cement paste specimens for all investigated calcination temperatures, substitution degrees and curing ages

(**Figure 5.10 - Figure 5.12**). The examination of the indices reveals that the strength enhancement of specimens at OPC replacement level of 5 wt.% using GWM powders calcined at 850°C and 950°C was led by the filler effect [105,106]. All samples with OPC substitution degrees from 5 wt.% up to 20 wt.% fulfilled the minimal SAI requirements according to [82] for all investigated curing ages. At curing age of 7 days (**Figure 5.10**), the specimens with a OPC replacement level above 25 wt.% did not fulfil the minimal requirement, probably related to the dilution effect with increasing pozzolan content which leads to an increased dispersion of cement particles and hence to a lower hydraulic reactivity. **Figure 5.11** and **Figure 5.12** show that, with increasing curing age, most of the specimens with higher OPC substitution degrees of 25-30 wt.% fulfil the minimal level of strength requirement as the pozzolanic reaction becomes more significant with development of additional CSH phases.

Figure 5.13 illustrates the calculated relative strength indices (RSI) of the hardened cement pastes after 56 days of curing age. The evaluation of the relative strength indices verify the previous analysis of the strength activity indices by showing a positive relative strength gain after 56 days of curing for the hardened cement pastes using higher OPC substitution degrees of 20-30 wt.% for all investigated calcination temperatures. The negative values for cement pastes using GWM powders calcined at 750°C at a replacement level from 5 to 15 wt.%, respectively, at 950°C at a replacement level of 10 wt.% indicate a relative strength loss by taking into account the substitution degree and the performance of the reference samples. This relative strength loss expresses that at lower substitution degrees, the contribution from pozzolanic reaction to the (relative) strength gain of the cement pastes is lower than the strength development by cement hydration of the reference sample. The highest potential of relative strength gain is reached by the cement pastes containing GWM powders calcined at 850°C [227] at an optimal OPC replacement level of 20 wt.%.

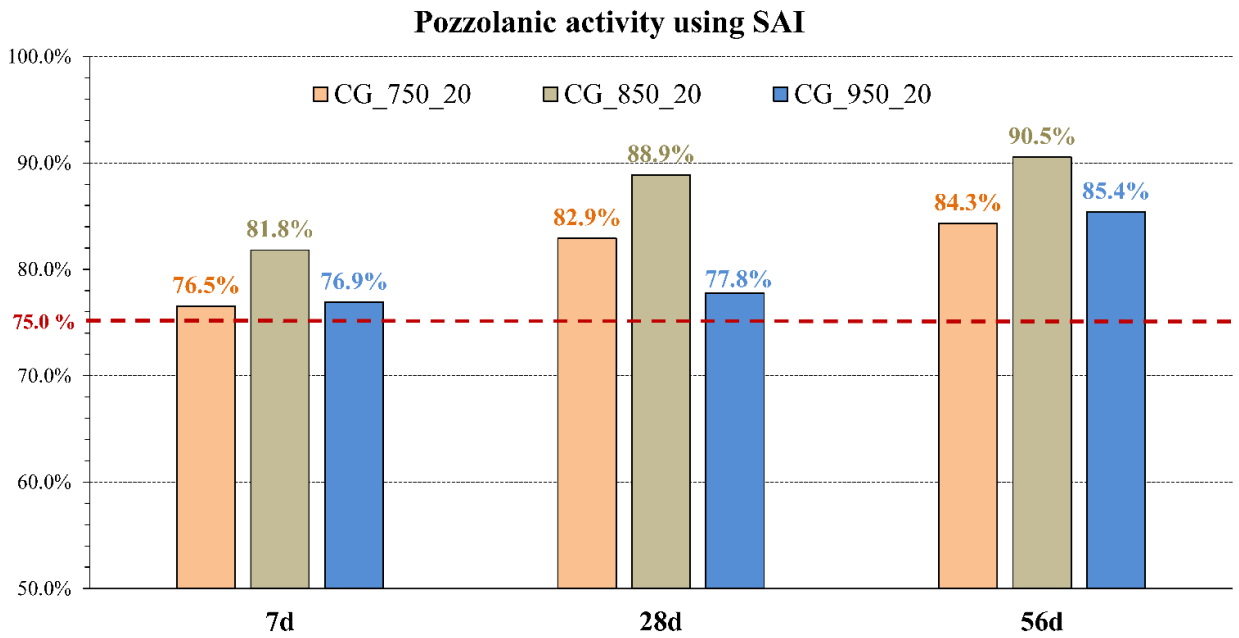

Figure 5.9 *- Strength activity indices of hardened cement pastes at OPC replacement level of 20 wt.% containing GWM powders calcined at 750°C, 850°C and 950°C; dashed line represents the limit for pozzolanic activity according to ASTM 618 [74]*

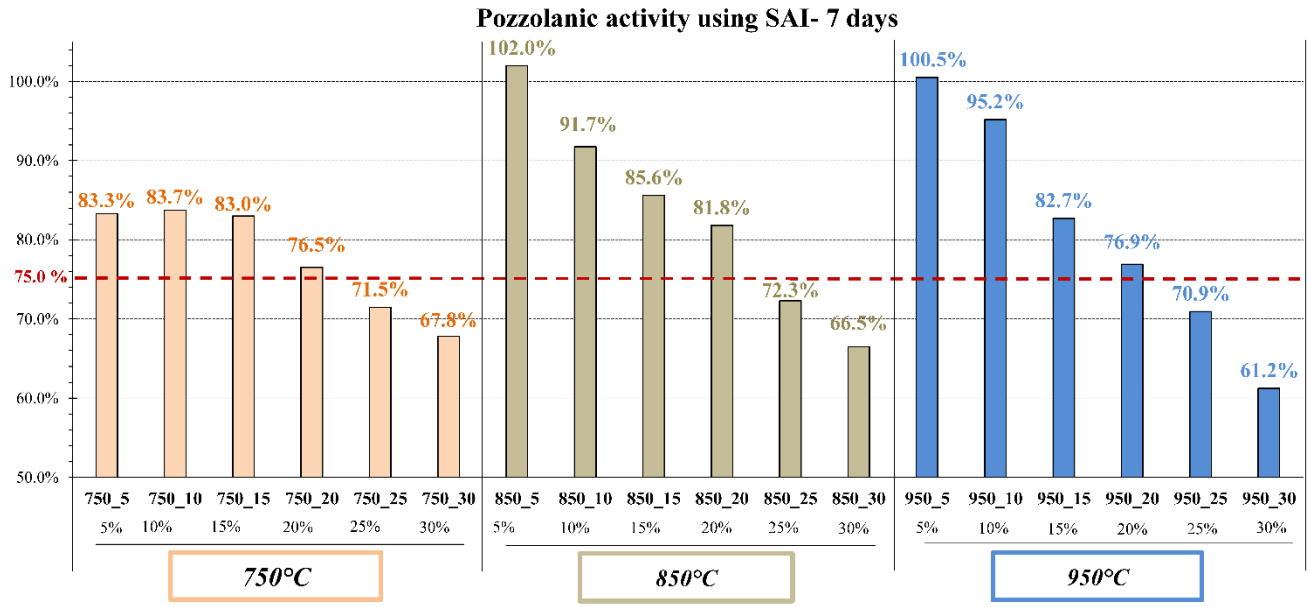

Figure 5.10 *- Strength activity indices of hardened cement pastes samples at 7 days of curing age*

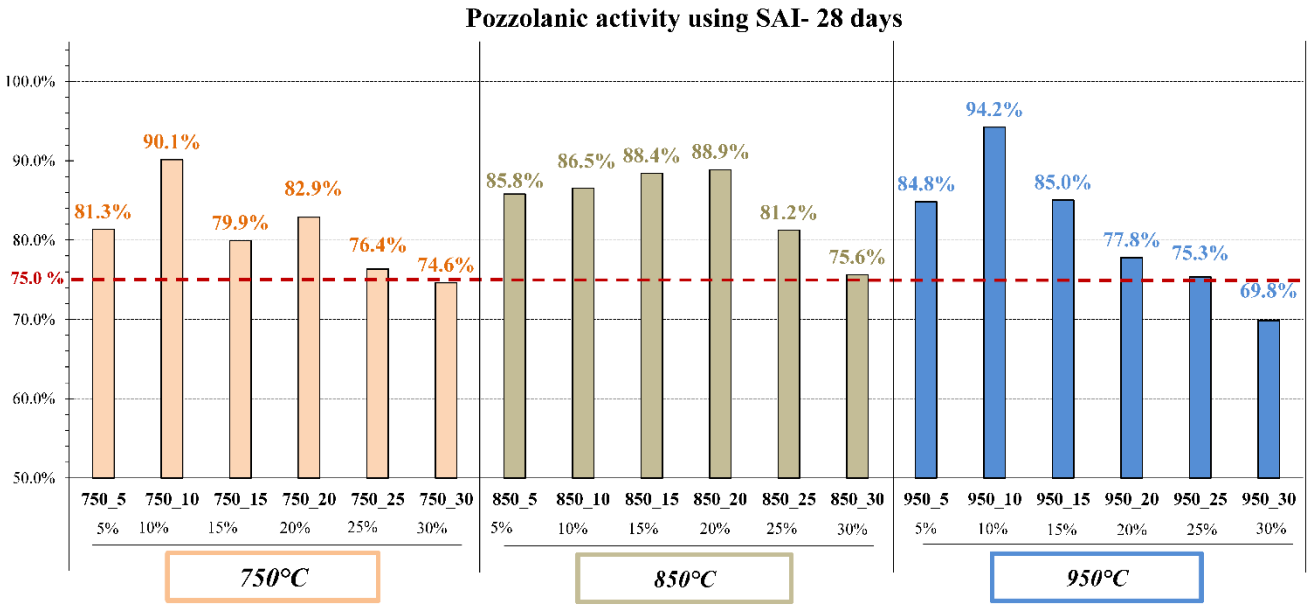

Figure 5.11 *- Strength activity indices of hardened cement pastes samples at 28 days of curing age*

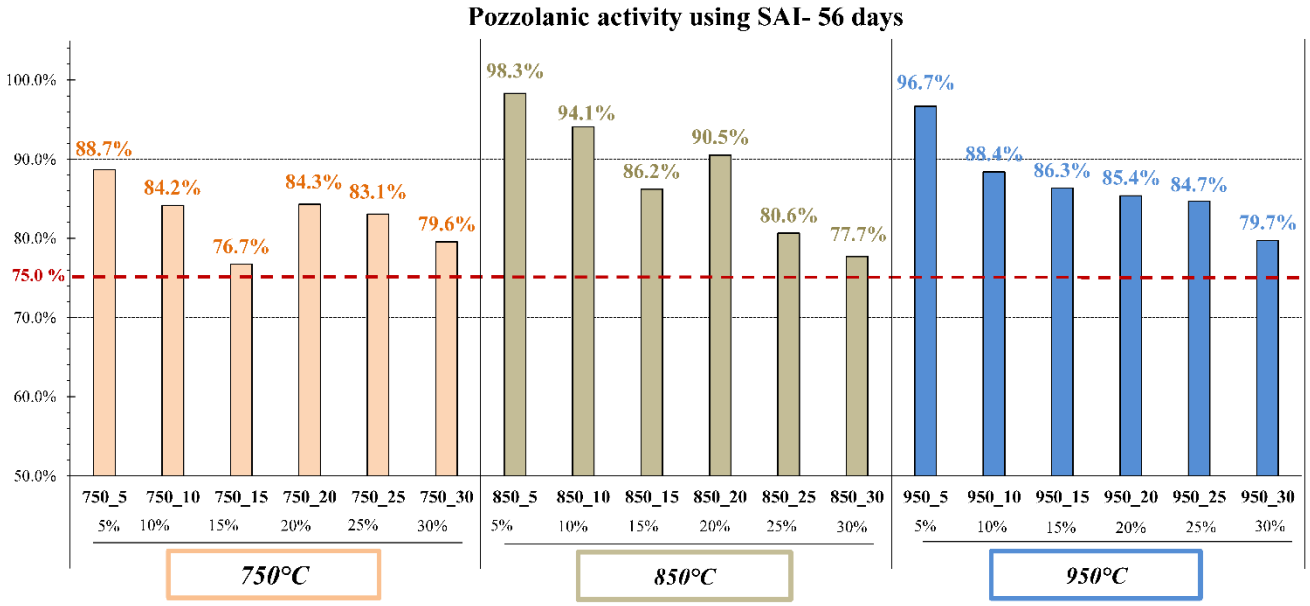

Figure 5.12 *- Strength activity indices of hardened cement pastes samples at 56 days of curing age*

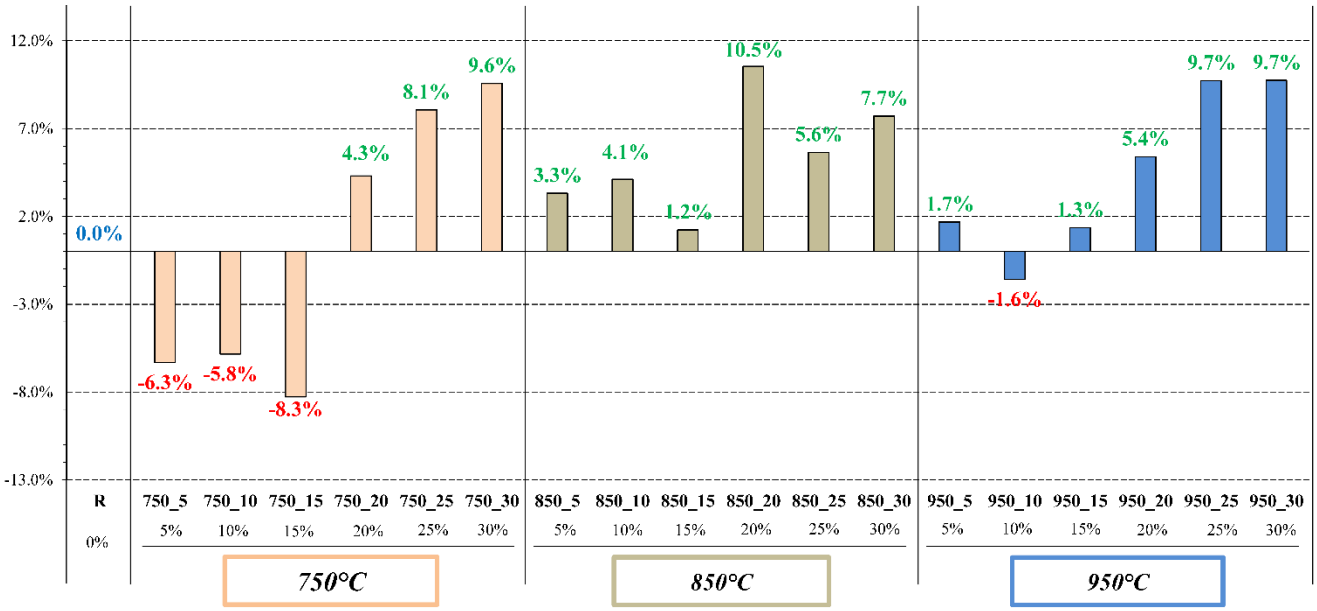

Figure 5.13 *- Evaluation of the mechanical performances (curing age of 56 days) of hardened cement pastes samples using the Relative Strength Index (RSI) method*

5.3.2.2 Phase composition of the hardened specimens by STA

Figure 5.14 shows the results of STA of CG_850_20. The TGA curve (green) shows a total mass reduction of 21.83%, which can be divided in three stages: The first mass loss of 9.63% from room temperature up to 250°C occurs due to the heating of the clay minerals, leading to the evaporation of capillary pore water, interlayer water and absorbed water of the CSH phases in the system. The second mass loss of 4.66% is related to the dehydration of calcium hydroxide (Portlandite). The third loss in mass of 7.54% from around 600°C up to 750°C can be attributed to the decarbonation of calcium carbonate ($CaCO_3$) in the binder system. Furthermore, the $CaCO_3$ carbonate results from the carbonation reaction of free Portlandite with CO_2 from air as no calcium carbonate was added in the initial mixture.

The DSC curve approves the findings of the TG analysis and presents three ranges with endothermic peaks. The first peaks around 100°C and 150°C represents the dehydration process of the different hydration products and aluminosilicate minerals due to the evaporation of capillary

pore water. The second endothermic peak around 450°C can be attributed to the dehydration of Portlandite. The final endothermic peaks observed between 700°C and 750°C correspond to the decarbonation of $CaCO_3$ [225,226].

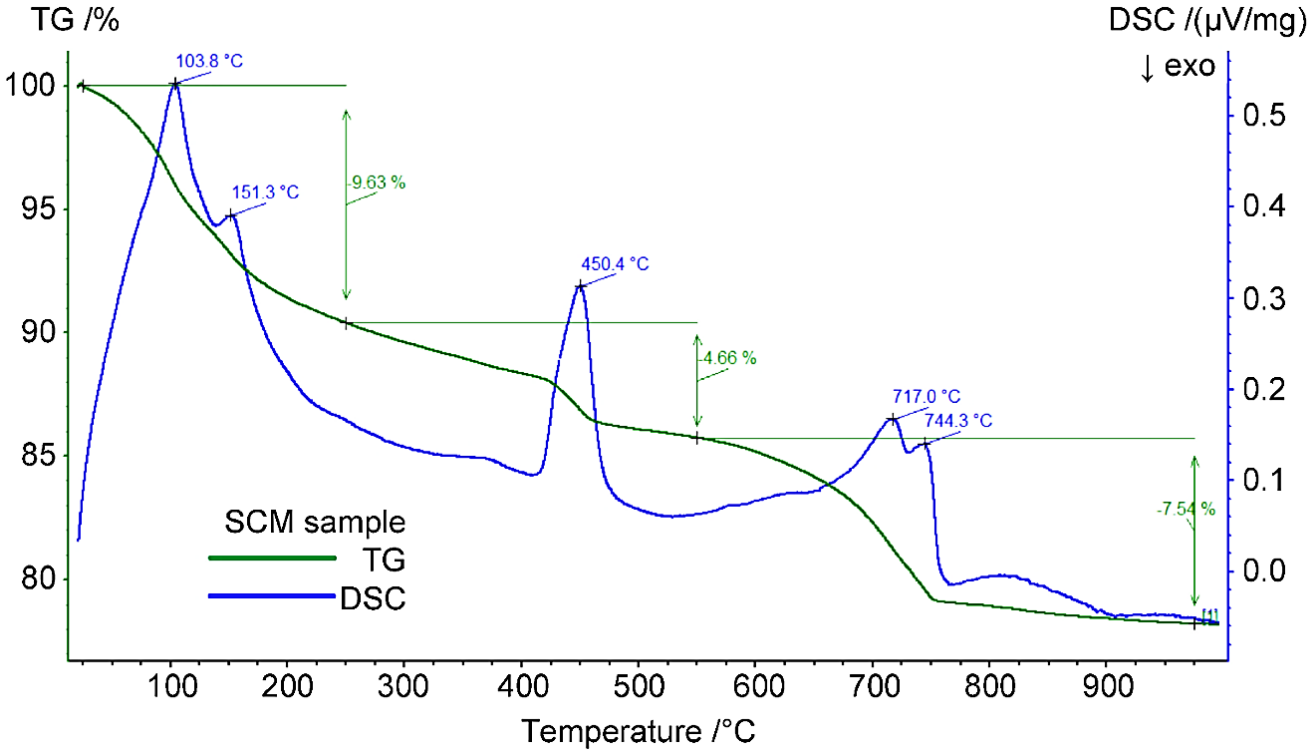

Figure 5.14 *- STA (TG-DSC) analysis of CG_850_20*

5.3.2.3 Analysis of the microstructure

Figure 5.15a-c illustrates the images of the microstructure of hardened specimens after 56 days, which were captured by performing SEM on small fractions of the compressed specimens with different replacement levels of CGWM. **Figure 5.15a** depicts the SEM image of the control sample and the formation of a compact microstructure of calcium silicate hydrates with Portlandite crystals can be observed with signs of local failures due to cracking of the hardened paste after the compression test. **Figure 5.15b** illustrates the microstructure of a hardened mixed paste with 20 wt.% of GWM powder calcined at 850°C. The bond between the hydrate phases and the

amorphous cementitious formations results in a compact and dense microstructure. Some irregular cracks were also observed due to the fractioning of the samples. Despite the presence of local aluminosilicate agglomerates, consisting of unmixed/semi-mixed compounds, the hardened mix paste of specimens with low PC replacement level is homogenous and less porous than for specimens with higher substitution degrees due to a better packing of its constituents (filler effect) and a higher degree of cement hydration (**Figure 5.15c**). The microstructural analysis of the different samples verify that a compact microstructural composition between the aluminosilicate-rich compounds and the cement-based products was established. This bond suggests the development of pozzolanic reactions between the calcined GWM powders and OPC.

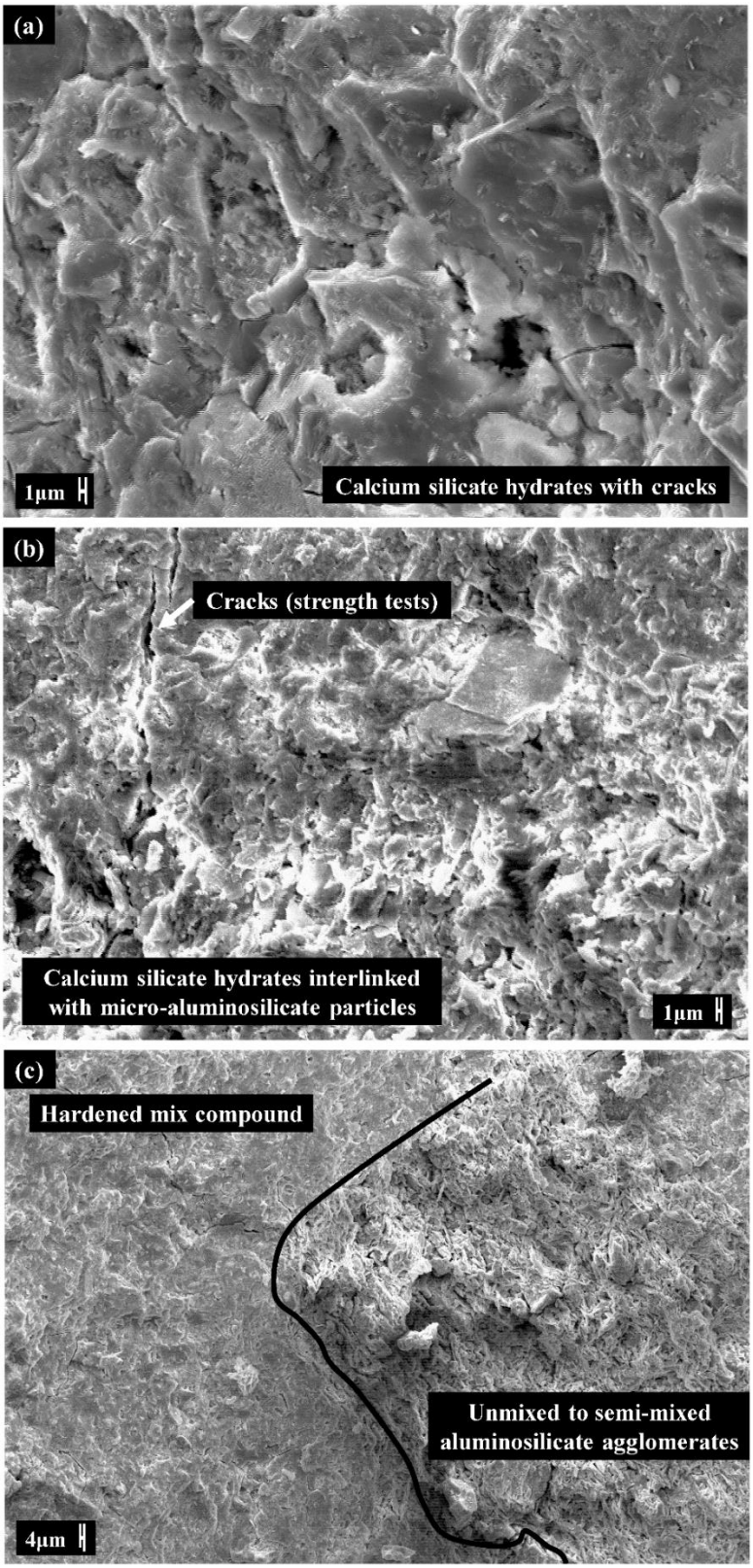

Figure 5.15 *- SEM images after 56 days of age: (a) reference mixture CG_R; (b) hardened mixtures CG_850_20; and (c) CG_850_5*

5.4 Conclusion

In the present study, gravel wash mud (GWM) powder, an aluminosilicate prime material, derived from a waste sludge from gravel quarrying and after undergoing a calcination process, was evaluated as a novel supplementary cementitious material. From the findings of the different investigations, the following conclusions can be drawn:

- The studied GWM powders are fine aluminosilicate-rich materials with a mean particle size around 7-9 μm depending on the applied calcination temperature. The mineralogy is mainly composed of quartz, illite and kaolinite as clay minerals, muscovite, hematite and a high amorphous portion.
- The evaluation of the mineralogy in combination with the STA analysis indicates that the increase of the calcination temperature led to the transfer of the clay phases into reactive hydrous and amorphous phases and therefore suggests the optimum calcination temperature for the GWM powders to be ranged above 750°C.
- The mechanical strength-based evaluation methods, the SAI and RSI methods applied on all investigated specimens, confirmed the pozzolanic activity of the CGWM powders.
- OPC substitution degrees ranging from 5% up to 25% by calcined GWM powders led to the development of a reliable, well-performing hardened cement paste/mortar products.
- The highest compressive strengths were achieved for specimens CG_850_5, CG_950_5 and CG_850_10 with 53.97MPa, 53.07 MPa and 51.66 MPa, respectively. However, the highest strength-enhancing potential regarding the mixing proportions and relative strength gain was observed for the samples containing GWM powders calcined at 850°C for one hour with a OPC replacement level of 20 wt.%. A pozzolanic composite cement of CEM

II/A-Q or CEM II/B-Q, standardized according to EN 197-1 [58] could be a medium-term option for the use of the calcined GWM powders.

- The associated environmental and economic benefits favour the use of CGWM powders as OPC substitution: The CO_2 emissions related to the calcination process of GWM powder (850°C) is lower than for the sintering (1450°C) of the prime materials during the production of Ordinary Portland cement. In addition, the waste material is no longer uneconomically landfilled due to its revalorisation as a partial OPC substitute. Nonetheless, further optimization are required, namely on the on-site removal of excess water of wet GWM to avoid extra transport costs if a practicable industrial usage of GWM is intended. From an environmental point of view, if compared directly with the range of different raw materials used to produce cement clinker, the environmental benefit of using GWM or similar industrial waste materials is evident considering the usage of a waste product and consequently the reduced depletion of limited natural resources required for cement clinker production.

This study confirms the pozzolanic activity of calcined GWM material as well as its strength-enhancing properties as filler material leading to higher compressive strengths for cementitious mixtures already at lower OPC substitution degrees. Even though promising results were obtained, further research on large-scale raw material processing, optimization of the mixing proportions, the study of the rheology, durability and other properties of fresh and hardened concrete mixture containing calcined GWM powders as alternative SCM, need to be carried out to implement a sustainable concrete product with a low carbon footprint for constructive applications.

Chapter 6 Publication III - Performance of lime-metakaolin pastes using gravel wash mud (GWM)

Abstract

The performance of ternary binders using lime, metakaolin (MK) and gravel wash mud (GWM) powders is studied for the development of novel lime-pozzolan pastes. This study examines the influence of varying mixture proportions using different types and compositions of lime powders and GWM at different treatment levels on the mechanical properties of lime-MK-GWM pastes. Various characterisation techniques including particle size distribution (PSD), X-ray fluorescence (XRF), X-ray diffraction (XRD), compressive strength tests, simultaneous thermal analysis (STA) and scanning electron microscopy (SEM), were applied on the different raw materials, respectively, on the hardened pastes to determine the reaction kinetics, the resulting microstructure and the mechanical performances of the lime-MK-GWM binder systems. Higher strength-enhancing contributions of thermally treated GWM powders (calcined at 850°C) leading to compressive strengths up to 18 MPa were confirmed and the strength-based evaluations revealed that hydrated lime-based pastes achieved higher mechanical performances than hydraulic lime-based binder systems.

Keywords - Gravel wash mud, Lime, Metakaolin, Calcined clays, Mineralogy, Mechanical properties, Pozzolanic activity.

6.1 Introduction

Combating climate change has undoubtedly become one of the major global priority concerns and its success crucially depends on the reduction of CO_2 emissions related to the cement industry, more precisely the cement clinker production [228–231]. In modern cement kilns, the production of 1 tonne of cement clinker generates around 800-840 kg gross CO_2 emissions [228,232], out of which about two third of the CO_2 emissions are released during the calcination reaction (decarbonation of calcium carbonate $CaCO_3$ into lime CaO and CO_2) and one third results from the combustion process itself [230,231]. Moreover, for further reduction of the overall carbon footprint of ordinary Portland cement (OPC), it is current practice for cement manufacturers to complement the Portland clinker by various cementitious products as partial clinker replacement materials or as additions, which are mainly reactive alumina-siliceous industrial co-products and are deemed to be low carbon in compliance with the cement standards [71]. In recent decades, extensive research was carried out to develop environmental friendly and sustainable binder technologies allowing to reduce the usage of cement clinker by using industrial by-products or waste materials, instead of already established and commercially available cement additions like fly ash (FA), ground granulated blast furnace slag (GGBS) and silica fume (SF) [86,88,90,112,233,234]. Especially in Europe, with the decline of the primary industrial activities in coal power stations, the steel industry and the ferro-alloy and silicon production, the availability of these resources has gradually dried up and remaining activities are no longer found sufficiently close to the cement production sites.

Most of the research studies investigate on supplementary cementitious materials (SCMs) and on how the clinker contents in Portland cement can be reduced without loss in workability, performance and durability. In particular, investigations on alternative SCMs using naturally

occurring raw clays mixes and waste clay products have risen worldwide [1,2,72,80,197,200,235]. Among recently investigated aluminosilicate materials figure the gravel wash mud (GWM) powders [2] and the sewage sludge ashes [235], which originally are waste products of industrial activities (sandstone quarry and sludge incineration plants). Their strength-enhancing potentials as promising alternative SCM in cement-based pastes, respectively in lime-pozzolan systems, were confirmed.

Furthermore, recent trends promote research on lime-based binder concepts without Portland cement clinker to develop mortars and concrete products using alternative cementitious materials like ground granulated blast-furnace slag, pulverised fuel ash, calcined clays, silica fume, rice husk ash, and brick dusts [86,142,146,236]. From a historical aspect, lime-pozzolan binders are the predecessor binder systems of Portland cement clinker and lime-pozzolan plasters have gained greater interest as valuable alternatives to OPC-based mortars for the restoration of historical buildings due to their better compatibility with historic lime-based building structures [136,137,143,152,237,238]. However, the increasing political and societal awareness on reducing the immediate impacts of climate change have imposed operational restrictions on intense CO_2-emitting industrial sectors like the cement industry. Therefore, in the recent years, the investigations on lime-pozzolan binders have significantly risen up [141,144,145,151,235,237,239–242]. In general, the hardening mechanism of pure lime binders is mainly driven by carbonation reaction, a slow reaction process where calcium hydroxide reacts with atmospheric CO_2 to form calcium carbonates [243,244]. However, in the presence of reactive, aluminosilicate-rich pozzolanic materials, the hydration reaction is favoured with formation of hydraulic components. The reaction mechanisms of binary lime-metakaolin binders systems were investigated in [142–144,146,241] and they confirmed that the main initial phases formed are

(cementitious) hydraulic products like calcium silicate hydrates (CSH), calcium aluminate silicate hydrates (CAH) and calcium aluminate silicate hydrates (CASH) resulting from the pozzolanic reaction between the calcium hydroxide-rich limes and the pozzolans. The compositional variety, the stability and the durability of these compounds depends on the amorphous phases in the alumina-siliceous materials, which strongly influence its pozzolanicity as well as the resulting mechanical performances [86]. Mechanical performances up to 28 MPa were reported in [237,242] for binary lime-silica fume pastes, ternary lime-silica fume-GGBS pastes and lime-fly ash-ceramic waste pastes; as well as compressive strength around 14 MPa for lime-MK pastes in combination with other pozzolanic additions. Furthermore, valuable research has been made into understanding the long-term characteristics of the corresponding lime-MK pastes [145,148]. Both studies concluded that with increasing curing age, the stability of the formed hydraulic compounds depends on the optimal MK content in correlation with consumable calcium hydroxide content to restrict the early carbonation reaction and promote later carbonate hardening.

However, most of the works focus mainly on the reaction kinetics of lime-MK systems for heritage restoration purposes, therefore, little is known about the impacts on the reaction mechanisms, the mechanical performances, the durability, the optimal composition (hydraulic or hydrated lime) and the performance-enhancing characteristics of lime-MK binders using alternative SCMs [152,235,240].

This paper focuses its investigations on the strength-enhancing pozzolanic character of gravel wash mud (GWM) as SCM in ternary lime-MK-GWM binder systems. GWM, a quarry waste product, was incorporated in lime-MK pastes using varying raw material compositions and different mix designs. The primary aim is to determine the optimal prime material compositions and to investigate towards optimal mix proportions by conducting a selected set of physiochemical

and mineralogical characterisation analyses and performance-based experimental assessments on the lime-MK-GWM products. Large series of lime-MK-GWM pastes were prepared including GWM in three different states of matter (pure, uncalcined and calcined at 850°C [1,2]), hydraulic lime, three different hydrated limes, MK and fine dolomitic sand. The physiochemical and mineralogical characterisations of selected raw materials were determined using laser diffraction granulometry, the X-ray fluorescence (XRF) analysis, the quantitative X-ray diffraction (XRD) analysis and the simultaneous thermal analysis (STA). The actual potential of ternary lime-MK-GWM pastes was drawn out based on the evaluation of hardened samples using mechanical strength tests combined with thermal analysis and scanning electron microscopy.

6.2 Materials and experimental program

6.2.1 Materials and material preparations

Three different hydrated limes, HL1 (ρ_{HL1} = 0.55 g/cm³) from Lhoist (Istein, Germany), HL2 (ρ_{HL2} = 0.52 g/cm³) and HL3 (ρ_{HL3} = 0.41 g/cm³) from Carmeuse S.A. (Belgium), were selected for this study to investigate the required characteristics of hydrated limes for optimal use. HL1 and HL3 are classified as calcium limes CL90-S (CaO+MgO content ≥ 90 wt.%; S stands for powder) and HL2 as CL80-S (CaO+MgO content ≥ 80 wt.%; S stands for powder), according to EN 459-1:2010 [245]. For the comparative trial test, a natural hydraulic lime (NHL, ρ_{NHL} = 0.65 g/cm³) from Chaux et enduits de Saint-Astier (France), classified as natural hydraulic lime NHL 3.5 ($Ca(OH)_2$ content ≥ 25 wt.%, 28-day compressive strength ≥ 3.5 MPa to ≤ 10 MPa) according to [245] was used.

The used metakaolin (MK, ρ_{MK} = 0.87 g/cm³) is produced by Argeco Développement (France)

according to NF P18-513 [246] by milling and calcining the raw kaolinite using the flash calcination method. In addition, a fine dolomitic sand (DS, ρ_{DS} = 1.71 g/cm³) from Carrières Feidt S.A. (Luxembourg) was used as fine aggregate.

Pure gravel wash mud (PGWM) was sampled from a decantation basin from a local sandstone quarry operated by Carrières Feidt S.A. (Luxembourg). The wet GWM has a water content of around 32 wt.% (with use of a flocculation reagent) [1]. After removal of the absorbed water and moisture by drying the sludge at 105°C in a laboratory drying chamber for two days, the dried GWM was fragmented and ground into a fine powder, denominated as uncalcined GWM (UGWM, ρ_{UGWM} = 0.75 g/cm³) powder. The calcination of the UGWM powder into a more reactive, amorphous raw material, henceforth referred to as calcined GWM (CGWM, ρ_{CGWM} = 0.73 g/cm³) powder, was performed in a laboratory chamber furnace with radiation heating by burning the fine powders from room temperature up to 850°C (heating rate of 5°C/min) [2]. After application of the peak temperature for one hour, the CGWM powder is let to cool down naturally inside the chamber furnace.

This study examines the suitability of the proposed MK-lime-GWM pastes as a potential alternative to OPC-based products for constructive applications. Prior to the investigated mixtures, preliminary strength-based evaluations were carried out to restrict the study range of the examined mixture proportions. Within this work, over 250 specimens were prepared based on varying mixing proportions of different types and compositions of lime powders (NHL, HL1, HL2 and HL3), GWM in different forms and treatment levels (PGWM, UGWM and CGWM), commercial Metakaolin (MK) and dolomitic sand (DS) as fine aggregate. The initial focus was on the selection of the adequate raw materials (types of lime and GWM) with the objective to restrict the range of examined mixture proportions towards optimum and the evaluation of the reaction mechanisms to

achieve best possible performances of the investigated binder concepts.

6.2.2 Paste compositions, mix proportion design and curing conditions

The mix design **(Table 6.1)** comprises three series of mixtures, which were adapted and prepared consecutively based on the findings of the respective preceding series. Three specimens of each mixture were prepared for each investigated curing age. The first series of mixtures (S1; curing ages of 7, 14, 28 days) consists of pastes based on pure, untreated GWM (PGWM), MK, and DS with two types of limes, namely natural hydraulic lime (NHL) or hydrated calcium lime (HL1). This primary set of mixtures examines the potential of binders using pure GWM as a potential raw material before any treatment procedures of this raw product are adopted which would lead to modifications of the mineralogy and the microstructure. In addition, a reliable statement on the choice of lime type (hydraulic or hydrated lime) as well as the range of acceptable mixture proportions was developed. Including additional mixture adjustments by taking into account the findings of the first series, the second series of mixtures (S2; curing ages of 7, 14, 28 and 90 days) examines pastes based on PGWM, MK and DS with three different hydrated limes HL1, HL2 and HL3, to evaluate the optimal physiochemical characteristics and compositions of hydrated limes using strength-based performance criteria. Based on the results of the second series of mixtures, the third and largest series of mixtures (S3; curing ages of 7, 28, 56 and 90 days) consists of pastes based on HL2, MK, DS and processed GWM powder (UGWM or CGWM), and a control lime-MK paste mixture without GWM content (REF). These series lead to the reported maximum performances of the proposed binder concepts with adapted mix design proportions. The water/binder (w/b) ratio was adjusted from one series to another from 0.3 to 0.5 and the

aggregate/binder (ag/b) ratio was kept constant at 0.7.

The mixing procedure was the same for all the series of mixtures: the amounts of binder components, namely GWM, MK, and lime, were dry-mixed at a mixing speed of 125 rpm for 15s. While maintaining the same mixing speed, half of the water is gradually added and let to mix for another 180s. Subsequently, the amount of DS is added with the remaining water and the compound is mixed for 90s at 125 rpm and finally 90s at 250 rpm. The fresh mixture pastes were cast in prismatic moulds (40 x 40 x 160 mm^3) and compacted for 15 seconds on a vibrating table. After casting, the moulds were covered with plastic plates of 5 mm thickness to prevent rapid desiccation. After hardening time of 24 hours, the specimens were demoulded, wrapped in cellophane foil to restrict moisture exchange with the surroundings and cured at ambient temperature until 24 hours before the uniaxial compression tests according to EN 196-1 [101].

	Mix proportions by mass					
Series 1 (S1)	NHL	HL1	MK	PGWM	w/b[a]	ag/b[b]
	[-]	[-]	[-]	[-]	[-]	[-]
PGA_NHL	1.00	-	2.00	1.00	0.30	0.70
PGB_NHL	1.00	-	1.66	1.25	0.30	0.70
PGC_NHL	1.00	-	0.70	1.40	0.30	0.70
PGA_HL1	-	1.00	2.00	1.00	0.30	0.70
PGB_HL1	-	1.00	1.66	1.25	0.30	0.70
PGC_HL1	-	1.00	0.70	1.40	0.30	0.70

	Mix proportions by mass						
Series 2 (S2)	HL1	HL2	HL3	MK	PGWM	w/b[a]	ag/b[b]
	[-]	[-]	[-]	[-]	[-]	[-]	[-]
PG_HL1	1.00	-	-	1.33	1.00	0.45	0.70
PG_HL2	-	1.00	-	1.33	1.00	0.45	0.70
PG_HL3	-	-	1.00	1.33	1.00	0.45	0.70

	Mix proportions by mass					
Series 3 (S3)	HL2	MK	UGWM	CGWM	w/b[a]	ag/b[b]
	[-]	[-]	[-]	[-]	[-]	[-]
REF	1.00	1.33	-	-	0.50	0.70
UG_1:1:1	1.00	1.00	1.00	-	0.50	0.70
UG_1:1:1.33	1.00	1.00	1.33	-	0.50	0.70

UG_1:1:1.66	1.00	1.00	1.66	-	0.50	0.70
UG_1:1.33:1	1.00	1.33	1.00	-	0.50	0.70
UG_1:1.33:1.33	1.00	1.33	1.33	-	0.50	0.70
UG_1:1.33:1.66	1.00	1.33	1.66	-	0.50	0.70
UG_1:1.66:1	1.00	1.66	1.00	-	0.50	0.70
UG_1:1.66:1.33	1.00	1.66	1.33	-	0.50	0.70
UG_1:1.66:1.66	1.00	1.66	1.66	-	0.50	0.70
CG_1:1:1	1.00	1.00	-	1.00	0.50	0.70
CG_1:1:1.33	1.00	1.00	-	1.33	0.50	0.70
CG_1:1:1.66	1.00	1.00	-	1.66	0.50	0.70
CG_1:1.33:1	1.00	1.33	-	1.00	0.50	0.70
CG_1:1.33:1.33	1.00	1.33	-	1.33	0.50	0.70
CG_1:1.33:1.66	1.00	1.33	-	1.66	0.50	0.70
CG_1:1.66:1	1.00	1.66	-	1.00	0.50	0.70
CG_1:1.66:1.33	1.00	1.66	-	1.33	0.50	0.70
CG_1:1.66:1.66	1.00	1.66	-	1.66	0.50	0.70

[a] w/b: water/binder ratio, binder equal to mass of lime, MK and GWM

[b] ag/b: binder/aggregate ratio; ag: dolomitic sand (DS)

***Table 6.1** - Mix proportions of studied mix series*

6.2.3 Experimental methods

The particle size distributions of NHL, HL1, HL2, HL3, UGWM, CGWM, DS and MK powders were determined by the laser diffraction technique using a particle size analyser (HELOS-RODOS-VIBRI from Sympatec GmbH, Germany). The chemical composition of the powder samples was determined by X-ray fluorescence method using a wavelength dispersive X-ray fluorescence spectrometer (S8 TIGER from Bruker AXS GmbH, Germany).

A powder X-ray diffractometer (D4 ENDEAVOR from Bruker AXS GmbH) using Cu K_α radiation was used to determine the mineralogy of the powders by quantitative X-ray diffraction analysis, following the Rietveld refinement principles. The characteristic d-spacings and diffraction peak intensities corresponding to specific crystalline phases, available in the powder samples, were detected using the XRD software DIFFRAC.EVA (Bruker AXS GmbH, Germany). The XRD patterns were processed using the software TOPAS (Bruker Corporation) using the

fundamental parameter approach for line profile fitting [213]. Moreover, the crystalline phases were described using appropriate structural data from ICSD database [2,189,216] before refinement of the diffractograms using the Rietveld method [214,247]. The amorphous contents were computed using quartz at 35% as an internal reference as described in [2,189].

The thermo-analytical technique applied on the hardened binder pastes was the simultaneous thermal analysis (STA), which merges the techniques to monitor the heat flow change (differential scanning calorimetry, DSC) and the mass change (thermogravimetric analysis, TGA) of a sample as a function of temperature.

The compressive strength of each mixture was measured on three replicate specimens for each curing age. The strength assessment was carried out using a compression test plant (TONICOMP III, Toni Technik GmbH, Germany), conform to the standard DIN EN 196-1 [101], with additional displacement transducers.

The microstructural composition of the hardened specimens were examined by scanning electron microscopy (SEM) using a “LEO 440 REM” unit (Carl Zeiss SMT AG, Germany). The examined samples were small fractions from the compressed specimens, which were prepared for the SEM analysis by applying a functional gold coating on the non-conductive.

6.3 Results and discussions

6.3.1 Physicochemical properties of the primary materials

Table 6.2 shows the chemical analysis of the used primary materials for the paste compositions. The different types of hydrated limes (HL1, HL2 and HL3) confirm a major CaO content, mainly resulting from the portlandite minerals. The natural hydraulic lime (NHL) shows a slightly lower

CaO content and a medium silica (SiO_2) content, resulting from the presence of argillaceous components during the firing process to produce calcium silicate compounds. The GWM powders (UGWM and CGWM) and the Metakaolin (MK) can be categorised as aluminosilicate-rich materials with high silica (SiO_2) and medium alumina (Al_2O_3) contents [1,2]. However, UGWM and CGWM show a slightly lower alumina (Al_2O_3) content, but higher ferrite (Fe_2O_3) content than MK, which explains the comparatively darker brownish-red colour of the GWM powders. The dolomitic sand (DS) shows high CaO, medium SiO_2 and MgO contents, which can be assigned to the high presence of calcium-magnesium carbonate phases (dolomite).

Sample	**Chemical composition**									
	SiO_2	Al_2O_3	Fe_2O_3	CaO	MgO	SO_3	Na_2O	K_2O	TiO_2	MnO
[-]	[%]	[%]	[%]	[%]	[%]	[%]	[%]	[%]	[%]	[%]
HL1	0.57	0.50	0.28	96.86	0.95	0.26	0.17	-	-	-
HL2	0.14	0.14	0.07	98.62	0.50	0.11	0.15	-	-	-
HL3	-	-	0.07	98.78	0.53	0.10	-	-	-	-
NHL	18.35	2.13	0.86	75.63	1.54	0.68	0.11	0.39	0.10	0.02
UGWM	64.97	19.50	9.35	0.41	1.66	0.09	0.24	2.72	0.85	0.06
CGWM	64.01	20.26	8.90	0.41	1.81	-	0.24	3.25	0.90	0.08
DS	22.54	4.79	5.16	49.25	13.91	0.18	-	2.54	0.57	0.20
MK	69.37	32.01	2.74	0.99	-	-	-	0.31	1.41	-

***Table 6.2** - Chemical composition of applied materials: HL1, HL2, HL3, UGWM, CGWM (calcined at 850°C), DS and MK powders*

The particle size distributions of the used materials are displayed in **Figure 6.1**. The different primary materials show a very fine PSD ranging from a fine clay particle size (< 2 µm) up to a coarse silt grain size (< 60 µm). Among the investigated materials, the three hydrated limes show the finest grain size range (d10-d90) from 0.7 to 5.5 µm with respective mean particle sizes (d50) and high specific surface areas of 2.23 µm and 1169.9 m^2/kg for HL1, 1.41 µm and 1597.2 m^2/kg for HL2, and respectively,1.45 µm and 1554.3 m^2/kg for HL3. In comparison, NHL presents a

higher average particle size of 7.54 µm and a lower specific surface area of 628.3 m^2/kg. The UGWM and CGWM powders follow very similar PSD with d50 of 7.36 µm resp. 8.36 µm and specific surface areas of 522.5 m^2/kg resp. 479.9 m^2/kg. CGWM is slightly coarser than UGWM due to clumping effect of the clay particles from the compaction of the minerals when exposed to high temperatures (850°C). MK and DS show comparatively coarser grain size distributions with average particle sizes of 22.15 µm resp. 24.49 µm and specific surface 308.6.9 m^2/kg resp. 479.9 m^2/kg. The different raw materials cover a wide range of particle size distributions, which suggests a compact packing density of the mixes between the different constituents of the lime-MK-GWM pastes [106,204,205].

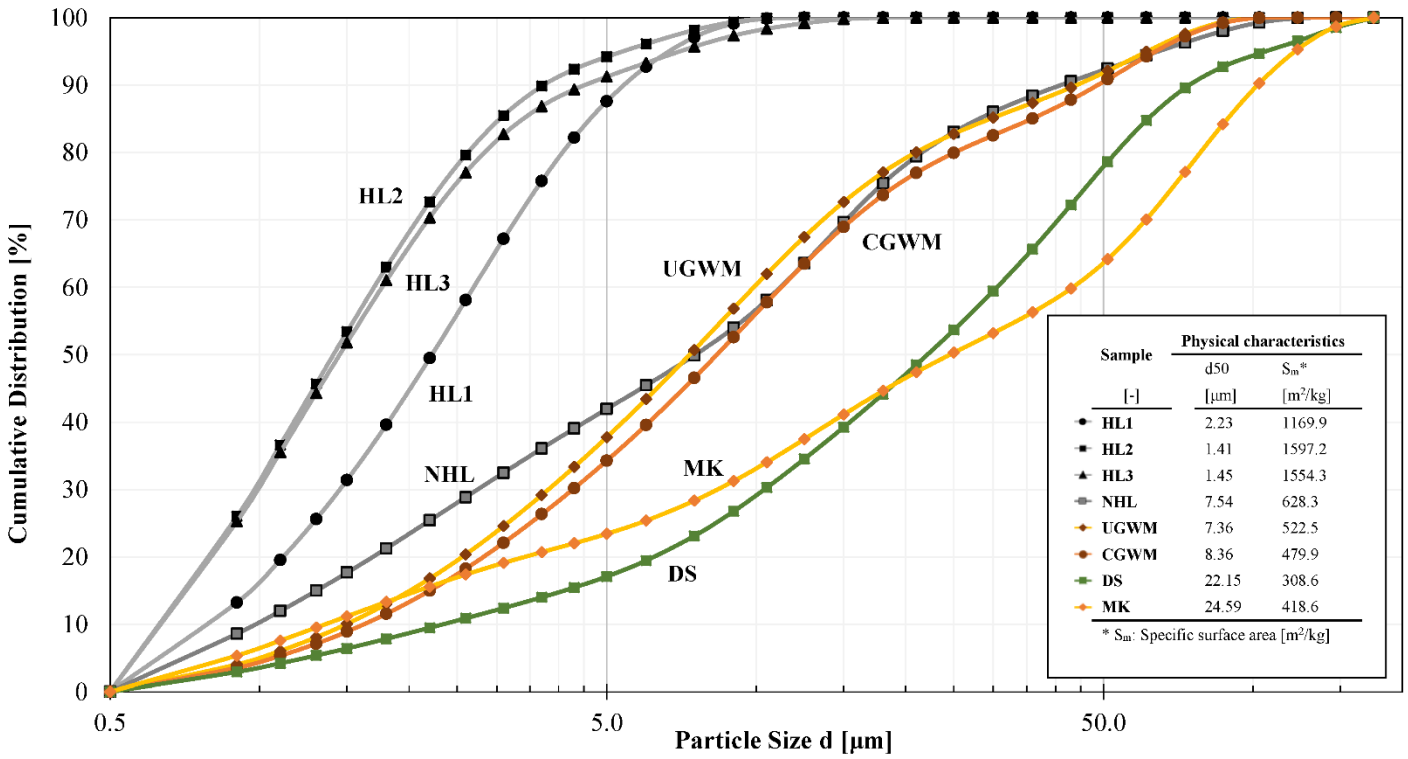

Figure 6.1 *- Particle size distribution and physiochemical characteristics of applied materials: HL1, HL2, HL3, UGWM, CGWM (calcined at 850°C), DS and MK powders*

6.3.2 Mineralogy and thermal analysis of the primary materials

XRD patterns of the UGWM and the CGWM are presented in **Figure 6.2**. The GWM powders indicate a strong reflection of quartz, medium peak intensities of muscovite, illite and kaolinite, and poor diffraction peaks of hematite. Traces of the phase shifts of kaolinite to XRD amorphous phases can be observed in the X-ray diffraction pattern of the UGWM and CGWM powders [1,2]. The quantitative XRD analysis of all the investigated materials is summarized in **Table 6.3**. The quantitative mineralogical evaluation, following the method described in [2,215], confirms for the GWM powders the high presence of amorphous components and the major crystalline phase as quartz, followed by muscovite, illite and kaolinite as medium phases and hematite respectively $KAl_3Si_3O_{11}$ as minor phases. Further comparison reveals the positive impact of thermal treatment (calcination) on the GWM powders, as a clear rise of the amorphous content results from the transition of kaolinite to XRD amorphous phases. In addition, a slight decrease in illite content and a phase transition of muscovite phases into $KAl_3Si_3O_{11}$ can be observed. Comparatively, the used metakaolin (MK) is majorly XRD amorphous with some content of quartz, which explains the high pozzolanicity of the commercial product. The hydrated lime powders HL1-HL3 consist primarily of portlandite (calcium hydroxide) and thereby also confirm the findings of the chemical analysis. The low calcite amounts can be explained either as remainders from the original limestone ($CaCO_3$) or as a result of carbonation of hydrated lime [248]. The main mineralogical phases observed for NHL were high contents of portlandite and calcite ($CaCO_3$), and medium contents of alite (C_3S) and belite (C_2S).

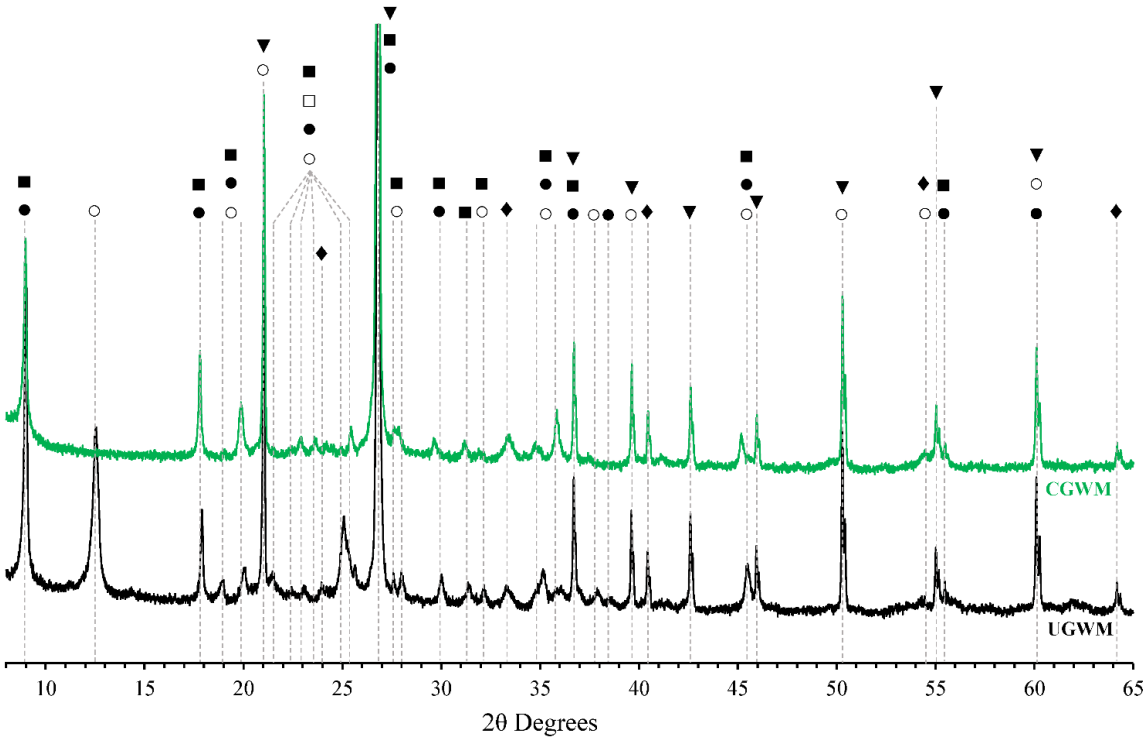

***Figure 6.2** - X-ray diffractogram of UGWM and CGWM: ▼ - Quartz, ■ - Muscovite, ● - Illite, ○ - Kaolinite, ♦ - Hematite, □ - $KAl_3Si_3O_{11}$*

Sample	Mineralogical composition [%]						
	Quartz[a]	Muscovite	Illite	Kaolinite	Hematite	$KAl_3Si_3O_{11}$	Amorph
UGWM	35.0	15.3	10.9	11.9	1.0	1.3	24.5
CGWM	35.0	8.4	12.8	0.5	2.2	7.0	34.1
	Portlandite	Calcite	Dolomite	Mica	Quartz	Amorph	
HL1	92.5	7.5	-	-	-	-	
HL2	98.9	1.1	-	-	-	-	
HL3	99.2	0.8	-	-	-	-	
DS	-	0.5	72.4	10.4	16.7	-	
MK	-	-	-	-	31.2	68.8	

	C_3S	C_2S	C_3A	C_4AF	Calcite	Portlandite	Anhydrite	Peri.[b]	Quartz	D.[b]	Amorph
NHL	12.2	17.9	2.8	2.8	28.1	29.8	0.1	0.4	2.6	0.4	2.9

[a] Quartz content fixed as standard

[b] Peri. - Periclase and D. - Dolomite

***Table 6.3** - Mineralogical composition of NHL, HL1-3, DS, MK, UGWM and CGWM powders*

6.3.3 Compressive strength tests of hardened specimens

6.3.3.1 Natural hydraulic lime vs hydrated lime

Figure 6.3 presents the results of the compressive strength test performed on the hardened prismatic specimens of the first series (S1) at 7, 14 and 28 days. The gradual gain in compressive strength for each mixing proportion over the investigated curing age validates the assumption that a strengthening structure is developed and thus the potential of lime-MK pastes using untreated, pure GWM as alternatives to cement-based products for construction applications. Overall, the mechanical strengths of the hardened pastes containing hydrated lime were higher than the strengths achieved by the mixtures containing natural hydraulic lime for all mixtures and curing ages, except for PGC_NHL at 7 days. The highest 28-day compressive strength of 13.3 MPa was achieved by hardened pastes containing hydrated lime, namely PGB_HL1, whereas the highest mechanical strength for hardened pastes containing natural hydraulic lime was reached by PGC_HL3 with 9.8 MPa.

Furthermore, for the hardened pastes containing hydraulic lime, on average around 70% of the 28-day compressive strength was already reached at 7 days of curing age due to predominant hydration reaction of hydraulic lime with formation of stable calcium silicate hydrate (CSH) phases over the first days [237,239]. The progressive development of additional CSH phases from pozzolanic reaction could not be traceably observed, mainly due to the lower availability of free calcium hydroxide in the binder system in opposition to the presence of high reactive MK and low reactive PGWM. In comparison, for the mixtures containing hydrated lime only about 55% of the 28-day compressive strength was achieved over the same time period (7 days). The hardening process of the hydrated lime-based pastes consists primarily of the formation of solid calcium

silicate hydrates which are formed from the pozzolanic reaction between calcium hydroxide and the reactive aluminosilicate minerals in the first hours and days [146]. Simultaneously, an additional increase in strength is considered due to the development of further reaction products from carbonation reaction with increasing hardening ages [141,248]. However, the strength-enhancing properties of pure GWM could not be identified, mainly due to its incorporation in the mixtures in its very low-reactive and untreated raw state.

The strength evolution of the hardened pastes of S1 validates the continuous hardening reactions of lime-MK pastes using pure GWM until 28 days of curing and the higher mechanical performances of mixtures using hydrated lime instead of hydraulic lime.

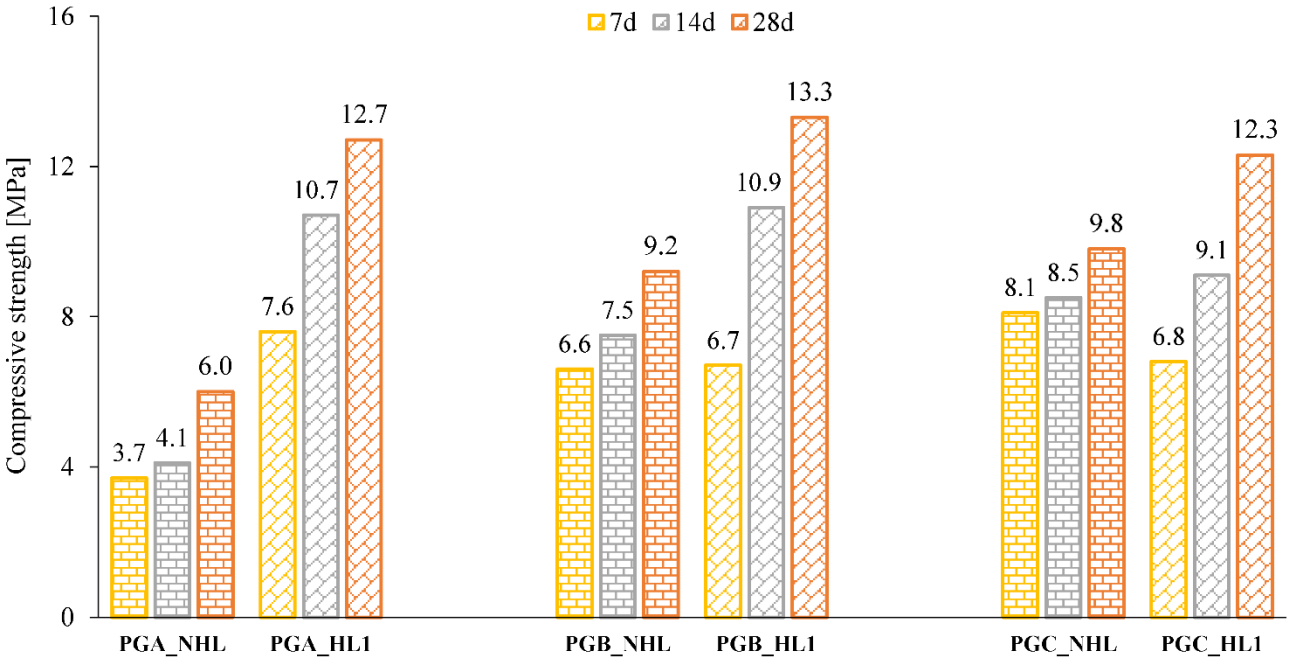

Figure 6.3 *- Development of the mechanical properties of hardened pastes from three different mixtures containing PGWM, MK, DS, and NHL or HL1*

6.3.3.2 Variation of the composition of hydrated lime

The compressive strength results at 7, 14, 28 and 90 days of the hardened lime-MK pastes containing PGWM and different hydrated limes (HL1, HL2 and HL3) with the same mixing

proportion are presented in **Figure 6.4**. As expected, the hardened pastes of the second series (S2) show very similar profile of strength gain with a gradual growth in compressive strength with increasing curing age. The strength evolution of HL2 and HL3 are almost identical, whereas HL1 shows a slightly lower strength development over the same period of time. All hardened pastes achieve compressive strengths slightly above 10 MPa at 28 days; however, at 90 days of curing age, the hardened pastes containing HL2 and HL3 reach highest mechanical strengths of 13.4 MPa, respectively, 13.3 MPa, whereas hardened pastes containing HL1 achieve maximal compressive strength of 11.5 MPa. One explanation could be the lower free calcium hydroxide content in HL1 as presented in **Table 6.2** and **Table 6.3**, leading to lower compressive strength gains from advancing pozzolanic reactions and carbonation to later curing ages. The strength evolution of the hardened pastes of S2 confirms the potential of hardened lime-MK pastes using pure GWM and hydrated lime to achieve promising mechanical performances from hydration, pozzolanic and carbonation reactions. Nonetheless, no clear influence of the addition of pure GWM on the reaction kinetics of the pastes and the resulting performances could be deducted. Therefore, the third series of mixtures was prepared and examined to assess the influence of incorporating uncalcined and calcined GWM powders on the performance of lime-MK binders.

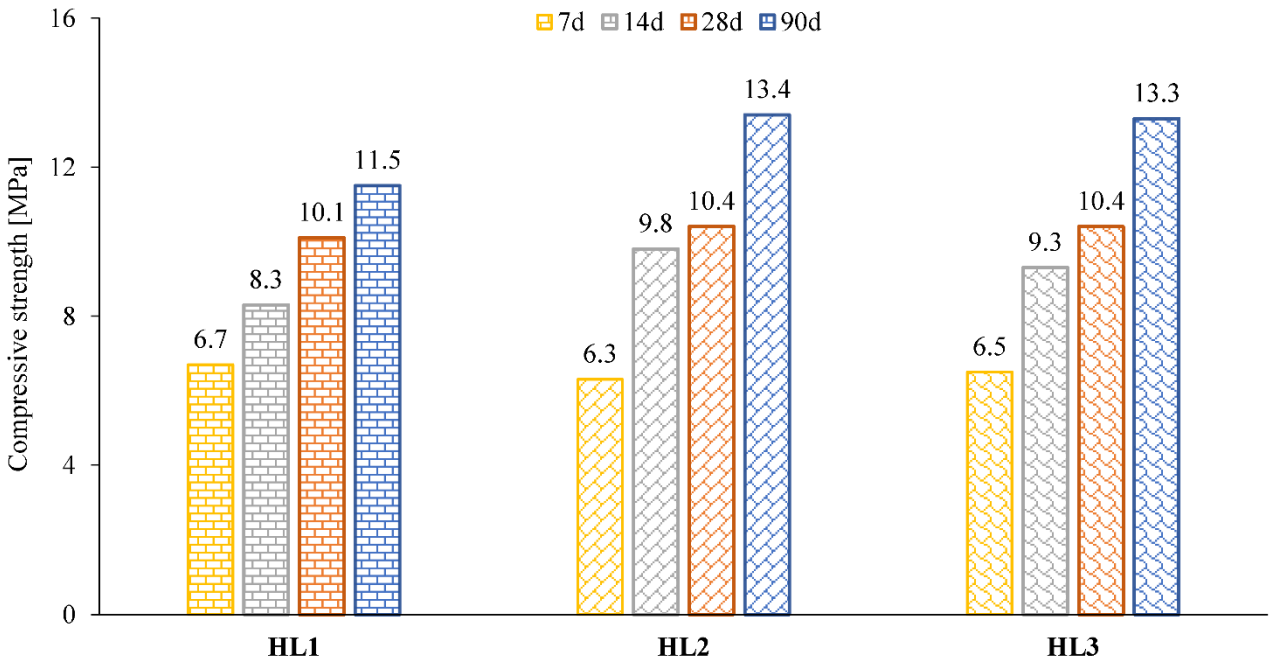

Figure 6.4 *- Development of the mechanical properties of hardened pastes containing PGWM, MK, DS, and HL1, HL2 or HL3*

6.3.3.3 Varying mixture design and use of UGWM and CGWM

Figure 6.5 and **Figure 6.6** present the compressive strength results at curing ages of 7, 28, 56 and 90 days performed on the hardened pastes of the third series of mixtures. **Figure 6.5** shows the compressive strength values of hardened pastes containing uncalcined GWM (UGWM) powders and **Figure 6.6** illustrates the mechanical strength values of the hardened pastes of the same mixing proportions containing calcined GWM (CGWM). The control specimen without GWM content (REF) reaches the highest 7-day compressive strength of 8.3 MPa among all the investigated mixtures, resulting from the early formation of calcium silicate hydrate phases from the pozzolanic reactions between the high reactive MK and the free calcium hydroxide. At curing ages up to 56 days, REF gradually increases in strength until a clear drop of the mechanical performance can be observed at 90 days. All tested specimens, except REF at 90 days and CG_1:1.33:1 at 56 days, show an increasing profile of compressive strengths with increasing

curing age up to 90 days. After 56 days of curing, the observed decrease in compressive strength of REF could be explained by the high lime content in the reference paste, leading to further carbonation of $Ca(OH)_2$ [145] and CSH phases (instability of the formed calcium silica hydrates) [249–251] as well as due to drying shrinkage (micro-cracking) and carbonation shrinkage induced strength losses [252,253]. Following the evolution of strength, the early reaction products are predominately resulting from the formation of calcium silicate hydrates from pozzolanic reactions of the active phases of the amorphous aluminosilicate precursors with the initial free calcium hydroxide. Due to the presence of the reactive pozzolan and the dominance of the pozzolanic reactions in the wet conditions at early curing ages, the carbonation reaction occurs from 28 days onwards. Furthermore, the carbonation of the remaining free lime drove forward further strength development and simultaneously additional networks of pozzolanic hydrates slowly formed above 28 days of curing age [237].

As expected, similar to the use of PGWM, the incorporation of UGWM in the lime-MK mixtures (**Figure 6.5**) did not show any clear improvement in the mechanical performances of the hardened pastes (maximal compressive strength of 13.8 MPa at 90 days by CG_1:1.33:1) compared to the reference mixture. The mechanical strength increased only slightly from 28 to 90 days for all hardened pastes. As concluded in the investigations carried out in [1,2], without additional thermal processing (calcination), GWM powders show very low pozzolanicity and therefore, the addition of UGWM lead to a dilution effect on the available reactive aluminosilicate materials in the pastes, leading to a lower rate of early pozzolanic reactions of MK and free calcium hydroxide.

Nonetheless, the incremental strength development pattern of all the lime-MK-UGWM pastes, compared to the already observed strength drop of the reference sample at 90 days of curing age, suggests that higher lime content (more unreacted calcium hydroxide) in the binder proportions

result in significant strength losses at longer curing ages [239].

As shown in **Figure 6.6**, for the same mixing proportions, significantly higher compressive strength values were obtained by the lime-MK-CGWM pastes than by lime-MK-UGWM pastes at all curing ages. In contrast to the lime-MK-UGWM pastes, the incorporation of the CGWM powders did not hinder the pozzolanic activity of the aluminosilicate materials of the mixtures. The highest compressive strength of 18.8 MPa was achieved by CG_1:1.66:1 at 90 days of curing age compared to 13.8 MPa by UG_1:1.66:1 (compressive strength gain of 36 %). The phase transition of GWM into a stable and more amorphous meta-state after thermal treatment at 850°C as well as the finer granulometry of the CGWM powder compared to the MK powder explain the strongly positive pozzolanic activity of MK-CGWM combination leading to the overall compressive strength improvements. Furthermore, the strength-based evaluations show that the improved mechanical performance is not directly related to the increasing MK content and/or CGWM content, but rather depends on the interrelated combinations of the ternary mixing proportions considering the lime:pozzolan ratio as well as the CGWM:MK ratio. The highest compressive strengths were observed for hardened lime-MK-CGWM pastes with lime:pozzolan ratios of 0.3-0.42 and CGWM:MK ratios of 0.6-1.0.

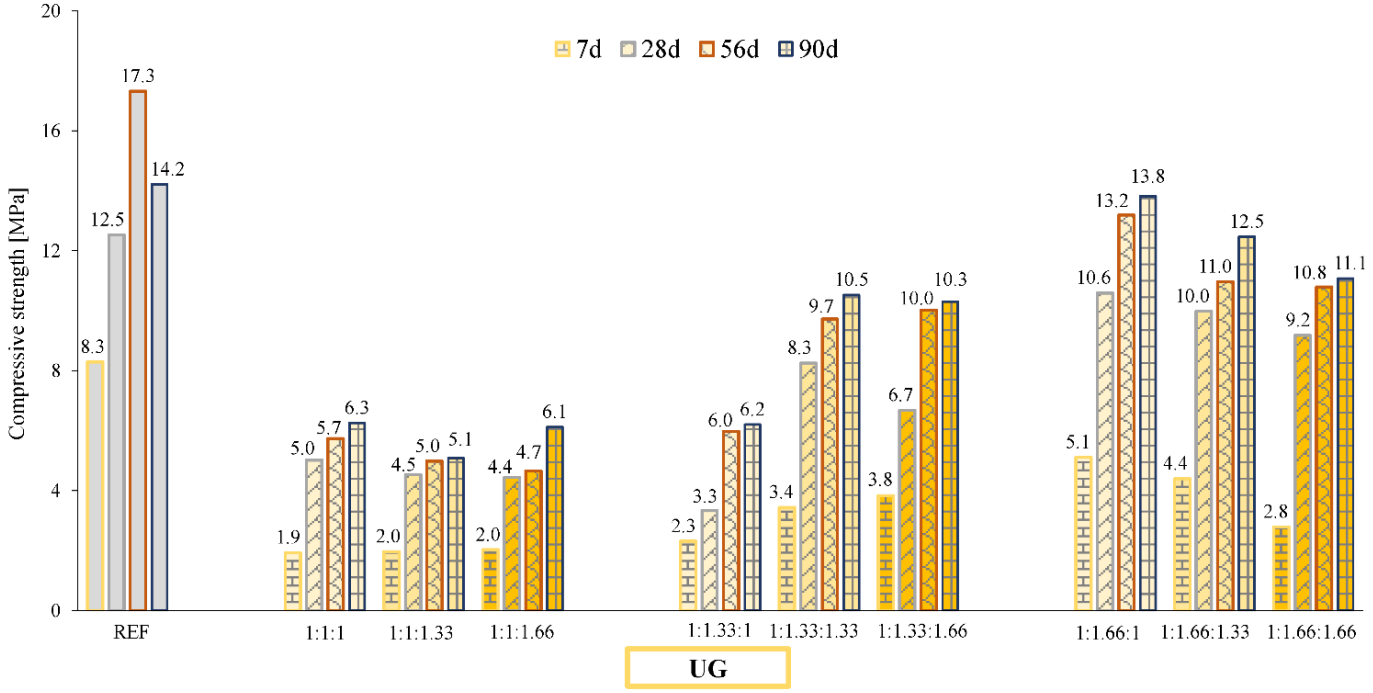

Figure 6.5 *- Development of the mechanical properties of hardened pastes containing UGWM, HL2, MK and DS*

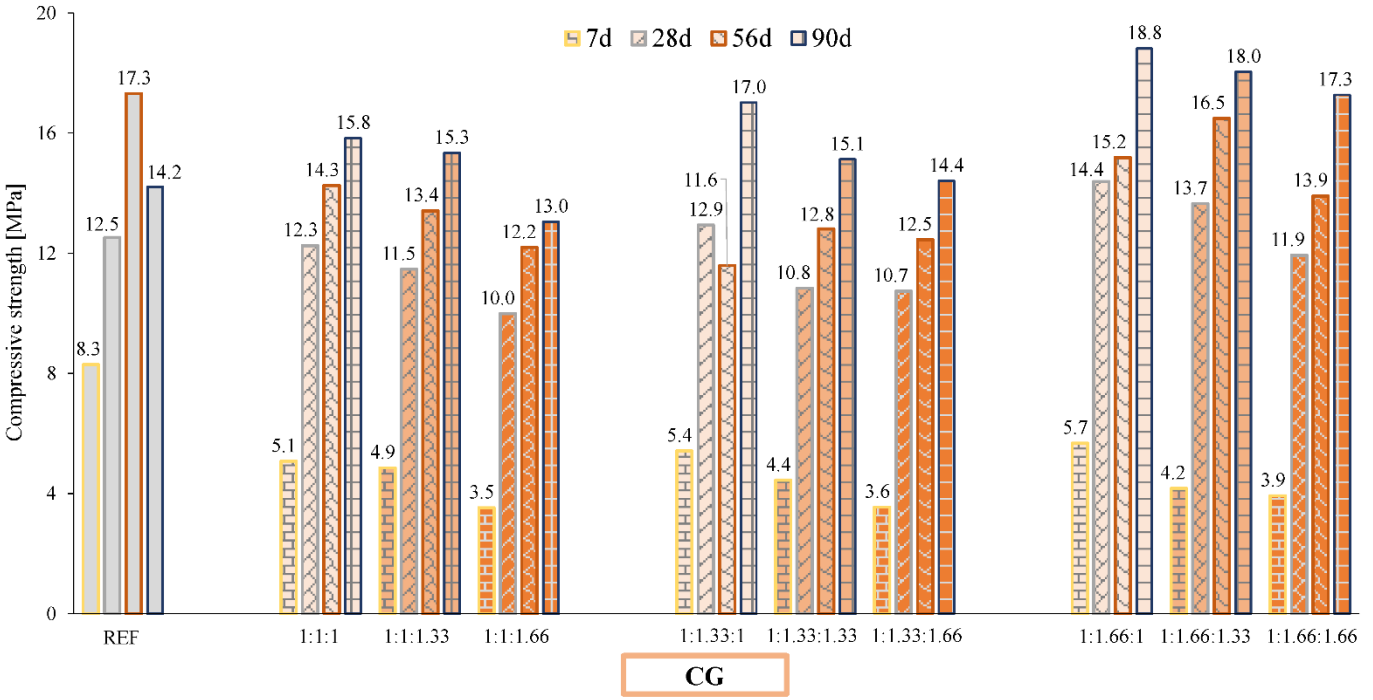

Figure 6.6 *- Development of the mechanical properties of hardened pastes containing CGWM, HL2, MK and DS*

6.3.4 Phase composition of the hardened specimens by STA

The evolution of the STA curves of the hardened specimen CG_1:1.66:1 is illustrated in **Figure 6.7.** The mass loss and the heat flow variation of the sample is monitored from ambient temperature up to 1000°C. A total mass drop of 24.13% can be observed following the TGA curve over the investigated temperature range. Three separate mass reduction segments can be pointed out, each segment can be attributed to a specific nature change (mass change in combination with endothermic and exothermic reactions) within the specimen: The first segment of gradual mass loss (-3.16%) can be perceived at a temperature of 250°C. This reduction represents the evaporation of the bound waters of the formed calcium silicate hydrates as products from the pozzolanic reactions and the absorbed water of calcium hydroxide as well as the burning of organic and/or volatile components. The second mass loss range (-1.55%) can be perceived from 250°C to 550°C due to decomposition of the AFm phases and calcium aluminate hydrate (CAH) phases, and the dehydroxylation of calcium hydroxide. The largest mass reduction from around 700°C up to about 800°C is mainly driven by the decarbonation of calcite ($CaCO_3$) in the hardened pastes until a constant mass state is reached. The corresponding DSC curve confirms the dehydration process of the different CSH products by the endothermic peak at about 230°C, then the endothermic peak at 574.6 °C corresponds to the phenomenon of quartz inversion (dolomitic sand) and the endothermic peaks observed between 740°C and 790°C can be attributed to the decarbonation of $CaCO_3$. These peaks confirm the carbonation reaction of free calcium hydroxide with CO_2 from air, leading to the formation of calcium carbonate ($CaCO_3$). Overall, the findings of the STA analysis are consistent with the results of the compressive strength test and confirm the formation of CSH phases (pozzolanic products) as well as the formation of $CaCO_3$ (carbonation products) as the dominant chemical reaction mechanisms of lime-MK-CGWM pastes.

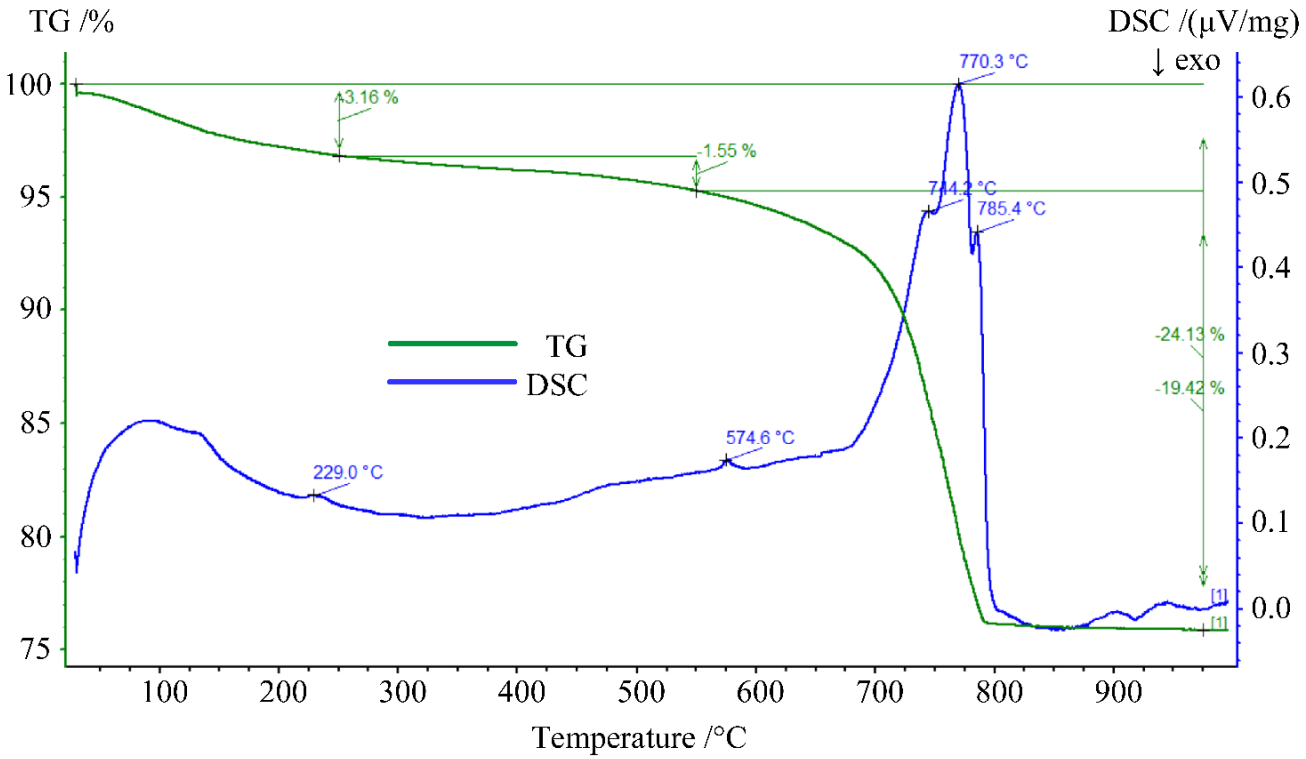

***Figure 6.7** - STA (TG-DSC) analysis of hardened specimen of CG_1:1.66:1*

6.3.5 Microstructural analysis

Scanning electron microscopy (SEM) was carried out on fractured samples to examine the resulting microstructural configurations of selected pastes after 56 days of curing age. **Figure 6.8a** presents the microstructure of a natural hydraulic lime-MK-PGWM paste (PCB_NHL), whereas **Figure 6.8b-e** illustrate the SEM micrographs of PCB_HL1, a hydrated lime-MK paste with PGWM. **Figure 6.8a** shows that medium quantities of reaction products were formed and a partially condensed microstructure was built with several visible cracks and micro gaps. In comparison, **Figure 6.8b** depicts a much denser structure with significant amount of amorphous compound forming a compact bond between the reaction products and the quartz particles. As expected, these SEM observations are consistent with the results of the compressive strength evaluation. **Figure 6.8c** confirms that the formation of a dense network of CSH phases as a result

of a pozzolanic reaction between free lime and the aluminosilicate raw materials. In the SEM micrographs (**Figure 6.8d**), amorphous cement-like compounds can be observed as well as traces of unreacted and reacted clay particles. Plate-like mineral formations indicate the presence of unreacted or semi-reacted metakaolinite. Moreover, some calcite crystals, resulting from the carbonation of lime, were observed, covered by the reaction products (**Figure 6.8e**), which confirms the strengthening capacities of the lime-pozzolan binder matrix by carbonation.

Overall, for the pastes using hydrated limes, a dense, homogenous microstructural composition between the aluminosilicate-rich compounds (clay minerals) and the reaction products was observed. This compact bond indicates that strong reaction products from pozzolanic reaction between GWM-MK and the hydrated lime were successfully synthesised. The formed binder matrix seems to be slightly weaker than that of usual cement-based pastes [238,254,255]. However, very promising compressive strength results show the benefit of using hydrated lime in combination with GWM powders to improve the microstructural configuration of the binders. Finally, some unreacted aluminosilicate constituents were observed in almost every sample, which suggest that further optimization of the mixing proportions of the applied quantities of each components could significantly enhance the properties of the ternary lime-MK-GWM pastes.

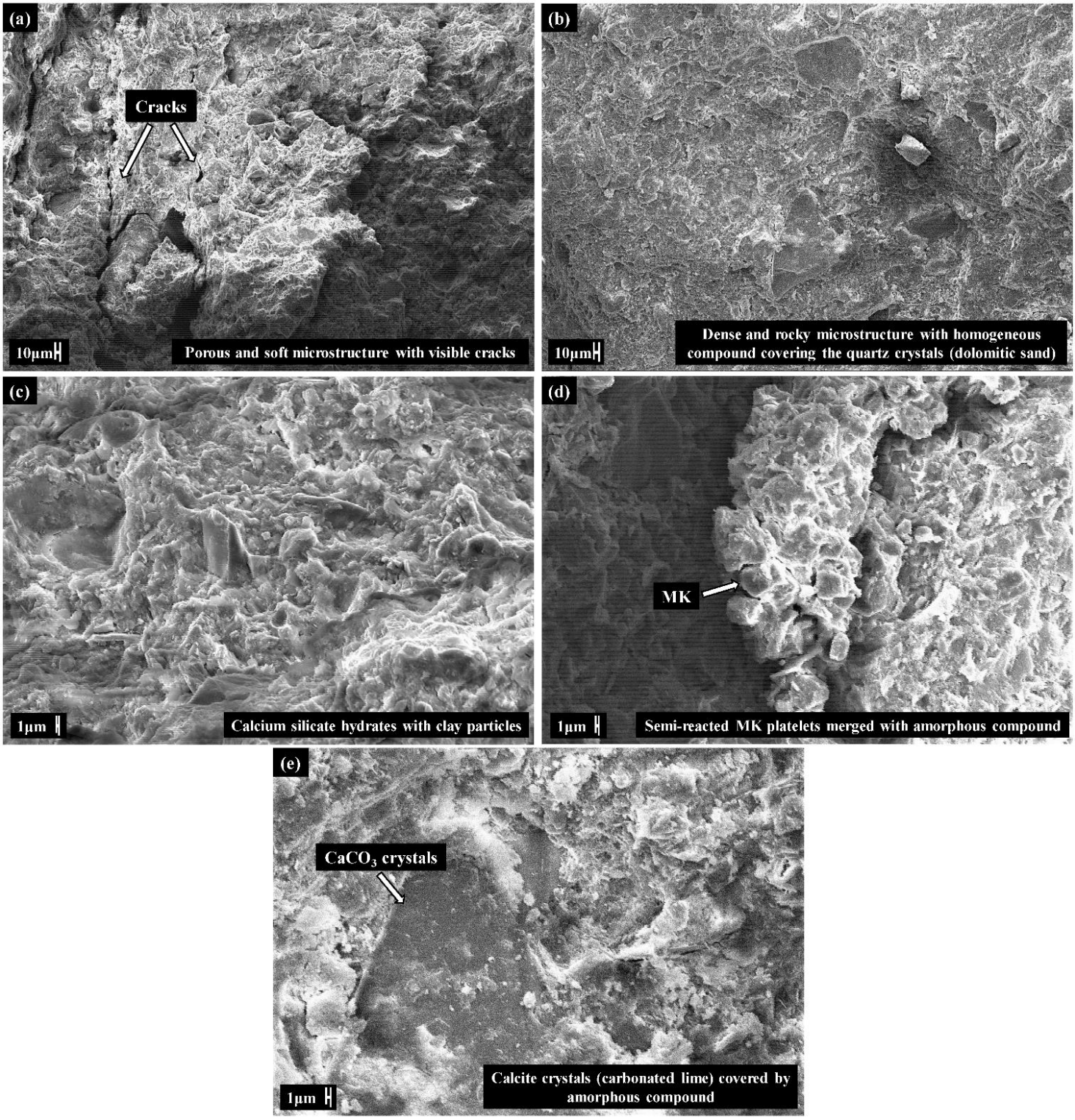

Figure 6.8 *- SEM micrographs of (a) PGB_NHL and (b)-(e) PGB_HL1 at curing age of 56 days*

6.4 Conclusion

In this work, an aluminosilicate-rich raw material, namely GWM powder, was incorporated in lime-based pastes to evaluate its strength-enhancing potential. Large varieties of lime-MK-GWM pastes with very promising mechanical properties were presented. From the presented results, considering the varying mixing proportions, the use of different types of lime powders, and GWM at different treatment levels, the following conclusions can be drawn from this study:

- XRD data indicate the beneficial effect of thermal treatment (calcination) on the mineralogy of GWM powders with a clear increase in amorphous content, resulting from the transition of kaolinite to metakaolin. The used metakaolin (MK) shows a very high amorphous content with a medium content of quartz. These findings indicate that both raw materials could exhibit medium to high pozzolanicity.
- For both hydraulic and hydrated lime systems, acceptable strengths for constructive applications were developed over the investigated curing ages. Considering the achieved mechanical performances, the use of hydrated lime is recommended instead of natural hydraulic lime as more dense and strength-enhancing reaction products from pozzolanic reaction were formed at early curing ages.
- The STA analysis as well as the SEM analysis of the microstructure, confirm the presence of the CSH phases and calcite ($CaCO_3$) as major reaction products.
- The examination of over 250 hardened specimens with varying lime-MK-GWM proportions and different curing ages suggests that the only consideration of the 28-day compressive strength as it is the case for traditional cement-based products is not recommendable for the lime-pozzolan binder systems due to the involved slower

pozzolanic reaction and carbonation reaction processes compared to the early hydration reaction.

- The highest compressive strength of 18.8 MPa was achieved by CG_1:1.66:1 at 90 days and the strength-based evaluation presents the use of calcined GWM as a very effective pozzolan in the ternary lime-MK-GWM binder systems. The achieved performances suggest that this composite concept can be considered as a potential low- to medium-strength material for construction applications.

Finally, the results of this study will contribute to further enrichment of investigations on waste materials as powerful SCMs as well as consequently promote their incorporation in lime-pozzolan binder systems. The establishment of calcined GWM as a competitive and alternative pozzolan requires further optimizations of the binder concepts, the analysis of long-term behaviour of the binder systems, and durable solutions regarding its full scalability into industrial processes need to be developed. It is important to divert existing waste management flows by stimulating optimization and innovation in the revalorisation of waste materials to limit the use of landfilling and to replace the “end-of-life” concept of industrial co-products by reusing or recycling them as raw materials. This will bring double benefit to environment as waste is eliminated from one system and later is used as a resource in another system.

Chapter 7 Manuscript IV - Properties of binary blended concrete using gravel wash mud (GWM) powders

Abstract

An alternative supplementary cementitious material (SCM) based on quarry waste sludge, namely gravel wash mud (GWM) powder, is investigated for its performance in blended cement pastes and concretes. Varying mix designs of blended cement pastes and concrete mixtures at OPC substitution degrees from 10 wt.% up to 30 wt.% by uncalcined and calcined GWM powders were examined at different curing ages using isothermal calorimetry, strength-based examinations, shrinkage test, carbonation test and scanning electron microscopy. The pozzolanic nature of the calcined GWM powder was confirmed; however, minor to no significant physiochemical contributions to the early hydration reactions were observed. The incorporation of calcined GWM powders up to OPC replacement levels of 20 wt.% showed an enhancement of the long-term properties of the hardened specimens, namely less drying shrinkage and reduced progression of carbonation compared to the control mixtures. Beneficial strength-enhancing effects were observed for binary blended concrete mixes using calcined GWM powders at OPC replacement levels of 10 wt.% and 20 wt.% and classified them as viable proportions for alternative SCM-based concretes. The revalorisation of the GWM, a quarry waste product, as a novel and competitive raw material resource for cement production, would provide an environmental-friendly and alternative solution to the expensive and inefficient end-of-life scenario of GWM at the landfills.

Keywords - Gravel wash mud, Concrete, SCM, Mechanical properties, Hydration kinetics, Carbonation.

7.1 Introduction

Concrete is incontestably the most used construction material, and it plays an essential role in the urbanisation of cities of industrialised countries as well as the rise of emerging countries to meet the living standards and the infrastructure requirements of rapidly growing populations worldwide, and its importance will continue to intensify in future [256]. The sustainable development of the construction industry has undoubtedly emerged to the focus of interest over the last decades as the progressive environmental consequences of the current concrete usage practices have further stimulated the urge for an appropriate and durable solution worldwide. Nonetheless, as the production of concrete is directly dependant on the acquirability of abundant local resources and their nature, current research outcomes are mainly able to come up with local up to regional solutions. The major portion of concrete's negative environmental impact is attributed to its principal binding agent, Ordinary Portland cement (OPC), whose production process, namely the clinkerisation process, generates high CO_2 emissions [228,232]. Current estimates state that the average yearly global cement production remained stable at around 4.1 Gt since 2013 [257–259]. However, the forecasts on the rise of the global population and its subsequent infrastructure development requirements suggest that global cement production will increase by more than 12% by 2050 [256].

Furthermore, the current expectations on the investigations and the advancements of the scientific and technological organisations collaborating with the cement industry are very high. The extent of the existing and future endeavours to mitigate the environmental impacts regarding the CO_2 emissions of the cement industry is correlated to the growing cement production rates and the speed of the technological progress of the sector. Therefore, various CO_2 mitigation strategies have been developed and established to formulate "eco-efficient" concretes [260]. One of the

proposed solutions is the clinker replacement by “low carbon” constituents with proven binding properties, namely supplementary cementitious materials (SCMs), to reduce the environmental impacts and to improve the durability of concrete products without compromising its competitiveness [8,261]. Consequently, the current European cement standard EN 197-1 [58] authorises the incorporation of six supplementary main constituents (blast furnace slag, silica fume, pozzolana, fly ash, burnt shale and limestone) in addition to Portland cement clinker in the composition of common cement types. Moreover, for instance, the French national addition of the European concrete standard NF EN 206/CN [262] permits the use of Metakaolin as a pozzolanic addition for concrete after conformity according to the national product standard NF P18-513 [246]. There exist numerous research work on the physicochemical and mineralogical characteristics of these SCMs, the extent and intensity of the involved reaction mechanisms in the cement-based compounds, and their influence on the mechanical performance and durability of the resulting blended cements and concrete products [59,67,71,86,90,112,122,151,205,263–270].

However, in most of the European countries, not all of these constituents are abundantly available locally and the stocks of these traditional “mainstream” SCMs, mostly artificial pozzolans like silica fume (SF), fly ash (FA) or granulated blast furnace slag (GBS), are gradually disappearing as a result of more substantial sectoral and environmental restrictions, and technological advances in primary industrial sectors like the steel industry or the coal-fired power stations. This increasing scarcity of traditional SCMs and the already existing depletion of naturally mined materials has promoted the construction industry to research on new alternative SCMs worldwide, mostly originating from various industrial waste flows [71,113,271–273].

In recent years, there is a substantially growing research interest in the valorisation of co-products or wastes from quarries (washing sludge), abandoned clay mines (medium-reactive clay deposits)

or other unused potential resources of diverse industrial origins to assess their aptitude for their use as SCMs in future blended cements and to provide larger flexibility to the local cement industry to encounter future challenges. Furthermore, the incorporation of these alternative waste-based SCMs in cementitious binders can reduce the environmental footprint of the quarries, and a potential stabilisation or even decrease of building materials' cost can be expected. A broad spectrum of local and regional industrial waste materials, which were not exploited to date and mainly landfilled, have been investigated to be incorporated as SCMs in blended cements or as additions in concrete. Among highly investigated waste products to reduce the clinker factor in future cements or to utilise as filler aggregates figure reservoir sludges [133], waste expanded perlites [135], waste glass sludges [274], granite quarry wastes [275], quarry wastes containing limestone, diabase and gneiss [276], quarry reservoir sludges [1–3], dolomitic quarry dust [277], marble stone dust [278], non-recyclable waste glass [128], ceramic wastes [128,240], clay-based construction wastes [127,279,280], and many more [208,210]. Most of the authors, researching the revalorisation of unutilised waste materials, report that independently of the reactivity of the waste-based SCMs, at lower replacement levels around 10 wt.%, improved hydration kinetics and strength development of the blends are foreseeable. Furthermore, depending on the nature of reactivity (potential to possess respectively build hydraulic or pozzolanic binding properties, or both) and the intrinsic characteristics of the waste products, at OPC replacement levels around 20 wt.%, the formation of additional hydration products at varying stages of the hydration process was observed, mostly leading to improved mechanical performances, reduced porosity (filling of micropores and improved interfacial transition zones), the enhancement of the microstructure and better durability (improved long-term behaviours and resistance to external deleterious effects) of the hardened products compared to the OPC-based reference mixtures [127,128,133,135,274–

281]. Nonetheless, most of the studies consist of early investigations on the suitability of the waste material to be considered as SCM in binder mixtures or blended cement mortars.

This work presents investigations on the performance of concrete formulations using a processed quarry waste material, namely gravel wash mud (GWM) powders, as SCM. Several series of cement pastes and concrete mixtures were prepared by incorporating GWM in two different forms (uncalcined and calcined at 850°C) and examined using a set of selected characterisation techniques. The substitution degrees of cement by GWM powders were fixed from 0 wt.% (reference mixture) up to 30 wt.% based on experiences from former works [1–3]. The water-binder ratio was kept constant at 0.4 for the composition of the paste mixtures and 0.42 for the concrete mixtures. A set of representative parameters regarding the early reaction kinetics, the time-dependent hygric volume change (dry shrinkage), the durability, the characteristics in the fresh state and the mechanical performances of binder and concrete products were compared to the properties and performances of reference paste- and concrete mixtures. The load-independent deformations due to hygrothermal impacts of the investigated blended cement pastes were determined by monitoring the evolution of shrinkage compared to the control mixture. The heat evolution profiles, respectively, the hydration heat flow of the blended pastes were monitored by isothermal conduction calorimetry. Furthermore, the mechanical properties of the hardened pastes, incorporating UGWM and CGWM at the investigated OPC replacement levels and stored at two different curing conditions (air- and water curing), were determined for selected curing ages up to 90 days. Concrete mixtures were prepared using the same OPC replacement levels as applied for the blended cement paste mixtures. The properties of fresh concrete, the compressive strengths and the elastic modulus of cylindrical concrete samples were determined, followed by the

measurement of the depth of carbonation as well as the analysis of the microstructural composition of fractured concrete samples by scanning electron microscopy (SEM).

7.2 Materials and experimental program

The objective of the conceptualised mix design and the applied experimental methods is to corroborate the performance of the proposed SCM, namely CGWM, to be incorporated in concrete mixtures as a promising alternative to only OPC-based concretes without compromising on the concrete's property requirements.

7.2.1 Materials and material preparations

A commercial Ordinary Portland cement (OPC) with grade CEM I 42.5 R according to EN 197-1[58] from Cimalux S.A. was used as the main binder of the different mixtures. The concrete mixtures were prepared with commercially available mixed sand and gravel aggregates of regional origin (Mosel sand and gravel mix, MSG) with a grain size range of 0/16 mm, certified according to DIN EN 12620 [282]. The gravel wash mud was obtained from a Luxembourgish sandstone quarry (Carrières Feidt S.A.) and was preprocessed by desiccation to constant mass at 105°C and later ground into a powder, hereafter referred to as the uncalcined GWM (UGWM) powder. The calcined GWM (CGWM) powder was produced by thermal treatment of UGWM powder at 850°C inside a laboratory chamber furnace (heating rate of about 5 °C/min) while maintaining the peak temperature for one hour, followed by a natural cooling down to room temperature. The calcination allowed to transform the base material (UGWM) with low pozzolanic activity into a more amorphous and medium-reactive artificial pozzolan (CGWM) [1–3].

7.2.2 Mix design and curing conditions

7.2.2.1 Binder paste compositions

The mix proportions of the investigated binder pastes are presented in **Table 7.1**. Seven different cement paste mixes were prepared to incorporate increasing proportions of UGWM powders, respectively CGWM powders, from 10 wt.% up to 30 wt.%, and a reference mixture (REF). The water/binder (w/b) ratio was fixed to 0.4, and no additional aggregates were added. Three replicate specimens were prepared for each mixture, and the investigated curing ages were 28 and 56 days. The same mixing procedure was applied for all mixtures and carried out, as described in [2]. The mixtures were poured in steel moulds (40 x 40 x 160 mm^3) according to EN 196-1 [101] and stored for 24h before demoulding. For REF, UG20 and CG20, additional specimens were prepared to examine the evolution of compressive strengths from 1 day up to 90 days. Furthermore, the impact of curing conditions (cured in air and water) on the evolution of compressive strength of REF and CG20 was investigated on additional samples.

Mixture[a]	Quantities per specimen (40x40x160mm^3)				
	Substitution degree	UGWM	CGWM[b]	OPC	w/b[c]
[-]	[wt.%]	[g]	[g]	[g]	[-]
REF	0	-	-	425	0.40
UG10	10	43	-	383	0.40
UG20	20	85	-	340	0.40
UG30	30	128	-	298	0.40
CG10	10	-	43	383	0.40
CG20	20	-	85	340	0.40
CG30	30	-	128	298	0.40

[a] For each curing age, three specimens of each mixture were prepared
[b] Calcination temperature of GWM = 850°C
[c] w/b: water/binder ratio, binder equal to cement or cement and CGWM

***Table 7.1** - Paste mixture compositions*

7.2.2.2 Concrete mixtures

In this study, the same binder proportions as for the binder pastes, namely cement substitution rates of 10 wt.%, 20 wt.% and 30 wt.% by UGWM respectively CGWM, were considered in the mix design of the concrete mixtures to study the characteristics in the fresh and hardened state of the investigated concretes. The volumetric mix design, as presented in **Table 7.2**, was applied to achieve concretes of class C40/50, according to DIN EN 206-1 [283]. For the concrete mixtures, the binder:aggregate (b:ag) ratio ranged around 1:3.7 and the water/binder ratio was fixed at 0,42 for all mixtures. The mixture C_REF without GWM powders was set as reference mixture. An increase of the mixture water content or the use of a superplasticiser to achieve the same consistency and workability (same slump values) was not considered in this study, as the performance of the hardened concrete, respectively the properties of the different binder matrices in the hardened composite structure were prioritised.

The mixing procedure was kept consistent for all the concrete mixtures: First of all, the fine and coarse aggregates are poured in the concrete mixer, and about two-thirds of the determined water quantity is added and briefly mixed. Then, the binder (cement only, respectively cement and GWM powder) is added and mixed for 30 s. Without interrupting the mixing process, the remaining water is poured in, followed by a mixing time of 90 s. After the mixing procedure, the consistency of all the fresh concrete mixtures was determined. All the specimen were cast in three layers, where each layer was compacted on a vibrating table until no further air bubbles appear (reduction of air voids) as prescribed by DIN EN 12390-2/A20 [284]. The samples were stored at room temperature for 24h. After demoulding, the specimens are stored and cured under water for 7 days, then dry storage at ambient temperature is applied until 28 days of curing age. The samples tested after 56 days are

submerged in water for 35 days and stored at room temperature for 21 days, according to DIN EN 12390-2/A20 [284].

Mixture[a]	Curing ages of 28 and 56 days; Quantities for 1 m^3 [kg/m^3]						
	Binder				Aggregates		
	Substitution degree	UGWM	CGWM[b]	OPC	Grain size (0/16 mm)	Water	w/b[c]
[-]	[wt.%]	[kg]	[kg]	[kg]	[kg]	[-]	[-]
C_REF	0	-	-	429	1200	180	0.42
C_CG10	10	-	43	386	1191	180	0.42
C_CG20	20	-	86	343	1183	180	0.42
C_CG30	30	-	129	300	1174	180	0.42
C_UG10	10	43	-	386	1191	180	0.42
C_UG20	20	86	-	343	1183	180	0.42
C_UG30	30	129	-	300	1174	180	0.42
ρ [kg/dm^3]		2.52	2.50	3.10	2.40	1.00	

[a] For the curing each curing age, three specimens of each mixture were prepared
[b] Calcination temperature of GWM = 850°C
[c] w/b: water/binder ratio, binder equal to cement or cement and CGWM

***Table 7.2** - Concrete mix design*

7.2.3 Experimental methods

7.2.3.1 Physicochemical and mineralogical properties of the primary materials

The grain size distribution of concrete aggregates (MSG) was examined using the dry sieving method, according to EN 933-1 [285]. The particle size distributions of the powder samples OPC, UGWM and CGWM, were determined by laser diffraction technique using a particle size analyser (HELOS-RODOS-VIBRI from Sympatec GmbH). A wavelength dispersive X-ray fluorescence spectrometer (S8 TIGER from Bruker AXS GmbH) was used to detect the elemental composition of the powder samples using the XRF method. A powder X-ray diffractometer (D4 ENDEAVOR

from Bruker AXS GmbH) using Cu K_α radiation was used to determine the mineralogy of the powders by X-ray diffraction analysis using the Rietveld refinement method [214].

7.2.3.2 Isothermal calorimetry, compressive strength test of the hardened pastes and shrinkage test

The analysis of early hydration phases of four cement pastes, namely one control mixture (cement only) and three cement pastes including CGWM powders at OPC replacement levels of 10, 20 and 30 wt.%, were determined using isothermal calorimetry. The rate and the extent of the hydration heat were monitored and quantified by a thermal activity monitor (TAM, TA Instruments) as a function of time at 20.0°C, and the mixtures were prepared at fixed w/b ratio of 0.4. Two separate measurements were performed to determine the evolution of the hydration heat for all samples: The first measurement was carried out for the first 30 minutes using the high sensitivity isothermal titration calorimetry [286,287], appropriate for the first rapid reactions (highly exothermic and high early hydration heat release). The second measurement was performed to monitor the heat release starting from 30 min up to 40 hours by isothermal microcalorimetry [288,289]. The measured thermal energy is converted into the heat flow in mW/g and the normalised cumulative heat release in J/g.

The compressive strength of the hardened binder pastes was measured using a compression testing plant (TESTING Bluhm & Feuerherdt GmbH, Germany), conform to the standard DIN EN 196-1 [101]. The presented compression strength results represent the average values of at least three valid tests on replicate specimens at the examined curing ages. The water- and air curing of the hardened specimens was performed at constant storage conditions. Further strength-based evaluations were conducted using the compressive strength results, namely the strength activity

index (SAI) [93,148,217,221] to evaluate the pozzolanicity of the GWM powders and the relative strength index (RSI), proposed by [2]. The RSI method allows determining the relative strength gain or loss of the cement pastes by taking into account the considered OPC replacement level by the GWM powder.

The unrestrained drying shrinkage test was conducted on the paste mixtures, which were cast in 40x40x160 mm^3 moulds with integrated attachment pins on both ends of the specimens. After 24h, the specimens were demoulded and were mounted on ball-bearing rollers of the measuring unit (**Figure 7.1**) using the attachment pins (free rotatable), assuring no obstruction for volume change in any direction (unrestrained). The conical contact tip of a digital displacement gauge was positioned on one side of the specimens to monitor the time-dependent volume contraction (shrinkage) by measuring the variation in the length of the specimen with time while a fixed pin horizontally constrained the other side.

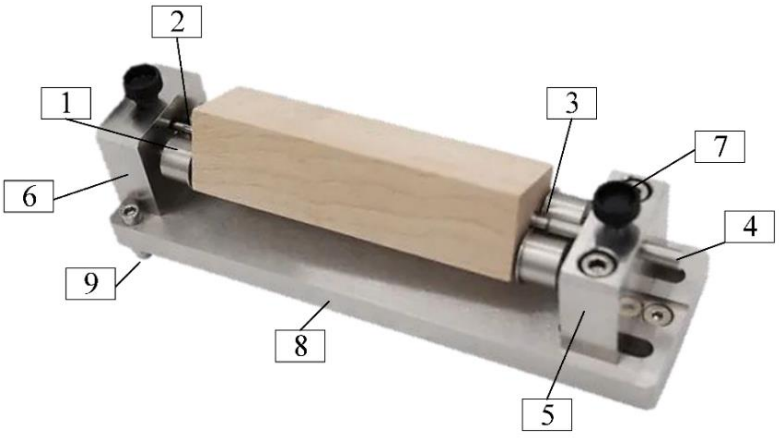

1. Ball-bearing rollers as support
2. Pin, replaced by digital displacement gauge
3. Pin, integrally cast-in or attached on both sides of specimen
4. Pin, used as horizontal constraint on one side
5. Bearing block, position adjustable
6. Bearing block, fixed
7. Locking mechanism
8.+ 9. Steel base plate, inclined position by supporting feet

***Figure 7.1** - Setup of the shrinkage test*

7.2.3.3 Characteristics of fresh concrete, mechanical properties of the examined concretes, carbonation test and scanning electron microscopy (SEM) analysis

The properties of the different fresh concrete were studied by measuring their consistency at the plastic state, directly after the preparation of the mixtures by concrete slump test, according to EN12350-2 [290]. The slump value is determined as the difference in height between the level of the standardised slump cone (Abrams cone; height = 300 mm) and the height of the collapsed fresh concrete after removing the cone in which it was compacted. The mixture C_REF was assigned as reference concrete to assess the workability of the concrete mixtures containing GWM powders.

The hardened concrete properties of all concrete specimens were tested by compressive strength test on cylinders (Ø150x300 mm) at 28 and 56 days of curing age using a compression testing machine (TESTING Bluhm & Feuerherdt GmbH, Germany), conform to the standard EN 206 [283] and according to EN 12390-3 [291]. Additionally, the modulus of elasticity (elastic modulus) of the different hardened concrete samples was determined according to EN 12390-13 [292]. Curing of the samples was performed according to DIN EN 12390-2/A20 [284], and before the compression tests, the surface irregularities of the cylindrical specimens were polished into plane contact surfaces to ensure a uniform pressure distribution.

The carbonation of the investigated concrete mixtures is assessed at curing ages of 28 and 56 days (specimens are cured under water for 7 days, then stored at room temperature until carbonation test) by applying an indicator fluid (phenolphthalein solution) on a freshly fractured concrete surface according to EN 14630 [293]. After the application of the indicator, the resulting violet area represents the non-carbonated concrete zones, and its distance to the outer concrete shell is measured as the carbonation depth.

The microstructure was examined on broken fractions of compressed concrete specimens (including gold sputter coating to prevent charging of the specimen and for higher resolution images) using a high performing JEOL JSM 6010 analytical scanning electron microscope with integrated elemental analysis by energy-dispersive X-ray spectroscopy (EDS), which allowed to produce high-quality microstructural observations by detection of secondary electrons (SEs), backscattered electrons (BSEs) and Auger electrons (AEs) from the interaction of the primary electron beam with the investigated specimens following a raster scan pattern

7.3 Results and discussions

7.3.1 Physicochemical properties and mineralogy of the primary materials

7.3.1.1 Particle size distribution of the used components

The grading curve of the mixed aggregates MSG, presented in **Figure 7.2**, was determined by sieve analysis and the grain-size distribution of MSG was classified to the A/B16 aggregate grading range (coarse- to medium-grained) according to EN 933-1 [285]. The GWM powders show the finest particle size distribution among all the examined materials (**Figure 7.2**). UGWM shows the finest grain size range (d10-d90) from 1.47 to 41.51 μm with respective mean particle sizes (d50) of 7.22 μm, whereas, owing to the clumping effect due to the calcination process, CGWM is slightly coarser with d10-d90 ranging from 1.68 μm to 58.30 μm and d50 of 9.02 μm. The OPC powder shows a mean particle size range of 11.32 μm.

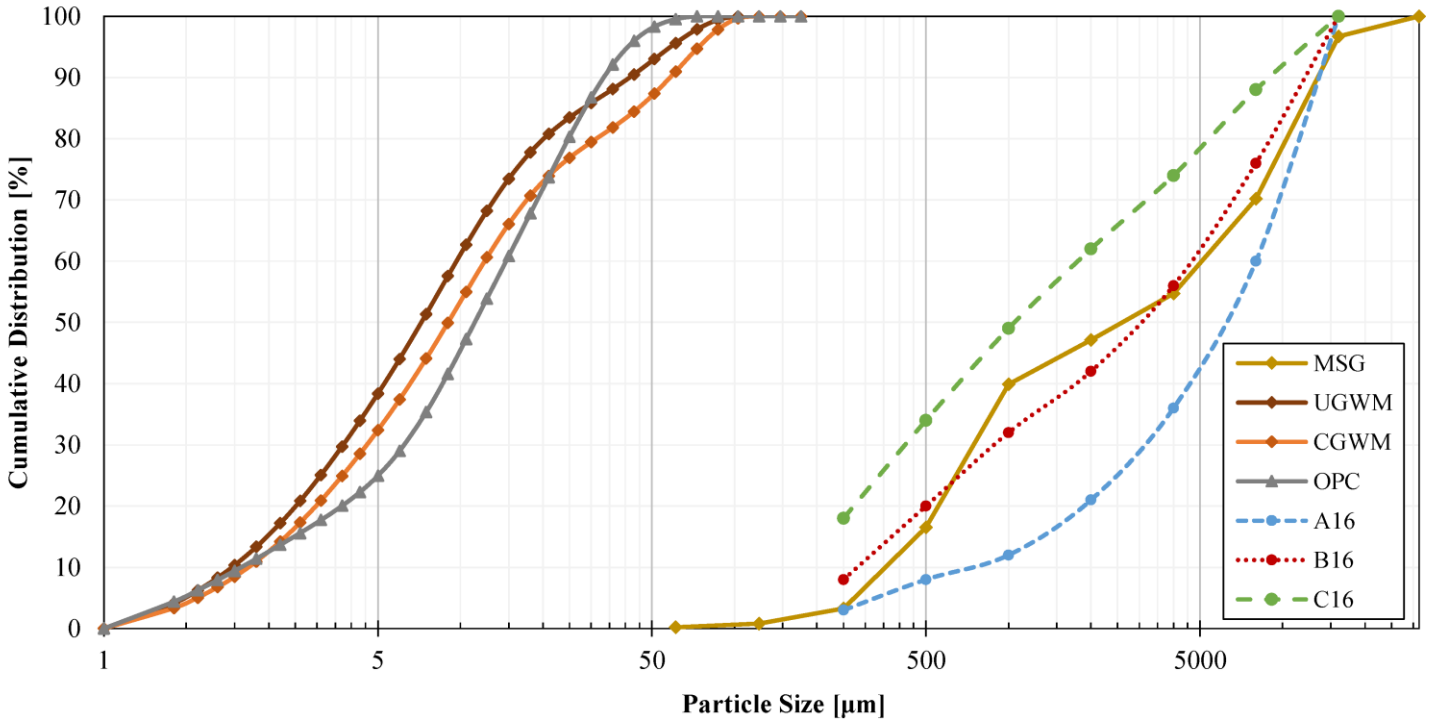

***Figure 7.2** - Particle size distribution of all used materials: UGWM, CGWM (calcined at 850°C), OPC powders and MSG aggregates; A/B/C 16 grading curves according to EN 933-1 [285]*

7.3.1.2 Chemical composition and mineralogy of the applied powders

The chemical compositions of the UGWM and CGWM powders are presented in **Table 7.3** and comply with the findings from other works [1–3] by confirming the aluminosilicate nature of the investigated materials with the primary elemental composition of SiO_2 (elevated content), Al_2O_3 and Fe_2O_3 (medium content). The chemical evaluation of OPC verifies the oxide composition of ordinary Portland cement of type CEM I 42.5 R with elevated CaO, moderate SiO_2, and minor Al_2O_3 and Fe_2O_3 contents [294,295].

The quantitative XRD analysis was carried out based on the method described in [2,215], and the mineralogical compositions of the binder constituents are summarised in **Table 7.4**. The used Ordinary Portland Cement, in addition to the traditional cement clinker phases (Alite, Belite, aluminoferrite and aluminate), revealed the presence of a hydrous calcium sulphate phase, namely

anhydrite ($CaSO_4$), as well as calcite ($CaCO_3$), Portlandite ($Ca(OH)_2$), and quartz (SiO_2). The main crystalline phases identified in the GWM powders were quartz, muscovite, followed by illite and kaolinite as clay minerals, hematite and the amorphous portions.

Sample	**Chemical composition**									
	SiO_2	Al_2O_3	Fe_2O_3	CaO	MgO	SO_3	Na_2O	K_2O	TiO_2	MnO
[-]	[%]	[%]	[%]	[%]	[%]	[%]	[%]	[%]	[%]	[%]
OPC	18.94	4.68	4.25	65.56	1.22	2.91	0.21	0.52	0.33	0.34
UGWM	65.06	19.53	9.37	0.41	1.66	0.09	0.24	2.72	0.85	0.06
CGWM	64.10	20.29	8.91	0.41	1.81	0.00	0.24	3.26	0.90	0.08

***Table 7.3** - Chemical composition of OPC, UGWM and CGWM powders*

Sample	**Mineralogical composition [%]**							
	C_3S	C_2S	C_4AF	C_3A	Anhydrite	Calcite	Portlandite	Quartz
OPC	52.2	24.6	11.8	1.7	2.6	4.8	1.8	0.5
	Quartz[a]	Muscovite	Illite	Kaolinite	Hematite	$KAl_3Si_3O_{11}$	Amorph	
UGWM[b]	35.0	16.5	13.2	11.3	0.6	1.5	21.9	
CGWM[b]	35.0	8.7	12.4	0.3	2.1	7.2	34.4	

[a] Quartz content fixed for normalisation of data; [b] Quantitative XRD data from [2]

***Table 7.4** - Mineralogical composition (quantitative) of OPC, UGWM and CGWM powders*

7.3.2 Early hydration kinetics, long-term volumetric changes due to shrinkage and mechanical performances of the hardened blended cement pastes

7.3.2.1 Hydration heat flow by isothermal calorimetry

The evolution of the heat flow profiles of the plain and binary cement pastes for the first 30 minutes are presented in **Figure 7.3a**, from 30 minutes up to 40 hours in **Figure 7.3b** and the cumulative heat release up to 40 hours in **Figure 7.3c**. During the initial phase of cement hydration (pre-

induction period) after addition of water, the rapid dissolution of the cement minerals, C_3A (calcium aluminate) and C_3S (alite), into unstable, reactive ions in the pore solution leads to the formation of stable solid phases accompanied with exothermic heat release. As shown in **Figure 7.3a**, the highest peaks of the initial hydration heat of each examined fresh pastes occurred in the first minutes after water addition and exhibited a non-monotonic progression as a slight leftward shift of the heat evolution curves of the cement pastes containing CGWM powders was observed. Furthermore, only for the cement pastes containing 10 wt.% of CGWM, a representative enhancement was traceable, mainly due to its positive contribution by the initial dissolution of additional ions to the saturation of the pore solution, which was not observed for the pastes with higher contents of CGWM (oversaturation of the pore solution with aluminate and silicate ions). Following the heat profile curves, illustrated in **Figure 7.3b**, no correlation between the incremental CGWM content and the heterogeneous nucleation of additional C-S-H phases could be observed as the released hydration heat declined with increasing OPC replacement levels by the CGWM powders. The decline of the hydration heat rates proportionally to the CGWM content becomes visible in **Figure 7.3c** as lower slopes are observed during the acceleration period, which confirms that the higher OPC replacement levels by a slow-reacting medium-pozzolanic material like CGWM reduce the extent of hydration reaction at early ages, and the overall dilution effect, as well as the agglomeration effect between the fine aluminosilicate particles, dominate their potential to act as nucleation sites for additional hydration of the cement grains. The higher hydration rates of the REF mixture are carried over all the examined hydration stages resulting in higher cumulative heat release up to 40 hours. These results regarding the evolution of the hydration heat release of the investigated cement pastes complement earlier findings [1–3] that the incorporation of higher amounts of CGWM in blended cement pastes exhibits minor to no

significant physiochemical effects as the CGWM powders could provide no larger interfacial surface area for higher hydration reaction rates (C-S-H seeding) by performing as nucleation sites during the early hydration stages of the cement matrices.

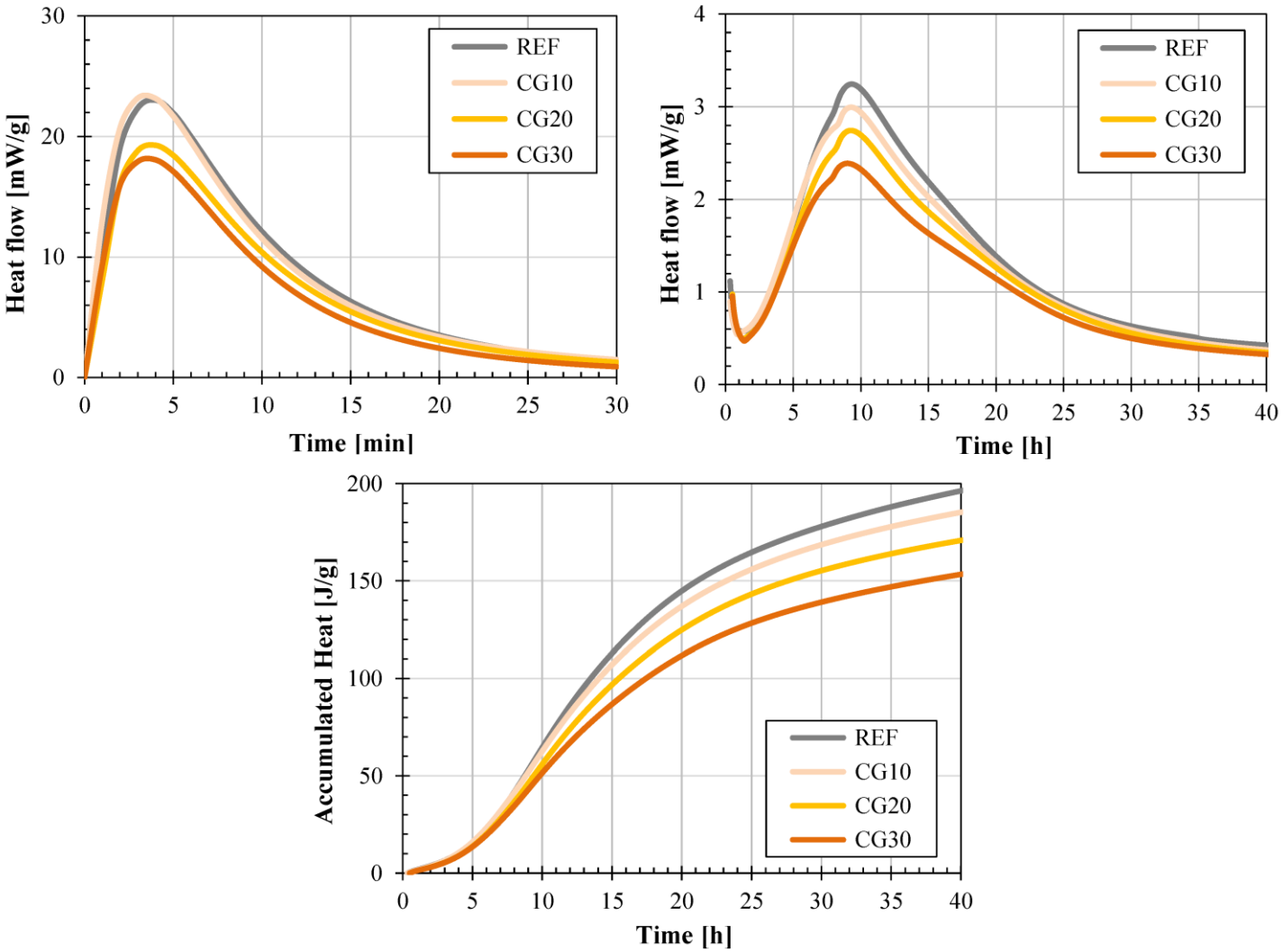

Figure 7.3 *- Isothermal calorimetric curves of REF, CG10, CG20 and CG30: a) heat flow from up to 30 min, b) heat flow from 30 min up to 40 h, c) accumulated heat release up to 40 h*

7.3.2.2 Shrinkage behaviour of blended cement pastes

The unrestrained drying shrinkage of hardening paste mixtures was measured as the variation in length due to volume change over time at constant storage conditions. The temperature [°C] and the relative humidity [%] were recorded over the entire measurement period and ranged around 21.3 ± 1.4 °C, respectively 56.7 ± 12.0 % of relative humidity (**Figure 7.4**). The drying shrinkage behaviours of the control mixture REF and the blended cement pastes CG10, CG20 and CG30 over 80 days is plotted in **Figure 7.4**. Overall, the drying shrinkage magnitudes of all specimens increased rapidly for the first two weeks, followed by slower increase rates in the subsequent months down to constancy. Over the whole examined time, REF exhibited the largest shrinkage values. CG10 and CG20 experienced almost identical evolution of the shrinkage values and therefore presented similar shrinkage behaviour, whereas CG30 exhibited a short swelling period in the first two days, followed by a larger shrinkage rate than REF until stabilising around the shrinkage magnitudes of CG10 and CG20 at 60 days. The expansive effects of swelling of the paste mixtures with higher CGWM contents can be related to the larger soaking of portions of mixture water by the aluminosilicate raw material, which influences the chemical and autogenous shrinkage of the cement-CGWM pastes at higher OPC replacement levels at early curing ages [296,297].

After 7 days of curing age, CG10, CG20 and CG30 experienced 18 %, 23 % and 15 % less contraction deformations than the control mixture. The maximum shrinkage values of REF, CG10, CG20 and CG30 up 80 days were at 508.6 μm/m, 489.4 μm/m, 484.1 μm/m and 469.8 μm/m, i.e. the experienced shrinkage is 4 %, 5 % and 8 % less for CG10, CG20 and CG30 than that of the reference mixture REF. The measured maximum shrinkage values comply within the indicative range for acceptable shrinkage deformations for standard concrete from 0.2 mm/m up to

0.6 mm/m [298]. The evaluation of the shrinkage magnitudes of the investigated pastes approves the positive enhancements of the time-dependant properties of blended cement pastes by incorporating CGWM as SCM due to the improved packing of the constituents and the formation of additional pozzolanic hydration products.

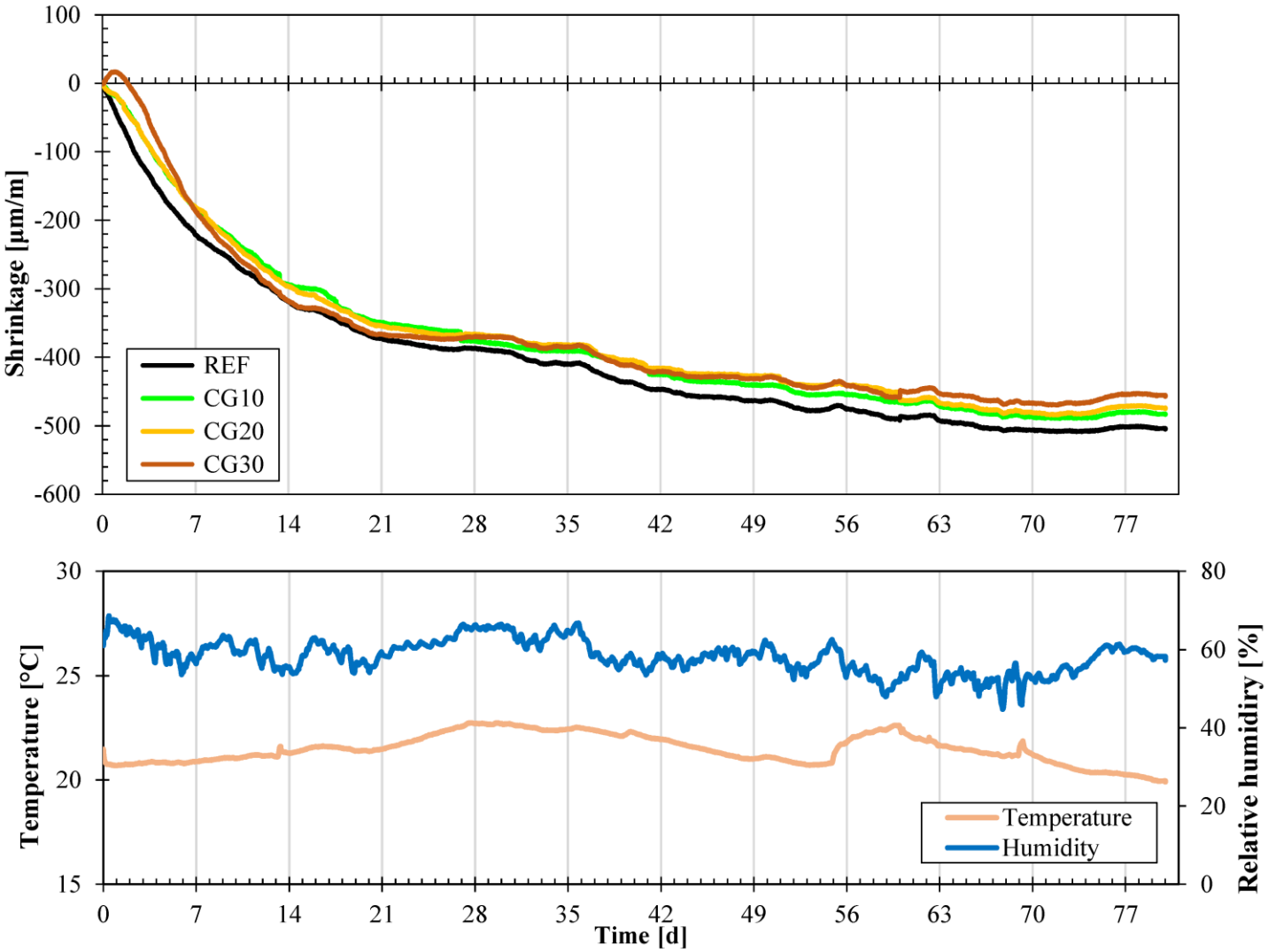

Figure 7.4 *- Evolution of shrinkage of the hardened paste mixtures REF, CG10, CG20 and CG30, including the development of relative humidity [%] and temperature [°C] up to 80 days*

7.3.3 Compressive strength tests of hardened specimens

The results of the 28- and 56-day compression strength tests of the hardened pastes with different OPC replacement levels by UGWM and CGWM powders are presented in **Figure 7.5**. The indicated values represent the mean compressive strengths out of at least three valid compression tests on replicates. For blended cement pastes containing 20 wt.% and 30 wt.% of GWM powders (both UGWM and CGWM), consistent gains in compressive strength from 28 days up to 56 days were considered. For REF, UG10 and CG10, a slight reduction of the compressive strength was observed from 28 days to 56 days.

Overall, the cement pastes containing GWM powders reached lower compressive strengths than the control mixture over the entire examined curing ages. At 28 days, the lower pozzolanicity of the UGWM powders compared to CGWM powders becomes evident as for same mixture proportions, lower compressive strengths are achieved by the hardened pastes containing UGWM at OPC replacement levels of 20 wt.% and 30 wt.%. The lower reactivity of UGWM becomes more significant with increasing curing age, as at 56 days, the compressive strengths of hardened pastes incorporating UGWM powders decrease with higher substitution degrees of OPC, whereas the mechanical performances of hardened pastes containing CGWM increase slightly with higher OPC replacement levels. This representative trend indicates the formation of additional hydration products due to pozzolanic reactions between the CGWM powders and unreacted calcium hydroxide (Portlandite), the main co-products from the hydration of cement clinker minerals. The SAI method (**Figure 7.6a**) and the RSI method (**Figure 7.6b**) were applied to assess the pozzolanic reactivity of UGWM and CGWM as potential OPC substitutes. According to ASTM C311 [102], the strength activity indices for hardened cement pastes are calculated for OPC replacement levels of 20 wt.% and the 75% minimum threshold according to ASTM C618 [74] represents the minimal

SAI requirement on calcined pozzolans after 28 days of curing age. As shown in **Figure 7.6a**, the computed SAI of UG20 does not fulfil the minimal requirement at 28 days of curing and indicates that the incorporation of the UGWM powder rather contributes to a dilution effect at higher OPC replacement levels which instead builds a physical constraint for the clinker hydration reactions than an improvement due to measurable pozzolanicity.

In comparison, the SAI of CG20 at 28 days of curing age surpasses the minimal requirement by 13.1 % and thereby confirms that the tested pozzolan, namely CGWM powder, can be considered as SCM [1–3] as it sufficiently contributes to the development of the required minimal strengths in an OPC-based mixture. As the SAI method, according to [74], is an indicative assessment method and does not evaluate the optimal substitution degree, the indices are computed for all hardened cement paste specimens at all curing ages. It can be observed that the hardened pastes containing UGWM powders fulfil the minimal threshold at later curing ages, as the development of additional calcium silicate hydrate (C-S-H) products due to later pozzolanic reactions becomes more significant.

The evaluation of the computed relative strength indices illustrated in **Figure 7.6b** confirms the previous statements from the comparative analysis of the absolute compression strength values as well as the SAI analysis. The assessment of the RSI verifies the positive contributions of UG10 and CG10 for all investigated curing ages, which suggest that for OPC replacement level of 10 wt.%, the physical filler effect of the GWM powders is rather predominant than the chemical contributions to the mechanical performances. Additionally, the negative contributions by relative strength loss of UG20 and UG30 at 28 days of curing age are also confirmed by the RSIs. Furthermore, positive relative strength gains up to 56 days of curing age for the hardened cement pastes using higher OPC substitution degrees of 20 wt.% and 30 wt.% by UGWM and CGWM are

observed.

Figure 7.7 illustrates the evolution of compressive strength results of hardened pastes of REF, UG20 and CG20 at 1, 3, 7, 28, 56 and 90 days (cured in air), and the strength development of REF and CG20 at 7, 28, 56 and 90 days (cured in water). By comparison of the mechanical performances of air-cured and water-cured specimens of the same mixing proportions, it can be concluded that the investigated specimens did not reveal any significant dissimilarities in terms of mechanical strength due to applied curing conditions [299], except for CG20 at 90 days. A gain of 10 % in compressive strength was observed for CG20_W compared to CG20 at 90 days, which can be explained by the continuous hydration of belite (C_2S) in water curing conditions at later ages [299], leading to the formation of calcium hydroxide (CH), which undergoes into a pozzolanic reaction with available CGWM to form additional hydration products. Furthermore, for the paste mixture REF, a representative decline in compressive strength was observed after 28 days of curing age in both examined curing conditions. The exact reason for the drop in strength is still unclear, but a possible explanation could be the applied high w/b ratio leading to larger volumetric shrinkage strains (drying shrinkage) in combination with proceeding carbonation reactions of the cement matrix with the presence of unreacted CH at increasing curing age, leading to the deterioration of specimens (cracks). This trend was not visible for all the blended cement paste mixtures containing UGWM and CGWM at any substitution degree, as the excess CH at later curing ages is consumed by the pozzolanic reaction with the examined SCM.

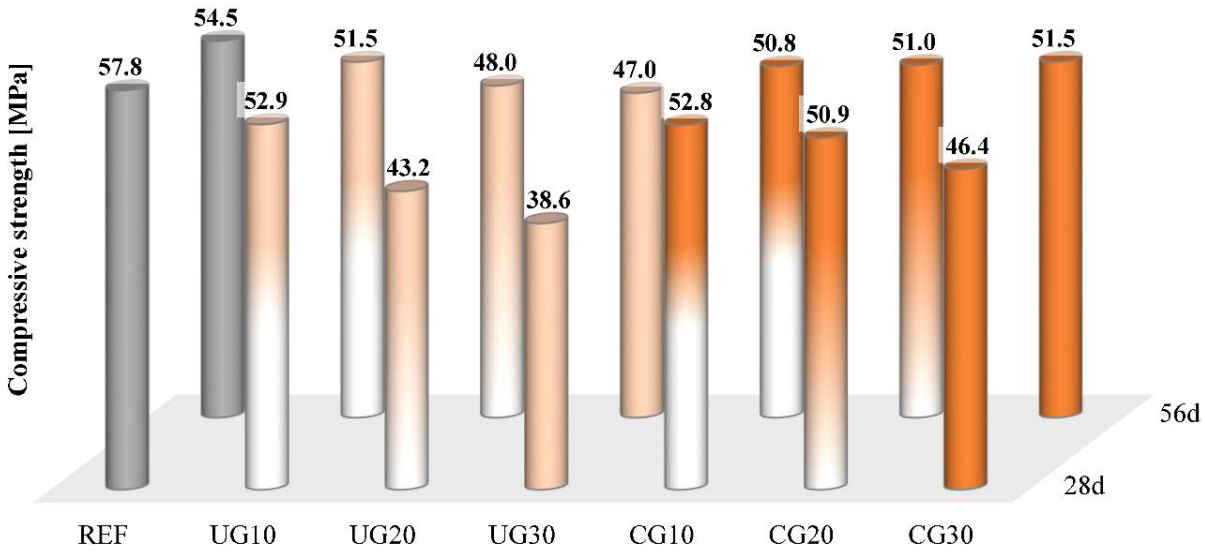

Figure 7.5 *- Evolution of the mechanical properties of hardened pastes of seven different paste mixtures, namely REF, UG10, UG20, UG30, CG10, CG20 and CG30 at 28 and 56 days of curing age*

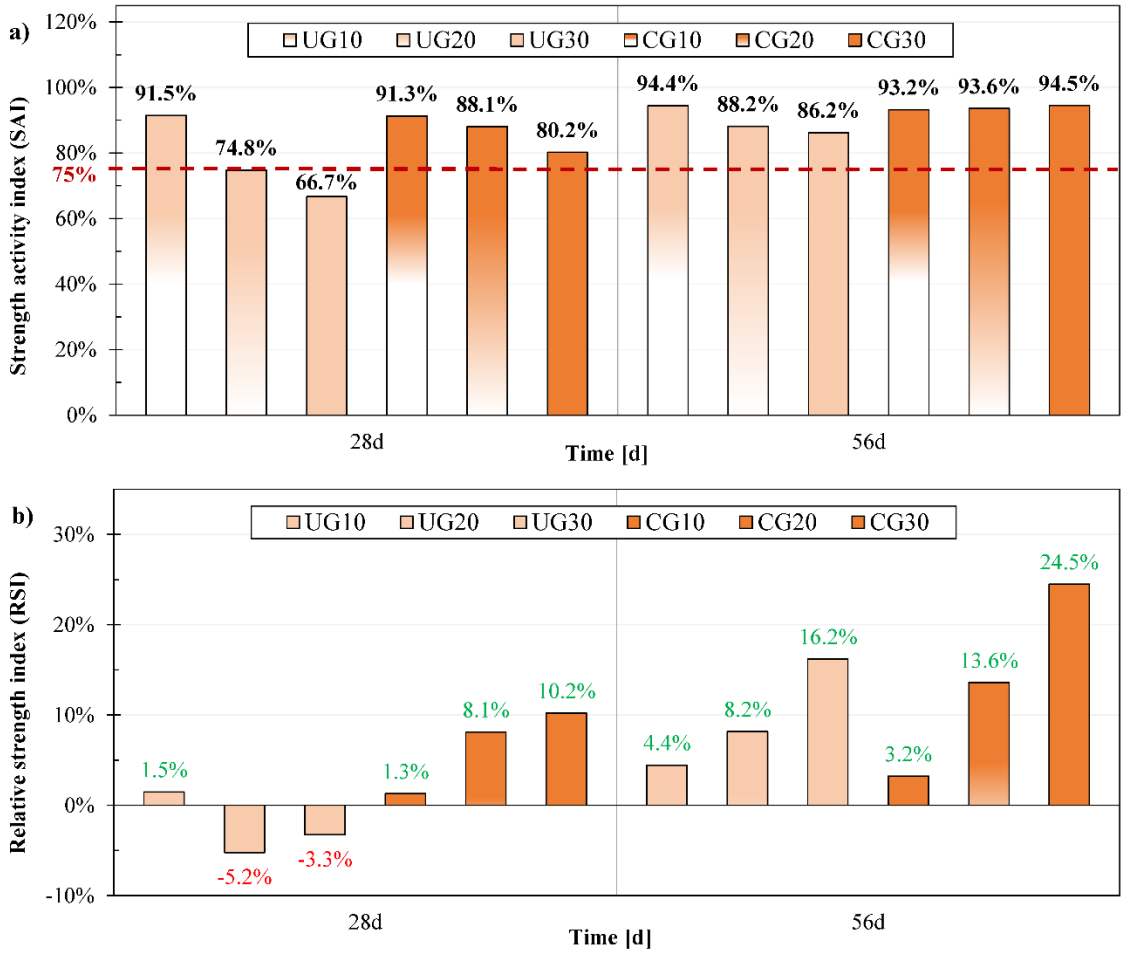

Figure 7.6 *- Strength-based evaluations: a) Strength activity index (SAI; dashed line represents the limit for pozzolanic activity according to ASTM C618 [74] and b) relative strength index (RSI) [2]*

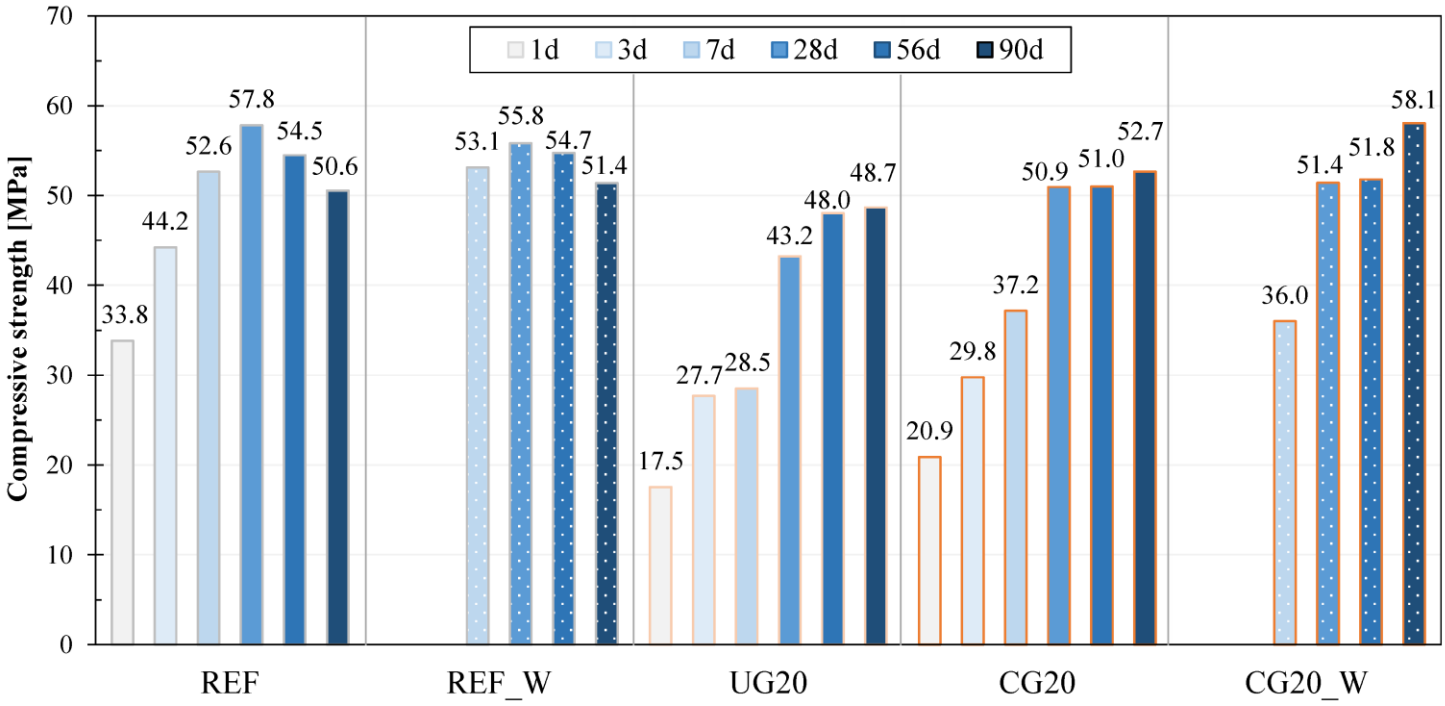

***Figure 7.7** - Evolution of the mechanical properties of hardened pastes from three different paste mixtures: REF, UG20 and CG20 (cured in the air), REF_W and CG20_W (cured in water) at 1, 3, 7, 28, 56 and 90 days of curing age (strength tests after 1 day and 3 days skipped for water cured specimens)*

7.3.4 Fresh concrete properties, compressive strength, carbonation test and SEM analysis of the investigated concrete mixtures

7.3.4.1 Properties of fresh concrete and the evolution of mechanical properties of the hardened concrete specimens

The results of the slump test are given in **Table 7.5**. From the evaluation of the results, it is confirmed that higher GWM powder content in the concrete mixes influences the fresh concrete properties as a significant reduction of the workability of concrete was observed. The major contribution to the reduction of the degree of workability with higher GWM powder contents can be attributed to the fineness (higher surface area [2,3]) of the aluminosilicate particles. Although overall, homogenous compaction of the fresh concrete was possible by vibration, these results are

in agreement with the findings from the literature [300–302] and suggest the usage of adequate dosage of superplasticisers to improve the flowability of concretes incorporating higher portions of SCMs (GWM powders) and, thereby, adapt the workability of the concretes for various constructive applications.

The properties and the evolution of the compressive strengths of the examined concrete mixtures after 28 days and 56 days are given in **Table 7.5** and illustrated in **Figure 7.8**, and the findings confirm that the incorporation of the different GWM powders influences the characteristics and the compressive strength of the binary blended concrete mixes. For all the investigated concrete mixes, the compressive strength increased with growing curing age, ranging from 25.6 MPa to 41.1 MPa after 28 days up to from 31.7 MPa to 46.5 MPa after 56 days. The binary concrete mixes C_UG10, C_CG10 and C_CG20 achieved the highest compressive strengths comparable to OPC concrete at around 40 MPa after 28 days and around 46 MPa after 56 days. At all examined curing ages, C_UG10 slightly exceeded the target compressive strength of the reference mixture, mainly due to the better packing of the constituents (filler effect) by the formation of a denser aggregate-blended cement paste matrix. Furthermore, the incorporation of higher portions of UGWM powders are revealed to have detrimental effects on the mechanical properties of blended concretes as the low reactivity of the UGWM powder hinders effectivity of pozzolanic reaction with the free Portlandite and rather build a physical obstruction to the hydration process (dilution effect). The development of elastic modulus (E_c) and the measured densities (ρ) of the different concrete mixes reflect and comply with the evolution of their mechanical strengths by producing lower values for concrete mixes with higher UGWM powder contents and comparable values to the reference mixture for C_UG10, C_CG10 and C_CG20.

The resulting mechanical parameters of the examined concrete mixes confirm the findings from

the strength assessments on the hardened blended cement pastes and implicate that the incorporation of UGWM powders at OPC replacement levels of 10 wt.%, and CGWM powders at OPC replacement levels of 10 wt.% and 20 wt.% in binary concrete mixes can be considered as viable and competitive proportions for alternative SCM-based concretes for various constructive applications without compromising on the concrete's mechanical performance.

Sample	Slump [mm]	ρ_{28} [kg/dm^3]	$f_{cyl,28}$ [MPa]	$\Delta f_{cyl,REF}$ [%]	$E_{c,28}$ [GPa]	ρ_{56} [kg/dm^3]	$f_{cyl,56}$ [MPa]	$\Delta f_{cyl,REF}$ [%]	$E_{c,56}$ [GPa]	Cd_{28} [mm]	Cd_{56} [mm]
C_REF	215.0	2.29	39.3	-	29.47	2.29	46.0	-	28.79	1.25	2.75
C_UG10	110.0	2.29	41.1	4.6%	29.45	2.29	46.5	1.21%	28.18	0.75	1.75
C_UG20	55.0	2.18	29.7	-24.5%	21.62	2.19	34.8	-24.31%	20.95	1.75	3.00
C_UG30	42.5	2.17	25.6	-34.8%	19.49	2.20	31.7	-31.05%	21.50	2.50	3.25
C_CG10	165.0	2.27	38.7	-1.6%	26.91	2.26	44.6	-2.96%	26.95	0.50	1.75
C_CG20	60.5	2.25	38.8	-1.3%	25.61	2.27	45.4	-1.30%	28.42	1.25	2.50
C_CG30	48.0	2.25	33.6	-14.5%	24.82	2.23	38.7	-15.92%	25.78	1.75	2.75

ρ_X – bulk density of concrete at X days of curing age
$f_{cyl,X}$ - compressive strength of concrete cylinder after X days
$E_{c,X}$ - elastic modulus of concrete at X days of curing age
Cd_X - carbonation depth after X days
$\Delta f_{cyl,REF}$ - difference of compressive strength between two curing ages or compared to the reference mixture

***Table 7.5** - Measured parameters and results of the strength tests of the examined concrete mixtures*

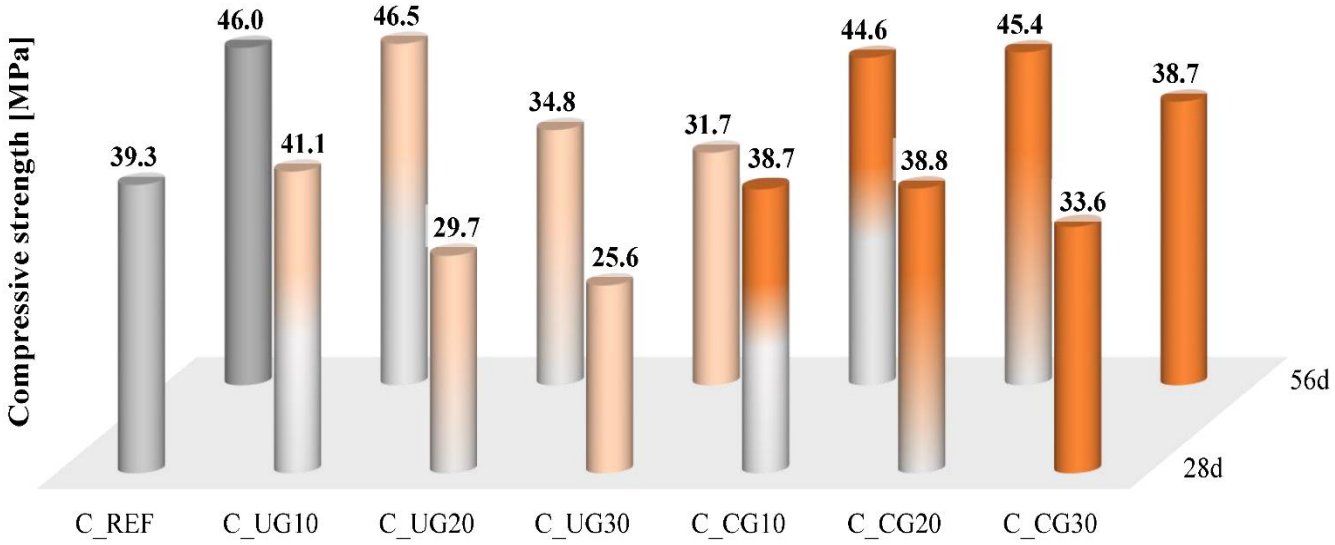

***Figure 7.8** - Evolution of the compressive strength of the examined concrete mixtures, namely C_REF, C_UG10, C_UG20, C_UG30, C_CG10, C_CG20 and C_CG30 at 28 and 56 days of curing age*

7.3.4.2 Depth of carbonation and microstructural analysis by SEM

The results of the measurement of the carbonation depths (Cd) of the investigated concrete samples after 28 days and 56 days are presented in **Table 7.5**. **Figure 7.9** shows the cross-sections of the investigated specimens after application of the phenolphthalein indicator solution after 56 days. The comparison of the carbonation depths of the concretes after 28 days reveals that at early curing ages the overall measured level of carbonation is very low (around 1 mm) as the hydration reactions are progressing and the interstices are being filled with hydration products to increase the strength development further. However, C_UG10, C_CG10 and C_CG20 already express lower or equal carbonation depths than the reference mixture C_REF. This positive enhancement can be explained by finer pore structure (denser packing of binder particles and additional hydration products) and the early pozzolanic reaction of available free $Ca(OH)_2$ with reactive CGWM powders. Whereas, for concretes with higher GWM powder contents, greater rates and depths of carbonation compared to the reference concrete C_REF were measured due to lower reactivity of UGWM in combination with the predominant dilution effect (less OPC available in the mixture) at early curing ages. Beyond that, at any examined time of exposure, the advancement of carbonation of the binary blended concretes incorporating 10 wt.% and 20 wt.% of CGWM were lower than in C_REF.

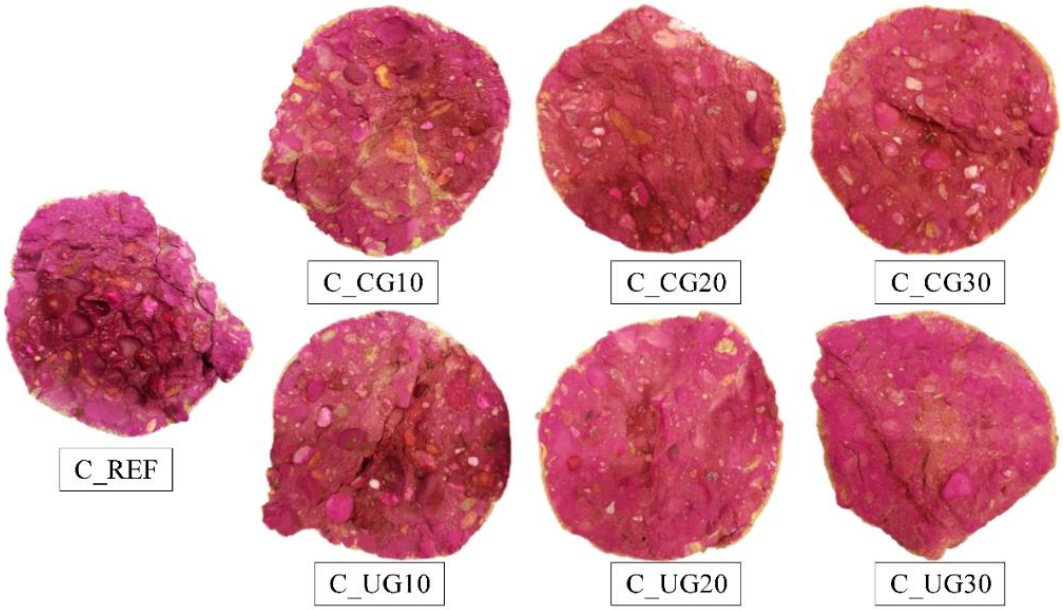

***Figure 7.9** - Carbonation depth test on cross-sections of C_REF, C_UG10, C_UG20, C_UG30, C_CG10, C_CG20 and C_CG30 after 56 days*

A selection of micrographs of broken fractions of all the investigated concrete mixtures are presented in **Figure 7.10**, **Figure 7.12** and **Figure 7.11**, which were produced by SEM analysis with verification using elemental analysis by EDS. **Figure 7.10** illustrates the microstructural features of the reference concrete C_REF. In **Figure 7.10a**, the development of a compact microstructure of hardened cement paste with dense and homogenous coverage of the quartz particles can be observed, whereas **Figure 7.10b** shows a well-formed framework of needle-like and amorphous C-S-H mineral formations of the same concrete mixture. **Figure 7.12** depicts a compilation of micrographs showing the microscale morphology of the concrete mixtures containing UGWM powders at varying OPC substitution degrees. In **Figure 7.12a** and **Figure 7.12b**, a dense microstructure of C_UG10, consisting of mainly calcium silicate hydrate phases without any traces of unmixed or unreacted aluminosilicate particles, was detected; additionally, at the interfacial transition zones between the cement matrix and the aggregates, extensive developments of needle-like, fibrillar and amorphous hydration products were localised, which explain the enhanced performances compared to the control mixture by an improved bond

between the hydrous and amorphous cementitious formations and the concrete aggregates. **Figure 7.12c**, **Figure 7.12d** and **Figure 7.12e** show the microstructural compositions of C_UG20, consisting of amorphous compounds with semi-reacted Portlandite crystals (CH), large aluminosilicate crystals covered by cementitious and pozzolanic hydration products and dispersed areas of unmixed, semi-mixed and unreacted aluminosilicate particles (UGWM) surrounded by amorphous cementitious formations, which suggests that some unreacted CH could not be bound by the low-reactive aluminosilicate particles of UGWM to form additional pozzolanic hydration products and thereby explain the decline of mechanical performance of concrete mixtures with higher UGWM proportions. The microstructure of C_UG30 (**Figure 7.12f**) reflects and explains the detrimental effect of higher UGWM contents in concrete mixtures on the resulting mechanical performances as larger entrapped air voids and micropores, as well as dispersed locations of unmixed or unreacted GWM powders, were detected across the investigated samples. This development also suggests that higher content of UGWM, resp. CGWM is not recommended to avoid larger proportions of unmixed/semi-mixed aluminosilicate or cementitious agglomerates (dilution effect). **Figure 7.11** presents the microstructure of broken fractions of concrete specimens incorporating CGWM powders at varying OPC replacement levels. Similar to C_UG10, the SEM micrograph of C_UG10 (**Figure 7.11a**) depicts a densely interlocked amorphous microstructure with no traceable semi-mixed or unreacted aluminosilicate particles. In **Figure 7.11b** and **Figure 7.11c**, the formation of dense microstructural networks of calcium silicate hydrates and calcium aluminosilicate hydrates covering local quartz particles and the formation of needle-like and fibrillar C-S-H phases and pozzolanic hydration products are identified. **Figure 7.11d** shows a spot of densely packed unreacted and semi-mixed aluminosilicate agglomerates. The SEM analysis of the different samples confirms a well-developed and dense microstructure of the

examined binary blended concretes with extensive formations of pozzolanic hydration products and the cementitious hydration products.

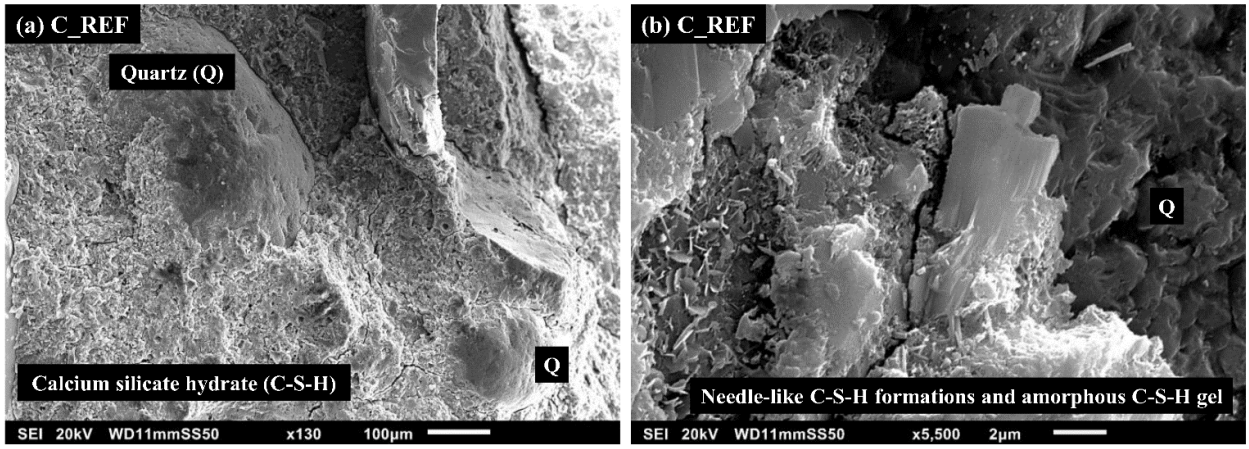

Figure 7.10 *- SEM micrographs of C_REF: a) quartz (Q) particles covered by compact hardened cement paste (x130); b) needle-like and amorphous calcium silicate hydrate (C-S-H) phases (x5500)*

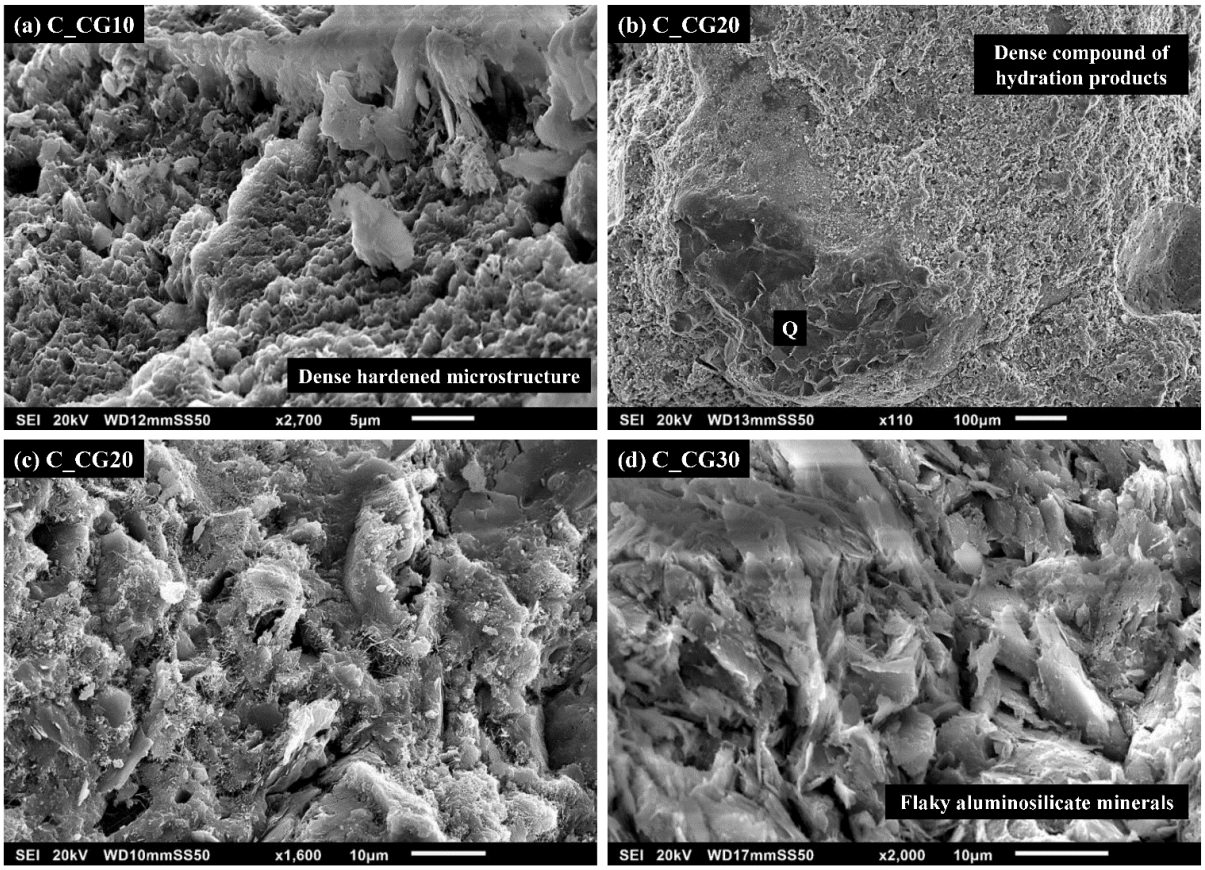

Figure 7.11 *- SEM micrographs of C_CG10, C_CG20 and C_CG30: a) Dense amorphous structure consisting of cementitious and pozzolanic hydration products (x2700); b) compact microstructure of calcium silicate hydrates and calcium aluminosilicate hydrates covering local quartz particles (x110); c) needle-like and fibrillar C-S-H phases and pozzolanic hydration products (x1600); d) Unreacted and semi-mixed aluminosilicate agglomerates (x2000)*

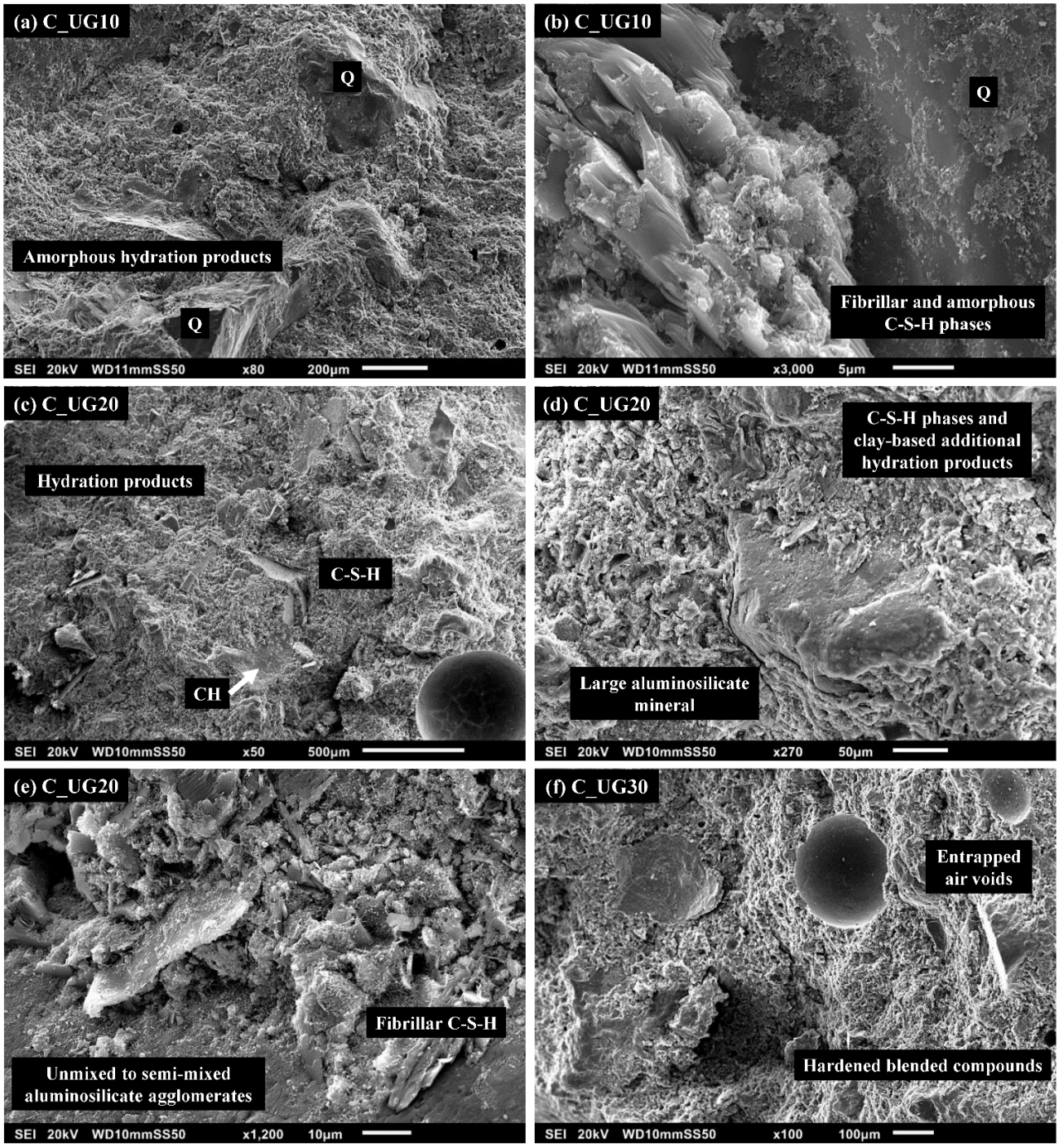

Figure 7.12 *- SEM micrographs of C_UG10, C_UG20 and C_UG30: a) Hardened amorphous blended paste with dense coverage of quartz particles (x80); b) Transition zone between large quartz grain and calcium silicate hydrate (C-S-H) phases (x3000); c) Amorphous compound with semi-reacted Portlandite (CH) (x50); d) Large aluminosilicate mineral covered by compact compound consisting of cementitious and pozzolanic hydration products (x270); e) unmixed, semi-mixed and aluminosilicate particles (UGWM) were discovered surrounded by fibrillar C-S-H phases (x1200); f) irregular hardened blended cement paste with distributed large air voids (x100)*

7.4 Conclusion

The work presents the results of investigations performed on blended cement pastes and concrete mixtures incorporating processed GWM powders (originating from quarry waste sludge) as potential alternative SCMs at varying OPC replacement levels from 10 wt.% up to 30 wt.%. From the key findings of the different examinations, the following can be drawn:

- The physicochemical characteristics and the mineralogy of the processed raw material, CGWM powder, originating from quarry waste sludge, exhibits medium-reactive pozzolanic behaviour and can be considered as an alternative SCM.
- The assessment of the hydration heat release of the blended cement pastes confirms that, at the early hydration stages, the incorporation of CGWM powders exhibits minor to no significant physiochemical effects and therefore does not actively contribute to the acceleration of the early hydration reaction by acting as nucleation sites of the cement matrices.
- The drying shrinkage magnitudes of the blended cement pastes containing CGWM powders as SCM are lower over the examined period of 80 days compared to the control mixture REF. The enhancement potential of the time-dependant properties of the blended cement pastes results from the improved packing of the constituents and the formation of additional pozzolanic hydration products, which induced a reduction of about 4-8 % of dry shrinkage values compared to REF.
- The GWM powders show a significant impact on the fresh concrete properties of the blended concrete mixes by greater reduction of the workability of the fresh compounds with increasing GWM powder content and therefore suggest the usage of an appropriate

superplasticiser to meet the flowability requirement on fresh concrete depending on desired applications.

- The assessment of the mechanical properties of the different concrete mixes implicates that the contents of UGWM powders at OPC replacement levels of 10 wt.%, and CGWM powders at OPC replacement levels of 10 wt.% and 20 wt.% in binary concrete mixes can be considered as viable and competitive proportions for alternative SCM-based concretes.
- For the examined time until 56 days of curing age, greater progress of carbonation was recorded for binary blended concrete using higher OPC substitution degrees by UGWM powders, whereas the advancement of carbonation of the binary blended concretes incorporating 10 wt.% and 20 wt.% of CGWM powders were lower compared to the reference concrete C_REF.
- The microstructural analysis of the different samples shows a firmly adhered and dense microstructural composition of the investigated specimens, mainly consisting of extensive formations of co-existing aluminosilicate-based pozzolanic hydration products and the clinker-based hydration products.

The usage of CGWM powders in binary blended concretes can contribute to cost-savings in the manufacture of constructive elements (derived of unused quarry waste), the reduction of the environmental impacts of the cement industry as well as the great potential to the enhancement of the durability performances of the final concrete products. Further studies are required to evaluate the challenges and opportunities inherent in the GWM-based concrete products, namely the transition to large-scale processes of the used treatment activity, the improvement of the rheology, the investigations on the durability performance against concrete degradation effects, and the economic and environmental assessment of the proposed technology at industrial scale.

Chapter 8 Summary

The main ambition of this research project is to revalorize gravel wash mud (GWM), which occurs as a waste product during industrial quarrying activities in Luxembourg, and to display its scope of performance as a potential raw material resource by suggesting GWM-based concepts for alternative cements for constructive applications.

The present summary draws together the core findings and conclusions of this cumulative dissertation entitled “Recycling of gravel wash mud for manufacturing CO_2-reduced cement”. In this writing, a series of background information, key objectives and extensive literature reviews on the main research topics, especially related to three different binder concepts and their accompanying themes, have been individually covered und very thoroughly explained. Notably, the necessity for alternatives cementitious products has been extensively discussed by providing significant contents on cement manufacture, the hydration process of OPC, the unavoidable intrinsic properties of OPC-based products and the current potentials of alternative cementitious concepts.

In a general context, the origin of the waste product, gravel wash mud (GWM), was explained from the geographical, geological, industrial and operational standpoint. Subsequently, the general topology, and the preparatory measures as well as the thermal treatment processes of the argillaceous GWM into the different powders were provided, before ending the presentation of the

main raw material by highlighting its quantity, its quality and the national availability of similar products.

After stating the general topical issues, the display of existing research gaps and the presentation of the main raw material GWM of this project, each of the investigated binder concepts on alkali-activated binders, blended cement pastes and ternary lime-MK-GWM binder pastes and the performance of binary blended concrete, are individually discussed in the corresponding research paper of this cumulative dissertation.

In conclusion, the first binder concept using the methods of alkaline activation on calcined GWM powders can be abandoned for GWM as main raw material. The investigated concept reveals in itself to be very promising, and existing works confirm that a well-formed microstructure can be developed by adapting various parameters regarding thermal activation, further adjustments on the applied w/b ratios and the usage of different alkaline solutions. However, the concept of alkaline activation is not suitable and applicable on the used calcined GWM powders, due to its physicochemical properties and its mineralogical composition that show a low to medium reactive aluminosilicate material, which suggested the requirement of a different type of activating agent.

The investigations on the suitability of calcined GWM powder as supplementary cementitious material were very fruitful as the presented findings confirm the pozzolanic activity of calcined GWM material as well as its strength-enhancing properties at low to medium OPC substitution degrees (second investigated concept). Overall, an OPC replacement level at 20 wt.% by calcined GWM powders led to the development of reliable, well-performing hardened mortars or concrete products. Higher OPC replacement levels than 30 wt.% are not recommendable for the development of concrete formulations, as the reaction products might be affected by secondary

issues like obstruction of the homogenous distribution of the binder paste or the presence of large unreacted GWM powders that can be considered as critical spots in the final products.

As a clear overview on the positioning of calcined GWM powders as valid SCM, **Figure 8.1** and **Figure 8.2** highlight a comparative classification of the mechanical performances of GWM-based blended cements and binary blended concretes compared to a selection of reported performances of pastes, respectively concretes from literature.

The third concept presented auspicious results for lime-MK-GWM-based binder mixtures for future applications in eco-efficient concrete formulations. The investigations suggest the use of hydrated lime instead of natural hydraulic lime as more dense and strength-enhancing reaction products from pozzolanic reaction were reported at early curing ages. Furthermore, the findings contributed to further verification of calcined GWM powders as competitive and powerful SCMs. Nonetheless, the extent of the current investigations presented in this research work suggests that the reliable incorporation of calcined GWM in lime-pozzolan binder systems requires further examinations on the long-term behaviour, the durability and the application potentials of these mixtures to satisfy common mortar or concrete-related conformity criteria for constructive purposes. In **Figure 8.3**, the performance of the best-performing lime-MK-GWM binder paste is compared to a selected set of lime-based paste from existing works.

Finally, this research work provides a solid fundamental basis to develop an appropriate revalorisation and management framework for GWM, a quarry waste product. As already mentioned several times in this dissertation:

“The aim is to replace the “end-of-life” concept of gravel wash mud by reusing or recycling it as new raw material.”

I believe that, within this thesis, a valuable scientific approach and a solid base for the usage of gravel wash mud has been delivered. I am also convinced that research is an endlessly iterative process, and absolute solutions do not exist, as there is always room for improvements. In my opinion, there are still enormous amounts of open questions and further research requirements, which could not be tackled within this time-limited project. Therefore, besides the required studies discussed in each research articles, some additional open questions, the already initiated research works and future potential projects following this research project are shortly highlighted in the outlook of this dissertation.

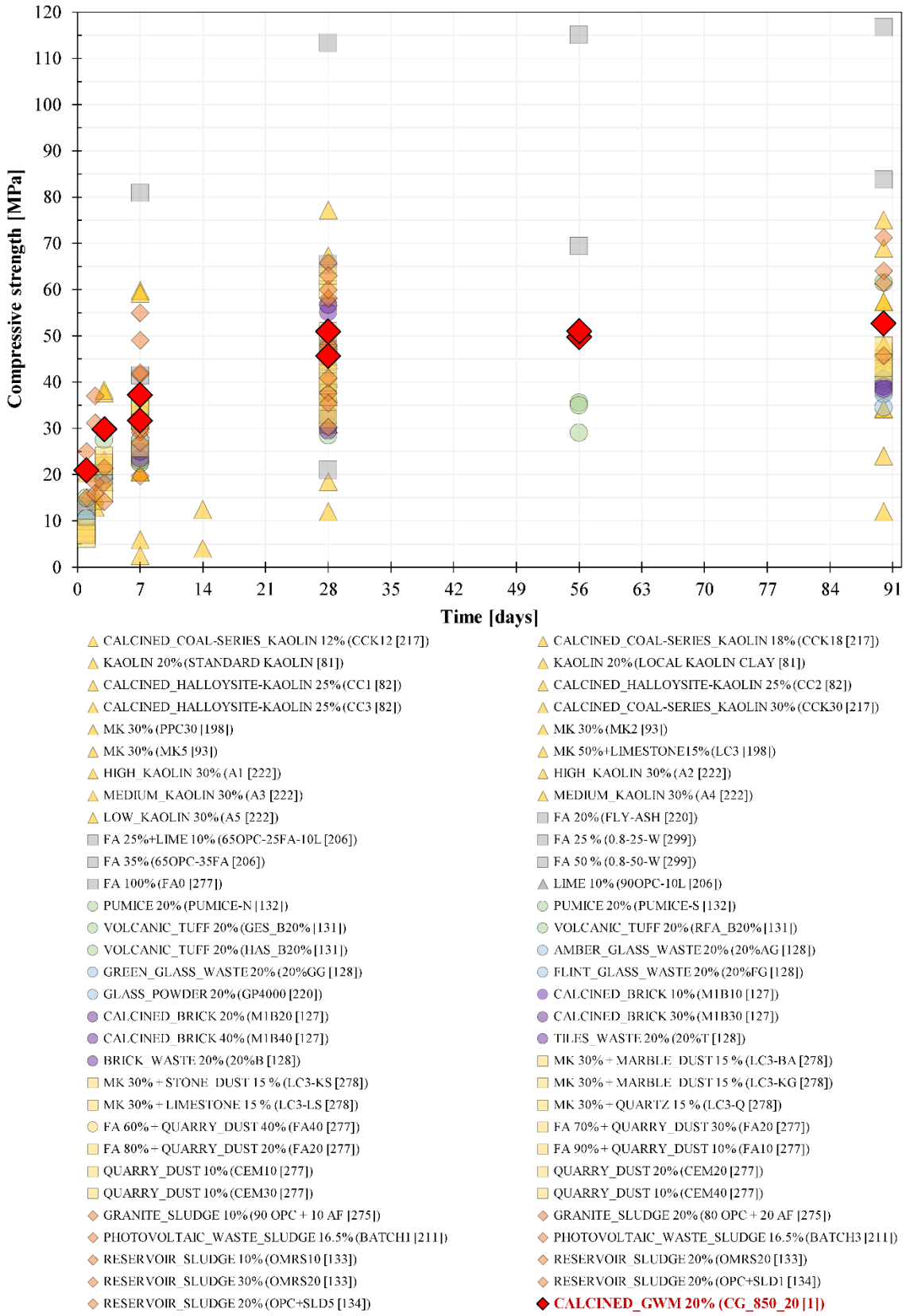

***Figure 8.1** - Positioning of the optimum blended cement paste (20 wt.% of calcined GWM)* [2,4] *in terms of compressive strength compared to selected pastes from literature*

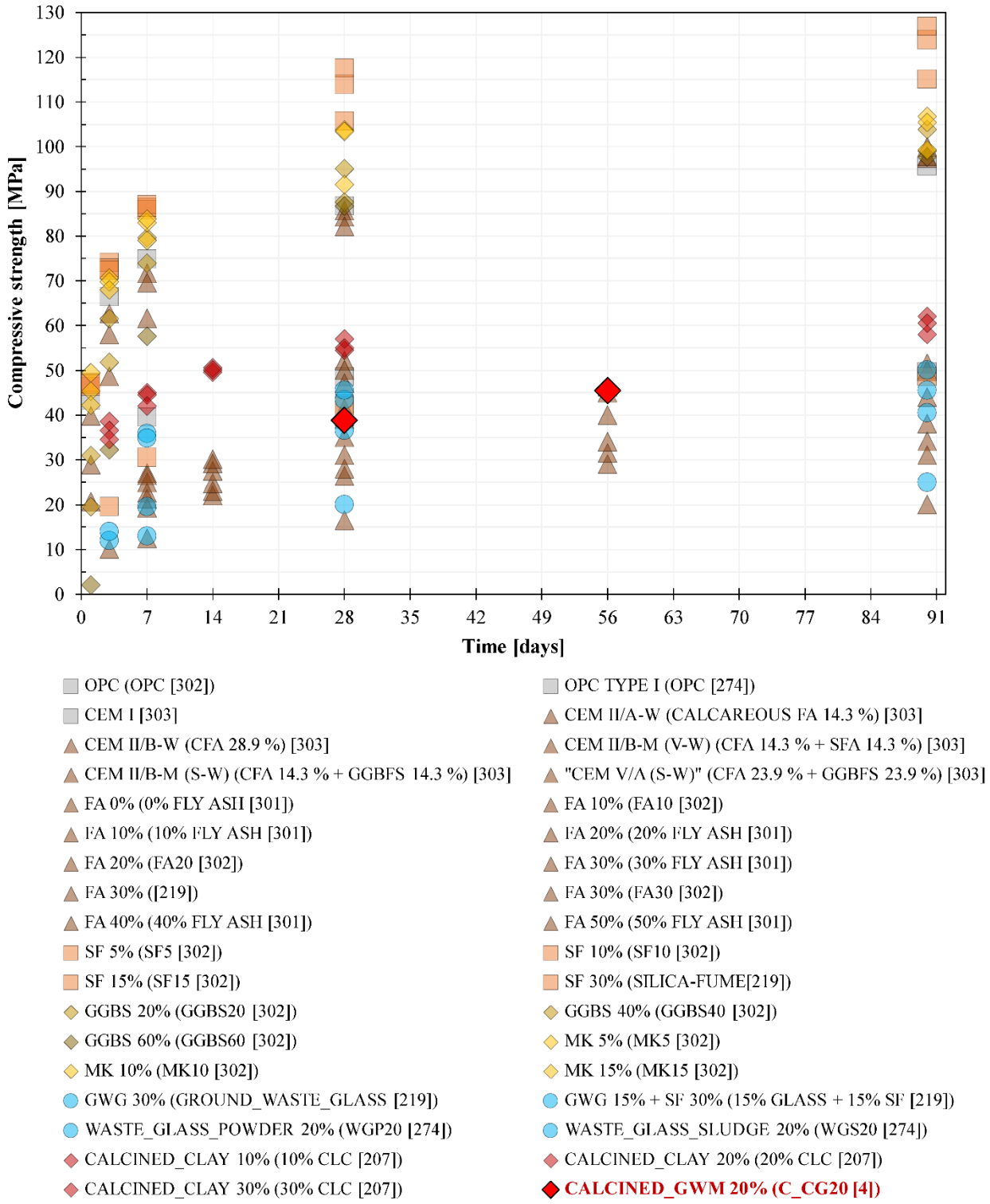

Figure 8.2 *- Ranking of the optimum blended concrete (20 wt.% of calcined GWM) [4] in terms of compressive strength compared to selected concretes from existing studies*

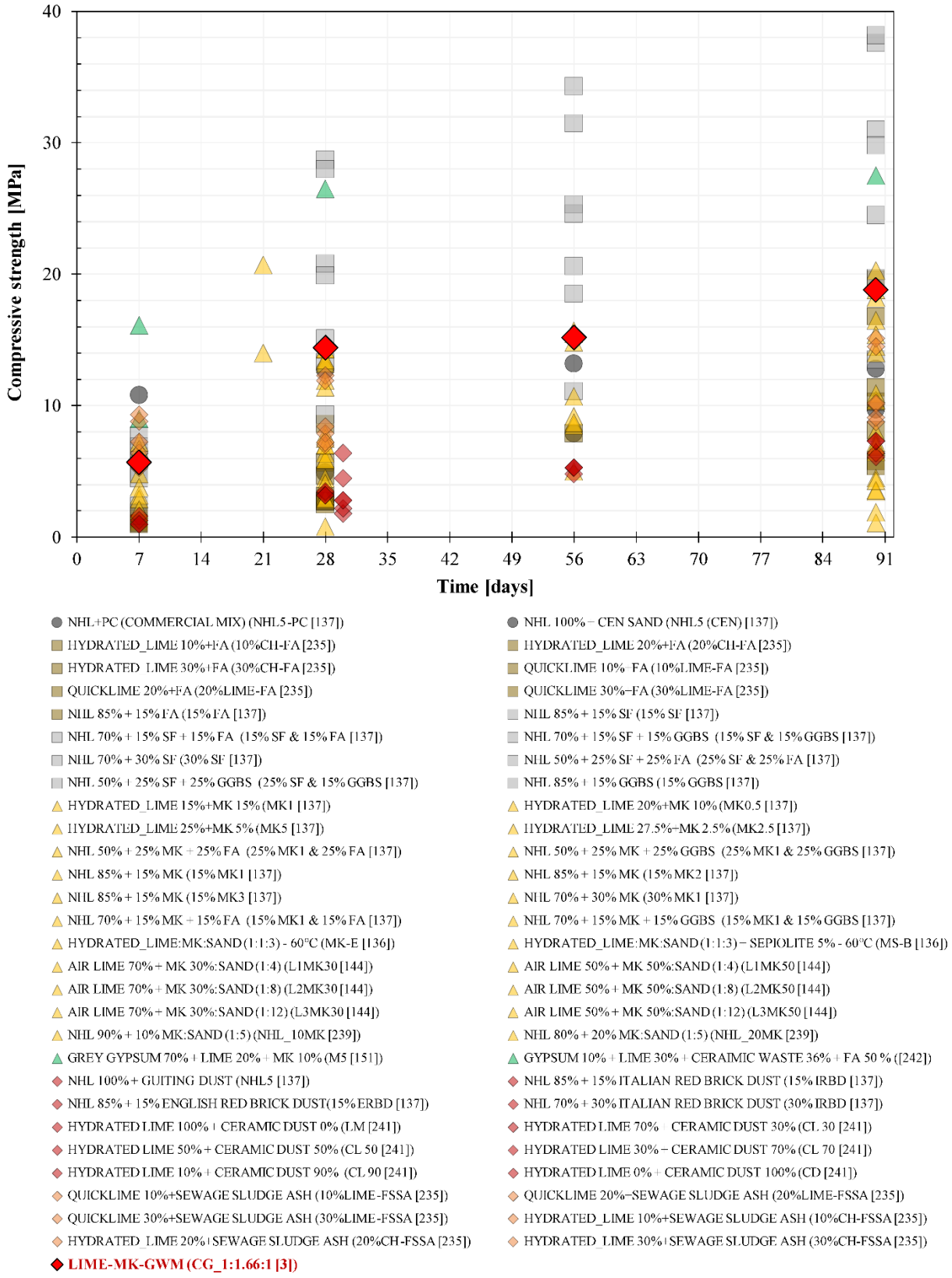

Figure 8.3 *- Classification of the best-performing ternary lime-MK-GWM binder paste [3] in terms of compressive strength compared to selected lime-based pastes from existing works*

Chapter 9 Outlook

The core findings and the framework of approaches applied in this research project have already been the basis for further projects in the field of valorisation of industrial by-products and waste products. Furthermore, although, the results are in line with published results of existing works, additional investigations on different aspects could be useful to further solidify and confirm the outcomes generated within this project. There exist many research trends and ambitious outlooks related to the research topics dealt with in this thesis. Their in-depth explanation and discussion would exceed the scope and the length of this cumulative dissertation, therefore, in the following, a short synopsis of the main outlooks are presented.

Optimization of the developed binders and concretes by adjusting the relevant parameters, the evaluation of long-term behaviour and the durability

The extent of the study on the variability of the relevant parameters of each concept was restricted due to the time-related constraints. For example, the optimal calcination temperature was set at 850°C among the tested temperatures of 550°C, 650°C, 750°C, 850°C and 950°C. However, the real optimum for GWM powder is probably ranged at around 800°C or even lower. This kind of sensitivity analysis must be carried out for all the relevant parameters like calcination temperature, calcination time, mixture proportions, water/binder ratio, etc., for each evaluated concept. The nuances of parameters might be not relevant for laboratory-scale investigations, but surely are

relevant cost-reducing aspects for industrial processes and could be determining factors for the success or failure of the scalability of the different concepts at industrial level. Furthermore, further examinations of the long-term behaviours and the durability of the different concepts need to be carried out to ensure that the GWM-based products fulfil the minimal requirement for cementitious mortars and concretes.

Life cycle assessment analyses on each proposed binder concept

The present research project assumes that the mitigation of the CO_2 emissions is achieved by the calcination process of clayey gravel wash mud, which requires less thermal energy and thus lower energy consumption than for cement clinker production. Although these logical assumptions are majorly supported by the findings from existing studies of similar industrial by-products, a factual verification of these operational and environmental efficiencies could not be carried out within this project. An established method for such a study is the life cycle assessment (LCA) method, which is a very efficient and powerful tool that helps taking decisions by evaluating the environmental impacts of a product while considering each of its life-cycle stages. This comparative environmental assessment, based on international standards, will help to get objectively both the global view as well as the process-related details of the proposed alternative binder concept. A reliable report needs to be generated that quantifies the significant environmental factors like carbon footprint, energy consumption, and the efficiency of the waste management practices to confirm the potential of GWM powder as a durable and eco-friendly raw material.

Create a critical mass of potential industrial wastes or unused by-products

In the Greater Region, there exist several exploitable sources of industrial by-products and wastes that have a great potential to be valorised as in the case of GWM. Partially, based on the fundamentals and the approaches to the promising results and realisations of this project

"CO2REDCEM", the outline of the project program for the proposal of the INTERREG project "CO2REDRES" was established and submitted. The European funding of the transnational project was granted, and the project has officially started since November 2020. In short, this cross-border initiative encourages the promotion of sustainable management (treatment) of secondary industrial resources to reduce the CO_2 emissions of the construction industry. One of the main objectives comprises the generation of a critical mass of potential unused industrial by-products and wastes, originating from quarries and abandoned industrial deposits from the Greater Region, to develop new concepts of energy-efficient and sustainable binder systems.

Transition from laboratory to industrial scale

Finally, the transition of the GWM powder production from laboratory to industrial-scale processes remains one of the main open topics, which require further investigations. It is essential to understand that each upscaling of a single processing step applied at laboratory scale is directly related to major investments in equipment and processing units at an industrial scale. Therefore, the assessment of the conversion of the main processes, namely water separation, drying process, calcination process and the powder production process, into an operational industrial production chain using existing processing technology and minor additional investments, determines the industrial viability of GWM.

List of Figures

CHAPTER 1

CHAPTER 3

CHAPTER 4

CHAPTER 5

CHAPTER 6

CHAPTER 7

CHAPTER 8

List of Tables

CHAPTER 3

CHAPTER 4

CHAPTER 5

CHAPTER 6

CHAPTER 7

Bibliography

[1] V.B. Thapa, D. Waldmann, J.-F. Wagner, A. Lecomte, Assessment of the suitability of gravel wash mud as raw material for the synthesis of an alkali-activated binder, Appl. Clay Sci. 161 (2018) 110–118. doi:10.1016/j.clay.2018.04.025.

[2] V.B. Thapa, D. Waldmann, C. Simon, Gravel wash mud, a quarry waste material as supplementary cementitious material (SCM), Cem. Concr. Res. 124 (2019) 105833. doi:10.1016/j.cemconres.2019.105833.

[3] V.B. Thapa, D. Waldmann, Performance of lime-metakaolin pastes using gravel wash mud (GWM), Cem. Concr. Compos. 114 (2020) 103772. doi:10.1016/j.cemconcomp.2020.103772.

[4] V.B. Thapa, D. Waldmann, Properties of binary blended concrete using gravel wash mud (GWM) powders, (2020).

[5] S. Ghoshal, F. Zeman, Carbon dioxide (CO2) capture and storage technology in the cement and concrete industry, in: Dev. Innov. Carbon Dioxide Capture Storage Technol., Woodhead Publishing Limited, 2010: pp. 469–491. doi:10.1533/9781845699574.5.469.

[6] N. Fonseca, J.D. Brito, L. Evangelista, The influence of curing conditions on the mechanical performance of concrete made with recycled concrete waste, Cem. Concr. Compos. 33 (2011) 637–643. doi:10.1016/j.cemconcomp.2011.04.002.

[7] R. Dhir, K. Paine, T. Dyer, A. Tang, Value-added recycling of domestic, industrial and construction arisings as concrete aggregate, Concr. Eng. Int. Spring (2004) 43–48.

[8] P. Hewlett, M. Liska, Lea's chemistry of cement and concrete, Butterworth-Heinemann, 2019.

[9] S.H. Kosmatka, M.L. Wilson, Design and Control of Concrete Mixtures, 15th ed., Portland

Cement Association, Skokie, Illinois, USA, 2011.

[10] QuarryScapes, The QuarryScapes Project: conservation of ancient stone quarry landscapes in the Eastern Mediterranean, (2017) (currently offline). http://www.quarryscapes.no/text/publications/factsheet5.pdf (accessed February 10, 2017).

[11] J.E. Bond, R. Coursaux, R.L. Worthington, Blending systems and control technologies for cement raw materials, IEEE Ind. Appl. Mag. 6 (2000) 49–59.

[12] Northwestern, Burning in a kiln – formation of cement clinker, (2017) (currently offline). http://iti.northwestern.edu/cement/monograph/Monograph3_4.html (accessed February 19, 2017).

[13] P.J. Jackson, Portland cement: classification and manufacture, in: P.C. Hewlett (Ed.), Lea's Chem. Cem. Concr., 4th ed., Elsevier, 1998.

[14] W. Lerch, The influence of gypsum on the hydration and properties of Portland cement pastes, Portland Cement Association, 1946.

[15] R. Benedix, Bauchemie: Einführung in die Chemie für Bauingenieure, Springer-Verlag, 2006.

[16] H. Le Chatelier, Recherches expérimentales sur la constitution des mortiers hydrauliques, Dunod, 1904.

[17] Verein Deutscher Zementwerke (vdz) e.V., Zement Taschenbuch, Verlag Bau+Technik, 2002.

[18] Portland Cement Association, Types and Causes of Concrete Deterioration, PCA R&D Spec. N. 2617. (2002) 1–16.

[19] S. Jacobsen, J. Marchand, L. Boisvert, Effect of cracking and healing on chloride transport in OPC concrete, Cem. Concr. Res. 26 (1996) 869–881. doi:10.1016/0008-8846(96)00072-5.

[20] J.G. Cabrera, Deterioration of concrete due to reinforcement steel corrosion, Cem. Concr. Compos. 18 (1996) 47–59. doi:10.1016/0958-9465(95)00043-7.

[21] W. Piasta, Analysis of carbonate and sulphate attack on concrete structures, Eng. Fail. Anal. 79 (2017) 606–614. doi:10.1016/j.engfailanal.2017.05.008.

[22] V.B. Thapa, D. Waldmann, A short review on alkali-activated binders and geopolymer binders, in: M. Pahn, C. Thiele, C. Glock (Eds.), Vielfalt Im Massivbau - Festschrift Zum 65. Geburtstag von Prof. Dr. Ing. Jürgen Schnell, Ernst & Sohn, 2018: pp. 576–591.

http://hdl.handle.net/10993/35284.

[23] J. Davidovits, Properties of Geopolymer Cements, First Int. Conf. Alkaline Cem. Concr. (1994) 131–149.

[24] F. Pacheco-Torgal, J. Castro-Gomes, S. Jalali, Alkali-activated binders: A review. Part 1. Historical background, terminology, reaction mechanisms and hydration products, Constr. Build. Mater. 22 (2008) 1305–1314. doi:10.1016/j.conbuildmat.2007.10.015.

[25] D.M. Roy, Alkali activated cements, opportunities and challenges, Cem. Concr. Res. 29 (1999) 249–254.

[26] J.S.J. Van Deventer, J.L. Provis, P. Duxson, D.G. Brice, Chemical Research and Climate Change as Drivers in the Commercial Adoption of Alkali Activated Materials, Waste and Biomass Valorization. 1 (2010) 145–155. doi:10.1007/s12649-010-9015-9.

[27] R. Féret, Slags for the manufacture of cement, Rev. Des Mater. Constr. Trav. Publics. (1939) 1–145.

[28] A. Purdon, The action of alkalis on blast-furnace slag, J. Soc. Chem. Ind. 59 (1940) 191–202.

[29] V.D. Glukhovsky, Soil silicates, Gosstroyizdat Publ. Kiev, USSR. (1959).

[30] J. Davidovits, Synthesis of new high temperature geo-polymers for reinforced plastics/composites, in: SPE PACTFC79, Soc. Plast. Eng., Brookfield Center, USA, 1979: pp. 151–154.

[31] R.F. Heitsmann, M. Fitzgerald, J.L. Sawyer, U.S. Patent No. 4.643.137, 1987.

[32] J. Davidovits, J.L. Sawyer, U.S. Patent No. 4.509.985, EP No.0153097, US4509985A, 1985.

[33] V.D. Glukhovsky, G.S. Rostovskaja, G. V. Rumyna, High strength slag-alkaline cements, in: Proc. Seventh Int. Congr. Chem. Cem. Vol. 3, 1980: pp. 164–8.

[34] A. Palomo, M.W. Grutzeck, M.T. Blanco, Alkali-activated fly ashes: A cement for the future, Cem. Concr. Res. 29 (1999) 1323–1329. doi:10.1016/S0008-8846(98)00243-9.

[35] S. Song, D. Sohn, H.M. Jennings, T.O. Mason, Hydration of alkali-activated ground granulated blast furnace slag, J. Mater. Sci. 35 (2000) 249–257. doi:10.1023/A:1004742027117.

[36] F. Puertas, S. Martinez-Ramirez, S. Alonso, T. Vazquez, Alkali-activated fly ash/slag cement: Strength behaviour and hydration products, Cem. Concr. Res. 30 (2000) 1625–

1632. doi:10.1016/S0008-8846(00)00298-2.

[37] Z. Xie, Y. Xi, Hardening mechanisms of an alkaline-activated class F fly ash, Cem. Concr. Res. 31 (2001) 1245–1249. doi:10.1016/S0008-8846(01)00571-3.

[38] M. Criado, A. Palomo, A. Fernandez-Jimenez, Alkali activation of fly ashes. Part 1: Effect of curing conditions on the carbonation of the reaction products, Fuel. 84 (2005) 2048–2054. doi:10.1016/j.fuel.2005.03.030.

[39] A. Fernández-Jiménez, A. Palomo, Characterisation of fly ashes. Potential reactivity as alkaline cements, Fuel. 82 (2003) 2259–2265. doi:10.1016/S0016-2361(03)00194-7.

[40] J.W. Phair, J.S.J. Van Deventer, Effect of silicate activator pH on the leaching and material characteristics of waste-based inorganic polymers, Miner. Eng. 14 (2001) 289–304. doi:10.1016/S0892-6875(01)00002-4.

[41] Z. Yunsheng, S. Wei, L. Zongjin, Composition design and microstructural characterization of calcined kaolin-based geopolymer cement, Appl. Clay Sci. 47 (2010) 271–275. doi:10.1016/j.clay.2009.11.002.

[42] M. Rowles, B. O'Connor, Chemical optimisation of the compressive strength of aluminosilicate geopolymers synthesised by sodium silicate activation of metakaolinite, J. Ma. 13 (2003) 1161–1165. doi:10.1039/b212629j.

[43] P.J. Schilling, L.G. Butler, A. Roy, H.C. Eaton, 29Si and 27Al MAS-NMR of NaOH-Activated Blast-Furnace Slag, J. Am. Ceram. Soc. 77 (1994) 2363–2368. doi:10.1111/j.1151-2916.1994.tb04606.x.

[44] A. Roy, P.J. Schilling, H.C. Eaton, P.G. Malone, W.N. Brabston, L.D. Wakeley, Activation of ground blast-furnace slag by alkali-metal and alkaline-Earth hydroxides., J. Am. Ceram. Soc. 75 (1992) 3233–3240. doi:10.1111/j.1151-2916.1992.tb04416.x.

[45] J.I. Escalante-García, A. V. Gorokhovsky, G. Mendoza, A.F. Fuentes, Effect of geothermal waste on strength and microstructure of alkali-activated slag cement mortars, Cem. Concr. Res. 33 (2003) 1567–1574. doi:10.1016/S0008-8846(03)00133-9.

[46] I.G. Richardson, A.R. Brough, G.W. Groves, C.M. Dobson, The characterization of hardened alkali-activated blast-furnace slag pastes and the nature of the calcium silicate hydrate (CSH) phase, Cem. Concr. Res. 24 (1994) 813–829. doi:10.1016/0008-8846(94)90002-7.

[47] S.D. Wang, K.L. Scrivener, Hydration products of alkali activated slag cement, Cem. Concr.

Res. 25 (1995) 561–571. doi:10.1016/0008-8846(95)00045-E.

[48] Z. Rajaokarivony-Andriambololona, J.H. Thomassin, P. Baillif, J.C. Touray, Experimental hydration of two synthetic glassy blast furnace slags in water and alkaline solutions (NaOH and KOH 0.1 N) at 40 C: structure, composition and origin of the hydrated layer, J. Mater. Sci. 25 (1990) 2399–2410. doi:10.1007/BF00638034.

[49] C. Shi, X. Wu, M. Tang, Hydration of alkali-slag cements at 150°C, Cem. Concr. Res. 21 (1991) 91–100. doi:10.1016/0008-8846(91)90035-G.

[50] S.D. Wang, P.X. Cheng, K.L. Scrivener, P.L. Pratt, Alkali-activated slag cement and concrete: a review of properties and problems, Adv. Cem. Res. 7 (1995) 93–102. doi:10.1680/adcr.1995.7.27.93.

[51] C. Shi, R.L. Day, A calorimetric study of early hydration of alkali-slag cements, Cem. Concr. Res. 25 (1995) 1333–1346. doi:10.1016/0008-8846(95)00126-W.

[52] J.L. Provis, Geopolymers and other alkali activated materials: why, how, and what?, Mater. Struct. 47 (2014) 11–25. doi:10.1617/s11527-013-0211-5.

[53] J. Davidovits, Gopolymer Cement, Inst. Geopolymer. (2013) 1–11.

[54] Insitut Géopolymère, À propos de la géopolymérisation, (2006). https://www.geopolymer.org/fr/science/a-propos-de-la-geopolymerisation/https://www.geopolymer.org/fr/science/a-propos-de-la-geopolymerisation/ (accessed June 12, 2017).

[55] J.H. Chen, J.S. Huang, Y.W. Chang, A preliminary study of reservoir sludge as a raw material of inorganic polymers, Constr. Build. Mater. 23 (2009) 3264–3269. doi:10.1016/j.conbuildmat.2009.05.006.

[56] F. Pacheco-Torgal, J. Castro-Gomes, S. Jalali, Investigations about the effect of aggregates on strength and microstructure of geopolymeric mine waste mud binders, Cem. Concr. Res. 37 (2007) 933–941. doi:10.1016/j.cemconres.2007.02.006.

[57] A. Poowancum, E. Nimwinya, S. Horpibulsuk, Development of room temperature curing geopolymer from calcined water-treatment-sludge and rice husk ash, in: K. Scrivener, A. Favier (Eds.), Calcined Clays Sustain. Concr., vol 10, RILEM Bookseries, Springer, Dordrecht, 2015: pp. 291–297. doi:10.1007/978-94-017-9939-3_36.

[58] EN 197-1:2011, Cement - Part 1: Composition, specifications and conformity criteria for common cements, European Committee for standardization, 2011.

[59] A. Wardhono, D.W. Law, A. Strano, The strength of alkali-activated slag/fly ash mortar blends at ambient temperature, Procedia Eng. 125 (2015) 650–656. doi:10.1016/j.proeng.2015.11.095.

[60] D.L.Y. Kong, J.G. Sanjayan, K. Sagoe-Crentsil, Comparative performance of geopolymers made with metakaolin and fly ash after exposure to elevated temperatures, Cem. Concr. Res. 37 (2007) 1583–1589. doi:10.1016/j.cemconres.2007.08.021.

[61] Z. Sun, H. Cui, H. An, D. Tao, Y. Xu, J. Zhai, Q. Li, Synthesis and thermal behavior of geopolymer-type material from waste ceramic, Constr. Build. Mater. 49 (2013) 281–287. doi:10.1016/j.conbuildmat.2013.08.063.

[62] ASTM C125-15b, Standard Terminology Relating to Concrete and Concrete Aggregates, ASTM Int. West Conshohocken, PA. (2015) 1–13. doi:10.1520/C0125-15B.2.

[63] I. Odler, Special Inorganic Cements (Modern Concrete Technology Series 8 (E & F.N. Spon)), Taylor & Francis, 2000.

[64] M.C. Gonçalves, F. Margarido, Materials for Construction and Civil Engineering - Science, Processing, and Design, Springer, Cham, 2015. doi:10.1007/978-3-319-08236-3_8.

[65] S.J. Virgalitte, M.D. Luther, J.H. Rose, B. Mather, L.W. Bell, B.A. Ehmke, P. Klieger, D.M. Roy, B.M. Call, R.D. Hooton, D.W. Lewis, M.J. Scali, R.K. Dhir, G.M. Idorn, V.M. Malhotra, ACI 233R-95 - Ground Granulated Blast-Furnace Slag as a Cementitious Constituent in Concrete, ACI Comm. Rep. 95 (2003) 1–18. doi:10.14359/1623.

[66] EN 197-1:2000, Cement - Composition, specifications and conformity criteria for common cements, European Committee for standardization, 2000.

[67] E. Özbay, M. Erdemir, H.I. Durmus, Utilization and efficiency of ground granulated blast furnace slag on concrete properties – A review, Constr. Build. Mater. 105 (2016) 423–434. doi:10.1016/j.conbuildmat.2015.12.153.

[68] F. Massazza, Pozzolana and Pozzolanic Cements, in: P. Hewlett (Ed.), Lea's Chem. Cem. Concr., Elsevier, 1998: pp. 471–631.

[69] M. Ahmaruzzaman, A review on the utilization of fly ash, Prog. Energy Combust. Sci. 36 (2010) 327–363. doi:10.1016/j.pecs.2009.11.003.

[70] R. Davis, A Review of Pozzolanic Materials and Their Use in Concretes, in: T. Stanton, R. Blanks (Eds.), Symp. Use Pozzolanic Mater. Mortars Concr., ASTM International, 1950: pp. 3–15. doi:10.1520/STP39401S.

[71] V.M. Malhotra, P.K. Mehta, Pozzolanic and Cementitious Materials, 1996.

[72] A. Seco, F. Ramirez, L. Miqueleiz, P. Urmeneta, B. Garcia, E. Prieto, V. Oroz, Types of Waste for the Production of Pozzolanic Materials – A Review, in: K.-Y. Show, G. Xinxin (Eds.), Ind. Waste, IntechOpen, Rijeka, 2012: pp. 141–150. doi:10.5772/36285.

[73] P. Fidjestol, R. Lewis, Microsilica as an addition, in: P. Hewlett (Ed.), Lea's Chem. Cem. Concr., 4th ed., Elsevier, 2003: pp. 679–712.

[74] ASTM C618-12a, Standard Specification for Coal Fly Ash and Raw or Calcined Natural Pozzolan for Use in Concrete, ASTM International, 2012.

[75] R. Siddique, M.I. Khan, Supplementary cementing Material, Springer-Verlag Berlin Heidelberg, 2011. doi:10.1007/978-3-642-17866-5.

[76] H. El-Diadamony, A.A. Amer, T.M. Sokkary, S. El-Hoseny, Hydration and characteristics of metakaolin pozzolanic cement pastes, HBRC J. 14 (2016) 150–158. doi:10.1016/j.hbrcj.2015.05.005.

[77] C. Real, M.D. Alcala, J.M. Criado, Preparation of silica from rice husks, J. Am. Ceram. Soc. 79 (1996). doi:10.1111/j.1151-2916.1996.tb08931.x.

[78] V. Della, I. Kuhn, D. Hotza, Rice husk ash as an elemente source for active silicaproduction, Mater. Lett. 57 (2002) 818–821. doi:10.1016/S0167-577X(02)00879-0.

[79] N. Zemke, E. Woods, Rice Husk Ash, California Polytechnic State University, 2009. http://www.cvbt-web.org/uploads/Rice_Husk_Ash/Nick_Emmet_RHA.pdf.

[80] B.B. Sabir, S. Wild, J. Bai, Metakaolin and calcinded clays as pozzolans for concrete: a review, Cem. Concr. Compos. 23 (2001) 441–454. doi:10.1016/S0958-9465(00)00092-5.

[81] A. Shvarzman, K. Kovler, G.S. Grader, G.E. Shter, The effect of dehydroxylation / amorphization degree on pozzolanic activity of kaolinite, 33 (2003) 405–416. doi:10.1016/S0008-8846(02)00975-4.

[82] A. Tironi, F. Cravero, A.N. Scian, E.F. Irassar, Pozzolanic activity of calcined halloysite-rich kaolinitic clays, Appl. Clay Sci. 147 (2017) 11–18. doi:10.1016/j.clay.2017.07.018.

[83] S. Donatello, M. Tyrer, C.R. Cheeseman, Comparison of test methods to assess pozzolanic activity, Cem. Concr. Compos. 32 (2010) 121–127. doi:10.1016/j.cemconcomp.2009.10.008.

[84] A.R. Pourkhorshidi, M. Najimi, T. Parhizkar, F. Jafarpour, B. Hillemeier, Applicability of the standard specifications of ASTM C618 for evaluation of natural pozzolans, Cem. Concr.

Compos. 32 (2010) 794–800. doi:10.1016/j.cemconcomp.2010.08.007.

[85] G.K. Al-chaar, M. Alkadi, D.A. Yaksic, L.A. Kallemeyn, The Use of Natural Pozzolan in Concrete as an Additive or Substitute for Cement Construction Engineering, 2011.

[86] R. Walker, S. Pavía, Physical properties and reactivity of pozzolans, and their influence on the properties of lime-pozzolan pastes, Mater. Struct. 44 (2011) 1139–1150. doi:10.1617/s11527-010-9689-2.

[87] M.M. Tashima, L. Soriano, J. Monzó, M. V. Borrachero, J.L. Akasaki, J. Payá, New method to assess the pozzolanic reactivity of mineral admixtures by means of pH and electrical conductivity measurements in lime:pozzolan suspensions, Mater. Construcción. 64 (2014) e032. doi:10.3989/mc.2014.00914.

[88] R.T. Thorstensen, P. Fidjestol, Inconsistencies in the pozzolanic strength activity index (SAI) for silica fume according to EN and ASTM, Mater. Struct. Constr. 48 (2015) 3979–3990. doi:10.1617/s11527-014-0457-6.

[89] S. Hollanders, R. Adriaens, J. Skibsted, Ö. Cizer, J. Elsen, Pozzolanic reactivity of pure calcined clays, Appl. Clay Sci. 132–133 (2016) 552–560. doi:10.1016/j.clay.2016.08.003.

[90] P. Suraneni, J. Weiss, Examining the pozzolanicity of supplementary cementitious materials using isothermal calorimetry and thermogravimetric analysis, Cem. Concr. Compos. 83 (2017) 273–278. doi:10.1016/j.cemconcomp.2017.07.009.

[91] EN 196-5:2005, Methods of testing cement - Part 5: Pozzolanicity test for pozzolanic cements, European Committee for standardization, 2005.

[92] University of Canterbury, Determination of Total Calcium and Magnesium Ion Concentration, Univ. Canterbury. (2018) 7. http://www.outreach.canterbury.ac.nz/chemistry/documents/calcium.pdf (accessed September 29, 2020).

[93] A. Tironi, M.A. Trezza, A.N. Scian, E.F. Irassar, Assessment of pozzolanic activity of different calcined clays, Cem. Concr. Compos. 37 (2013) 319–327. doi:10.1016/j.cemconcomp.2013.01.002.

[94] J. Qian, J. Qin, Z. Zhang, Y. Shen, Z. Ye, P. Hou, How to evaluate pozzolanic activity of sulfate-rich fly ash, Adv. Cem. Res. 28 (2015) 1–10. doi:10.1680/adcr.15.00027.

[95] M. Frías, E. Villar-Cociña, M.I.S. De Rojas, E. Valencia-Morales, The effect that different pozzolanic activity methods has on the kinetic constants of the pozzolanic reaction in sugar

cane straw-clay ash/lime systems: Application of a kinetic-diffusive model, Cem. Concr. Res. 35 (2005) 2137–2142. doi:10.1016/j.cemconres.2005.07.005.

[96] A. Bahurudeen, M.S. Hemalatha, M. Santhanam, Need of an efficient procedure for the evaluation of pozzolanic performance of supplementary cementitious materials, Indian Concr. J. 90 (2016) 80–92.

[97] W.J. McCarter, D. Tran, Monitoring pozzolanic activity by direct activation with calcium hydroxide, Constr. Build. Mater. 10 (1996) 179–184. doi:10.1016/0950-0618(95)00089-5.

[98] N.Y. Mostafa, P.W. Brown, Heat of hydration of high reactive pozzolans in blended cements: Isothermal conduction calorimetry, Thermochim. Acta. 435 (2005) 162–167. doi:10.1016/j.tca.2005.05.014.

[99] M.I. Sánchez De Rojas, M. Frias, The pozzolanic activity of different materials, its influence on the hydration heat in mortars, Cem. Concr. Res. 26 (1996) 203–213. doi:10.1016/0008-8846(95)00200-6.

[100] N.Y. Mostafa, S.A.S. El-Hemaly, E.I. Al-Wakeel, S.A. El-Korashy, P.W. Brown, Characterization and evaluation of the pozzolanic activity of Egyptian industrial by-products: I: Silica fume and dealuminated kaolin, Cem. Concr. Res. 31 (2001) 467–474. doi:10.1016/S0008-8846(00)00485-3.

[101] DIN EN 196-1:2016-11, Methods of Testing Cement - Part 1: Determination of Strength, European Committee for standardization, 2016.

[102] ASTM C311-05, Standard Test Methods for Sampling and Testing Fly Ash or Natural Pozzolans for Use in Portland-Cement Concrete, 2004. doi:10.1520/C0311-05.

[103] BS 3892-1:1997, Pulverized-fuel ash. Specification for pulverized-fuel ash for use with Portland cement, 1997.

[104] A. Goldman, A. Bentur, The influence of microfillers on enhancement of concrete strength, Cem. Concr. Res. 23 (1993) 962–972. doi:10.1016/0008-8846(93)90050-J.

[105] G.C. Isaia, A.L.G. Gastaldini, R. Moraes, Physical and pozzolanic action of mineral additions on the mechanical strength of high-performance concrete, Cem. Concr. Compos. 25 (2003) 69–76. doi:10.1016/S0958-9465(01)00057-9.

[106] H. Moosberg-Bustnes, B. Lagerblad, E. Forssberg, The function of fillers in concrete, Mater. Struct. Constr. 37 (2004) 74–81. doi:10.1617/13694.

[107] G.C. Cordeiro, R.D. Toledo Filho, L.M. Tavares, E.M.R. Fairbairn, Pozzolanic activity and

filler effect of sugar cane bagasse ash in Portland cement and lime mortars, Cem. Concr. Compos. 30 (2008) 410–418. doi:10.1016/j.cemconcomp.2008.01.001.

[108] C. Jaturapitakkul, J. Tangpagasit, S. Songmue, K. Kiattikomol, Filler effect and pozzolanic reaction of ground palm oil fuel ash, Constr. Build. Mater. 25 (2011) 4287–4293. doi:10.1016/j.conbuildmat.2011.04.073.

[109] W. Kroehong, T. Sinsiri, C. Jaturapitakkul, Effect of palm oil fuel ash fineness on packing effect and pozzolanic reaction of blended cement paste, Procedia Eng. 14 (2011) 361–369. doi:10.1016/j.proeng.2011.07.045.

[110] R. Snellings, G. Mertens, J. Elsen, Supplementary Cementitious Materials, Rev. Mineral. Geochemistry. 74 (2012) 211–278. doi:10.2138/rmg.2012.74.6.

[111] F.P. Glasser, S. Diamond, D.M. Roy, Hydration Reactions in Cement Pastes Incorporating Fly Ash and Other Pozzolanic Materials, in: MRS Proc., 1986: p. 167. doi:10.1557/PROC-85-167.

[112] M.C.G. Juenger, R. Siddique, Recent advances in understanding the role of supplementary cementitious materials in concrete, Cem. Concr. Res. cli (2015) 71–80. doi:10.1016/j.cemconres.2015.03.018.

[113] B. Lothenbach, K. Scrivener, R.D. Hooton, Supplementary cementitious materials, Cem. Concr. Res. 41 (2011) 1244–1256. doi:10.1016/j.cemconres.2010.12.001.

[114] A. Tironi, C.C. Castellano, V. Bonavetti, M.A. Trezza, A.N. Scian, E.F. Irassar, Blended Cements Elaborated with Kaolinitic Calcined Clays, Procedia Mater. Sci. 8 (2015) 211–217. doi:10.1016/j.mspro.2015.04.066.

[115] G. Quercia, A. Lazaro, J.W. Geus, H.J.H. Brouwers, Characterization of morphology and texture of several amorphous nano-silica particles used in concrete, Cem. Concr. Compos. 44 (2013) 77–92. doi:10.1016/j.cemconcomp.2013.05.006.

[116] J. Zhang, Q. Wang, Z. Wang, Optimizing design of high strength cement matrix with supplementary cementitious materials, Constr. Build. Mater. 120 (2016) 123–136. doi:10.1016/j.conbuildmat.2016.05.100.

[117] A. Fernandez, J.L. Garcia Calvo, M.C. Alonso, Ordinary Portland Cement composition for the optimization of the synergies of supplementary cementitious materials of ternary binders in hydration processes, Cem. Concr. Compos. 89 (2018) 238–250. doi:10.1016/j.cemconcomp.2017.12.016.

[118] S.C. Taylor-Lange, E.L. Lamon, K.A. Riding, M.C.G. Juenger, Calcined kaolinite-bentonite clay blends as supplementary cementitious materials, Appl. Clay Sci. 108 (2015) 84–93. doi:10.1016/j.clay.2015.01.025.

[119] K. Abdelli, M. Tahlaiti, R. Belarbi, M.N. Oudjit, Influence of the origin of metakaolin on pozzolanic reactivity of mortars, Energy Procedia. 139 (2017) 230–235. doi:10.1016/j.egypro.2017.11.201.

[120] N. Beuntner, Leistungsfähigkeit großtechnisch calcinierter Tone und deren Wirksamkeit in zementären Systemen, Bochum, 2013.

[121] E. Badogiannis, G. Kakali, S. Tsivilis, Metakaolin as supplementary cementitious material, J. Therm. Anal. Calorim. 81 (2005) 457–462. doi:10.1007/s10973-005-0806-3.

[122] Y. Farnam, B. Zhang, J. Weiss, Evaluating the use of supplementary cementitious materials to mitigate damage in cementitious materials exposed to calcium chloride deicing salt, Cem. Concr. Compos. 81 (2017) 77–86. doi:10.1016/j.cemconcomp.2017.05.003.

[123] E. Vejmelková, M. Keppert, P. Rovnaníková, M. Ondráček, Z. Keršner, R. Černý, Properties of high performance concrete containing fine-ground ceramics as supplementary cementitious material, Cem. Concr. Compos. 34 (2012) 55–61. doi:10.1016/j.cemconcomp.2011.09.018.

[124] M.F.M. Zain, M.N. Islam, F. Mahmud, M. Jamil, Production of rice husk ash for use in concrete as a supplementary cementitious material, Constr. Build. Mater. 25 (2011) 798–805. doi:10.1016/j.conbuildmat.2010.07.003.

[125] R.S. Almenares, L.M. Vizcaíno, S. Damas, A. Mathieu, A. Alujas, F. Martirena, Industrial calcination of kaolinitic clays to make reactive pozzolans, Case Stud. Constr. Mater. 6 (2017) 225–232. doi:10.1016/j.cscm.2017.03.005.

[126] S. Wild, J.M. Khatib, M. O'Farrell, Sulphate resistance of mortar, containing ground brick clay calcined at different temperatures, Cem. Concr. Res. 27 (1997) 697–709. doi:10.1016/S0008-8846(97)00059-8.

[127] R.D. Toledo Filho, J.P. Gonçalves, B.B. Americano, E.M.R. Fairbairn, Potential for use of crushed waste calcined-clay brick as a supplementary cementitious material in Brazil, Cem. Concr. Res. 37 (2007) 1357–1365. doi:10.1016/j.cemconres.2007.06.005.

[128] L.A. Pereira-de-Oliveira, J.P. Castro-Gomes, P.M.S. Santos, The potential pozzolanic activity of glass and red-clay ceramic waste as cement mortars components, Constr. Build.

Mater. 31 (2012) 197–203. doi:10.1016/j.conbuildmat.2011.12.110.

[129] L.R. Steiner, A.M. Bernardin, F. Pelisser, Effectiveness of ceramic tile polishing residues as supplementary cementitious materials for cement mortars, Sustain. Mater. Technol. 4 (2015) 30–35. doi:10.1016/j.susmat.2015.05.001.

[130] Y. Labbaci, B. Labbaci, Y. Abdelaziz, A. Mekkaoui, A. Alouani, The use of the volcanic powders as supplementary cementitious materials for environmental-friendly durable concrete, Constr. Build. Mater. 133 (2017) 468–481. doi:10.1016/j.conbuildmat.2016.12.088.

[131] A. Ababneh, F. Matalkah, Potential use of Jordanian volcanic tuffs as supplementary cementitious materials, Case Stud. Constr. Mater. 8 (2018) 193–202. doi:10.1016/j.cscm.2018.02.004.

[132] S. Seraj, R. Cano, R.D. Ferron, M.C.G. Juenger, The role of particle size on the performance of pumice as a supplementary cementitious material, Cem. Concr. Compos. 80 (2017) 135–142. doi:10.1016/j.cemconcomp.2017.03.009.

[133] W.Y. Kuo, J.S. Huang, T.E. Tan, Organo-modified reservoir sludge as fine aggregates in cement mortars, Constr. Build. Mater. 21 (2007) 609–615. doi:10.1016/j.conbuildmat.2005.12.009.

[134] O. Rodríguez, L. Kacimi, A. López-delgado, M. Frías, A. Guerrero, Characterization of Algerian reservoir sludges for use as active additions in cement : New pozzolans for eco-cement manufacture, 40 (2013) 275–279. doi:10.1016/j.conbuildmat.2012.10.016.

[135] Ł. Kotwica, W. Pichór, E. Kapeluszna, A. Różycka, Utilization of waste expanded perlite as new effective supplementary cementitious material, J. Clean. Prod. 140 (2017) 1344–1352. doi:10.1016/j.jclepro.2016.10.018.

[136] A. Sepulcre-Aguilar, F. Hernández-Olivares, Assessment of phase formation in lime-based mortars with added metakaolin, Portland cement and sepiolite, for grouting of historic masonry, Cem. Concr. Res. 40 (2010) 66–76. doi:10.1016/j.cemconres.2009.08.028.

[137] E. Aggelakopoulou, A. Bakolas, A. Moropoulou, Properties of lime-metakolin mortars for the restoration of historic masonries, Appl. Clay Sci. 53 (2011) 15–19. doi:10.1016/j.clay.2011.04.005.

[138] S. Wild, J.M. Khatib, A. Jones, Relative strength, pozzolanic activity and cement hydration in superplasticised metakaolin concrete, Cem. Concr. Res. 26 (1996) 1537–1544.

doi:10.1016/0008-8846(96)00148-2.

[139] A. Arizzi, G. Cultrone, Aerial lime-based mortars blended with a pozzolanic additive and different admixtures: A mineralogical, textural and physical-mechanical study, Constr. Build. Mater. 31 (2012) 135–143. doi:10.1016/j.conbuildmat.2011.12.069.

[140] E. Vejmelková, M. Keppert, Z. Keršner, P. Rovnaníková, R. Černý, Mechanical, fracture-mechanical, hydric, thermal, and durability properties of lime-metakaolin plasters for renovation of historical buildings, Constr. Build. Mater. 31 (2012) 22–28. doi:10.1016/j.conbuildmat.2011.12.084.

[141] V. Nezerka, Microstructure, Chemical Processes and Experimental Investigation of Lime-Based Mortars, (2012) 26.

[142] A.L. Gameiro, A.S. Silva, M. do R. Veiga, A.L. Velosa, Lime-metakaolin hydration products: A microscopy analysis, Mater. Technol. 46 (2012) 145–148.

[143] A. Gameiro, A. Santos Silva, R. Veiga, A. Velosa, Hydration products of lime-metakaolin pastes at ambient temperature with ageing, Thermochim. Acta. 535 (2012) 36–41. doi:10.1016/j.tca.2012.02.013.

[144] A. Gameiro, A. Santos Silva, P. Faria, J. Grilo, T. Branco, R. Veiga, A. Velosa, Physical and chemical assessment of lime-metakaolin mortars: Influence of binder:aggregate ratio, Cem. Concr. Compos. 45 (2014) 264–271. doi:10.1016/j.cemconcomp.2013.06.010.

[145] A.S. Silva, A. Gameiro, J. Grilo, R. Veiga, A. Velosa, Long-term behavior of lime-metakaolin pastes at ambient temperature and humid curing condition, Appl. Clay Sci. 88–89 (2014) 49–55. doi:10.1016/j.clay.2013.12.016.

[146] J. Cabrera, M.F. Rojas, Mechanism of hydration of the metakaolin-lime-water system, Cem. Concr. Res. 31 (2001) 177–182. doi:10.1016/S0008-8846(00)00456-7.

[147] M.F. Rojas, J. Cabrera, The effect of temperature on the hydration rate and stability of the hydration phases of metakaolin-lime-water systems, Cem. Concr. Res. 32 (2002) 133–138. doi:10.1016/S0008-8846(01)00642-1.

[148] A. Bakolas, E. Aggelakopoulou, A. Moropoulou, S. Anagnostopoulou, Evaluation of pozzolanic activity and physicomechanical characteristics in metakaolin-lime pastes, J. Therm. Anal. Calorim. 84 (2006) 157–163. doi:10.1007/s10973-005-7262-y.

[149] S. Andrejkovičová, A.L. Velosa, F. Rocha, Air lime-metakaolin-sepiolite mortars for earth based walls, Constr. Build. Mater. 44 (2013) 133–141.

doi:10.1016/j.conbuildmat.2013.03.008.

[150] S. Andrejkovičová, A.L. Velosa, E. Ferraz, F. Rocha, Influence of clay minerals addition on mechanical properties of air lime-metakaolin mortars, Constr. Build. Mater. 65 (2014) 132–139. doi:10.1016/j.conbuildmat.2014.04.118.

[151] A. Vimmrová, M. Keppert, O. Michalko, R. Černý, Calcined gypsum-lime-metakaolin binders: Design of optimal composition, Cem. Concr. Compos. 52 (2014) 91–96. doi:10.1016/j.cemconcomp.2014.05.011.

[152] G. Matias, P. Faria, I. Torres, Lime mortars with heat-treated clays and ceramic waste: A review, Constr. Build. Mater. 73 (2014) 125–136. doi:10.1016/j.conbuildmat.2014.09.028.

[153] Geology Luxembourg, Overview of the geology of Luxembourg, Geol. - Portail Luxemb. Des Sci. La Terre. (2009). http://www.geology.lu/index.php/geologie-du-luxembourg/apercu-geologique/10-overview-of-the-geology-of-luxembourg (accessed September 16, 2020).

[154] Geology Luxembourg, Carte géologique en ligne, Geol. - Portail Luxemb. Des Sci. La Terre. (2020). http://www.geologie.lu/index.php/geologie-du-luxembourg/carte-geologique (accessed September 16, 2020).

[155] Geoportail.lu, Geoportail Luxembourg, (2020). https://map.geoportail.lu (accessed September 16, 2020).

[156] A.R. Mora, The effect of alkali-activated binder on clay-silt (PS<20μm) from gravel wash mud, University of Trier, 2018.

[157] AASHTO T11, Standard Method of Test for Materials Finer Than 75-μm (No. 200) Sieve in Mineral Aggregates by Washing, American Association of State Highway and Transportation Officials, 2005.

[158] A. Thomé, Das Konzept der Geosynthese und Anwendung ausgewahlter Syntheseparameter auf einen Kieswascheschlamm im Laborversuch zur Eruierung seines Potenzials zur Geopolymerisation, University of Trier, 2008.

[159] D.W.Y. Cardenas, Alternative low CO_2 cement through substitution of clinker by a waste product from gravel mining, University of Trier, 2016.

[160] P. Friedlingstein, R.M. Andrew, J. Rogelj, G.P. Peters, J.G. Canadell, R. Knutti, G. Luderer, M.R. Raupach, M. Schaeffer, D.P. Van Vuuren, C. Le Quéré, Persistent growth of CO2 emissions and implications for reaching climate targets, Nat. Geosci. 7 (2014) 709–715.

doi:10.1038/NGEO2248.

[161] D. García-Gusano, H. Cabal, Y. Lechón, Long-term behaviour of CO2 emissions from cement production in Spain: Scenario analysis using an energy optimisation model, J. Clean. Prod. 99 (2015) 101–111. doi:10.1016/j.jclepro.2015.03.027.

[162] Z. Liu, D. Guan, W. Wei, S.J. Davis, P. Ciais, J. Bai, S. Peng, Q. Zhang, K. Hubacek, G. Marland, R.J. Andres, D. Crawford-Brown, J. Lin, H. Zhao, C. Hong, T.A. Boden, K. Feng, G.P. Peters, F. Xi, J. Liu, Y. Li, Y. Zhao, N. Zeng, K. He, Reduced carbon emission estimates from fossil fuel combustion and cement production in China, Nature. 524 (2015) 335–338. doi:10.1038/nature14677.

[163] D.A. Salas, A.D. Ramirez, C.R. Rodríguez, D.M. Petroche, A.J. Boero, J. Duque-Rivera, Environmental impacts, life cycle assessment and potential improvement measures for cement production: A literature review, J. Clean. Prod. 113 (2016) 114–122. doi:10.1016/j.jclepro.2015.11.078.

[164] C. Shi, A.F. Jiménez, A. Palomo, New cements for the 21st century: The pursuit of an alternative to Portland cement, Cem. Concr. Res. 41 (2011) 750–763. doi:10.1016/j.cemconres.2011.03.016.

[165] J. Davidovits, D.C. Comrie, J.H. Paterson, D.J. Ritcey, Geopolymeric concretes for environmental protection, Concr. Int. 12 (1990) 30–40.

[166] J.L. Provis, J.S.J. van Deventer, Geopolymers: Structures, Processing, Properties and Industrial Applications, Elsevier, 2009.

[167] F. Pacheco-Torgal, Z. Abdollahnejad, A.F. Camões, M. Jamshidi, Y. Ding, Durability of alkali-activated binders: A clear advantage over Portland cement or an unproven issue?, Constr. Build. Mater. 30 (2012) 400–405. doi:10.1016/j.conbuildmat.2011.12.017.

[168] A.M. Aguirre-Guerrero, R.A. Robayo-Salazar, R.M. de Gutiérrez, A novel geopolymer application: Coatings to protect reinforced concrete against corrosion, Appl. Clay Sci. 135 (2017) 437–446. doi:10.1016/j.clay.2016.10.029.

[169] G. Le Saoût, V. Kocaba, K. Scrivener, Application of the Rietveld method to the analysis of anhydrous cement, Cem. Concr. Res. 41 (2011) 133–148. doi:10.1016/j.cemconres.2010.10.003.

[170] J.L. Provis, Alkali-activated materials, Cem. Concr. Res. 114 (2018) 40–48. doi:10.1016/j.cemconres.2017.02.009.

[171] J.L. Provis, A. Palomo, C. Shi, Advances in understanding alkali-activated materials, Cem. Concr. Res. 78 (2015) 110–125. doi:10.1016/j.cemconres.2015.04.013.

[172] R.J. Myers, S.A. Bernal, J.L. Provis, Phase diagrams for alkali-activated slag binders, Cem. Concr. Res. 95 (2017) 30–38. doi:10.1016/j.cemconres.2017.02.006.

[173] K. Wianglor, S. Sinthupinyo, M. Piyaworapaiboon, A. Chaipanich, Effect of alkali-activated metakaolin cement on compressive strength of mortars, Appl. Clay Sci. 141 (2017) 272–279. doi:10.1016/j.clay.2017.01.025.

[174] S.D. Wang, K.L. Scrivener, P.L. Pratt, Factors affecting the strength of alkali-activated slag, Cem. Concr. Res. 24 (1994) 1033–1043. doi:10.1016/0008-8846(94)90026-4.

[175] C. Ferone, F. Colangelo, R. Cioffi, F. Montagnaro, L. Santoro, Use of reservoir clay sediments as raw materials for geopolymer binders, Adv. Appl. Ceram. 112 (2013) 184–189. doi:10.1179/1743676112Y.0000000064.

[176] B. Molino, A. De Vincenzo, C. Ferone, F. Messina, F. Colangelo, R. Cioffi, Recycling of clay sediments for geopolymer binder production. A new perspective for reservoir management in the framework of Italian Legislation: The Occhito reservoir case study, Materials (Basel). 7 (2014) 5603–5616. doi:10.3390/ma7085603.

[177] F. Messina, C. Ferone, A. Molino, G. Roviello, F. Colangelo, B. Molino, R. Cioffi, Synergistic recycling of calcined clayey sediments and water potabilization sludge as geopolymer precursors: Upscaling from binders to precast paving cement-free bricks, Constr. Build. Mater. 133 (2017) 14–26. doi:10.1016/j.conbuildmat.2016.12.039.

[178] V. Balek, M. Murat, The emanation thermal analysis of kaolinite clay minerals, Thermochim. Acta. 282–283 (1996) 385–397. doi:10.1016/0040-6031(96)02886-9.

[179] A. Buchwald, M. Hohmann, K. Posern, E. Brendler, The suitability of thermally activated illite/smectite clay as raw material for geopolymer binders, Appl. Clay Sci. 46 (2009) 300–304. doi:10.1016/j.clay.2009.08.026.

[180] A. Buchwald, M. Vicent, R. Kriegel, C. Kaps, M. Monzó, A. Barba, Geopolymeric binders with different fine fillers - Phase transformations at high temperatures, Appl. Clay Sci. 46 (2009) 190–195. doi:10.1016/j.clay.2009.08.002.

[181] M.C. Bignozzi, S. Manzi, I. Lancellotti, E. Kamseu, L. Barbieri, C. Leonelli, Mix-design and characterization of alkali activated materials based on metakaolin and ladle slag, Appl. Clay Sci. 73 (2013) 78–85. doi:10.1016/j.clay.2012.09.015.

[182] E. Gartner, H. Hirao, A review of alternative approaches to the reduction of CO2 emissions associated with the manufacture of the binder phase in concrete, Cem. Concr. Res. 78 (2015) 126–142. doi:10.1016/j.cemconres.2015.04.012.

[183] J.-F. Wagner, Paläogeographische Entwicklung der triadischen Randfazies Luxemburgs, Zeitschrift Der Dtsch. Geol. Gesellschaft. Band 140 (1989) 311–331. doi:10.1127/zdgg/140/1989/311.

[184] M. Lucius, Erläuterungen zur geologischen Karte Luxemburgs - Das Gutland, Publ. Du Serv. Géologique Luxemb. Luxemb. (1948).

[185] M. Lucius, Geologie Luxemburgs: Erläuterungen zu der geologischen Spezialkarte Luxemburgs - Das Oesling, Publ. Du Serv. Géologique Luxemb. Luxemb. (1950).

[186] J.M. Cowley, Diffraction physics, Third edit, Elsevier Science B.V., 1995. doi:10.1016/B978-0-444-82218-5.X5000-7.

[187] F.O. Aramide, Effects of sintering temperature on the phase developments and mechanical properties ifon clay. Leonardo Journal of Sciences 2015;26:67-82., Leonardo J. Sci. (2015) 67–82.

[188] S. Brunauer, P.H. Emmett, E. Teller, Adsorption of Gases in Multimolecular Layers, J. Am. Chem. Soc. 60 (1938) 309–319. http://pubs.acs.org/doi/abs/10.1021/ja01269a023.

[189] M. Paul, D. Ag, W. Dyckerhoff, Application of the Rietveld method in the cement industry, (2005) 1–3.

[190] B.B. Kenne Diffo, A. Elimbi, M. Cyr, J. Dika Manga, H. Tchakoute Kouamo, Effect of the rate of calcination of kaolin on the properties of metakaolin-based geopolymers, J. Asian Ceram. Soc. 3 (2015) 130–138.

[191] H.K. Tchakoute, C.H. Rüscher, J.N.Y. Djobo, B.B.D. Kenne, D. Njopwouo, Influence of gibbsite and quartz in kaolin on the properties of metakaolin-based geopolymer cements, Appl. Clay Sci. 107 (2015) 188–194. doi:10.1016/j.clay.2015.01.023.

[192] J. Ke, M. Mcneil, L. Price, N.Z. Khanna, N. Zhou, Estimation of CO2 emissions from China's cement production: Methodologies and uncertainties, 57 (2013) 172–181. doi:10.1016/j.enpol.2013.01.028.

[193] E. Benhelal, G. Zahedi, E. Shamsaei, A. Bahadori, Global strategies and potentials to curb CO2 emissions in cement industry, J. Clean. Prod. 51 (2013) 142–161. doi:10.1016/j.jclepro.2012.10.049.

[194] W. Shen, L. Cao, Q. Li, W. Zhang, G. Wang, Quantifying CO2 emissions from China's cement industry, Renew. Sustain. Energy Rev. 50 (2015) 1004–1012. doi:10.1016/j.rser.2015.05.031.

[195] N. Li, D. Ma, W. Chen, Projection of cement demand and analysis of the impacts of carbon tax on cement industry in China, Energy Procedia. 75 (2015) 1766–1771. doi:10.1016/j.egypro.2015.07.457.

[196] Y. Cancio, U. Heierli, A.R. Favier, R.S. Machado, K.L. Scrivener, J. Fernando, M. Hernández, G. Habert, Limestone calcined clay cement as a low-carbon solution to meet expanding cement demand in emerging economies, 2 (2017) 82–91. doi:10.1016/j.deveng.2017.06.001.

[197] K. Scrivener, F. Martirena, S. Bishnoi, S. Maity, Calcined clay limestone cements (LC3), Cem. Concr. Res. 114 (2017) 49–56. doi:10.1016/j.cemconres.2017.08.017.

[198] F. Avet, K. Scrivener, Investigation of the calcined kaolinite content on the hydration of Limestone Calcined Clay Cement (LC3), Cem. Concr. Res. 107 (2018) 124–135. doi:10.1016/j.cemconres.2018.02.016.

[199] K.L. Scrivener, V.M. John, E.M. Gartner, Eco-efficient cements: Potential economically viable solutions for a low-CO2cement-based materials industry, Cem. Concr. Res. 114 (2018) 2–26. doi:10.1016/j.cemconres.2018.03.015.

[200] H. Yanguatin, J. Tobón, J. Ramírez, Pozzolanic reactivity of kaolin clays , a review, Rev. Ing. Construcción. 32 (2017) 13–24. doi:10.4067/S0718-50732017000200002.

[201] F. Avet, X. Li, K. Scrivener, Determination of the amount of reacted metakaolin in calcined clay blends, Cem. Concr. Res. 106 (2018) 40–48. doi:10.1016/j.cemconres.2018.01.009.

[202] E. John, T. Matschei, D. Stephan, Cement and Concrete Research Nucleation seeding with calcium silicate hydrate – A review, Cem. Concr. Res. 113 (2018) 74–85. doi:10.1016/j.cemconres.2018.07.003.

[203] T. Oey, A. Kumar, J.W. Bullard, N. Neithalath, G. Sant, The Filler Effect : The Influence of Filler Content and Surface Area on Cementitious Reaction Rates, 14th Int. Congr. Chem. Cem. (2015) 1–33.

[204] J. Tangpagasit, R. Cheerarot, C. Jaturapitakkul, K. Kiattikomol, Packing effect and pozzolanic reaction of fly ash in mortar, Cem. Concr. Res. 35 (2005) 1145–1151. doi:10.1016/j.cemconres.2004.09.030.

[205] I. Mehdipour, A. Kumar, K.H. Khayat, Rheology, hydration, and strength evolution of interground limestone cement containing PCE dispersant and high volume supplementary cementitious materials, Mater. Des. 127 (2017) 54–66. doi:10.1016/j.matdes.2017.04.061.

[206] K. De Weerdt, M. Ben Haha, G. Le Saout, K.O. Kjellsen, H. Justnes, B. Lothenbach, Hydration mechanisms of ternary Portland cements containing limestone powder and fly ash, Cem. Concr. Res. 41 (2011) 279–291. doi:10.1016/j.cemconres.2010.11.014.

[207] D. Zhou, R. Wang, M. Tyrer, H. Wong, C. Cheeseman, Sustainable infrastructure development through use of calcined excavated waste clay as a supplementary cementitious material, J. Clean. Prod. 168 (2017) 1180–1192. doi:10.1016/j.jclepro.2017.09.098.

[208] E. Aprianti S, A huge number of artificial waste material can be supplementary cementitious material (SCM) for concrete production – a review part II, J. Clean. Prod. 142 (2017) 4178–4194. doi:10.1016/j.jclepro.2015.12.115.

[209] E. Aprianti, P. Shafigh, S. Bahri, J.N. Farahani, Supplementary cementitious materials origin from agricultural wastes - A review, Constr. Build. Mater. 74 (2015) 176–187. doi:10.1016/j.conbuildmat.2014.10.010.

[210] J.M. Paris, J.G. Roessler, C.C. Ferraro, H.D. Deford, T.G. Townsend, A review of waste products utilized as supplements to Portland cement in concrete, J. Clean. Prod. 121 (2016) 1–18. doi:10.1016/j.jclepro.2016.02.013.

[211] G. Quercia, J.J.G. Van Der Putten, G. Hüsken, H.J.H. Brouwers, Photovoltaic's silica-rich waste sludge as supplementary cementitious material (SCM), Cem. Concr. Res. 54 (2013) 161–179. doi:10.1016/j.cemconres.2013.08.010.

[212] P.F.G. Banfill, Alternative materials for concrete- Mersey silt as fine aggregate, Build. Environ. 15 (1980) 181–190. doi:10.1016/0360-1323(80)90035-9.

[213] R.W. Cheary, A.A. Coelho, J.P. Cline, Fundamental parameters line profile fitting in laboratory diffractometers, 109 (2004) 1–25. doi:10.6028/jres.002.

[214] H.M. Rietveld, A profile refinement method for nuclear and magnetic structures, J. Appl. Crystallogr. 2 (1969) 65–71. doi:10.1107/S0021889869006558.

[215] M. Paul, Quality control of autoclaved aerated concrete by means of X-ray diffraction, (2018) 111–116. doi:10.1002/cepa.894.

[216] A.H. De Aza, A.G. De La Torre, M.A.G. Aranda, F.J. Valle, S. De Aza, Rietveld Quantitative Analysis of Buen Retiro Porcelains, 87 (2004) 449–454.

doi:doi/abs/10.1111/j.1551-2916.2004.00449.x.

[217] Y. Liu, S. Lei, M. Lin, Y. Li, Z. Ye, Y. Fan, Assessment of pozzolanic activity of calcined coal-series kaolin, Appl. Clay Sci. 143 (2017) 159–167. doi:10.1016/j.clay.2017.03.038.

[218] C. Jaturapitakkul, K. Kiattikomol, S. Songpiriyakij, A Study of Strength Activity Index of Ground Coarse Fly Ash with Portland Cement, Sci. Asia. 25 (1999) 223–229.

[219] Y. Shao, T. Lefort, S. Moras, D. Rodriguez, Studies on concrete containing ground waste glass, Cem. Concr. Res. 30 (2000) 91–100. doi:10.1016/S0008-8846(99)00213-6.

[220] C. Shi, Y. Wu, C. Riefler, H. Wang, Characteristics and pozzolanic reactivity of glass powders, Cem. Concr. Res. 35 (2005) 987–993. doi:10.1016/j.cemconres.2004.05.015.

[221] D.P. Bentz, A. Durán-Herrera, D. Galvez-Moreno, Comparison of ASTM C311 Strength Activity Index Testing versus Testing Based on Constant Volumetric Proportions, J. ASTM Int. 9 (2012) 104138. doi:10.1520/JAI104138.

[222] A. Tironi, M.A. Trezza, A.N. Scian, E.F. Irassar, Kaolinitic calcined clays: Factors affecting its performance as pozzolans, Constr. Build. Mater. 28 (2012) 276–281. doi:10.1016/j.conbuildmat.2011.08.064.

[223] R.L. Coble, Effects of particle-size distribution in initial-stage sintering, J. Am. Ceram. Soc. 56 (1973) 461–466.

[224] V.-G. Lee, T.-H. Yeh, Sintering effects on the development of mechanical properties of fired clay ceramics, Mater. Sci. Eng. A. 485 (2008) 5–13.

[225] B. Wunderlich, Thermal analysis of polymeric materials, Springer Science & Business Media, 2005. doi:10.1520/C0618-12A.

[226] R.C. Mielenz, N.C. Schieltz, M.E. King, Thermogravimetric analysis of clay and clay-like minerals, Clay Clay Miner. (1953) 285–314.

[227] S. Ferreiro, M.M.C. Canut, J. Lund, D. Herfort, Influence of fineness of raw clay and calcination temperature on the performance of calcined clay-limestone blended cements, Appl. Clay Sci. 169 (2019) 81–90. doi:10.1016/J.CLAY.2018.12.021.

[228] M. Gimenez, CO2 uses in the cement industry, Carbon Capture Util. Storage - SETIS. (2016) 34–35. doi:10.1007/978-3-030-30908-4_5.

[229] R.M. Andrew, Global CO2 emissions from cement production, Earth Syst. Sci. Data. 10 (2018) 195–217. doi:10.5194/essd-10-195-2018.

[230] R.M. Andrew, Global CO2 emissions from cement production , 1928 – 2017, Earth Syst.

Sci. Data. 10 (2018) 2213–2239. doi:10.5194/essd-10-2213-2018.

[231] Ecofys, Methodology for the free allocation of emission allowances in the EU ETS post 2012 - Sector report for the lime industry, 2009. https://ec.europa.eu/clima/sites/clima/files/ets/allowances/docs/bm_study-lime_en.pdf.

[232] WBCSD Cement Sustainability Initiative, Getting the Numbers Right - GCCA in NumbeRs, GNR Proj. Report. CO2. (2017). https://www.wbcsdcement.org/index.html (accessed April 3, 2020).

[233] S. Ferreiro, D. Herfort, J.S. Damtoft, Effect of raw clay type, fineness, water-to-cement ratio and fly ash addition on workability and strength performance of calcined clay – Limestone Portland cements, Cem. Concr. Res. 101 (2017) 1–12. doi:10.1016/j.cemconres.2017.08.003.

[234] S. Samad, A. Shah, Role of binary cement including Supplementary Cementitious Material (SCM), in production of environmentally sustainable concrete: A critical review, Int. J. Sustain. Built Environ. 6 (2017) 663–674. doi:10.1016/j.ijsbe.2017.07.003.

[235] Y. Zhou, J. Li, J. xin Lu, C. Cheeseman, C.S. Poon, Sewage sludge ash: A comparative evaluation with fly ash for potential use as lime-pozzolan binders, Constr. Build. Mater. 242 (2020) 118160. doi:10.1016/j.conbuildmat.2020.118160.

[236] R.L. Day, C. Shi, Influence of the fineness of pozzolan on the strength of lime natural-pozzolan cement pastes, Cem. Concr. Res. 24 (1994) 1485–1491. doi:10.1016/0008-8846(94)90162-7.

[237] E.R. Grist, K.A. Paine, A. Heath, J. Norman, H. Pinder, Compressive strength development of binary and ternary lime-pozzolan mortars, Mater. Des. 52 (2013) 514–523. doi:10.1016/j.matdes.2013.05.006.

[238] B.A. Silva, A.P. Ferreira Pinto, A. Gomes, Natural hydraulic lime versus cement for blended lime mortars for restoration works, Constr. Build. Mater. 94 (2015) 346–360. doi:10.1016/j.conbuildmat.2015.06.058.

[239] J. Grilo, A. Santos Silva, P. Faria, A. Gameiro, R. Veiga, A. Velosa, Mechanical and mineralogical properties of natural hydraulic lime-metakaolin mortars in different curing conditions, Constr. Build. Mater. 51 (2014) 287–294. doi:10.1016/j.conbuildmat.2013.10.045.

[240] G. Matias, P. Faria, I. Torres, Lime mortars with ceramic wastes: Characterization of

components and their influence on the mechanical behaviour, Constr. Build. Mater. 73 (2014) 523–534. doi:10.1016/j.conbuildmat.2014.09.108.

[241] M. Jerman, V. Tydlitát, M. Keppert, M. Čáchová, R. Černý, Characterization of early-age hydration processes in lime-ceramic binders using isothermal calorimetry, X-ray diffraction and scanning electron microscopy, Thermochim. Acta. 633 (2016) 108–115. doi:10.1016/j.tca.2016.04.005.

[242] M.S. Morsy, A.M. Rashad, H. Shoukry, M.M. Mokhtar, S.A. El-Khodary, Development of lime-pozzolan green binder: The influence of anhydrous gypsum and high ambient temperature curing, J. Build. Eng. 28 (2020) 101026. doi:10.1016/j.jobe.2019.101026.

[243] R.M.H. Lawrence, T.J. Mays, P. Walker, D. D'Ayala, Determination of carbonation profiles in non-hydraulic lime mortars using thermogravimetric analysis, Thermochim. Acta. 444 (2006) 179–189. doi:10.1016/j.tca.2006.03.002.

[244] J. Lanas, J.L.P. Bernal, M.A. Bello, J.I.A. Galindo, Mechanical properties of natural hydraulic lime-based mortars, Cem. Concr. Res. 34 (2004) 2191–2201. doi:10.1016/j.cemconres.2004.02.005.

[245] EN 459-1:2010, Building lime - Part 1: Definitions, specifications and conformity criteria, European Committee for standardization, 2010.

[246] NF P18-513:2012-08-01, Addition for concrete - Metakaolin - Specifications and conformity criteria, AFNOR, 2012.

[247] H.M. Rietveld, The Rietveld Method : a retrospection, 225 (2010) 545–547. doi:10.1524/zkri.2010.1356.

[248] M. Erans, S.A. Nabavi, V. Manović, Carbonation of lime-based materials under ambient conditions for direct air capture, J. Clean. Prod. 242 (2020). doi:10.1016/j.jclepro.2019.118330.

[249] K. Suzuki, T. Nishikawa, S. Ito, Formation and carbonation of C-S-H in water, Cem. Concr. Res. 15 (1985) 213–224. doi:10.1016/0008-8846(85)90032-8.

[250] P.A. Slegers, P.G. Rouxhet, Carbonation of the hydration products of tricalcium silicate, Cem. Concr. Res. 6 (1976) 381–388. doi:10.1016/0008-8846(76)90101-0.

[251] K. Kobayashi, K. Suzuki, Y. Uno, Carbonation of concrete structures and decomposition of CSH, Cem. Concr. Res. 24 (1994) 55–61. doi:10.1016/0008-8846(94)90082-5.

[252] H. Ye, A. Radlińska, J. Neves, Drying and carbonation shrinkage of cement paste containing

alkalis, Mater. Struct. Constr. 50 (2017). doi:10.1617/s11527-017-1006-x.

[253] E.G. Swenson, P.J. Sereda, Mechanism of the carbonatation shrinkage of lime and hydrated cement, J. Appl. Chem. 18 (2007) 111–117. doi:10.1002/jctb.5010180404.

[254] S. Diamond, The microstructure of cement paste and concrete - A visual primer, Cem. Concr. Compos. 26 (2004) 919–933. doi:10.1016/j.cemconcomp.2004.02.028.

[255] M.J. Purton, Comparison of the binding properties of hydrated lime and cement in brick manufacture, J. Appl. Chem. 20 (1970) 293–299. doi:10.1002/jctb.5010200907.

[256] International Energy Agency (IEA), Technology Roadmap - Low-Carbon Transition in the Cement Industry, 2018. https://www.iea.org/reports/technology-roadmap-low-carbon-transition-in-the-cement-industry.

[257] International Energy Agency (IEA), Cement, IEA, Paris. (2020). https://www.iea.org/reports/cement (accessed August 30, 2020).

[258] US Geological Survey, Cement Production Globally and in The U.S. from 2010 to 2019 (in Million Metric Tons), Stat. Inc. (2020). https://www-statista-com.proxy.bnl.lu/statistics/219343/cement-production-worldwide/ (accessed August 30, 2020).

[259] Global Cement Magazine, Cement production worldwide from 1995 to 2019 (in billion tons), Stat. Inc. (2019). https://www-statista-com.proxy.bnl.lu/statistics/1087115/global-cement-production-volume/ (accessed August 30, 2020).

[260] F. Pacheco-Torgal, S. Jalali, J. Labrincha, V.M. John, Eco-efficient concrete, Woodhead Publishing Limited, 2013.

[261] M. Thomas, Supplementary Cementing Materials in Concrete, CRC Press - Taylor & Francis Group, 2013.

[262] NF EN 206/CN, Concrete - Specification, performance, production and conformity - National addition to the standard NF EN 206, AFNOR, 2014.

[263] Z. Shi, M.R. Geiker, K. De Weerdt, B. Lothenbach, J. Kaufmann, W. Kunther, S. Ferreiro, D. Herfort, J. Skibsted, Durability of portland cement blends including calcined clay and limestone: Interactions with sulfate, chloride and carbonate ions, RILEM Bookseries. 10 (2015) 133–141. doi:10.1007/978-94-017-9939-3_17.

[264] W. Huang, H. Kazemi-Kamyab, W. Sun, K. Scrivener, Effect of replacement of silica fume with calcined clay on the hydration and microstructural development of eco-UHPFRC,

Mater. Des. 121 (2017) 36–46. doi:10.1016/j.matdes.2017.02.052.

[265] K. Scrivener, Calcined Clays for Sustainable Concrete, 2018. doi:10.1007/978-94-024-1207-9.

[266] R. Gmür, K.C. Thienel, N. Beuntner, Influence of aging conditions upon the properties of calcined clay and its performance as supplementary cementitious material, Cem. Concr. Compos. 72 (2016) 114–124. doi:10.1016/j.cemconcomp.2016.05.020.

[267] P. He, M. Wang, S. Fu, D. Jia, S. Yan, J. Yuan, J. Xu, P. Wang, Y. Zhou, Effects of Si/Al ratio on the structure and properties of metakaolin based geopolymer, Ceram. Int. 42 (2016) 14416–14422. doi:10.1016/j.ceramint.2016.06.033.

[268] D. Nied, M. Zajac, M. Ben Haha, C. Stabler, Assessing the Synergistic Effect Between Limestone and Metakaolin and Novel Methodology to Assess the Reactivity of Calcined Clays Composite Cements based on Limestone and Metakaolin, (2015).

[269] F. Avet, E. Boehm-Courjault, K. Scrivener, Investigation of C-A-S-H composition, morphology and density in Limestone Calcined Clay Cement (LC3), Cem. Concr. Res. 115 (2019) 70–79. doi:10.1016/j.cemconres.2018.10.011.

[270] S. Tongbo, W. Bin, Z. Lijun, C. Zhifeng, Meta-kaolin for high performance concrete, RILEM Bookseries. 10 (2015). doi:10.1007/978-94-017-9939-3_58.

[271] M.I. Sánchez De Rojas, J. Rivera, M. Frías, Influence of the microsilica state on pozzolanic reaction rate, Cem. Concr. Res. 29 (1999) 945–949. doi:10.1016/S0008-8846(99)00085-X.

[272] M. Frías, M.I. Sánchez De Rojas, Microstructural alterations in fly ash mortars: Study on phenomena affecting particle and pore size, Cem. Concr. Res. 27 (1997) 619–628. doi:10.1016/S0008-8846(97)00026-4.

[273] R. Siddique, Waste Materials and By-Products in Concrete, Springer, Berlin, Heidelberg, 2008. doi:10.1007/978-3-540-74294-4.

[274] H. Lee, A. Hanif, M. Usman, J. Sim, H. Oh, Performance evaluation of concrete incorporating glass powder and glass sludge wastes as supplementary cementing material, J. Clean. Prod. 170 (2018) 683–693. doi:10.1016/j.jclepro.2017.09.133.

[275] G. Medina, I.F. Sáez del Bosque, M. Frías, M.I. Sánchez de Rojas, C. Medina, Granite quarry waste as a future eco-efficient supplementary cementitious material (SCM): Scientific and technical considerations, J. Clean. Prod. 148 (2017) 467–476. doi:10.1016/j.jclepro.2017.02.048.

[276] R.A. Schankoski, P.R. de Matos, R. Pilar, L.R. Prudêncio, R.D. Ferron, Rheological properties and surface finish quality of eco-friendly self-compacting concretes containing quarry waste powders, J. Clean. Prod. 257 (2020). doi:10.1016/j.jclepro.2020.120508.

[277] E. Cohen, A. Peled, G. Bar-Nes, Dolomite-based quarry-dust as a substitute for fly-ash geopolymers and cement pastes, J. Clean. Prod. 235 (2019) 910–919. doi:10.1016/j.jclepro.2019.06.261.

[278] S. Krishnan, S.K. Kanaujia, S. Mithia, S. Bishnoi, Hydration kinetics and mechanisms of carbonates from stone wastes in ternary blends with calcined clay, Constr. Build. Mater. 164 (2018) 265–274. doi:10.1016/j.conbuildmat.2017.12.240.

[279] J. Dang, J. Zhao, W. Hu, Z. Du, D. Gao, Properties of mortar with waste clay bricks as fine aggregate, Constr. Build. Mater. 166 (2018) 898–907. doi:10.1016/j.conbuildmat.2018.01.109.

[280] E. Asensio, C. Medina, M. Frías, M.I. Sánchez de Rojas, Fired clay-based construction and demolition waste as pozzolanic addition in cements. Design of new eco-efficient cements, J. Clean. Prod. 265 (2020). doi:10.1016/j.jclepro.2020.121610.

[281] J.M. Paris, J.G. Roessler, C.C. Ferraro, H.D. Deford, T.G. Townsend, A review of waste products utilized as supplements to Portland cement in concrete, J. Clean. Prod. 121 (2016) 1–18. doi:10.1016/j.jclepro.2016.02.013.

[282] DIN EN 12620:2013, Aggregates for concrete; German version EN 12620:2013, European Committee for standardization, 2013.

[283] DIN EN 206:2017-01, Concrete - Specification, performance, production and conformity; German version EN 206:2013+A1:2016, European Committee for standardization, 2017.

[284] DIN EN 12390-2/A20:2015-12, Testing hardened concrete - Part 2: Making and curing specimens for strength tests; Amendment A20, European Committee for standardization, 2015.

[285] DIN EN 933-1:2012-03, Tests for geometrical properties of aggregates - Part 1: Determination of particle size distribution - Sieving method; German version EN 933-1:2012, European Committee for standardization, 2012.

[286] L.H. Grierson, J.C. Knight, R. Maharaj, The role of calcium ions and lignosulphonate plasticiser in the hydration of cement, Cem. Concr. Res. 35 (2005) 631–636. doi:10.1016/j.cemconres.2004.05.048.

[287] N.N. Salim, A.L. Feig, Isothermal titration calorimetry of RNA, Methods. 47 (2009) 198–205. doi:10.1016/j.ymeth.2008.09.003.

[288] E.J. Prosen, P.W. Brown, G. Frohnsdorff, F. Davis, A multichambered microcalorimeter for the investigation of cement hydration, Cem. Concr. Res. 15 (1985) 703–710. doi:10.1016/0008-8846(85)90072-9.

[289] J.M. Díez, J. Madrid, A. Macías, Characterization of cement-stabilized Cd wastes, Cem. Concr. Res. 27 (1997) 337–343. doi:10.1016/S0008-8846(97)00017-3.

[290] DIN EN 12350-2:2019-09, Testing fresh concrete - Part 2: Slump test; German version EN 12350-2:2019, European Committee for standardization, 2019.

[291] DIN EN 12390-3:2019-10, Testing hardened concrete - Part 3: Compressive strength of test specimens; German version EN 12390-3:2019, European Committee for standardization, 2019.

[292] DIN EN 12390-13:2014-06, Testing hardened concrete - Part 13: Determination of secant modulus of elasticity in compression; German version EN 12390-13:2013, European Committee for standardization, 2014.

[293] DIN EN 14630:2007-01, Products and systems for the protection and repair of concrete structures - Test methods - Determination of carbonation depth in hardened concrete by the phenolphthalein method; German version EN 14630:2006, European Committee for standardization, 2007.

[294] C. Jakob, D. Jansen, N. Ukrainczyk, E. Koenders, U. Pott, D. Stephan, J. Neubauer, Relating Ettringite Formation and Rheological Changes during the Initial Cement Hydration: A Comparative Study Applying XRD Analysis, Rheological Measurements and Modeling, Materials (Basel). 12 (2019) 2957. doi:10.3390/ma12182957.

[295] U. Pott, C. Jakob, D. Jansen, J. Neubauer, D. Stephan, Investigation of the Incompatibilities of Cement and Superplasticizers and Their Influence on the Rheological Behavior, Materials (Basel). 13 (2020) 977. doi:10.3390/ma13040977.

[296] B. Sabir, S. Wild, J. Bai, Metakaolin and calcined clays as pozzolans for concrete: A review, Cem. Concr. Compos. 23 (2001) 441–454. doi:10.1016/S0958-9465(00)00092-5.

[297] S. Wild, J.M. Khatib, L.J. Roose, Chemical shrinkage and autogenous shrinkage of Portland cement-metakaolin pastes, Adv. Cem. Res. 10 (1998) 109–119. doi:10.1680/adcr.1998.10.3.109.

[298] D. Küchlin, O. Hersel, Betontechnische Daten - Augabe 2017, Ausgabe 20, HeidelbergCement AG, 2017.

[299] P. Termkhajornkit, T. Nawa, K. Kurumisawa, Effect of water curing conditions on the hydration degree and compressive strengths of fly ash – cement paste, Cem. Concr. Compos. 28 (2006) 781–789. doi:10.1016/j.cemconcomp.2006.05.018.

[300] J. Bai, S. Wild, B.B. Sabir, J.M. Kinuthia, Workability of concrete incorporating pulverized fuel ash and metakaolin, Mag. Concr. Res. 51 (1999) 207–216. doi:10.1680/macr.1999.51.3.207.

[301] R. Siddique, Effect of fine aggregate replacement with Class F fly ash on the mechanical properties of concrete, Cem. Concr. Res. 33 (2003) 539–547. doi:10.1016/S0008-8846(02)01000-1.

[302] M.A. Megat Johari, J.J. Brooks, S. Kabir, P. Rivard, Influence of supplementary cementitious materials on engineering properties of high strength concrete, Constr. Build. Mater. 25 (2011) 2639–2648. doi:10.1016/j.conbuildmat.2010.12.013.

[303] D. Jóźwiak-Niedźwiedzka, M. Sobczak, K. Gibas, Carbonation of concretes containing calcareous fly ashes, Roads Bridg. - Drog. i Most. 12 (2013) 223–236. doi:10.7409/rabdim.013.016.